THE GEOMICROBIOLOGY OF SUSPENDED AQUATIC FLOCS: LINKS BETWEEN MICROBIAL ECOLOGY, $FE^{(III/II)}$-REDOX CYCLING, & TRACE ELEMENT BEHAVIOUR

By

AMY V.C. ELLIOTT, H.B.Sc., Ecology & Evolution Specialization

A Thesis Submitted to the School of Graduate Studies

in Partial Fulfillment of the Requirements for

the Degree Doctor of Philosophy

McMaster University

McMaster University DOCTOR OF PHILOSOPHY (2013) Hamilton, Ontario (Geochemistry)

TITLE: 'The geomicrobiology of suspend aquatic flocs: links between microbial ecology, $Fe^{(III/II)}$-redox cycling and trace element behaviour'

AUTHOR: Amy V.C. Elliott, H.B.Sc. (The University of Western Ontario)

SUPERVISOR: Dr. Lesley A. Warren

PAGES: i...n

ABSTRACT

This doctoral research comparatively assesses the biogeochemical properties of suspended aquatic flocs through a integrated field-laboratory approach; providing new insight into the linkages among floc associated bacteria, floc-reactive solid phases and trace metal uptake.

Results show flocs to possess a distinct geochemistry, microbiology and composition from bed sedimentary materials in close proximity (<0.5m) across 6 widely varying aquatic systems. Of significant note, in all systems investigated, resident floc microbial cells and associated natural organic materials (NOM) were found to facilitate the concentration of trace elements (TEs: Ag, As, Cu, Ni and Co) specifically through the collection/nucleation of highly reactive, amorphous Fe^{III}-oxyhydroxide minerals (FeOOH); resulting in localized floc-Fe-mineral precipitates and enhanced reactivity. Further, the Fe-enrichment of floc and of floc bio-mineral constituents in turn provides an important and novel lens through which to examine how environmental microbial communities, microbial metabolism and Fe^{III}/Fe^{II} redox transformations interact. The results were the discovery of floc-hosted, $Fe^{III/II}$-redox cycling bacterial consortia across diverse oxygenated ($O_2^{Sat.}$=1-103%) aquatic systems, which were not predicted to sustain bacterial Fe-metabolism. Both environmental and experimentally-developed consortial aggregates constituted multiple genera of aero-intolerant Fe^{III}-reducing and Fe^{II}-oxidizing bacteria together with oxygen consuming organotrophic species. These findings highlight that the implementation of geochemical thermodynamic constraints alone as a guide to investigating and interpreting microbe-geosphere interactions may not accurately capture processes occurring *in situ.*

Seasonal investigation of microbial $Fe^{III/II}$-redox transformations highlighted the interdependence of floc Fe-redox cycling consortia members, revealing that cold conditions and a turnover in putative Fe-reducing community membership extinguishes the potential for coupled Fe-redox cycling by wintertime floc bacteria. Further, the observed summer-winter seasonal turnover of *in situ* floc community membership corresponded with an overall shift from dominant Fe to S redox cycling bacterial communities. This significantly impacted observable floc Fe and TE (Cd, Pb) geochemistry, resulting in a shift in floc associated Fe-phases from dominantly $Fe^{(III)}_{(s)}$ to $Fe^{(II)}_{(s)}$, and, in turn, corresponded to a large decrease of TE uptake by flocs under ice.

Table of Contents

LIST OF FIGURES

LIST OF TABLES

PREFACE

This dissertation contains three results chapters which represent manuscripts for peer-reviewed publication. Chapter 3 has been published as: *"Comparative floc-bed sediment trace element partitioning across variably contaminated aquatic ecosystems';* Elliott, A.V.C., Plach, J.M., Droppo, I.G., and Warren, L.A. Environmental Science & Technology., **2012,** 46 (1), pp. 209-231 DOI: 10.1021/es202221u". Chapter 4 is currently under review (Chemical Geology) as: "*Collaborative microbial Fe-redox cycling by pelagic floc bacteria cross diverse oxygenated aquatic systems';* Elliott, A.V.C., Plach, J.M., Droppo, I.G., and Warren, L.A. Chapter 5 will be submitted July 2013 (Environmental Science & Technology) as "*Seasonal changes in microbial community structure, $Fe^{(III/II)}$-redox cycling, and trace element geochemistry of pelagic flocs in a circumneutral, remote lake';* Elliott, A.V.C., and Warren L.A.

These papers represent the results of research carried out by the author under the supervision of Dr. Lesley Warren in partial fulfillment of a Ph. D. degree. Collaboration with the other authors of the published papers consisted of analyses selected by the thesis author of samples prepared by the thesis author; most significantly the assistance with sample collection and initial processing (Chapter 3), fluorescence imaging and ESEM (Chapter 4) and editing of manuscript text (Chapters 3, 4) provided by Janina M. Plach, PhD. candidate, McMaster University, with which the thesis author was closely involved. The author of this thesis under the guidance of Dr. Lesley Warren carried out the literature review, laboratory microcosm experimentation, fluorescence imaging and TEM imaging (Chapter 5), data analyses and interpretation, and writing and revision of these chapters.

CHAPTER 1: INTRODUCTION

Environmental bacteria are the primary intermediaries of biosphere-geosphere interactions. They act as biogeochemical catalysts, utilizing environmental redox couples to drive a diverse range of metabolisms and detoxification pathways, and thereby mediate kinetically inhibited but thermodynamically favourable reactions. Bacterial membranes and associated extracellular polymeric substances (EPS) are also geochemically reactive substrates and can serve both as potent sorbents for a wide range of differentially reactive trace metal elements (e.g.[1-4]) as well as nucleation sites for the precipitation of a host of authigenic minerals (e.g. [5-7]). In this manner, environmental bacteria actively manipulate, regulate and catalyze important geochemical processes. These include the formation of geologically significant minerals (e.g.[8, 9]), the geochemical cycling of essential elements (e.g. C, N, P, and S [10-15]), and the bioavailability and fate of both inorganic and organic contaminants within the biosphere [16-20]. Furthermore, bacteria rarely interact with their environment in isolation; rather, they participate in syntrophic relationships as components of multi-guild cooperatives often associated with macrostructures such as consortial aggregates (e.g. [21, 22]) or sessile biofilm communities [23-25]. In this manner, diverse lineages of environmental bacteria intimately co-exist and collectively influence biogeochemical cycling of elements. Geomicrobiology is a field that seeks to understand and characterize these often complex interrelationships between microbial ecology, microbial metabolism and geochemical process.

1.1 THE GEOMICROBIOLOGY OF IRON

As the fourth most abundant element on the Earth's surface, iron (Fe) plays a particularly important role in environmental biogeochemistry. $Fe^{(III/II)}$-redox transformations are critically implicated in environmental contaminant behaviour[16, 17, 26, 27], are utilized as a key interpretative markers for Earth's geological and atmospheric record [8, 9, 28, 29], and participate in the biogeochemical cycling of carbon,

nitrogen, sulfur and phosphorous[10-12, 14, 15, 17]**.** Although the transformation of Fe in the major global pools is seen as a consequence of geological processes operating over millions of years of Earth history, microorganisms mediating $Fe^{(III)}/Fe^{(II)}$ redox cycling are deeply rooted in the universal phylogenetic tree and have been implicated in planetary biogeochemistry during the Archaean and early Proterozoic Eons [28, 30]. Thus the geomicrobiology of Fe, and in particular, elucidating a role for microbial metabolism in environmental $Fe^{(III/II)}$ redox transformations, has been the subject of intense interest in recent years, having large implications across disciplines ranging from astrobiology to the development of biomining and bioremediation technologies.

To date, modern Fe-metabolizing bacteria are largely known from a variety geochemical 'niche' environments (i.e. anoxic to low redox boundaries where oxygen <50μM or pH <3.0; [9, 31-34]; Figure 1.1). These include anaerobic respiration by dissimilatory ferric iron ($Fe^{(III)}$) reducing bacteria (IRB) in groundwater, soils and non-sulfidogenic sedimentary environments [9, 34] as well as the bacterially catalyzed oxidation of ferrous ($Fe^{(II)}$) iron by chemolithotrophic bacteria (IOB) in both highly acidic aerobic systems [35] and circumneutral anoxic to microoxic environments (e.g. groundwater seeps, the rhizosphere of wetland plants and biogenic iron oxyhydroxide (BIOS) mat communities) by specialized, often appendaged, bacteria [36, 37].

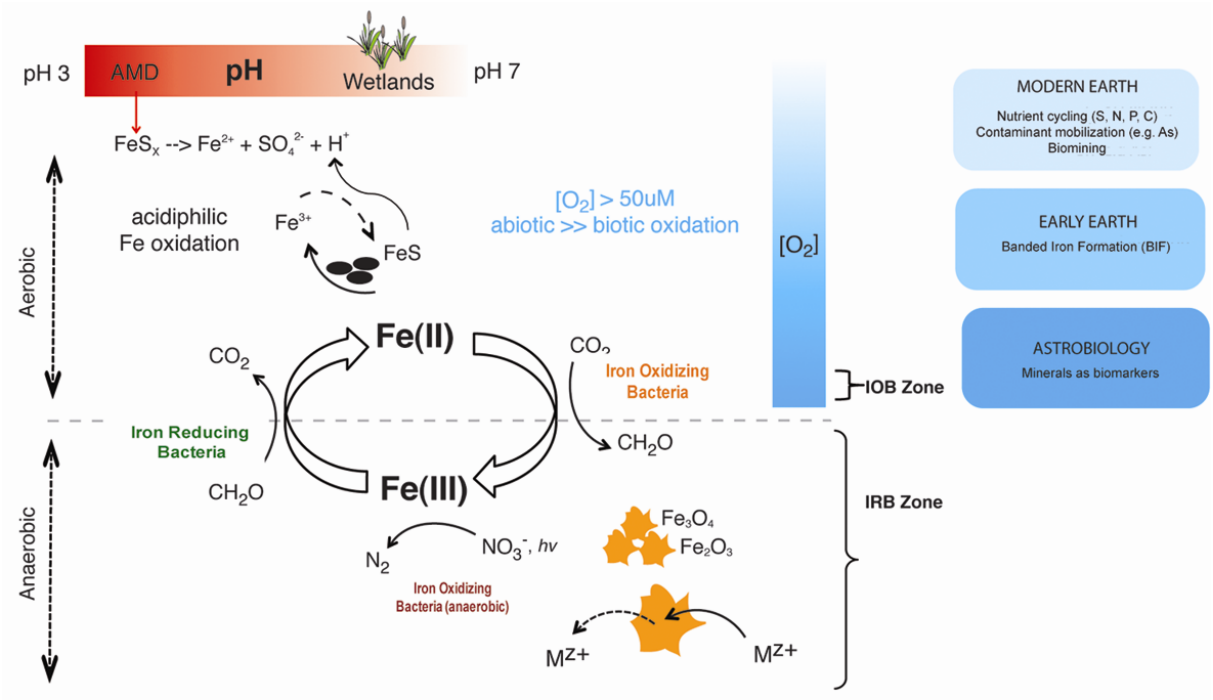

FIGURE 1.1. Geochemical niche of known $Fe^{(III/II)}$-redox cycling bacteria. The biogeochemical redox cycling of Fe has important implications for both ancient and modern planetary biogeochemistry as a control over Fe mobility, bioavailability and metal (M^{z+}) contaminant mobilization/sequestration reactions. However, $Fe^{(III/II)}$-redox cycling bacteria (IRB, IOB) are currently thought to be differentially segregated to a select range of geochemical 'niche' environments (i.e. O_2 ≤50µM or pH≤3.0). At pH>3.0, the rapid abiotic oxidation of $Fe^{(II)}$ by O_2 outcompetes microbial IOB catalysis of $Fe^{(II)}$ oxidation, limiting opportunity for survival. Similarly, IRB activity is restricted to anoxic conditions due to metabolic inhibition and toxicity of molecular oxygen. This has directed scientific investigation to date and accordingly our understanding of the biogeochemical Fe-redox cycle. However this view discounts the capacity of environmental bacterial communities to collectively engineer their immidate microenvironment through the creation of aggregates or biofilms; thus IRB and IOB may have a greater biogeography and importance to the global biogeochemical Fe-redox cycle than is currently appreciated (*Chapt.4).*

1.1.1 $Fe^{(III)}$-reducing bacteria (IRB).

The discovery of dissimilatory iron reducing bacteria (IRB) **(Eq. 1)** transformed the understanding of Fe geochemistry in soils and sediments. In fact, even microbial-oriented texts considered $Fe^{(III)}$ reduction in sedimentary environments to be primarily an abiotic process up until the early 1980s ([9, 34, 38]). A major reason for this line of thinking is that $Fe^{(III)}$ is only soluble under extremely acidic conditions (~pH < 3.0), hydrolyzing and subsequently precipitating as highly insoluble $Fe^{(III)}$(hydro)oxides above pH=5 (**Eq. 2**). This $Fe^{(III)}_{(s)}$ was considered inaccessible to microbial metabolism [34, 39] (i.e. could not serve as a terminal electron acceptor (TEA) in respiration).

Eq.1: $CH_3COO^- + 8Fe^{(III)}(OH)_3 \rightarrow 8Fe^{(II)} + 2HCO_3^- + 15OH^- + 5H_2O$

Eq. 2: $Fe^{(III)} + H_2O \rightarrow Fe^{(III)}(OH)^{2+} + H^+$ **logK= -2.19**

$Fe^{(III)}(OH)^{2+} + H_2O \rightarrow Fe^{(III)}(OH)^{+} + H^+$ **logK= -3.48**

$Fe^{(III)}(OH)^{+} + H_2O \rightarrow Fe^{(III)}(OH)_3 + H^+$ **logK= -5.22**

It is now well established that microbial metabolic catalysis primarily controls $Fe^{(III)}$ reduction in non-sulfidogenic environments [17, 34, 39-41]. It is considered the dominant respiratory pathway in the absence of more energetically favourable metabolites according to the redox ladder (e.g. $Mn^{(IV)}$ and nitrate [17, 39]) and can be responsible for driving the oxidation of as much as 75% of the organic matter oxidized in natural aquatic systems ([42]). Further, dissimilatory IRB have now been documented to utilize a wealth of differentially reactive/bioavailable $Fe^{(III)}$-$oxides_{(s)}$ as TEAs including amorphous oxyhydroxides ($Fe^{(III)}OOH$), crystalline $Fe^{(III)}_{(s)}$ (e.g. hematite, goethite,[40, 43, 44]) as well as a variety of $Fe^{(III)}$-bearing clay meineras (e.g. chlorite, palygorskite, illite, and most notably, smectites such as nontronite ([45, 46 47]).

The two most well described dissimilatory $Fe^{(III)}$-reducing bacterial species are the organotrophs *Geobacter sp.* and *Shewenella sp.*,[48, 49] which are currently identified as the most numerically dominant IRB species in anoxic environments (i.e. groundwater and bottom sediments of anoxic hypolimnion of stratified lakes, ([48, 50]). It is of important note that enzymatic $Fe^{(III)}$ reduction not only manifests in

bacteria as a form of respiration, in which $Fe^{(III)}$ serves as a dominant or exclusive TEA, but also may accompany fermentation in which $Fe^{(III)}$ serves as a supplementary electron acceptor. In microbial fermentative metabolism, there is no electron transport chain as in respiration; rather electrons from NADH generated during glycolysis are transferred to the carbon source itself[39]. It is thought that $Fe^{(III)}$ serves as a supplementary electron acceptor during this process as a means to dispose of excess reducing power [39]. Further, lithoautotrophs, such as *Sulfobacillus acidophilus*, *Acidimicrobium ferrooxidans* and *Acidithiobacillus ferrooxidans* can also respire with $Fe^{(III)}$, using reduced sulfur species (S^0 , H_sS, SO_3^{2-}) as an electron donor ([39, 51, 52]). Most of these bacteria have been isolated from acidic environments and complete this reaction both under aerobic and anaerobic conditions.

While dissimilatory iron reduction is now a well established and accepted bacterial metabolic pathway, both the molecular biology and the actual mechanism by which IRB transfer electrons from the cell surface to that of a $Fe^{(III)}_{(s)}$ remain heavily debated[39]. Accordingly, there is currently a lack of a conserved, identifiable functional gene to use as a genetic proxy for $Fe^{(III)}$ respiration activity (as compared to, for instance, dissimilatory sulphate reduction metabolism). The prevailing paradigm involves the requirement of direct contact (Figure 1.2). Early evidence for this process demonstrated that $Fe^{(III)}$-reduction was inhibited when contact between an organotrophic IRB and $Fe^{(III)}_{(s)}$ was prevented utilizing a semi-permeable membrane; i.e. the barrier permits the passage of only soluble reductants while simultaneously providing equivalent pH and redox potential on either side of the membrane[39, 53]. The authors proposed electron transfer involved the utilization of outer-membrane *c*-type cytochromes **(**Figure 1.2**).** Similarly, Lower et al. (2007) suggested that the formation of specific bonds between hematite (TEA) and outer-membrane cytochromes MtrC and OmcA in *Shewanella oneidensis* strain MR-1 are involved in transferring electrons during anaerobic respiration [54]. In contrast, a recently proposed and exciting alternative to the cytochrome-contact model for $Fe^{(III)}_{(s)}$ reduction is the utilization of specialized pili or 'nanowires' by bacteria as a direct physical link to a ferric oxide surface ([55]). Reguera et al (2006) demonstrated that IRB (*Geobacter sp*.) produced specialized pili during growth on $Fe^{(III)}_{(s)}$ oxides

but not on soluble $Fe^{(III)}$ (Figure 1.2**).** Further, these 'nanowires' were exclusively localized to the side of attachment of the $Fe^{(III)}_{(s)}$ and when the gene mediating nanowire production (*pilA*) was knocked-out, the bacteria i) showed no pili production ii) could no longer reduce solid phase $Fe^{(III)}$ but iii) retained the ability to utilize $Fe^{(III)}_{(aq)}$ species [55]. They proposed that this indicated that IRB requires pili in order to reduce $Fe^{(III)}$oxides, acting as 'wire conductors' of electrons and effectively shuttling electrons from the electron transport chain to the $Fe^{(III)}_{(s)}$ surface**.**

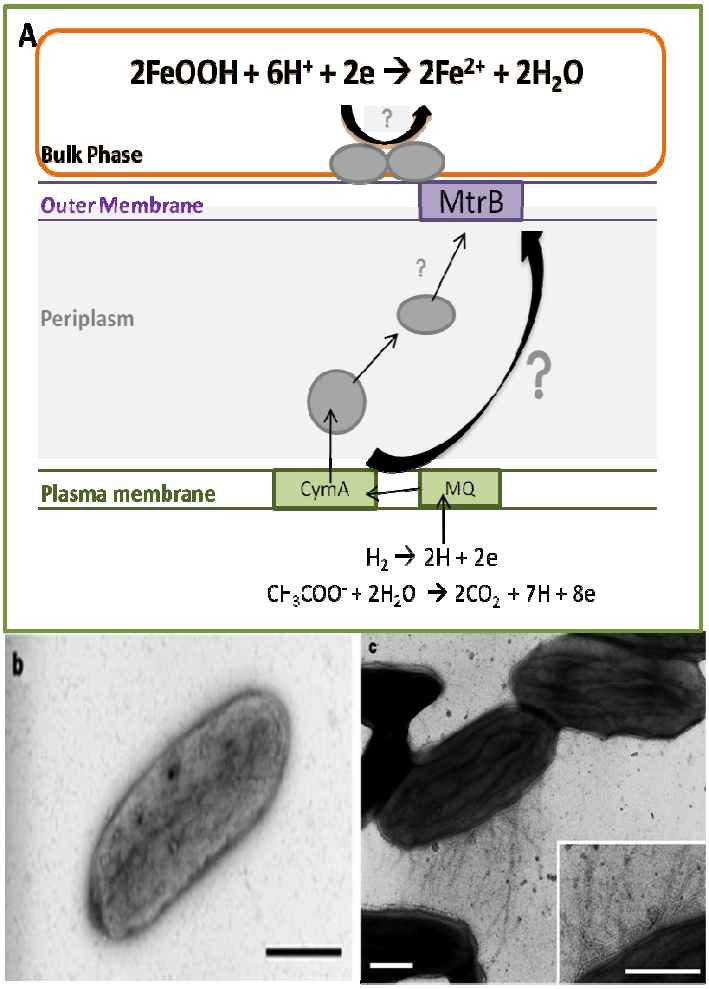

Figure 1.2 The molecular biology of dissimilatory ferric iron reduction is not well constrained. It is known that different genera of bacteria will use different strategies to deliver electrons to $Fe^{(III)}_{(s)}$, i.e. an external, solid terminal electron acceptor (TEA).**A)** The use of membrane-bound c-type cytochromes have been implicated to shuttle electrons during direct contact with $Fe^{(III)}_{(s)}$. **B,C)** Recently, pili production (or 'nanowires') have been implicated in IRB activity, whereby pili are only produced when bacterial cells metabolize $Fe^{(III)}_{(s)}$ phases (B) and are absent when cells are presented with a soluble $Fe^{(III)}$ source (C). (*Figures reproduced with alternation from Ehrlich & Neman, 2009; Konhauser, 2007; Regeura et al. 2005*)

1.1.2 $Fe^{(II)}$-oxidizing bacteria (IOB)

Most of the evidence for autotrophic $Fe^{(II)}$ oxidizing metabolism (**Eq. 3**) comes from the study of acidophilic bacteria which commonly dominate low-pH environments, including acid mine drainage (AMD) and acidic hydrothermal vents (e.g. *Acidithiobacillus ferrooxidans, Leptosprilimm spp., Thiobacillus ferrooxidans*) [51, 56, 57]. This derives from the physiological challenge of bacterial growth via the utilization of $Fe^{(II)}$ as a sole energy source. Of all the potential lithotrophic energy sources, the oxidation of $Fe^{(II)}$ yields the lowest Gibbs free energy (G◦) with energetic yield estimates from -41.8 kJ mol-1 to 27.2 kJ mol-1[36, 39] (Eq. 3). Further, in order to gain energy by capturing electrons from the oxidation of $Fe^{(II)}$ to $Fe^{(III)}$ oxidation, an IOB must be able to out-compete the rapid abiotic oxidation of $Fe^{(II)}$ by molecular oxygen[32] (Eq. 4).

Eq. 3: $$26Fe^{2+} + 0.5O_2 + 6CO_2 + 26H^+ \rightarrow C_6H_{12}O_6 + 26Fe^{3+} + 7H_2O$$

Eq. 4: $$-d[Fe(II)]/dt = k]Fe(II)][OH^-]^2[O_2]$$

$$k = 8(\pm 2.5)*10^{13} min^{-1} atm^{-1} mol^{-2} L^{-2}$$

As is evident from Eq. 4 and 5, pH strongly regulates the abiotic reaction kinetics of $Fe^{(II)}$oxidation. Thus the most efficient way for an IOB to gain access to their electron donor is to grow at very low pH (i.e. pH<4). For these reasons, microbial $Fe^{(II)}$ oxidation has historically been considered a geochemical 'niche' metabolism; that is, demonstrating a very restricted biogeography and low overall importance to the global biogeochemical Fe redox cycle. Nevertheless, acidophilic IOB bacteria have been recognized for decades, characterized in various environments, and include strict autotrophs, mixotrophs and heterotrophs widely dispersed amongst the Bacterial and Achaeal domains [39, 51, 56, 57]. Importantly, acidophilic IOB demonstrate significant geochemical importance within the 'environmental niche' which they do inhabit. For example, the oxidative dissolution of $Fe^{(II)}$sulfide minerals by acidophilic Fe (and sulfur) oxidizing species (e.g. *Acidithiobacillus ferrooxidans),* catalyzes the production acid mine drainage (AMD;

Eq. 6, 7) a globally-relevant phenomenon which results in substantial environmental degradation and water contamination.

Eq. 5: $FeS_2 + 3.5O_2 + H_2O \rightarrow Fe^{(II)}+ + 2SO_4^{2-} + 2H^+$

Eq. 6: $Fe_{1-xS} + (2-0.5x)O_2 + xH2O \rightarrow (1-x)Fe^{(III)} + SO_4^{2-} + 2xH^+$

The molecular biology of iron oxidation, known from acidophiles, is much better constrained than in dissimilatory iron reducers to date. A widely accepted model[39, 58] involves the rapid electron transfer from molar excess of $Fe^{(II)}$ to the enzyme rusticyanin which is catalyzed by iron rusticyanin oxidoreductase, which consists of c-type cytochromes (e.g. Cyc1, CycA1) (Figure 1.3) [57]

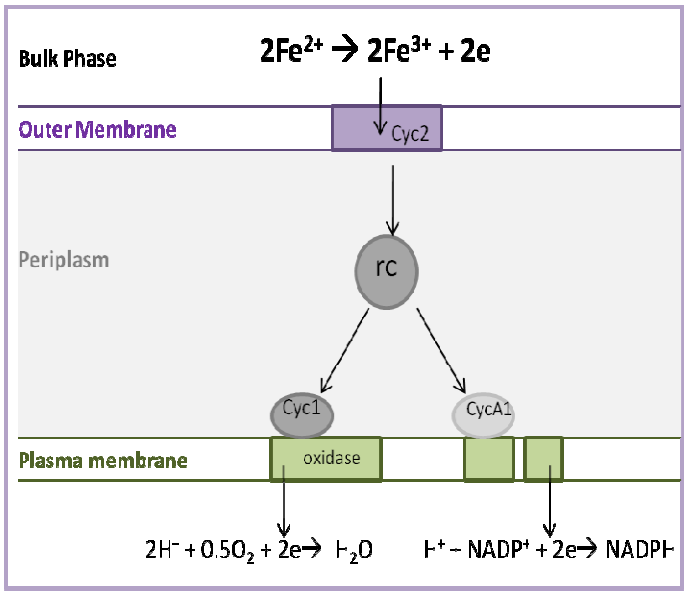

Figure 1.3. Much of the molecular insight into microbial $Fe^{(II)}$-oxidizing metabolism come from the study of acidophiles, in particular, *Acidithiobacillus ferrooxidans*. This organism uses $Fe^{(II)}$ both as an energy source as well as a reducing power for assimilation of carbon for biosynthesis (i.e. the burden of autotrophy). Arrows indicate direction of electron flow. (*Figure reproduced with alteration from Erlich & Newman, 2006; Konhauser, 2007*)

While the acidophilic, aerobic, microbial oxidation of $Fe^{(II)}$ has long been recognized, the relatively recent identification of neutrophilic, microaerophilic $Fe^{(II)}$ bio-oxidation extended the range of bacterial IOB metabolism beyond highly acidic environments[59-63]. Neutrophilic IOB are thought to overcome the $Fe^{(II)}$ stability problem (Eq. 3,4) by subsisting in low redox boundaries (i.e. where oxygen <50µM, [31, 36]) where they are thus able to effectively compete with abiotic $Fe^{(II)}$-oxidation. The most widely characterized neutrophilic IOB are specialized, appendaged species. These include the stalk-forming *Galionella spp*. and the sheath- forming *Leptothrix spp.* which, in turn, have been documented in a diverse range of bulk microoxic environments. These include the roots of wetland plants, ground water seeps, the Lohi hydrothermal vent site (marine) and microbial mat communities (BIOS) ([60, 64-68]. In fact, the distinctive

morphology and growth habit *in situ* of many neutrophilic IOB (i.e. stalks and sheaths) as often been used specifically for environmental identification of IOB as specific organisms (e.g.[69, 70-72]), and, further, to study their distribution[69, 73, 68, 74, 66, 75]. One reason for the often reliance on morphology and growth habit *in situ* for IOB identification is that many IOB species are enigmatic and have resisted laboratory isolation efforts to obtain in pure culture. For this reason, virtually nothing is known about neutrophilic IOB molecular biology nor mechanisms by which neutrophilic IOB oxidize $Fe^{(II)}$. Also yet to be fully elucidated is the actual metabolic and/or physiological function of the so-called 'sheaths' and 'stalks' on these specialized microorganisms and whether these appendages directly or passively contribute to the bacterial metabolic function, although this has been subject to recent, intense research focus [76, 77].

Another significant advancement in the understanding and characterization of IOB was the discovery that bacterial $Fe^{(II)}$ oxidizing activity does not always require molecular oxygen as a terminal electron acceptor. Recent evidence indicates that ferrous iron oxidation, coupled to the reduction of nitrate, perchlorate, and chlorate (i.e. anaerobic IOB metabolism) can occur in a variety of anoxic environments [37, 62, 7858]. Further, photoautotrophic, anaerobic $Fe^{(II)}$ oxidation has also been demonstrated as a viable microbial metabolism, whereby IOB oxidize $Fe^{(II)}$ to generate ATP and utilize light energy to generate the reducing powered required to fix CO_2 into biomass (**Eq. 8**). This is in contrast to all other autotrophic IOB which must utilize ferrous iron both as a reducing power and to generate ATP (i.e. the 'burden' of autotrophy;) ([58]

Eq. 8: $\mathbf{24Fe^{2+} + 6CO_2{}^{+} + 66H_2O \rightarrow C_6H_{12}O_6 + 24Fe(OH)_3 + 48H^+}$

1.1.3 Coupled Microbial $Fe^{(III/II)}$-redox cycling

The discovery of microbially-mediated $Fe^{(III)}$ reduction and $Fe^{(II)}$ oxidation significantly expanded the appreciation of the impact of microbes and their activities on geochemical processes and, further, points towards the possibility that environmental bacteria could in fact perpetuate a dynamic $Fe^{(III/II)}$ redox cycle

(Figure 1.4). However, microbial catalyzed $Fe^{(II)}$-oxidation and $Fe^{(III)}$-reduction activities are largely considered restrictively segregated to these select range of low oxygen and/or highly acidic geochemical niche environments (Figure 1.1). Moreover, due to these differential restrictions on IRB (absence of O_2) and IOB (e.g. low O_2) metabolism, they are classically thought to occur in segregated microenvironmental contexts, limiting the possibility of their co-occurrence and thus the potential for widespread, coupled microbial $Fe^{(III/II)}$-redox cycling. Such a strategy would have ecological benefits as well as biogeochemical ramifications.

For example, sustained microbial Fe redox cycling has been proposed within a select range of bulk redox interfacial environments including groundwater seeps, the roots of wetland plants and the sediment-water interface in hypolimnion of productive lake systems([58, 79-81]). The majority of evidence supporting the potential coupling of microbial metabolism to the cycling of Fe relies on *in vitro* $Fe^{(III)}$-reduction and $Fe^{(II)}$-oxidizing experiments using separately cultured isolates, *in situ* observation of characteristic Fe encrusted microbial morphologies (e.g. the stalked-forming *Galionella spp*. and the sheath- forming *Leptothrix spp.*) via microscopic techniques (e.g. phase contrast, TEM, ESEM) and 16S rDNA Sanger-sequencing demonstrating the co-occurrence of classically known and/or 'type' species of IRB and IOB within the environment. For example, Blothe & Roden (2009) assessed the potential for bacterial Fe redox cycling within a circumneutral ground water seep environment. $Fe^{(III)}$-reduction and $Fe^{(II)}$-oxidation cultures, together with most-probable-number (MPN) results, supported the presence of both IRB and IOB[79]. Further 16S rDNA sequencing from the Fe seep revealed the presence of 'type' iron-metabolizing organisms including *Shewanella spp., Gallionella spp., Leptothrix spp.* and *Comamonas spp.* ([79]). Similarly, Bruun et al. (2010) use a combination of phase-contrast and fluorescent (SBYR-green) microscopies, cultivation and sequencing techniques to provide multiple lines of evidence for a coupling of biologic Fe redox in another fresh water iron-rich ground water seep [81].

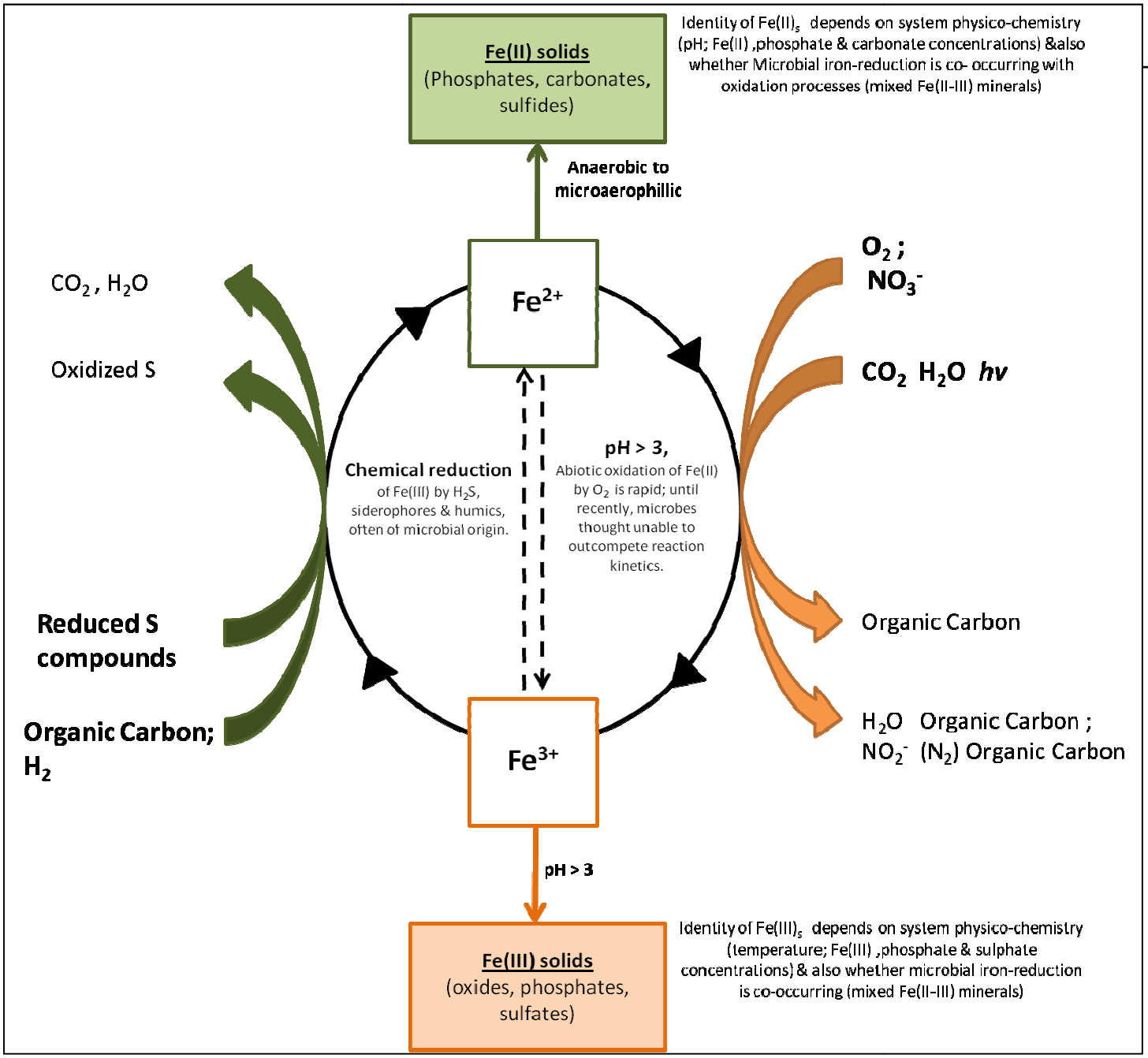

FIGURE 1.4. Major microbial metabolisms perpetuating the biogeochemical cycling of Fe. Dissimilatory ferric iron ($Fe^{(III)}$) reducing (IRB) metabolisms (green arrows) include both heterotrophic and autotrophic pathways. IRB activity can result in the generation of aqueous ferrous iron species (Fe^{II}), solid-phase $Fe^{(II)}$-bearing minerals (e.g. siderite and vivianite) and mixed valence $Fe^{(II)}$-$Fe^{(III)}$ mineral assemblages such as magnetite and green rust. Autotrophic ferrous iron (Fe^{II}) oxidizing bacterial (IOB) are indicated by orange arrows. Molecular oxygen can be used as an electron acceptor by IOB in both acidic (pH<3) and microoxic circumneutral environments. The use of nitrate as an electron donor has yet only been identified by IOB isolated from anaerobic, circumneutral aqueous environments. Photosynthetic IOB oxidize $Fe^{(II)}$ to generate ATP and utilize light energy to generate the reducing powered required to fix CO_2 into biomass. This is in contrast to all other autotrophic IOB which must utilize ferrous iron both as a reducing power and to generate ATP. (Emerson,David 2010; Weber,Karrie A. 2006; Konhauser, K. O. 2007; Ehrlich, H.L. 2009)

The perceived bulk-system geochemical restrictions thought to severely restrict where IOB and IRB can sustain their metabolism has directed scientific investigation and accordingly our understanding of the biogeochemical Fe-redox cycle (Figure 1.4). However, this view largely discounts both syntrophic, cooperative metabolism among diverse guilds of bacteria as well as the capacity for environmental bacterial communities to collectively decouple from immediate bulk system conditions through the creation of consortial aggregates or stratified biofilm communities[21, 22, 82-84] . For example, the microbial zonation model afforded by redox ladder view of the environment predicts that active dissimilatory $Fe^{(III)}$ reducers would only occur/ have importance in anaerobic, nitrate-depleted environments. However, evidence form marine systems supports the existence of $Fe^{(III)-}$ and $Mn^{(IV)-}$ reducing bacteria subsisting within low oxygen microzones in pelagic macro-aggregates (>1mm) under bulk oxygenated regimes (marine snow, marine aggregates, cyanobateria colonies) using microelectrodes and chemical redox indicators [85-88]. Similarly, a cooperative aggregate-production strategy has been identified in the µm-scale coupling of anaerobic bacterial sulfur (S^0) reduction with autotrophic, oxygen-driven reduced sulfur oxidation in AMD consortial aggregates [21]. These recent findings have large implications for the prediction of microbial metabolic activity given a set of bulk-system physicochemical conditions and highlights that the implementation of geochemical thermodynamic constraints alone as a guide to investigating and interpreting microbe-geosphere interactions may not accurately capture processes occurring *in situ*.

1.2 MICROBIAL-MINERAL-METAL INTERACTIONS

Trace metal concentrations in surface waters have increased in the past several decades as a result of anthropogenic inputs, impairing water quality and posing risks to ecosystem as well as public health. Assessing these risks requires an understanding of the key processes and dominant variables controlling metal behaviour, distribution and ultimate fate within aquatic environments[17]. Environmental bacteria are increasing recognized as 'geochemical agents'[39] and actively manipulate, regulate and catalyze important geochemical processes [17, 23, 47, 89-

[92]. Given the extensive biological nature of suspended aquatic floc (*section 1.2.1*), floc-colonizing bacteria likely actively influence floc trace element geochemistry both through participation in floc-associated mineral formation and dissolution reactions, as well as through their ability to modify the geochemical conditions of their immediate environment through natural metabolic processes.

1.2.1. Suspended aquatic flocs- 'a microbial engineered' aquatic system compartment

It is well known that bed sedimentary materials dynamically concentrate and partition trace elements (TEs) amongst constituent reactive solid phases with a variety of specific physico-chemical and biological controls, making bed sediments a key compartment controlling TE behavior and ultimate fate within natural aquatic environments[17]. Investigation of TE geochemistry of suspended sedimentary materials or suspended particulate matter (SPM) has also received a great deal of attention in the last several decades. This is largely owing to i) the ability of SPM to sequester large quantities of metal contaminants relative to bottom sediments [93-95] (ii) being highly mobile [96, 97], SPM is likely an important vector for trace metal transport; iii) SPM likely acts as an important link between the highly bioavailable aqueous phase and bed sediment (classical metal-sink) system compartments. However, little direct evaluation of SPM metal partitioning patterns or constituent phases responsible for metal scavenging has occurred[93-95, 98] and none to date have compared SPM-associated TE concentrations and partitioning patterns across a suite of variably impacted natural aquatic systems. Further, natural SPM is largely considered to exist as biologically flocculated particles or suspended aquatic flocs[99]. Flocs are increasingly recognized as an important constituent for the transport of cohesive sediments and associated contaminants in aquatic environments and may be derived from overland wash-off of soil aggregates, re-suspended bottom sediments and/or formed directly in suspension via a complex flocculation process.[99] Regardless of their origin, flocs within the watercolumn are in a continual state of flux due to changing hydraulic, biological, and chemical factors[96, 97, 99]. The development and stabilization of suspended flocs, in turn, is highly influenced by

the activity of floc-colonizing bacteria and associated extracellular polymeric substances (EPS) (e.g. [96, 97, 100]). EPS fibrils are produced by microbes as a primary mechanism of attachment to sediment particles, protection from predation, as well as for nutrient assimilation [58, 101]. While EPS often represents a low mass relative to the other floc components, it can represent a significant volume of the overall floc structure and is generally thought to make up the framework for the overall floc architecture[97] due to the enormous surface area and general 'sticky' nature of EPS ([97, 100-104]). While floc structure, size and composition can vary considerably across aquatic systems and energy regimes (e.g. [96, 97, 105, 106]) what is common among floc is this underlying microbial nature of its formation and stabilization, with bacterial-produced EPS as the dominant bridging mechanism between the floc components-microbial, mineral and organic [97, 99, 100] .

The complex composition, as well as the increasing appreciation of the interacting physical, chemical and biological interactions within flocs, and within the systems where they occur, has given rise to a recent reconsideration about what constitutes flocculated SPM within the watercolumn. Droppo et al (1997, 2001) define a flocculated particle as an '*individual micro-ecosystem (composed of a matrix of water, inorganic and organic particles) with autonomous and interactive physical, chemical and biological functions or behaviours operating within the floc matrix.*' This substantive 'ecological' nature of floc, as well as microbial influences on floc architecture and development, thus suggests that the floc microbial community will influence floc TE behaviour in ways not currently captured by geochemical models, i.e., linkages amongst microbial activity, metabolism and geochemical microniche development. Thus suspended floc represents both an important aquatic system compartment influencing environmental trace metal behaviour, as well as an unique lens with which to examine how environmental microbial communities and geochemical processes interact. To date, characterization of these floc roles has not been reported in the literature.

1.2.2 Potential Microbial-FeOOH-metal interactions in suspended aquatic flocs

The substantial biological nature of floc suggests that floc-associated organic materials (i.e. cells, EPS) are likely important for floc TE geochemistry. For example, bacterial surfaces are amphoteric and can be considered analogous to mineral surfaces in terms of trace element sorption processes e.g.[1, 7, 17]. The reactivity of bacterial cell membranes is due to the wide range of associated functional groups (e.g. carboxyl, phospohryl, amino groups with pKa values within the ranges 4.5 -6, 6.5 -7.8 and 9.9 -10.2, respectively) that can sorb metals with binding affinities and bond strengths that vary amongst elements for the same surface sites [1, 2, 107-109]. Similarly, the substantive EPS fibril network of floc, being very small in diameter (4-20 nm[96, 110]), not only provides a large reactive surface area for direct sorption of metal elements but also a nucleation template for the development and/or entrapment of highly metal-reactive phases (e.g., amorphous Fe (oxy)hydroxide minerals, $Fe^{(III)}OOH_{(s)}$ [5, 6]) which could result in localized floc-mineral precipitates and thus enhanced TE reactivity.

Iron (oxy)hydroxides ($Fe^{(III)}OOH_{(s)}$) likely play a substantial role in influencing floc metal behaviour. The role of $Fe^{(III)}OOH_{(s)}$ as efficient scavengers of TEs has been widely documented (e.g. [2, 98, 111-116]) and they are considered of particular importance for aqueous TE geochemistry due to i) their ubiquitous presence in aquatic systems, ii) the highly reactive nature of their surfaces, and iii) tendency to precipitate as surface coatings on organics and other minerals. Trace metal elements, in turn, can be sequestered by $Fe^{(III)}OOH_{(s)}$ by number of processes including: surface reactions such as ion exchange reactions (non-specific adsorption), specific adsorption (e.g. to surface hydroxyl groups), and co-precipitation [17, 33]. Although both $Fe^{(III)}OOH_{(s)}$ and organics are well-characterized sorbents in aquatic systems[17, 112], organic-Fe associations often results in complex, non-additive metal sorption behavior e.g. [1, 2, 7, 98] that will be especially important within suspended floc. For example, cell-associated Fe-oxyhydroxide coatings may create new reactive surfaces available for metal sequestration leading to enhanced floc TE reactivity. Further, it has been demonstrated that bacterial-associated organic polymers preferentially induce the formation of amorphous Fe

oxyhydroxides (e.g. ferrihydrite), and tend to slow re-crystallization to other forms [5, 76]. Amorphous $Fe^{(III)}_{(s)}$ are characteristically more reactive than their crystalline counterparts (e.g. goethite) due to their poorly ordered crystal structure and thus greater density of exposed reactive surface sites[117]. In contrast, $Fe^{(III)}_{(s)}$ mineral coatings on organics may simultaneously mask underlying reactive surfaces on bacterial cell walls and EPS[1, 7]. While the metal reactivity of isolated bacterial cells and oxyhydroxide mineral surface are well characterized, the combined reactivity of heterogeneous bacterial-oxides is still not fully understood despite the prevalent occurrence of organic-minerals composites in the environment.

1.2.3 Floc hosted microbial $Fe^{(III/II)}$-redox cycling & implications for floc trace metal geochemistry

Results of this doctoral research (*Chapter 3*) identified floc microbial communities and associated natural organic materials (NOM) to facilitate the scavenging of TEs specifically through the collection/nucleation of highly reactive amorphous Fe^{III}-oxyhydroxide minerals ($Fe^{(III)}OOH_{(s)}$), resulting in localized floc-Fe-mineral precipitates and enhanced reactivity. Further, recent investigations have shown environmental aggregate structures to allow environmental microbial communities to effectively de-couple from bulk solution conditions, i.e., provide hospitable microenvironments under bulk conditions thought to be toxic or inhibitory to sustainable substrate supplies [21-23, 84]. Thus environmental aggregates may well be important structures for more wider Fe biogeochemical cycling (i.e. Figure 1.4), outside of classical geochemical niche environments (Figure 1.1), that have yet to be fully appreciated. This leads to a number of novel questions concerning floc-associated microbial Fe dynamics and potential implications for floc metal behaviour.

Particularly relevant for floc TE geochemistry are bacteria that could catalyze $Fe^{(III/II)}$-redox reactions (i.e. IRB, IOB: *section 1.1*) within the floc microhabitat (Figure 1.5). That is, by affecting the cycling of Fe, and associated Fe-minerals, floc bacteria would not only effect the mobility of Fe as well as its local accumulation, but also, in turn, the mobility and concentrations of associated TEs.

For example, the reduced carbon in floc EPS polymers and other floc-associated organics (e.g. detrital matter, humic and fulvic acids) are potential electron donors for floc-microbes; $Fe^{(III)}_{(s)}$ (e.g. ($Fe^{(III)}OOH_{(s)}$) are potential electron acceptors. This iron-reduction reaction in turn may be mediated by heterotrophic dissimilatory $Fe^{(III)}$ reducing bacteria (IRB), coupling floc-organic oxidation to iron reduction (*Eq. 1, section 1.1.1*), or autotrophic sulfur bacteria coupling the oxidation of reduced sulfur species to the reduction of Fe(III) (*Eq.1 , section 1.1.1*). While IRB activity is typically thought restricted to bulk anoxic environments in aquatic systems (e.g. bottom sediments, hypolimnion), potentially low oxygen microenvironments could exist within the matrix of suspended floc aggregates, similar to what has been previously documented in both marine snow aggregates and sessile microbial biofilms (e.g. [84, 86, 87, 118]). Indeed, emerging results from marine snow and "iron snow" aggregates in lakes of acid mine drainage systems indicate that Fe metabolizing bacteria can occur in pelagic systems, typically associated with diverse communities [85, 119]. If, in turn, redox gradients do exist within the floc matrix, coupled redox recycling of Fe could occur, similar to the cooperative redox-cycling strategy identified coupling anaerobic bacterial sulfur (S^0) reduction with autotrophic, oxygen-driven reduced sulfur oxidation in AMD consortial aggregates [21]. That is, the resulting IRB-produced $Fe^{(II)}$ is then available to provide and an electron donor for $Fe^{(II)}$ oxidizing microbes to generate energy, reduced carbon, and re-generate $Fe^{(III)}$ (Figures 1.4, 1.5). IOB activity would also afford a degree of control over localization of $Fe^{(III)}_{(s)}$ precipitation and, in turn, confers several advantages to the resident floc microbial community including prevention of entombment from precipitating $Fe^{(III)}_{(s)}$, and IOB cells may gain an energetic benefit from the localized protons released from mineral formation (*Eq. 2, section 1.1*).

$Fe^{(III)}$-reduction and $Fe^{(II)}$-oxidation activities by resident floc IRB and IOB activity could profoundly affect both floc-metal behaviour as well as surrounding bulk solution geochemistry. Figure 1.5 presents a proposed schematic summarizing the hypothesized potential processes that may occur in floc linking microbial iron metabolism and TE geochemistry. IRB activity could result in a dynamic reductive dissolution of $Fe^{(III)}$ minerals and concomitant co-mobilization of previously bound

trace elements in addition to $Fe^{(II)}$ (e.g. [16, 19, 120]). This is one of the most well documented impacts of dissimilatory ferric iron reduction by environmental bacteria. Increases in aqueous trace metal concentrations as a result of IRB activity occur due both i) decreasing Fe-hydroxide surface area and sorption sites as a result of reductive dissolution of the $Fe^{(III)}_{(s)}$ sorbent phase; and ii) biogenic (i.e. from IRB) $Fe^{(II)}$ competing with trace metals for sorption sites. For example, laboratory batch experiments of microbial reduction of $Ni^{(II)}$and $Co^{(II)}$ substituted goethite showed the release of these metals into aqueous solution [27] and microbial iron reduction activity has also been shown responsible for the mobilization of previously absorbed arsenic in ground water [16, 121, 122]. The production of secondary mineral phases is also a major consequence of IRB and IOB activity, with solid identity determined by numerous interacting factors including: the production rate of $Fe^{(II)}$, concentration and identity of potential electron donors (e.g. H_2, acetate), crystallinity of ferric iron acceptor, occurrence of sorbed species and solution chemistry (e.g. phosphate concentrations) [27, 123, 124]. This has important implications for TE-mobility and TE sorption processes as different secondary Fe minerals have profoundly different sorbent capacities (Table 1.1). For example, Cooper et al. (2006) have reported that not only can IRB activity result in the mobilization of trace metals, but upon re-exposure to microoxic conditions, IRB activity resulted in a selective re-sequestration of a range of previously sorbed metals into a more recalcitrant, acid-insoluble phase (they propose goethite). [27] This decrease in lability was positively correlated to the amount of ferrihydrite available to IRB bacteria and the authors propose that the process was stimulated through sequential steps of microbial iron reduction and subsequent auto-oxidation of sorbed $Fe^{(II)}$ under microaerophilic conditions [27]. Further, microbial reduction experiments with a range of divalent cations (Cd, Co, Ni, Pb, Zn) indicate that all metals showed some degree of re-sequestration, with those cations with the most similar ionic radius to ferrous iron being preferentially incorporated[27].

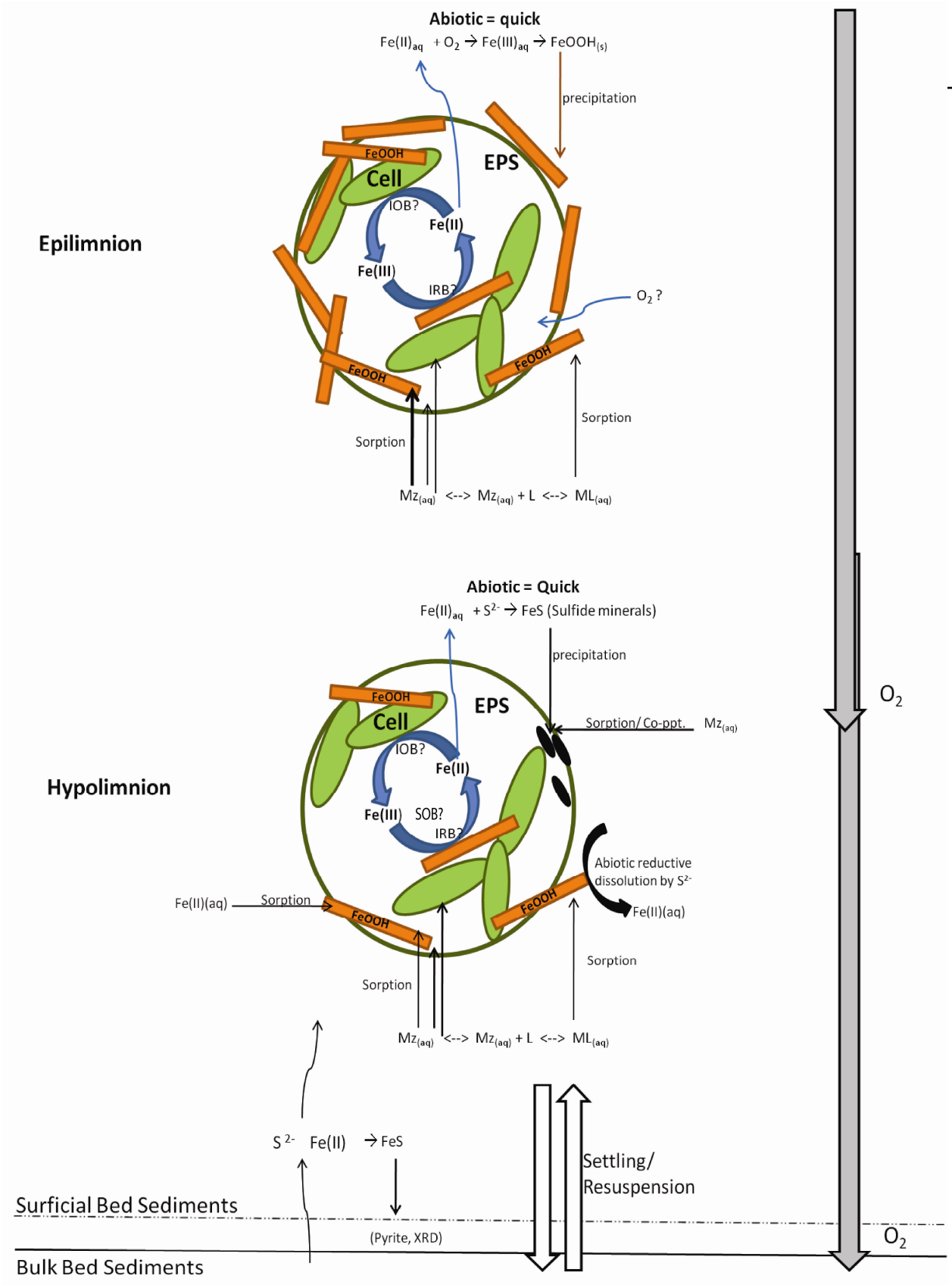

Figure 1.5 Conceptual diagram of hypothesized microbial-Fe-metal dynamics within suspended aquatic flocs. L represents inorganic/organic ligand; ML represents metal-ligand complex in solution. Microbial metabolisms that could be important for floc metal dynamics include dissimilatory iron reducing bacteria, and autotrophic iron oxidizing bacteria. Resident floc Fe-bacteria would affect the local cycling of Fe, thus not only effecting the mobility of Fe as well as its local accumulation, but also, in turn, the mobility and concentrations of associated trace metals.

TABLE 1.1: Different Fe minerals have different capacity for metal uptake from aqueous solution, in part mediated by number of reactive surface sites/group

Mineral	Estimated No. Of reactive surface sites/nm2
Ferrihydrite	15-20
Magnetite	1.7-2.4
Vivianite	1.58
Goethite	5.6-17

Data compiled from (Stumm and Morgan, 1996; Drever, 1997, Langmuir, 1997)

1.3 THESIS OUTLINE

Although widely appreciated, our understanding of the often complex interrelationships between microbial ecology, microbial metabolism and geochemical processes is limited; however, it is increasingly apparent that microbial activity catalyses and influences important geochemical processes in natural aquatic systems. Further, an important principle of geomicrobiology is that bacteria rarely interact with their environment in isolation; rather, they exist as multi-guild cooperatives in consortial aggregates (e.g. [21, 22]) or biofilm communities [23-25]. In this manner, diverse lineages of environmental bacteria intimately co-exist and *collectively* influence biogeochemical cycling. Such impacts on macroscale geochemistry are not well described.

The substantive biological nature of pelagic floc aggregates, as well as bacterial influences on floc architecture and development, provides for a unique and important lense through which to examine how environmental microbial communities and geochemical processes interact. For example, resident floc-microbes may influence floc trace element behaviour in ways not currently captured by geochemical models, i.e., linkages amongst microbial metabolism, geochemical microniche development, and both the type and concentration of constituent reactive sorbent-phases. The overall objective of this doctoral dissertation is thus to comparatively assess the biogeochemical properties of suspended flocs through an integrated field-laboratory approach, providing new insight into the linkages among floc-associated bacteria, floc-reactive solid phases and TE uptake (Figures 1.5, 2.1). To date, characterization of these floc roles has not been reported in the literature.

Chapters 3-5 present the major research findings of this thesis. Chapter 3 presents an assessment of floc trace element (TEs: Cu, Ni, Ag, Co, As) biogeochemistry across six varying aquatic systems in Ontario, Canada. Across all systems investigated, floc associated organic materials (cells, EPS) were found to facilitate the concentration of TEs through the collection/nucleation of highly reactive amorphous Fe^{III}-oxyhydroxide minerals ($Fe^{(III)}OOH$). This Fe-enrichment of floc and of floc bio-mineral constituents lead to a number of novel questions concerning floc-associated microbial Fe dynamics and potential implications for floc

TE geochemistry. Addressing these questions is the focus of Chapters 4-5. Chapter 4 describes the characterization of floc-hosted, $Fe^{(III/II)}$-redox cycling bacterial consortia across diverse oxygenated ($O_2^{\%SAT.}$=1-103%) aquatic systems not predicted to sustain microbial Fe metabolism. This expansion of aero-intolerant Fe-bacteria into the oxygenated pelagic regions of lakes has large implications in current models of modern and ancient Fe biogeochemistry. Furthermore, these results highlight that the implementation of geochemical thermodynamic constraints alone as a guide to investigating and interpreting microbe-geosphere interactions may not accurately capture processes occurring *in situ.* Chapter 5 presents a seasonal investigation of $Fe^{(III/II)}$-redox transformations by floc bacteria collected from a pristine, remote lake within the nature preserve area of Algonquin Park, ON, Canada. Results indicate that cold conditions and a turnover in putative Fe-reducing community membership extinguishes the potential for coupled Fe-redox cycling by wintertime floc bacteria specifically through the removal of neutrophilic IOB metabolic guilds. Further, the seasonal turnover in floc community membership also corresponded with an overall shift from dominant Fe to S redox cycling bacterial communities. This significantly impacted floc TE biogeochemistry, due to associated changes in the nature of floc associated solid Fe-phases and, in turn, resulted in a large decrease of TE (Cd, Pb) uptake by flocs under ice. Chapter 6 summarizes the major findings of Chapters 3-5 and offers suggestions and recommendations for future work.

1.4 REFERENCES

1. Small, T. D., Warren, L. A., Roden, E. E. & Ferris, F. G. Sorption of strontium by bacteria, Fe (III) oxide, and bacteria-Fe (III) oxide composites. *Environ. Sci. Technol.* **33**, 4465-4470 (1999).

2. Small, T. D., Warren, L. A. & Ferris, F. G. Influence of ionic strength on strontium sorption to bacteria, Fe (III) oxide, and composite bacteria-Fe (III) oxide surfaces. *Appl. Geochem.* **16**, 939-946 (2001).

3. Gadd, G. M. Bioremedial potential of microbial mechanisms of metal mobilization and immobilization. *Curr. Opin. Biotechnol.* **11**, 271-279 (2000).

4. Ngwenya, B. T., Sutherland, I. W. & Kennedy, L. Comparison of the acid-base behaviour and metal adsorption characteristics of a gram-negative bacterium with other strains. *Appl. Geochem.* **18**, 527-538 (2003).

5. Chan, C. S., Fakra, S. C., Edwards, D. C., Emerson, D. & Banfield, J. F. Iron oxyhydroxide mineralization on microbial extracellular polysaccharides. *Geochim. Cosmochim. Acta* **73**, 3807-3818 (2009).

6. Chan, C. S. *et al*. Microbial polysaccharides template assembly of nanocrystal fibers. *Science* **303**, 1656-1658 (2004).

7. Warren, L. A. & Ferris, F. G. Continuum between sorption and precipitation of Fe (III) on microbial surfaces. *Environ. Sci. Technol.* **32**, 2331-2337 (1998).

8. Chaudhuri, S. K., Lack, J. G. & Coates, J. D. Biogenic magnetite formation through anaerobic biooxidation of Fe(II). *Applied and Environmental Microbiology* **67**, 2844-2848 (2001).

9. Lovely, D. R., Stolz, J. F., Nord, G. L. & Phillips, E. J. P. Anaerobic production of magnetite by a dissimilatory iron reducing microogranism. *Nature* **330**, 252 (1987).

10. Zhuang, G., Yi, Z., Duce, R. A. & Brown, P. R. Link between iron and sulphur cycles suggested by detection of Fe(n) in remote marine aerosols. *Nature* **355**, 537-539 (1992).

11. Luther, G. W., *et al*. Chemical speciation drives hydrothermal vent ecology. *Nature* **410**, 813-816 (2001).

12. Senn, D. B. & Hemond, H. F. Nitrate Controls on Iron and Arsenic in an Urban Lake. *Science* **296**, 2373-2376 (2002).

13. Shi, D., Xu, Y., Hopkinson, B. M. & Morel, F. M. M. Effect of Ocean Acidification on Iron Availability to Marine Phytoplankton. *Science* **327**, 676-679 (2010).

14. Boyd, P. W. & Ellwood, M. J. The biogeochemical cycle of iron in the ocean. *Nature Geosci* **3**, 675-682 (2010).

15. Li, Y., Yu, S., Strong, J. & Wang, H. Are the biogeochemical cycles of carbon, nitrogen, sulfur, and phosphorus driven by the "FeIII–FeII redox wheel" in dynamic redox environments? *J Soils Sediments* **12**, 683-693 (2012).

16. Islam, F. S. *et al*. Role of metal-reducing bacteria in arsenic release from Bengal delta sediments. *Nature* **430**, 68-71 (2004).

17. Warren, L. A. & Haack, E. A. Biogeochemical controls on metal behaviour in freshwater environments. *Earth-Science Reviews* **54**, 261-320 (2001).

18. Stumm, W. & Sulzberger, B. The cycling of iron in natural environments: considerations based on laboratory studies of heterogeneous redox processes. *Geochimica et Cosmochimica Acta* **56**, 3233-3257 (1992).

19. Borch, T. *et al*. Biogeochemical redox processes and their impact on contaminant dynamics. *Environ. Sci. Technol.* **44**, 15-23 (2009).

20. Feris, K. *et al*. Effect of Ethanol on Microbial Community Structure and Function During Natural Attenuation of Benzene, Toluene, and o-Xylene in a Sulfate-reducing Aquifer. *Environ. Sci. Technol.* **42**, 2289-2294 (2008).

21. Norlund, K. L. I. *et al*. Microbial Architecture of Environmental Sulfur Processes: A Novel Syntrophic Sulfur-Metabolizing Consortia. *Environ. Sci. Technol.* **43**, 8781-8786 (2009).

22. Dekas, A. E., Poretsky, R. S. & Orphan, V. J. Deep-Sea Archaea Fix and Share Nitrogen in Methane-Consuming Microbial Consortia. *Science* **326**, 422-426 (2009).

23. Warren, L. A. & Kauffman, M. E. Microbial Geoengineers. *Science* **299**, 1027-1029 (2003).

24. Konopka, A. Microbial ecology: searching for principles. *Microbe* **1**, 175 (2006).

25. Gault, A. G. *et al*. Seasonal Changes In Mineralogy, Geochemistry and Microbial Community of Bacteriogenic Iron Oxides (BIOS) Deposited in a Circumneutral Wetland. *Geomicrobiol. J.* **29**, 161-172 (2012).

26. Gorra, R. *et al*. Dynamic Microbial Community Associated with Iron-Arsenic Co-Precipitation Products from a Groundwater Storage System in Bangladesh. *Microbial ecology JID - 7500663*

27. Cooper, D. C., Picardal, F. F. & Coby, A. J. Interactions between microbial iron reduction and metal geochemistry: Effect of redox cycling on transition metal speciation in iron bearing sediments. *Environ. Sci. Technol.* **40**, 1884-1891 (2006).

28. Konhauser, K. O. *et al*. Could bacteria have formed the Precambrian banded iron formations? *Geology* **30**, 1079-1082 (2002).

29. Rasmussen, B. & Buick, R. Redox state of the Archean atmosphere: Evidence from detrital heavy minerals in ca. 3250â€“2750 Ma sandstones from the Pilbara Craton, Australia. *Geology* **27**, 115-118 (1999).

30. Walker, J. C. G. Suboxic diagenesis in banded iron formations. *Nature* **309**, 340-342 (1984).

31. Druschel, G. K., Emerson, D., Sutka, R., Suchecki, P. & Luther, G. W.,III. Low-oxygen and chemical kinetic constraints on the geochemical niche of neutrophilic iron(II) oxidizing microorganisms. *Geochim. Cosmochim. Acta* **72**, 3358-3370 (2008).

32. Singer, P. C. & Stumm, W. Acidic mine drainage: the rate-determining step. *Science* **167**, 1121-23 (1970).

33. Langmuir, D. in *Aqueous Environmental Geochemistry* (ed McConnin, R.) (Prentice Hall, Upper Saddle River, New Jersey, 1997).

34. Lovely, D. R. in *Environmental Microbe-Metal Interactions* (ed Lovely, D. R.) 3-30 (ASM Press, Washington, DC, 2000).

35. Baker, B. J. & Banfield, J. F. Microbial communities in acid mine drainage. *FEMS Microbiol. Ecol.* **44**, 139-152 (2003).

36. Emerson, D., Fleming, E. J. & McBeth, J. M. Iron-Oxidizing Bacteria: An Environmental and Genomic Perspective. *Annual Review of Microbiology, Vol 64, 2010* **64**, 561-583 (2010).

37. Weber, K. A., Achenbach, L. A. & Coates, J. D. Microorganisms pumping iron: anaerobic microbial iron oxidation and reduction. *Nature Reviews Microbiology* **4**, 752-764 (2006).

38. A.J.B., Z. & W., S.,. in *Biology of Anaerobic Microorgansisms* (ed A.J.B. Zehnder) 1-38 (John Wiley & Sons, Inc., 1988).

39. Ehrlich, H. L. & Newman, D. K. Geomicrobiology. (2009).

40. Fritzsche, A. *et al*. Fast microbial reduction of ferrihydrite colloids from a soil effluent. *Geochim. Cosmochim. Acta* **77**, 444-456 (2012).

41. Wang, X., Yang, J., Chen, X., Sun, G. & Zhu, Y. Phylogenetic diversity of dissimilatory ferric iron reducers in paddy soil of Hunan, South China. *Journal of Soils and Sediments* **9**, 568-577 (2009).

42. Mark Jensen, M., Thamdrup, B., Rysgaard, S., Holmer, M. & Fossing, H. Rates and regulation of microbial iron reduction in sediments of the Baltic-North Sea transition. *Biogeochemistry* **65**, 295-317 (2003).

43. Lentini, C. J., Wankel, S. D. & Hansel, C. M. Enriched iron(III)-reducing bacterial communities are shaped by carbon substrate and iron oxide mineralogy. *Frontiers in Microbiology* **3** (2012).

44. Langley, S. *et al*. A Comparison of the Rates of Fe(III) Reduction in Synthetic and Bacteriogenic Iron Oxides by Shewanella putrefaciens CN32. *Geomicrobiol. J.* **26**, 57-70 (2009).

45. Kostka, J. E., Dalton, D. D., Skelton, H., Dollhopf, S. & Stucki, J. W. Growth of Iron(III)-Reducing Bacteria on Clay Minerals as the Sole Electron Acceptor and Comparison of Growth Yields on a Variety of Oxidized Iron Forms. *Appl. Environ. Microbiol.* **68**, 6256-6262 (2002).

46. Shelobolina Evgenya, S. *et al*. Isolation of phyllosilicate-iron redox cycling microorganisms from an illite-smectite rich hydromorphic soil. *Frontiers in Microbiology* **3** (2012).

47. Dong, H., Jaisi, D. P., Kim, J. & Zhang, G. Microbe-clay mineral interactions. *Am. Mineral.* **94**, 1505-1519 (2009).

48. Lovley, D. R., Holmes, D. E. & Nevin, K. P. in *Advances in Microbial Physiology* (ed Pool, R. K.) (Academic Press, 2004).

49. Kostka, J. E. & Nealson, K. H. in *Techniques in Microbial Ecolgy* (eds Burlage, R. S., Atlas, R., Stahl, D., Geesey, G. & Sayler, G.) (Oxford University Press, Inc., New York, New York, 1998).

50. Thamdrup, B. in *Advances in Microbial Ecology* (ed Schink, B.) (Kluwer Academic/Plenum Publishers, New York, 2000).

51. Pronk, J. T., de Buyn, J. C., & Kuen, J. G. Anaerobic growth of Thiobacillus ferrixdans. Appleid and Environmental microbiology. *Applied and Environmental Microbiology* **58**, 2227-2230 (1992).

52. Bridge, T. A. M. & D.B., J. Reduction of soluble iron and reduction dissolution of ferric iron containg mineral by moderatly themophilic iron-oxidzing bacteria. *Applied and Environmental Microbiology*, 2181-2186 (1998).

53. Munch, J. C. & Ottow, J. Reductive transformation mechanism of ferric oxides in hydromorphic soils. *Ecological Bulletins*, 383-394 (1983).

54. Lower, B. H. *et al*. Specific bonds between an iron oxide surface and outer membrane cytochromes MtrC and OmcA from Shewanella oneidensis MR-1. *J. Bacteriol.* **189**, 4944-4952 (2007).

55. Reguera, G. *et al*. Extracellular electron transfer via microbial nanowires. *Nature* **435**, 1098-1101 (2005).

56. Schrenk, M. O., Edwards, K. J., Goodman, R. M., Hamers, R. J. & Banfield, J. F. Distribution of Thiobacillus ferrooxidans and Leptospirillum ferrooxidans: implications for generation of acid mine drainage. *Science* **279**, 1519-1522 (1998).

57. Blake, R. & Jonson, D. B. in *Enviromental Microbe-Metal Interactions* (ed Lovely, D. R.) 53-78 (ASM Press, 2000).

58. Konhauser, K. O. in *Introduction to Geomicrobiology* (Blackwell Science Ltd, Cornwall, United Kingdom, 2007).

59. Emerson, D. & Moyer, C. Isolation and characterization of novel iron-oxidizing bacteria that grow at circumneutral pH. *Appl. Environ. Microbiol.* **63**, 4784-4792 (1997).

60. Emerson, D. & Floyd, M. M. Enrichment and isolation of iron-oxidizing bacteria at neutral pH. *Environ. Microbiol.* **397**, 112-123 (2005).

61. Widdel, F. *et al*. Ferrous iron oxidation by anoxygenic phototrophic bacteria. *Nature* **362**, 834-836 (1993).

62. Weber, K. A. *et al*. Anaerobic nitrate-dependent iron(II) bio-oxidation by a novel lithoautotrophic betaproteobacterium, strain 2002. *Appl. Environ. Microbiol.* **72**, 686-694 (2006).

63. Bloethe, M. & Roden, E. E. Composition and Activity of an Autotrophic Fe(II)-Oxidizing, Nitrate-Reducing Enrichment Culture. *Appl. Environ. Microbiol.* **75**, 6937-6940 (2009).

64. Emerson, D. Potential for Iron-reduction and Iron-cycling in Iron Oxyhydroxide-rich Microbial Mats at Loihi Seamount. *Geomicrobiol. J.* **26**, 639-647 (2009).

65. Weiss, J. V. *et al*. Characterization of neutrophilic Fe(II)-oxidizing bacteria isolated from the rhizosphere of wetland plants and description of Ferritrophicum radicicola gen. nov sp nov., and Sideroxydans paludicola sp nov. *Geomicrobiol. J.* **24**, 559-570 (2007).

66. Emerson, D. & Weiss, J. V. Bacterial iron oxidation in circumneutral freshwater habitats: Findings from the field and the laboratory. *Geomicrobiol. J.* **21**, 405-414 (2004).

67. Neubauer, S. C., Emerson, D. & Megonigal, J. P. Life at the Energetic Edge: Kinetics of Circumneutral Iron Oxidation by Lithotrophic Iron-Oxidizing Bacteria Isolated from the Wetland-Plant Rhizosphere. *Appl. Environ. Microbiol.* **68**, 3988-3995 (2002).

68. Emerson, D. & Revsbech, N. P. Investigation of an Iron-Oxidizing Microbial Mat Community Located near Aarhus, Denmark: Field Studies. *Applied and Environmental Microbiology* **60**, 4022-4031 (1994).

69. Ferris, F. G., Hallberg, R. O., Lyven, B. & Pedersen, K. Retention of strontium, cesium, lead and uranium by bacterial iron oxides from a subterranean environment. *Appl. Geochem.* **15**, 1035-1042 (2000).

70. Emerson, D. & Moyer, C. L. Neutrophilic Fe-oxidizing bacteria are abundant at the Loihi Seamount hydrothermal vents and play a major role in Fe oxide deposition. *Appl. Environ. Microbiol.* **68**, 3085-3093 (2002).

71. Roden, E. E., Sobolev, D., Glazer, B. & Luther, G. W. Potential for microscale bacterial Fe redox cycling at the aerobic-anaerobic interface. *Geomicrobiol. J.* **21**, 379-391 (2004).

72. Gault, A. G. *et al*. Microbial and geochemical features suggest iron redox cycling within bacteriogenic iron oxide-rich sediments. *Chem. Geol.* **281**, 41-51 (2011).

73. Fleming, E. J. *et al*. Hidden in plain sight: discovery of sheath-□forming, iron □oxidizing Zetaproteobacteria at Loihi Seamount, Hawaii, USA. *FEMS Microbiol. Ecol.* (2013).

74. Emerson, D. & Revsbech, N. P. Investigation of an iron-oxidizing microbial mat community located near Aarhus, Denmark: laboratory studies. *Appl. Environ. Microbiol.* **60**, 4032-4038 (1994).

75. James, R. E. & Ferris, F. G. Evidence for microbial-mediated iron oxidation at a neutrophilic groundwater spring. *Chem. Geol.* **212**, 301-311 (2004).

76. Chan, C. S., Fakra, S. C., Emerson, D., Fleming, E. J. & Edwards, K. J. Lithotrophic iron-oxidizing bacteria produce organic stalks to control mineral growth: implications for biosignature formation. *The ISME journal* **5**, 717-727 (2010).

77. Singer, E. *et al*. Mariprofundus ferrooxydans PV-1 the first genome of a marine Fe (II) oxidizing Zetaproteobacterium. *PLoS One* **6**, e25386 (2011).

78. Weber, K. A. & Coates, J. D. in *Microbially Mediated Anaerobic Iron(II) Oxidation at Circumneutral pH* (eds Hurst, C. et al.) 1154, 2007).

79. Blothe, M. & Roden, E. E. Microbial iron cycling in two different circumneutral pH iron-rich habitats. *Abstracts of the General Meeting of the American Society for Microbiology* **106**, 385-386 (2006).

80. Eric, R. *et al*. The microbial ferrous wheel in a neutral pH groundwater seep. *Frontiers in Microbiology* **3** (2012).

81. Bruun, A., Finster, K., Gunnlaugsson, H. P., Nornberg, P. & Friedrich, M. W. A Comprehensive Investigation on Iron Cycling in a Freshwater Seep Including Microscopy, Cultivation and Molecular Community Analysis. *Geomicrobiol. J.* 27, 15-34 (2010).

82. Hunter, R. C. & Beveridge, T. J. Application of a pH-Sensitive Fluoroprobe (C-SNARF-4) for pH Microenvironment Analysis in*Pseudomonas aeruginosa* Biofilms. *Applied and Environmental Microbiology* 7, 2501-2510 (2005).

83. Hunter, R. C., Hitchcock, A. P., Dynes, J. J., Obst, M. & Beveridge, T. J. Mapping the Speciation of Iron in Pseudomonas aeruginosa Biofilms Using Scanning Transmission X-ray Microscopy. *Environ. Sci. Technol.* 42, 8766-8772 (2008).

84. Haack, E. A. & Warren, L. A. Biofilm Hydrous Manganese Oxyhydroxides and Metal Dynamics in Acid Rock Drainage. *Environ. Sci. Technol.* 37, 4138-4147 (2003).

85. Balzano, S., Statham, P. J., Pancost, R. D. & Lloyd, J. R. Role of microbial populations in the release of reduced iron to the water column from marine aggregates. *Aquat. Microb. Ecol.* **54**, 291 (2009).

86. Ploug, H., Kuhl, M., Bucholz-Cleven, B. & Jorgensen, B. B. Anoxic aggregtes- an ephemeral phenomenon in the pelagic environment? *Aquatic Microbial Ecology* **13**, 285-294 (1997).

87. Ploug, H., Iversen, M., Koski, M. & Buitenhuis, E. T. Production, oxygen respiration rates, and sinking velocity of copepod fecal pellets: Direct measurements of ballasting by opal and calcite. *Limnol. Oceanogr. 53 (2)*, 469-476 (2008).

88. Ploug, H. *et al*. Carbon, nitrogen and O2 fluxes associated with the cyanobacterium Nodularia spumigena in the Baltic Sea. *The ISME journal* **5**, 1549-1558 (2011).

89. Hohmann, C., Winkler, E., Morin, G. & Kappler, A. Anaerobic Fe(II)-Oxidizing Bacteria Show As Resistance and Immobilize As during Fe(III) Mineral Precipitation. *Environ. Sci. Technol.* **44**, 94-101 (2010).

90. Posth, N. R., Huelin, S., Konhauser, K. O. & Kappler, A. Size, density and composition of cellâ€“mineral aggregates formed during anoxygenic phototrophic Fe(II) oxidation: Impact on modern and ancient environments. *Geochim. Cosmochim. Acta* **74**, 3476-3493 (2010).

91. Fortin, D. & Langley, S. Formation and occurrence of biogenic iron-rich minerals. *Earth-Sci. Rev.* **72**, 1-19 (2005).

92. Douglas, S. & Beveridge, T. J. Mineral formation by bacteria in natural microbial communities. *FEMS Microbiol. Ecol.* **26**, 79-88 (1998).

93. Stecko, J. R. & Bendell-Young, L. Contrasting the geochemistry of suspended particulate matter and deposited sediments within an estuary. *Appl. Geochem.* **15**, 753-775 (2000).

94. Sondi, I., et al. Particulates and the environmental capacity for trace metals: A small river as a model for a land-sea transfer system: the Rasa River estuary. *Sci. Total Environ.* **155**, 173-185 (1994).

95. Santiago, S. *et al*. Nutrient, heavy metal and organic pollutant composition of suspended and bed sediments in the Rhone River. *Aquat. Sci.* **56**, 220-242 (1994).

96. Droppo, I. G. Structural controls on floc strength and transport. *Canadian Journal of Civil Engineering* **31**, 569-578 (2004).

97. Droppo, I. G., Leppard, G. G., Flannigan, D. T. & Liss, S. N. The freshwater floc: a functional relationship of water and organic and inorganic floc constituents affecting suspended sediment properties. *Water Air Soil Pollut.* **99**, 43-54 (1997).

98. Warren, L. A. & Zimmerman, A. P. Suspended particulate oxides and organic matter interactions in trace metal sorption reactions in a small urban river. *Biogeochemistry* **24**, 21-34 (1994).

99. Droppo, I. G. Rethinking what constitutes suspended sediment. *Hydrol. Process.* **15**, 1551-1564 (2001).

100. Liss, S. N., Droppo, I. G., Flannigan, D. T. & Leppard, G. G. Floc architecture in wastewater and natural riverine systems. *Environmental science & technology* **30**, 686 (1996).

101. Costerton, J. W. *et al*. Bacterial biofilms in nature and disease. *Annual Reviews in Microbiology* **41**, 435-464 (1987).

102. Hall-Stoodley, L., Costerton, J. W. & Stoodley, P. Bacterial biofilms: from the natural environment to infectious diseases. *Nature Reviews Microbiology* **2**, 95-108 (2004).

103. Characklis, W. G. & Cooksey, K. E. Biofilms and microbial fouling. *Adv. Appl. Microbiol.* **29**, 93-138 (1983).

104. Bhaskar, P. V. & Bhosle, N. B. Microbial extracellular polymeric substances in marine biogeochemical processes. *Curr. Sci.* **88**, 45-53 (2005).

105. Droppo, I. G. *et al*. Dynamic existence of waterborne pathogens within river sediment compartments. Implications for water quality regulatory affairs. *Environ. Sci. Technol.* **43**, 1737-1743 (2009).

106. Biggs, C. A. & Lant, P. A. Activated sludge flocculation: on-line determination of floc size and the effect of shear. *Water Res.* **34**, 2542-2550 (2000).

107. Reddy, K. J., Soper, B. W., Tang, J. & Bradley, R. L. Phenotypic variation in exopolysaccharide production in the marine, aerobic nitrogen-fixing unicellular cyanobacterium Cyanothece sp. *World Journal of Microbiology and Biotechnology* **12**, 311-318 (1996).

108. Alvarado Quiroz, N.,G., Hung, C. & Santschi, P. H. Binding of thorium (IV) to carboxylate, phosphate and sulfate functional groups from marine exopolymeric substances (EPS). *Mar. Chem.* **100**, 337-353 (2006).

109. Yin, Y., Hu, Y. & Xiong, F. Biosorption properties of Cd (II), Pb (II), and Cu (II) of extracellular polymeric substances (EPS) extracted from Aspergillus fumigatus and determined by polarographic method. *Environ. Monit. Assess.*, 1-6 (2013).

110. National Water, R. I. & Leppard, G. G. in *Evaluation of electron microscope techniques for the description of aquatic colloids* , 1991).

111. Lu, P. *et al*. Lead coprecipitation with iron oxyhydroxide nano-particles. *Geochim. Cosmochim. Acta* **75**, 4547-4561 (2011).

112. Fortin, D., Leppard, G. G. & Tessier, A. Characteristics of lacustrine diagenetic iron oxyhydroxides. *Geochimica et Cosmochimica Acta* **57**, 4391-4404 (1993).

113. Millward, G. E. & Moore, R. M. The adsorption of Cu, Mn and Zn by iron oxyhydroxide in model estuarine solutions. *Water Res.* **16**, 981-985 (1982).

114. Davis, J. A. & Leckie, J. O. Surface ionization and complexation at the oxide/water interface II. Surface properties of amorphous iron oxyhydroxide and adsorption of metal ions. *J. Colloid Interface Sci.* **67**, 90-107 (1978).

115. Langley, S. *et al*. Sorption of Strontium onto Bacteriogenic Iron Oxides. *Environ. Sci. Technol.* **43**, 1008-1014 (2009).

116. KomÃ¡rek, M., VanÄ›k, A. & Ettler, V. Chemical stabilization of metals and arsenic in contaminated soils using oxidesâ€“A review. *Environmental Pollution* **172**, 9-22 (2013).

117. Trivedi, P. & Axe, L. Ni and Zn sorption to amorphous versus crystalline iron oxides: Macroscopic studies. *J. Colloid Interface Sci.* **244**, 221-229 (2001).

118. Li, B. & Bishop, P. L. Micro-profiles of activated sludge floc determined using microelectrodes. *Water research*, 1248-1258 (2004).

119. Lu, S. *et al*. Insights into the structure and metabolic function of microbes that shape pelagic iron-rich aggregates (iron snow). *Appl. Environ. Microbiol.* (2013).

120. Langley, S. *et al*. Strontium desorption from bacteriogenic iron oxides (BIOS) subjected to microbial Fe(III) reduction. *Chem. Geol.* **262**, 217-228 (2009).

121. Nickson, R. *et al*. Arsenic poisoning of Bangladesh groundwater. *Nature* **395**, 338-338 (1998).

122. Oremland, R. S. & Stolz, J. F. Arsenic, microbes and contaminated aquifers. *Trends Microbiol.* **13**, 45-49 (2005).

123. Hansel, C. M. *et al*. Secondary mineralization pathways induced by dissimilatory iron reduction of ferrihydrite under advective flow. *Geochim. Cosmochim. Acta* **67**, 2977-2992 (2003).

124. Borch, T., Masue, Y., Kukkadapu, R. K. & Fendorf, S. Phosphate imposed limitations on biological reduction and alteration of ferrihydrite. *Environ. Sci. Technol.* **41**, 166-172 (2007).

CHAPTER 2: METHODS

2.1 INTRODUCTION

Evaluation and characterization of floc geochemistry and environmental bacterial community dynamics for this doctoral work has required an integrated biogeochemical approach, including field investigation together with standard geochemical and microbiological techniques. This also necessitated the adaptation of molecular and classical microbiological protocols to reflect the realities of environmental microbial community functioning and also to overcome inhibitory affects of complex environmental sample composition on standard molecular procedures. Chapters 3, 4 and 5 contain specific materials and methods sections detailing protocols used to address the objectives outlined in those chapters; some redundancy is therefore unavoidable. The objectives of this chapter are to provide a general overview of the approach utilized to address the outlined objectives of this dissertation (*section 1.3*), as well as to provide greater detail and rationale than exists in subsequent chapters.

2.2 SAMPLING STRATEGY

The overall objective of this doctoral dissertation was to comparatively assess the biogeochemical properties of suspended flocs, providing new insight into the linkages among floc-associated bacteria, floc-reactive solid phases and trace element uptake. For each chapter, field sites and sampling locations were specifically chosen to encompass environmental gradients in either 1) types and levels of contamination, or 2) watercolumn physicochemical conditions (Figure 2.1). This provided for the ability to test specific hypotheses. For example, that floc trace element (TE: Ag, Ni, As, Cu, Co) partitioning and concentrations will differ from bed sedimentary materials, reflecting both type and abundance of solid sorbant phases (*Chapter 3*); or, e.g., that that bulk system [O_2] will not inhibit floc enabled, coupled $Fe^{(III/II)}$-redox cycling by co-occurring floc IRB and IOB (*Chapter 4*).

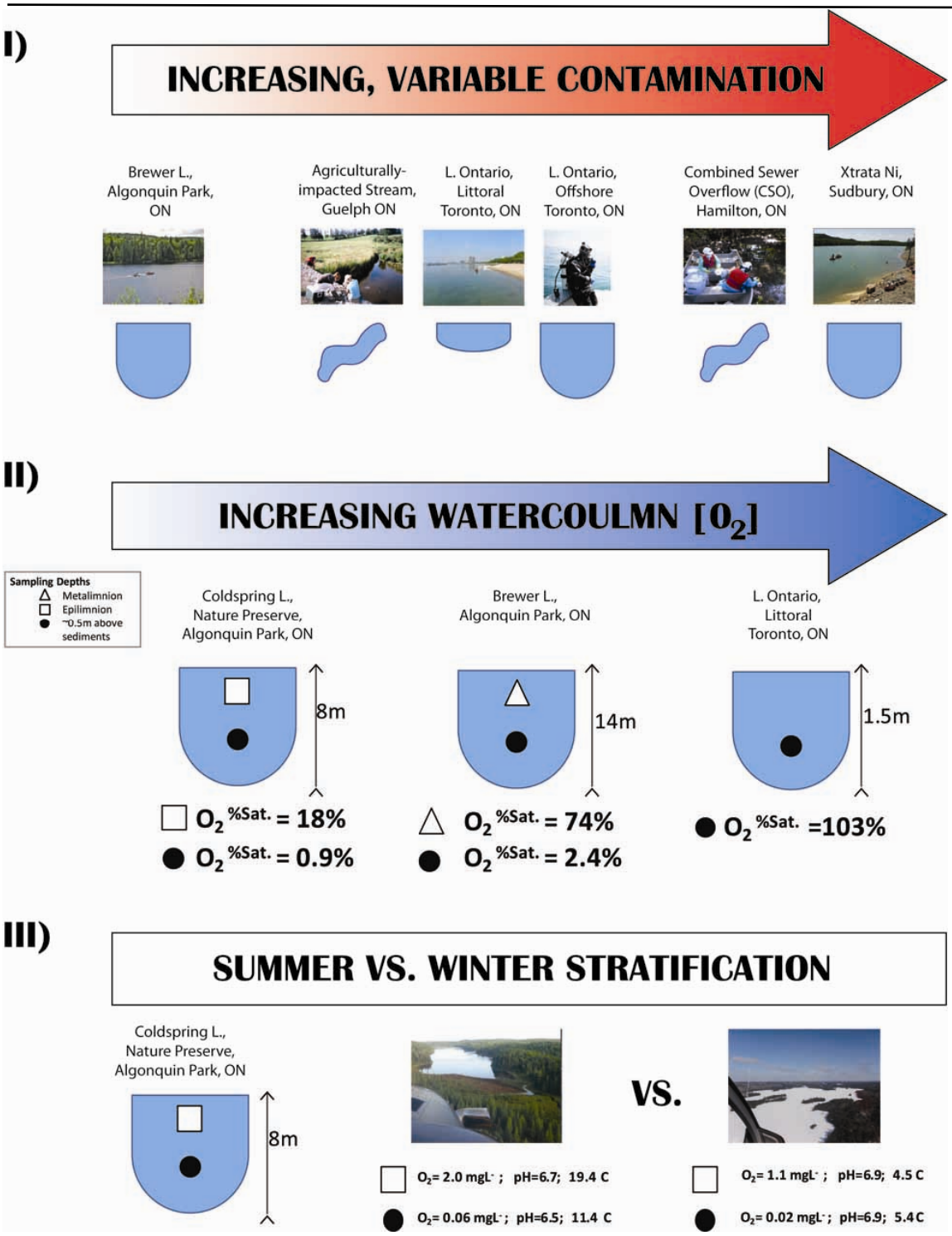

Figure 2.1 For each objective of this doctoral work, field sites and sampling locations were specifically chosen to encompass environmental gradients in either **I)** types and levels of contamination, and distinct aquatic system 'types'; **II)** watercolumn oxygen concentrations; **III)** assessment of seasonal changes in system physicochemical conditions

Sampling campaigns at each site of floc collection provided water column survey information (pH, $[O_2]$, °C, SPC: DataSonde-Surveyor 4A, Hydrolab Corporation, TX) and water, suspended floc and bed sediment samples. Surficial (0-1 cm) bed sediment samples were collected by extruding SCUBA-diver retrieved polycarbonate cores (6 cm diameter, 45 cm length) as to minimize sediment disturbance; cores were extruded immediately after retrieval. Flocs from all sites were collected using continuous flow centrifugation (CFC: Westfalia Model KA 2-06-075) whereby water (>2000L) was pumped ($6Lmin^{-1}$, 9470rpm) into CFC bowls [1-3]. When it was required (*Chapters 4, 5*), flocs were collected simultaneously from discrete, non-mixing strata within the watercolumn by placing CFCs (two) on a barge or on ice cover (Figure 2.2) and using tubing of different lengths to target selected water column depth for floc collection. When possible, flocs were taken at calm and base flow conditions reflecting the majority of the year when flocs are in "equilibrium" with their flow conditions (i.e. carrying capacity of the flow will support a given floc size) and when settling and re-suspension would be minimal.

After collection, flocs and bed sedimentary materials for imaging analyses, targeted metabolic isolation cultures and laboratory co-enrichment experiments were stored at 4°C for a maximum of 12–16h prior to processing in the laboratory. This was to prevent detrimental freeze/thaw effects on floc communities (e.g. cell lysis). Flocs for environmental community identification (16S), bulk organic content (LOI), mineralogical analyses (XRD), and trace element analyses (sequential extractions) were immediately frozen on dry ice and stored at -20ºC or at -80ºC until processing. This was to prevent genomic DNA degradation as well as microbial activity/Redox effects on floc/sediment solid phase constituents.

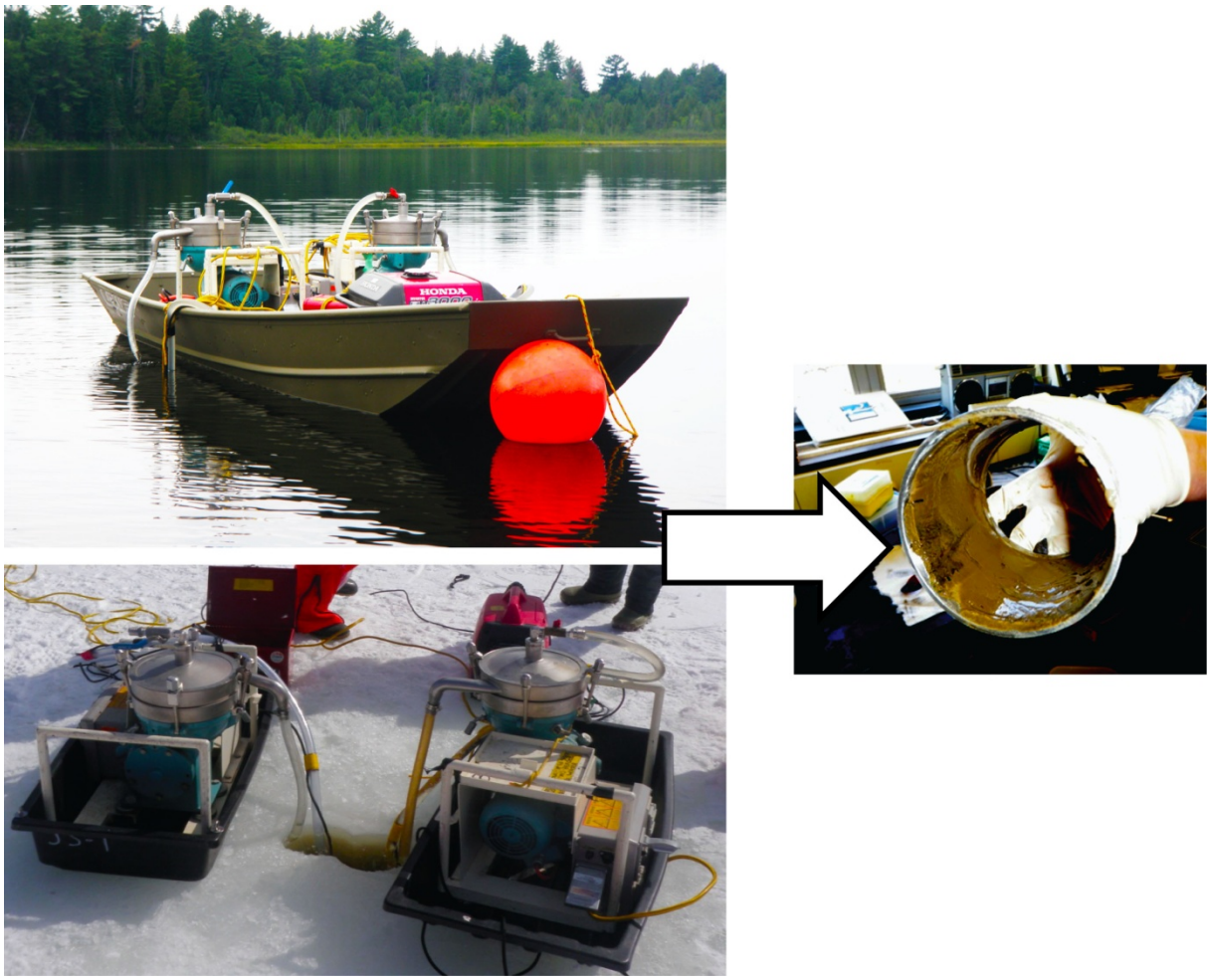

Figure 2.2 In chapters 4 and 5 suspended flocs were collected simultaneously from discrete, non-mixing strata within the watercolumn by placing CFCs (two) on a barge or on ice cover

2.3 CHARACTERIZING FLOC BACTERIAL COMMUNITIES

2.3.1 Targeted metabolic isolations vs. enrichment of consortia

Advances in molecular biology continue to generate powerful tools that can improve our ability to identify environmental bacteria as well as our understanding of the biochemistry, function and expression of microbial metabolism. However, an overemphasis on genetics can largely ignore the microbial ecology of bacterial communities and findings from genomics without ecological and biogeochemical characterization can be difficult to link to processes occurring within natural systems. Experimentation on enrichment cultures and isolation of targeted microbial metabolism are techniques which allow for the identification of particular physiological types within environmental bacterial communities, and also the identification and characterization of microbial interactions in the context of biogeochemical cycles.

A goal of this dissertation was to evaluate whether iron-oxidizing bacteria (IOB) and iron-reducing bacteria (IRB) co-occur within pelagic flocs across a range of oxygenated freshwater. As universal functional genes that would genetically confirm the presence of either $Fe^{(III)}$ respiration or $Fe^{(II)}$ lithoautotrophic metabolic activity are currently lacking, the confirmation of these metabolisms required the use of geochemical, microbiological and molecular biological tools to demonstrate floc associated IRB and IOB occurrence and specifically metabolic activity. A functional biogeochemical approach at addressing these questions was utilized by specifically culturing and characterizing bacterial consortial communities associated with $Fe^{(III)}$-reduction and $Fe^{(II)}$-oxidation activities. The identification and characterization of Fe-bacteria involved (1) the isolation and confirmation of target Fe-metabolism (IRB, IOB) following widely applied targeted isolation approaches as well as (2) laboratory microcosm co-enrichment experiments comparing $Fe^{(III)}$ and $Fe^{(II)}$ evolution as well as mineral formation associated with enriched Fe-redox cycling consortia from environmental floc under increasing oxygen concentrations.

In the geomicrobiological literature, there is ambiguity surrounding the terms 'isolation' versus 'enrichment' cultures. Here, the term 'isolation' specifically refers to the use of classical, well-accepted isolation protocols for Fe-bacterial metabolism:

the opposing gradient tube method (IOB: [4, 5]) and heterotrophic ferric-iron reduction under strictly anoxic conditions (IRB, [6]). Both these metabolic isolation procedures involved restricting available electron donors and acceptors over multiple generations (n>90, over 2 years) to sustain the metabolism of 'isolated' bacteria as well as testing ability to grow on other substrates. Positive results from targeted metabolic isolations relative to abiotic controls unequivocally demonstrate the presence of bacteria capable of completing that respective metabolic reaction. These techniques has been used in a variety of recent and important studies on microbial Fe-metabolism (e.g. [7-10]).

In contrast, 'enrichment' techniques describe the selection of multi-strain consortia or a mixed bacterial culture capable of performing a targeted metabolism/ function (e.g. perchlorate reduction, [11]); it is often the goal of classical microbiology, in turn, to physically reduce the diversity within mixed enrichment cultures so as to specifically assign a single organism to a specific metabolic process [12-14]. However, here, as the hypothesis was that syntrophic partnerships of IRB and IOB are required to enable Fe redox cycling within pelagic flocs, the goal was not to isolate/ reduce enrichments to pure strains but rather to enrich and sustain a mixed community capable of coupling these two aero-intolerant Fe metabolisms under environmentally relevant (i.e. oxygenated) conditions. Indeed the overwhelming failure of traditional isolation culturing for retrieval of representative bacteria from most natural environmental communities[12, 15, 16] underscores the importance of ecological interactions and potential syntrophy in many relevant biogeochemical processes driven by microbial activity. Thus, in this doctoral work, the term 'enrichment' refers to laboratory experimentation on floc consortia (i.e. multiple OTUs of floc-bacteria enriched from their respective parent, whole floc community). The goal of laboratory enrichments was to test whether floc IRB and IOB could be simultaneously *co-enriched* from the same environmental floc samples under increasing oxygen regimes and, in turn, to provide insight into how aero-tolerant IOB and IRB may operate *in situ*. This is distinct from previous investigations in which separately isolated IOB and IRB from different environmental contexts are then experimentally added together to assess coupled microbial Fe redox (e.g. [17, 18])

and also from studies employing *in situ* observations and environmental sequencing of bulk communities to infer coupled IRB and IOB activity (e.g. [19, 20]).

2.3.2. Targeted isolation of floc IOB

Neutrophilic, microaerophilic, $Fe^{(II)}$-oxidizing floc bacteria (IOB) were isolated using a modified gradient tube method[4, 5]. Opposing gradients of oxygen and $Fe^{(II)}$ were created in screw-top borosilicate glass vials (17 x 60mm). An aliquot of floc (~50 µL) was inoculated along a vertical axis without pre-treatment under sterile conditions; this allowed floc IOB to grow at the manufactured anoxic-oxic interface (Figure 2.3). Isolations for each site of sample collection were done in replicates of 4-6. The 'ferrous-Fe plug' was created using 1% (w/v) high melt agarose and equal volumes of MWMM (Table 2.1) and $Fe^{(II)}$ (as $FeCl_2$). The gel-stabilized top layer was created using 0.15% low melt agarose to MWMM along with 1 ul of trace minerals per mL of medium (Table 2.1). The pH of isolation media was adjusted to within the range of 6.1-6.5 by bubbling with sterile CO_2 gas. The top layer was allowed to solidify a minimum of 2 hours, but no longer than 6, prior to inoculation. Solid phase Fe-oxide bands of positive cultures were allowed to develop for ~4 weeks before approximately 10% of the band was extracted and similarly inoculated into a fresh gradient tube [10]. Negative controls were created both by i) inoculation with gamma-sterilized floc samples, and ii) empty (i.e. sample-free) tubes. Floc IOB isolated in this manner were identified by 16S rRNA sequencing and subsequent phylogenetic analysis (*see section 2.5*)

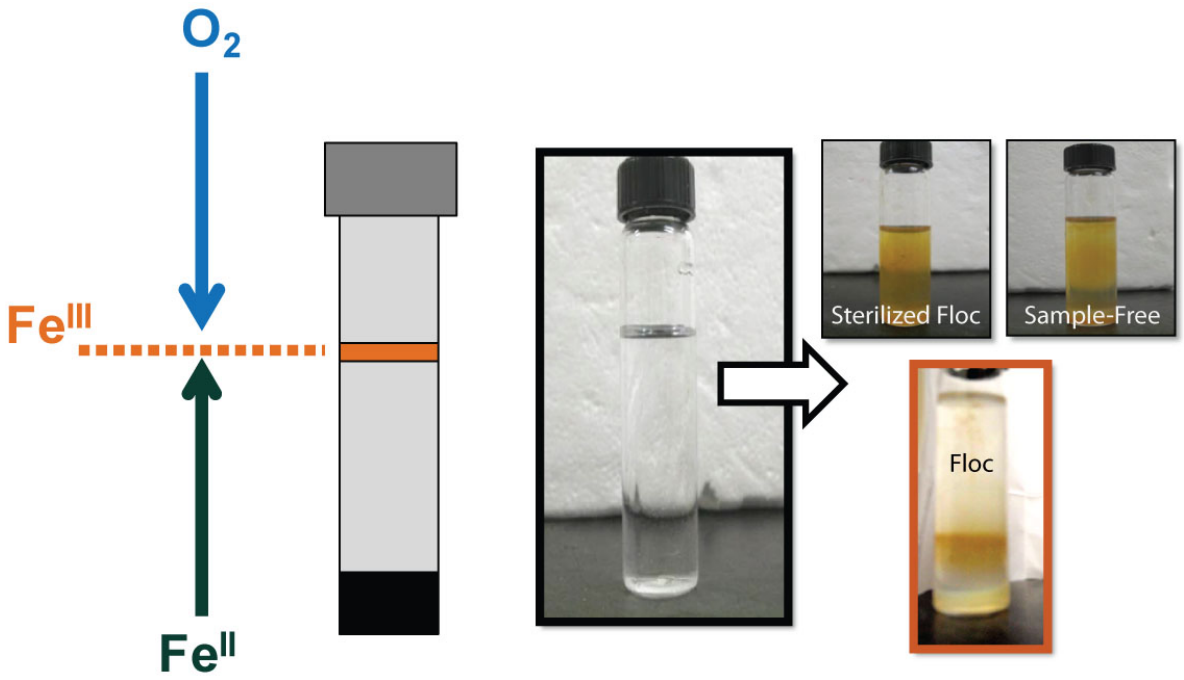

Figure 2.3 Gel stabilized opposing gradient tube method used in this dissertation for the targeted metabolic isolation of putative IOB (modified from Emerson and Moyer, 1997). Opposing gradients of molecular oxygen (oxic head space) and ferrous-Fe (as Fe_2Cl) were created in screw top borosilicate vials. Positive results were scored on the generation and localization of $Fe^{(III)}_{(s)}$ relative to abiotic controls: gamma-sterilized floc samples; empty (i.e. sample-free) tubes.

Table 2.1. Supplements added to IOB isolation media as described in Emerson & Floyd, "Enrichment and Isolation of Iron-Oxidizing Bacteria at Neutral pH" as modifications on Kucera and Wolfe's (1957) process for growing microaerophilic lithotrophs.

Wolfe's Trace Minerals Supplement	MWMM Media (1L)
0.5 EDTA g/L	1 g NH_4Cl
3 g/L $MgSO_4 - 7H_2O$	0.2 g $MgSO_4 - 7H_2O$
0.5 g/L $MnSO_4 - H_2O$	0.1 g $CaCl_2 - 2H_2O$
1 g/L NaCl	0.05 g K_2HPO_4
0.1 g/L $FeSO_4 - 7H_2O$	
0.1 g/L $Co(NO_3)_2 - 6H_2O$	
0.1 g/L $CaCl_2$ (anhydrous)	
0.1 g/L $ZnSO_4 - 7H_2O$	
0.01 g/L $CuSO_4 - 5H_2O$	
0.01 g/L $AlK(SO_4)_2$ (anhydrous)	
0.01 g/L H_3BO_3	
0.01 g/L $Na_2MoO_4 - 2H_2O$	
0.001 g/L Na_2SeO_3 (anhydrous)	
0.01 g/L $Na_2WO_4 - 2H_2O$	
0.02 g/L $NiCl_2 - 6H_2O$	

2.3.3. Targeted isolation of floc IRB

Isolation of anaerobic, dissimilatory $Fe^{(III)}$-reducing floc bacteria (IRB) was accomplished using a modified *Shewanella putrefactions* specific liquid media following the procedures detailed by Kostka & Nealson (1998) under strictly anoxic conditions. An aliquot of floc (~1 mL) was inoculated to ~150mL of M1 basal media (pH=6.5) without pre-treatment under sterile conditions. Isolations for each site of sample collection were done in replicates of 3. M1 media was prepared according to Kostka & Nealson (1998); variable concentration ranges were provided for several of the media components in this protocol, and only these components will be addressed herein. 10mM of sodium acetate was provided as an electron donor; 50mM of $Fe^{(III)}$-citrate was provided as the electron acceptor. These $Fe^{(III)}$ and carbon concentrations were chosen i) to represent the relatively high overall total Fe content of *in situ* parent floc samples (up to 113 mg Fe/g floc, 0.6 mg organic C/ g floc; $Fe_{(aq)}$=0.02-9.72 mg/L. Table S1), and ii) to mimic electron donor and acceptor concentrations utilized in recent and important investigations of microbial Fe-redox transformations (e.g. [21-26]). All isolation cultures were conducted in the dark to prevent photo-reduction of ferric-Fe. Positive growth of isolations were scored on the evolution of $Fe^{(II)}$ (ferrozine assay: [27, 28]) and colour change of the medium that accompanied microbial $Fe^{(III)}$-reduction [6, 29]. Negative controls were created both by i) inoculation with gamma-sterilized floc samples, and ii) empty (i.e. sample-free) media. All cultivated floc-IRB isolates (n>90 generations over two years) garnered in this manner also metabolize synthetic solid-phase $Fe^{(III)}$ as ferrihydrite ($FeOOH^{Amorphous}$). Floc IRB isolated in this manner were identified by 16S rRNA sequencing and subsequent phylogenetic analysis (*see section 2.5*)

2.3.4 Laboratory co-enrichment experiments.

To assess microbial Fe-redox cycling by floc bacterial consortia under the range of oxygenated conditions occurring in selected field sites (Figure 2.1), microcosm co-enrichment experiments were performed on environmental parent floc samples collected from all sites, from all depths of floc collection (*Chapter 4*). A factorial experimental design was implemented to assess oxygen impact on floc Fe-bacteria under oxic ($O_2^{Average}$ = 6.0 mgL^{-}), microoxic ($O_2^{Average}$ = 0.19-0.22 mgL^{-}

^{1}) and anoxic (O_2 = 0 mgL^{-1}) conditions. By exposing each environmental floc sample from the three environmental systems that encompassed 1%-103% O_2 saturation levels to all three experimental O_2 treatment levels, we could then assess bulk oxygen impact on the ability of floc IRB-IOB to survive wide ranging oxygen conditions and whether there were any links between bulk oxygen concentration and floc associated biomineral formation. Experimental microcosms (5 environmental samples X 3 O_2 experimental treatment levels) tracked microbial community dynamics (16S rRNA, described above), consortia morphology (imaging analyses) and Fe geochemistry ($Fe^{(II)}_{aq}$, $Fe^{(III)}_{aq}$, Fe biomineral formation (XRD)). We hypothesized that, as molecular oxygen is required for coupled IOB-IRB metabolism, floc Fe-bacteria isolates (*section 4.2.2.1*) would be co-enriched only within the oxygenated microcosms. Further, ferrous-Fe accumulation, indicative of IRB-activity, would accumulate in all three treatments. However, [$Fe^{(II)}$] across the experimental treatments would vary reflecting differential ongoing $Fe^{(II)}$-oxidation (both biotic and abiotic) under the three different oxygenated conditions. Thus, a negative-IOB control (i.e. IOB removed from enriched communities by incubation in anaerobic chamber, confirmed via 16S sequencing) comparatively assessed Fe-geochemical outcome (i.e. biominerals formed, $Fe^{(II)}$-accumulation) under oxygenated conditions. It was hypothesized that varying experimental O_2 conditions, as well as IOB-removal in "IRB-only" controls, would influence Fe-biominerals formed by the enriched communities; reflecting the active Fe-bacterial metabolisms present as well as the generation of aggregate associated low oxygen/anoxic microenvironments, required to sustain active Fe-metabolism at these experimental oxygenated conditions.

All co-enrichment microcosms were set-up in minimal salts liquid media[6] spiked with acetate (electron donor, 10mM), ferric-$Fe^{(III)}$ (10mM as $Fe^{(III)}$-citrate; i.e. no $Fe^{(II)}$ source provided) and were maintained over multiple successive generations (N>50 over 2 years) in the dark. These $Fe^{(III)}$ and carbon concentrations were chosen i) to represent the relatively high overall total Fe content of *in situ* parent floc samples (up to 113 mg Fe/g floc, 0.6 mg organic C/ g floc; $Fe_{(aq)}$=0.02-9.72 mg/L. Table S1), and ii) to mimic electron donor and acceptor concentrations utilized in

recent and important investigations of microbial Fe-redox transformations (e.g. [21-26]. Further, a soluble Fe source was utilized in order to allow for the tracking of *in situ* bio-mineral formation in the experimental microcosms (i.e. no exogenous Fe-mineral source introduced). Multiple investigations report that different species of IRBs are capable of reducing *both* solid phase and soluble $Fe^{(III)}$; (e.g.[21, 30, 31]) Similarly, all floc consortia enriched in laboratory microcosms here with soluble Fe also metabolize synthetic solid-phase $Fe^{(III)}$ as ferrihydrite ($FeOOH^{Amorphous}$). Further, active reduction of soluble phase $Fe^{(III)}$ under oxygenated conditions results in the re-precipitation of ferric-Fe solids[32]. Thus, in addition to ferrous-Fe accumulation within oxygenated microcosms, the transition in speciation of Fe concentrations from soluble to solid phases can also be used as an indicator of Fe-bacterial activity under oxygenated conditions.

Microoxic treatment conditions ($O_2^{Average}$ = 0.19-0.22 mgL^{-1}) were achieved by setting flasks up at a liquid volume to flask volume ratio of 0.88, covered with a double-layer of aluminum foil to permit gas diffusion and left static, which produced similar microoxic conditions in previous studies [6, 33, 34]. Oxic treatment conditions were achieved by placing flasks at 175 r.p.m. on a Forma Orbital Shaker 420 (Controlled Environment Equipment, Marietta, OH, USA) which increase mixing and aeration of the solutions. Anoxic conditions were achieved by incubation in an anaerobic chamber. In the oxic treatments, oxygen concentrations started at 100% saturation and decreased over the first 12-24 hours before stabilizing at O_2^{Oxic} = 6.0 mgL^{-1}. Oxygenated microcosms do not accumulate $Fe^{(II)}$ the absence of acetate. Preservation of Fe-metabolic function (i.e. IOB and IRB activity) during and post the co-enrichment process was intermediately confirmed by re-growth trials in both i) opposing gradient tubes (IOB); and ii) *Shewanella putrefaciens* specific isolation media (IRB) as described above (*section 2.4.2).* Experimental control 'IRB-only systems' were created by eliminating oxygen-consuming members of the floc-consortia by incubation in an anaerobic chamber and was confirmed by 16S sequencing and visualization (fluorescent imaging, absence of IOB-sheathed morphotype).

2.3.5 DNA Extractions, Sanger 16S sequencing, 454 Pyrosequencing

In this dissertation, sequencing of 16S rRNA genes was used for the identification and characterization of i) whole *in situ* floc ii) IOB and IRB isolates and iii) Fe-bacterial consortial communities co-enriched in laboratory experiments. Total genomic DNA was extracted from i) parent floc samples (whole floc community) ii) targeted Fe-metabolic isolations (IOB, IRB) and iii) laboratory co-enrichment microcosms (enriched Fe-bacteria consortial community) using the PowerSoil DNA Isolation Kit (MO Bio Laboratories, Carlsbad, CA). DNA from floc IOB and IRB isolates and co-enrichment experiments was extracted in duplicate from excised Fe-oxide bands (IOB) or filtered solids (>0.22μm) (IRB, co-enrichments) following the manufacturer supplied protocols. DNA from environmental floc samples was extracted in n=6 from ~0.25g of homogenized floc sediment samples, and later pooled prior to amplification.

Extracted genomic DNA was amplified by polymerase chain reaction (PCR) using universal bacterial primers 27F and 1492R to amplify nearly the complete 16S rRNA gene (*Chapters 4 and 5*). The PCR reaction was carried out in a total of 50 μL, the total formulation/constituents of which varied depending on sample type due to inhibitory affects of environmental sample composition on Taq Polymerase. Optimization of PCR reactions involved diluting the genomic DNA sample to reduce the concentration of inhibiting substances (co-enrichment experiments, 1:10 or 1:100 dilutions), increasing volume of genomic DNA added (environmental samples, if template concentration was suspected to be low), addition of bovine serum albumin (BSA) to remove inhibiting metal ions (high Fe-concentration in both environmental samples and isolation techniques), and increasing the concentration of Mg^{2+} and/or Taq in cases of suspected Taq inhibition. Positive controls of genomic Escherichia coli DNA and negative controls of PCR reagents with no DNA were run simultaneously with environmental samples. The thermocycler program consisted of an initial 3 minute denaturation at 94°C, followed by 30 cycles of 45 second denaturation at 94°C, 30 second annealing at 55.5°C and 45 second elongation at 72°C. A final elongation step was carried out for 10 minutes.

PCR products were never frozen prior to purification/cloning and instead were stored at 4°C until processing (up to a maximum of 48h); this was found to greatly improve cloning efficiency. Amplification products were subsequently purified with the QIA-quick PCR Purification kit (Qiagen) and ligated into the linear Plasmid Vector pCR4 supplied with the TOPO TA kit (Invitrogen). Cloning efficiency was improved by the addition of 3' A-overhangs post-amplification. Final products were transformed into One Shot Chemically Competent *Escherichia coli* (Invitrogen) by heat shock following the manufacturer's protocol. Sequencing was completed with ABI BigDye terminator chemistry, using a 3730 DNA analyzer (Applied Biosystems, Foster City, CA and Institute for Molecular Biology and Biotechnology, McMaster University, ON, Canada).

All subsequent phylogenetic analyses were conducted using MEGA version 5.0 software[35]. Multiple sequence alignments were accomplished using the MUSCLE algorithm, manually edited and regions of ambiguous alignment removed. Operational taxonomical units (OTUs) were binned at 97% similarity. Identified OTUS were subsequently analyzed against the NCBI (US) database using the mega-BLAST algorithm and also assigned to a taxonomical hierarchy proposed in Bergey's Manual of Systematic of Bacteriology, release 6.0., using the RDP classifier tool [36].The Maximum Likelihood (ML) tree-searching method was utilized for phylogenetic tree construction. A phylogenetic tree is a graphical representation of the relationships of different OTUs (16S sequences) to each other and to their ancestral sequences (trees made easy). The ML algorithm constructs a phylogenetic tree by finding the tree which maximizes the probability of observing the data (i.e. 16S sequence alignments) (Mega software). Phylogram topologies were bootstrapped 1,000 times to assess support for nodes and subsequently utilized as input files for UniFrac analyses, *Chapter 5* (*section 2.5.1*).

Additionally, Pyrosequencing (*Chapter 5*) was carried out by Mr. DNA Next Generation Sequencing and Bioinformatics Services (Shallowater, TX, U.S.A) using Roche 454 FLX genome sequencer system and FLX Titanium reagents (Roche Applied Sciences, IN, U.S.A) as described previously[37, 38]. Pyrosequencing technology is a high throughput technique, i.e. a larger number of sequences can be

read in a single run. This, in turn, allows for a very large sampling depth and thus the detection not only of the most dominant microbial community members but also of low-abundance (i.e. 'rare') taxa. The universal Eubacterial primers 27F (5'-AGRGTTTGATCMTGGCTCAG) and 530R (5'-CCGCNGCNGCTGGCAC) were used to amplify approximately 500bp of the variable regions V1 to V3. The Ribosomal Database Project (RDP) Pyrosequencing pipeline was used to process and analyze resultant 16S rRNA sequences derived from 454 sequencing (Michigan State University; http://pyro.cme.msu.edu/index.jsp[39]) including: alignment, clustering, and dereplication. All sequences (both 454 and Sanger 16S) were analyzed against the NCBI (US) database using the mega-BLAST algorithm and also assigned to a taxonomical hierarchy using the RDP classifier tool. Representative sequence identification and classification from all OTUs (binned at 97% similarity) was performed using the Basic Local Alignment Search Tool (BLAST) and RDP classification tool[36]. Further phylogenetic analyses were conducted using MEGA version 5.0 software [35]. Multiple sequence alignments were accomplished using the MUSCLE algorithm, manually edited and regions of ambiguous alignment removed. The Maximum Likelihood (ML) tree-searching method was utilized for phylogenetic tree construction. Phylogram topologies were bootstrapped 1,000 times to assess support for nodes and subsequently utilized as input files for UniFrac analyses (*section 2.5.1*)

2.3.6 Whole Community Clustering and PCA Analyses.

A major goal of both 16S Sanger and 454 Pyrosequencing is to comparatively assess environmental bacterial community structure and composition either between environments (e.g. impacted vs. reference system sites; along a environmental gradient) or over temporal scales temporally within a single site (e.g. seasonal time frames). UniFrac is aka "the unique fraction metric' (http://bmf.colorado.edu/unifrac [40, 41]) is a phylogenetic distance metric and clustering algorithm developed for this purpose, which, in turn, has been applied in a wide variety of medical microbiological and human 'microbiome' (e.g. [42-44]) as well as environmental studies (e.g. [45-47]) (Figure 2.4). Unifract measures the distance (i.e.

difference) between communities based on the lineages they contain (Figure 2.4**).** In this dissertation, UniFrac was used to evaluate changes between i) *in situ* floc and ii) floc Fe-bacterial consortia communities across seasons (summer-winter) and with depth down the watercolumn (metalimnion vs. hypolimnion) (*Chapter 5*). Unifract is distinct from other widely utilized metrics in that it accounts for the different degrees of similarity between 16S rRNA gene sequences and thus garners more information than comparable taxon-based metrics that bin 16S rRNA genes based on 97-99% similarity; thus the impact of utilization of arbitrary OTU thresholds prior to statistical analyses was reduced[41] (Figure 2.4). Further, both qualitative ($UniFrac^{Unweighted}$) and quantitative ($UniFract^{Weighted}$, accounting for relative lineage abundance) metrics were used. This allowed for the delineation of the relative importance of changes in community membership (here defined as the presence/absence of specific bacterial lineages, $UniFrac^{Unweighted}$) versus changes in bacterial lineage abundance (i.e. overall community structure, $UniFract^{Weighted}$) in contributing to variations and clustering patterns observed between floc communities [41, 48]. The Unifract Significance test[41] was used to assess pair-wise differences between each floc community using both weighted ($P^{Weighted}$) and unweighted ($P^{Unweighted}$) UniFrac metrics. Multivariate statistic measures, hierarchal clustering (UPGMA) and Principle Coordinates Analyses (PCA), were utilized compare floc communities simultaneously [40]. The first three principle components of PCA were subsequently regressed with site physicochemical and floc composition data as to identify which variables have the largest impact on floc community membership ($UniFrac^{Unweighted}$) and overall floc community structure ($UniFract^{Weighted}$) [48]. This, in turn, provided insight into the factors that structure both whole floc community Fe-bacterial community diversity.

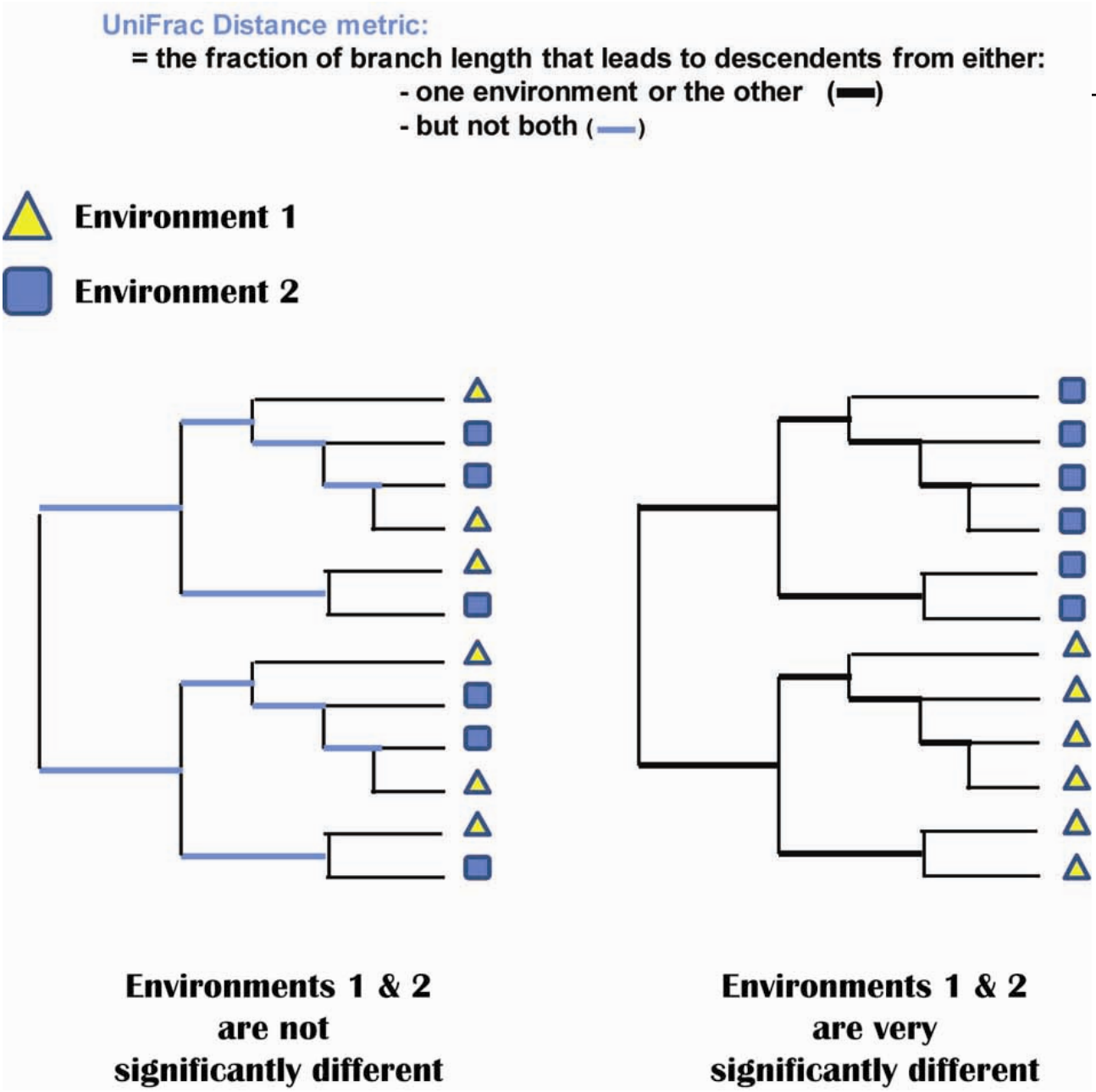

Figure 2.4 Unifract distance metric to compare and cluster whole bacterial communities. (modified from Knight & Lozupone 2005; Lozupone et al. 2007). Unifract measures the distance (i.e. difference) between bacterial communities based on the lineages they contain (i.e. 16S). Here, two distinct bacterial communities are depicted, yellow triangles vs. blue squares. On **the left**, environments 1 and 2 are not significantly different as the majority of the branch length within the phylogenetic tree is shared (i.e. intuitively, if two environments are so similar, few adaptation would be needed to transfer from one community to another: e.g. boreal forest oligotrophic lakes in Ontario vs. Quebec). However, if two communities are very different (**right hand column**) most of the nodes in the phylogenetic tree would have descendants only from one community, and thus most of the branch length in the tree would not be shared (i.e. belonging to one environment or another). Again, intuitively, if two environments are so distinct that an organism adapted to one could not survive in the other (e.g. acid thermal springs vs. marine ice).

2.5 References

1. Rees, T. F., Leenheer, J. A. & Ranville, J. F. Use of a single-bowl continuous-flow centrifuge for dewatering suspended sediments: Effect on sediment physical and chemical characteristics. *Hydrol. Process.* 5, 201-214 (1991).

2. Elliott, A. V. C., Plach, J. M., Droppo, I. G. & Warren, L. A. Comparative Floc-Bed Sediment Trace Element Partitioning Across Variably Contaminated Aquatic Ecosystems. *Environ. Sci. Technol.* 46, 209-216 (2012).

3. Plach, J. M., Elliott, A. V. C., Droppo, I. G. & Warren, L. A. Physical and Ecological Controls on Freshwater Floc Trace Metal Dynamics. *Environ. Sci. Technol.* 45, 2157-2164 (2011).

4. Emerson, D. & Floyd, M. M. Enrichment and isolation of iron-oxidizing bacteria at neutral pH. *Environ. Microbiol.* 397, 112-123 (2005).

5. Emerson, D. & Moyer, C. Isolation and characterization of novel iron-oxidizing bacteria that grow at circumneutral pH. *Appl. Environ. Microbiol.* 63, 4784-4792 (1997).

6. Kostka, J. E. & Nealson, K. H. in *Techniques in Microbial Ecolgy* (eds Burlage, R. S., Atlas, R., Stahl, D., Geesey, G. & Sayler, G.) (Oxford University Press, Inc., New York, New York, 1998).

7. Francis, C. A., Obraztsova, A. Y. & Tebo, B. M. Dissimilatory metal reduction by the facultative anaerobe Pantoea agglomerans SP1. *Appl. Environ. Microbiol.* 66, 543-548 (2000).

8. Lentini, C. J., Wankel, S. D. & Hansel, C. M. Enriched iron(III)-reducing bacterial communities are shaped by carbon substrate and iron oxide mineralogy. *Frontiers in Microbiology* 3 (2012).

9. Roden, E. E. *et al*. Extracellular electron transfer through microbial reduction of solid-phase humic substances. *Nature Geosci* 3, 417-421 (2010).

10. Swanner, E. D., Nell, R. M. & Templeton, A. S. Ralstonia species mediate Fe-oxidation in circumneutral, metal-rich subsurface fluids of Henderson mine, CO. *Chem. Geol.* 284, 339-350 (2011).

11. Attaway, H. & Smith, M. Reduction of perchlorate by an anaerobic enrichment culture. *J. Ind. Microbiol.* 12, 408-412 (1993).

12. Vartoukian, S. R., Palmer, R. M. & Wade, W. G. Strategies for culture of 'unculturable' bacteria. *FEMS Microbiol. Lett.* 309, 1-7 (2010).

13. Gerhardt, P., Murray, R., Wood, W. A. & Krieg, N. R. in *Methods for general and molecular bacteriology* (American Society for Microbiology Washington, DC, 1994).

14. Jokinen, C. C. *et al*. An enhanced technique combining pre-enrichment and passive filtration increases the isolation efficiency of Campylobacter jejuni and Campylobacter coli from water and animal fecal samples. *J. Microbiol. Methods* (2012).

15. Eilers, H., Pernthaler, J., GlÃ¶ckner, F. O. & Amann, R. Culturability and In Situ Abundance of Pelagic Bacteria from the North Sea. *Appl. Environ. Microbiol.* 66, 3044-3051 (2000).

16. Jeanthon, C. *et al*. Diversity of cultivated and metabolically active aerobic anoxygenic phototrophic bacteria along an oligotrophic gradient in the Mediterranean Sea. *Biogeosciences Discussions* 8, 4421 (2011).

17. Roden, E. E., Sobolev, D., Glazer, B. & Luther, G. W. Potential for microscale bacterial Fe redox cycling at the aerobic-anaerobic interface. *Geomicrobiol. J.* 21, 379-391 (2004).

18. Bloethe, M. & Roden, E. E. Microbial Iron Redox Cycling in a Circumneutral-pH Groundwater Seep. *Appl. Environ. Microbiol.* 75, 468-473 (2009).

19. Lu, S. *et al*. Insights into the structure and metabolic function of microbes that shape pelagic iron-rich aggregates (iron snow). *Appl. Environ. Microbiol.* (2013).

20. Gault, A. G. *et al*. Microbial and geochemical features suggest iron redox cycling within bacteriogenic iron oxide-rich sediments. *Chem. Geol.* 281, 41-51 (2011).

21. Shelobolina Evgenya, S. *et al*. Isolation of phyllosilicate-iron redox cycling microorganisms from an illite-smectite rich hydromorphic soil. *Frontiers in Microbiology* 3 (2012).

22. Coby, A. J., Picardal, F., Shelobolina, E., Xu, H. & Roden, E. E. Repeated Anaerobic Microbial Redox Cycling of Iron. *Appl. Environ. Microbiol.* 77, 6036-6042 (2011).

23. Fritzsche, A. *et al*. Fast microbial reduction of ferrihydrite colloids from a soil effluent. *Geochim. Cosmochim. Acta* 77, 444-456 (2012).

24. Miot, J. *et al*. Iron biomineralization by anaerobic neutrophilic iron-oxidizing bacteria. *Geochim. Cosmochim. Acta* 73, 696-711 (2009).

25. Kappler, A., Johnson, C. M., Crosby, H. A., Beard, B. L. & Newman, D. K. Evidence for equilibrium iron isotope fractionation by nitrate-reducing iron(II)-oxidizing bacteria. *Geochim. Cosmochim. Acta* 74, 2826-2842 (2010).

26. Lovely, D. R., Stolz, J. F., Nord, G. L. & Phillips, E. J. P. Anaerobic production of magnetite by a dissimilatory iron reducing microogranism. *Nature* 330, 252 (1987).

27. Stookey, L. L. Ferrozine---a new spectrophotometric reagent for iron. *Anal. Chem.* 42, 779-781 (1970).

28. Viollier, E., Inglett, P. W., Hunter, K., Roychoudhury, A. N. & Van Cappellen, P. The ferrozine method revisited: Fe(II)/Fe(III) determination in natural waters. *Appl. Geochem.* 15, 785-790 (2000).

29. Lin, B. *et al*. Phylogenetic and physiological diversity of dissimilatory ferric iron reducers in sediments of the polluted Scheldt estuary, Northwest Europe. *Environ. Microbiol.* 9, 1956-1968 (2007).

30. Reguera, G. *et al*. Extracellular electron transfer via microbial nanowires. *Nature* 435, 1098-1101 (2005).

31. Roden, E. E. Geochemical and microbiological controls on dissimilatory iron reduction. *Comptes Rendus Geoscience* 338, 456-467 (2006).

32. Langmuir, D. in *Aqueous Environmental Geochemistry* (ed McConnin, R.) (Prentice Hall, Upper Saddle River, New Jersey, 1997).

33. Norlund, K. L. I. *et al*. Microbial Architecture of Environmental Sulfur Processes: A Novel Syntrophic Sulfur-Metabolizing Consortia. *Environ. Sci. Technol.* 43, 8781-8786 (2009).

34. Warren, L. A., Norlund, K. L. I. & Bernier, L. Microbial thiosulphate reaction arrays: the interactive roles of Fe(III), O2 and microbial strain on disproportionation and oxidation pathways. *Geobiology* 6, 461-470 (2008).

35. Tamura, K. *et al*. MEGA5: Molecular Evolutionary Genetics Analysis Using Maximum Likelihood, Evolutionary Distance, and Maximum Parsimony Methods. *Molecular Biology and Evolution* 28, 2731-2739 (2011).

36. Wang, Q., Garrity, G. M., Teiedje, J. M. & Cole, J. R. Naive Bayesian classifier for rapid assignmnet of rRNA aequences into the new bacterial taxonomy. *Appl. Environ. Microbiol.* 73, 5261 (2007).

37. Dowd, S. E. *et al*. Evaluation of the bacterial diversity in the feces of cattle using 16S rDNA bacterial tag-encoded FLX amplicon pyrosequencing (bTEFAP). *BMC Microbiology* 8, 125 (2008).

38. Wolcott, R. D., Gontcharova, V., Sun, Y. & Dowd, S. E. Evaluation of the bacterial diversity among and within individual venous leg ulcers using bacterial tag-encoded FLX and titanium amplicon pyrosequencing and metagenomic approaches. *BMC Microbiology* 9, 226-237 (2009).

39. Cole, J. R. *et al*. The Ribosomal Database Project: improved alignments and new tools for rRNA analysis. *Nucleic Acids Research* 37, D145 (2009).

40. Lozupone, C. A., Hamady, M. & Knight, R. UniFrac – An online tool for comparing microbial community diversity in a phylogenetic context. *BMC Bioinformatics* 7, 371 (2006).

41. Lozupone, C. & Knight, R. UniFrac: a New Phylogenetic Method for Comparing Microbial Communities. *Appl. Environ. Microbiol.* 71, 8228-8235 (2005).

42. Turnbaugh, P. J. *et al*. A core gut microbiome in obese and lean twins. *Nature* 457, 480-484 (2008).

43. Cui, Z. *et al*. Complex sputum microbial composition in patients with pulmonary tuberculosis. *BMC microbiology* 12, 276 (2012).

44. Koenig, J. E. *et al*. Succession of microbial consortia in the developing infant gut microbiome. *Proceedings of the National Academy of Sciences* 108, 4578-4585 (2011).

45. Werner, J. J. *et al*. Bacterial community structures are unique and resilient in full-scale bioenergy systems. *Proceedings of the National Academy of Sciences* 108, 4158-4163 (2011).

46. Evans, S. E. & Wallenstein, M. D. Soil microbial community response to drying and rewetting stress: does historical precipitation regime matter? *Biogeochemistry* 109, 101-116 (2012).

47. Yavitt, J. B., Yashiro, E., Cadillo-Quiroz, H. & Zinder, S. H. Methanogen diversity and community composition in peatlands of the central to northern Appalachian Mountain region, North America. *Biogeochemistry* 109, 117-131 (2012).

48. Lozupone, C. A., Hamady, M., Kelley, S. T. & Knight, R. Quantitative and Qualitative Î² Diversity Measures Lead to Different Insights into Factors That Structure Microbial Communities. *Appl. Environ. Microbiol.* 73, 1576-1585 (2007).

CHAPTER 3: COMPARATIVE FLOC-BED SEDIMENT TRACE ELEMENT PARTITIONING ACROSS VARIABLY CONTAMINATED AQUATIC ECOSYSTEMS

Reproduced with permission from: Elliott, A.V.C., Plach, J.M., Droppo, I.G., and Warren, L.A. *Environmental Science & Technology.,* **2012,** *46* (1), pp. 209-231 DOI: 10.1021/es202221u

ABSTRACT

Significantly higher concentrations of Ag, As, Cu, Ni and Co are found in floc compared to bed sediments across six variably impacted aquatic ecosystems. In contrast to the observed element and site-specific bed sediment trace element (TE) partitioning patterns, floc TE sequestration is consistently dominated by amorphous oxyhydroxides (FeOOH), which account for 30–79% of floc total TE concentrations, irrespective of system physico-chemistry or elements involved. FeOOH consistently occur in significantly higher concentrations in floc than within bed sediments. Further, comparative concentration factors indicate significantly higher TE reactivity of floc-FeOOH relative to sediment-FeOOH in all systems investigated, indicating that both the greater abundance and higher reactivity of floc-FeOOH contribute to enhanced floc TE uptake. Results indicate that floc-organics (live cells and exopolymeric substances, EPS) directly predict floc-FeOOH concentrations, suggesting an organic structural role in the collection/templating of FeOOH. This, in turn, facilitates the sequestration of TEs associated with floc-FeOOH formation, imparting the conserved FeOOH "signature" on floc TE geochemistry across sites. Results demonstrate that the organic rich nature of floc exerts an important control over TE geochemistry in aquatic environments, ultimately creating a distinct solid with differing controls over TE behavior than bed sediments in close proximity (<0.5 m).

3.1 Introduction

Flocculated suspended particulate matter (SPM) is increasingly recognized as an important constituent for the transport of cohesive sediments and associated contaminants in aquatic environments.[1] Flocs (conglomerates of multiple inorganic and organic particles) within the water-column may be derived from overland wash-off of soil aggregates, re-suspended bottom sediments and/or formed directly in suspension via a complex flocculation process.[1] Regardless of their origin, flocs within the water column are in a continual state of flux due to changing hydraulic, biological, and chemical factors.[1,2] It has been demonstrated, however, that the stabilization and continued development of flocs in aquatic environments is largely controlled by the activity of floc-colonizing microorganisms and their associated exopolymeric substances (EPS), produced as a means of attachment, protection from predation, and nutrient assimilation.[1,3,4] Flocs engender different hydrodynamic and reactive properties compared to their constituent particles due to modified effective grain size, shape, porosity, density, and composition that will have important implications for the fate and behavior of associated trace element (TE) contaminants.[1,2,5,6] As both SPM and floc are used in the literature, here we specifically define floc as follows: complex matrix of fine-grained inorganic particles (e.g. clays, silts, oxyhydroxides and carbonate minerals) within a network of active microbial communities and organics derived from microbial metabolism (e.g. EPS, humic and fulvic acids).[1,4,6] Floc can comprise the majority of the SPM pool, particularly under lower energy regimes, e.g. the sediment-water interface or pelagic regions of lacustrine systems, where flocs can stabilize and develop.[1,6] The architecture and composition of floc, its suspension within the water column and its high surface area to volume ratio collectively suggest that floc TE concentrations are likely higher than those of bed sediments. Further, the substantive EPS fibril network of floc, being very small in diameter (4-20 nm[7,8]), not only provides a large reactive surface area for sorption of TEs but also an important nucleation template for the development and/or entrapment of TE-reactive minerals (e.g., Fe oxyhydroxides, FeOOH[9]) resulting in localized floc-mineral precipitates and thus enhanced TE reactivity. The microbial nature and diffusive microenvironment of

floc[3] may also facilitate the development of internal redox gradients within the floc-microenvironment, enabling the microbial-catalysis of redox sensitive mineral precipitation-dissolution reactions (e.g., Fe/Mn (hydro)oxides[10]). This would profoundly affect floc TE behavior, resulting in both the sequestration of TEs associated with Fe/Mn oxide formation, as well as TE release associated with the reductive dissolution of these sorbant phases. Although Fe/Mn oxyhydroxides and organics are well-characterized sorbents in aquatic systems[11], organic-Fe associations can result in complex, non-additive TE sorption behavior[12] that will be especially important within suspended floc. These characteristics, the substantive biological components of floc and the underlying microbial nature of floc formation, suggest floc TE partitioning will also differ from bed sediments, reflecting both type and concentration of solid sorbant phases.

To date a number of studies have demonstrated floc to be a significant TE sorbant (e.g., ref 13). However, very few studies have specifically assessed suspended floc TE partitioning patterns or constituent phases responsible for TE scavenging[6,14-16] and none to date have compared floc TE concentrations and partitioning patterns across a suite of variably impacted natural aquatic systems. As with all natural samples, where heterogeneous multi-component solids are the norm, quantification of whole floc TE concentrations is not sufficient to predict TE behavior and fate.[17] The goal of this work was to address these gaps in understanding through specific inclusion of floc in assessment of freshwater TE behavior. Thus the objectives of this field investigation were to quantitatively characterize: 1. floc, aqueous and bed sediment trace element (Ag, Ni, As, Cu, Co) concentrations; 2. key floc sorbent solid phases; and 3. controls on floc trace element sequestration processes both within and across a suite of six variably impacted freshwater environments.

3.2 Materials & methods

3.2.1 Site Description. Six aquatic ecosystems located in Ontario, Canada, that varied in physico-chemistry, exposure to contaminants and types of contamination were selected for comparison (see Table S1, Supporting Information, for detailed

information on sites): i) Ni mine tailings impoundment, Sudbury; ii/iii) Lake Ontario, Toronto; nearshore and offshore sites; iv) a combined sewer outfall (CSO), Hamilton; v) an agriculturally-impacted stream, Guelph; and vi) Brewer Lake, Algonquin Park. Sampling campaigns at each site provided water column survey information (pH, [O_2], °C, SPC: DataSonde-Surveyor 4A, Hydrolab Corporation, TX) and water, suspended floc and bed sediment samples over the summer of 2008 (14-May through 2-September) (Table S1).

3.2.2 Sampling Protocol. Both water column and suspended floc samples were collected <0.5 m above the sediment-water interface. Floc at this proximity to the sediment-water interface were chosen for analysis as they will constitute the "building blocks" of bed sediments upon settling and exist within the same bulk physico-chemical zone as surficial bed sediments, enabling comparison. At all sites floc was collected under calm and base flow conditions, the dominant flow regime conditions for most of the year, when flocs are in equilibrium with their flow conditions (i.e., the carrying capacity of the flow will support a given floc size) and thus when settling and re-suspension are minimal. All sampling equipment and containers for trace element (TE) analysis were prepared by soaking in 10% (v/v) HCl (Sigma-Aldrich) for >24h followed by five rinses with ultra pure water (UPW:18.2 Ωmcm^{-1}, Milli-Q, Millipore). Water samples for TE analysis were collected using Van dorn sampler, passed serially through syringe filters (Acrodisc 0.45 μm, 0.2 μm), and acidified to 2% v/v with trace metal grade HNO3 (OPTIMA HNO3, Seastar Chemicals Inc. Pa.). Water samples were also collected for dissolved inorganic and organic carbon (DIC/ DOC) analysis.[18] Procedural blanks were collected by flushing UPW though an acid-clean Van dorn as well as syringe filters. Suspended floc samples were collected using continuous flow centrifugation (CFC: Westfalia Model KA 2-06-075) whereby water (>2000 L) was pumped (6 L min^{-1}) into CFC bowls with a rotational speed of 9470 rpm. Percent recovery of floc at each field site was >90% (assessed by weight comparison of CFC inflow and outflow filtered water samples on glass-fiber Whatman filters following the standard method 2540D 19). Surficial (0-1 cm) bed sediment samples were collected by

extruding SCUBA-diver retrieved polycarbonate cores (6 cm diameter, 45 cm length) immediately after retrieval. All sediment samples were frozen on dry ice in the field and stored at -20°C until analysis. Floc for imaging analyses were collected from diver-retrieved plankton chambers.

3.2.3 Trace Element Analyses. Aqueous trace element ($[TE]_D$:dissolved, <0.2 μm) and solid-phase (surficial bed sediments, suspended floc) TE concentrations were quantified in triplicate by inductively coupled plasma mass spectrometry (ICP-MS: As, Co, Cu, Ag, Mn, and Ni: Perkin Elmer SCIEX ELAN 6100, Woodbridge, ON, Canada). Solid-phase TE analysis followed a sequential extraction technique involving microwave digestion[20] which partitions sediment associated TEs into six operationally defined reactive solid matrix fractions: 1. exchangeable (loosely bound, labile sediment TEs); 2. carbonates and/or acid soluble sulfides; 3. amorphous Fe/Mn oxyhydroxides; 4. crystalline Fe/Mn oxides; 5. oxidizable organics and/or sulfides; 6. TEs held within residual mineral lattices. Total floc and sediment TE concentrations ($[TE]^{Total}$: $\mu molg^{-1}$) were determined by summing the individual concentrations in each of the six operationally defined fractions. Analytical procedural controls were included in each digestion assay and ICP-MS run for the detection of reagent and procedural associated contamination; matrix effects associated with ICP-MS were corrected using matrix-matched standard curves. Blank analysis indicated negligible contamination for all elements analyzed. Analytical accuracy was assessed by the co-extraction of certified reference materials (Buffalo River 8047, Bovine Liver 1577b: NIST Standard Reference Materials). The sum of the extracted concentrations of the reference material was within the certified range for all TEs analyzed. Complete sample digestion for the most contaminated (Ni mine tailings, Sudbury) and most remote (Brewer lake, Algonquin Park) sites did not exceed a 10% difference in comparison to totals obtained from the summation of the operationally defined fractions (Table S3).

3.2.4 Sediment Composition. Floc and bed sediment dry weights were determined by heating of triplicate samples at 80 °C over 24h to a constant weight. Bulk organic

and carbonate content were estimated by loss on ignition at 550 °C for 2 h (g organic C/g sediment) followed by 950 °C for 1 h (g carbonate mineral/g sediment). Concentrations of amorphous and crystalline Fe oxyhydroxides within the floc/sediments were estimated assuming (i) that the concentration of Fe measured in associated extraction steps estimates solid Fe oxyhydroxides or Fe oxide concentrations (Colorimetric analysis, Ultraspec 3000, UV/visible spectrophotometer, Pharmacia Biotech, Cambridge, U.K.),[6,14,20] and (ii) ferrihydrite (molar mass: 168.70; density = 3.8 g cm^3) and goethite (molar mass: 88.85; density = 4.3 g cm^3) are representative of amorphous and crystalline mineralogy respectively.[23] X-ray diffractometry (XRD) was used to determine bulk mineralogical composition of floc and bed sediments (Siemens D5005 X-ray diffractometer). Bulk XRD analysis identified the main crystalline components of both floc and bed sediments to be similar within each site (Table S2).

3.2.5 Imaging. Environmental scanning electron microscopy (ESEM; ESEM system 2020, Version 3.53, FEI company) of floc allowed for the enhanced observation of specific components, including cells and EPS material. Transmission electron microscopy (TEM) followed a 4-fold multistep technique to enhanced visualization of floc ultrastructure.[3] Ultrathin sections were imaged in transmission mode at an accelerated voltage of 80 kV using a JEOL 1200 Ex II TEMSCAN scanning transmission electron microscope. Viability of floc microbial communities was assessed using epifluorescence microscopy and the LIVE/ DEAD BacLight nucleic acid staining technique. Samples (~10 mg) were suspended in 1 mL 0.085% NaCl solution; 0.5 μL of LIVE/DEAD BacLight staining solution was added to the mixture, incubated for 15 minutes in the dark and spotted on gelatin-coated slides [0.25% gelatin and 0.01% $KCr(SO_4)^2$]. Slides were viewed using Leica LEITZ DMRX epifluorescence microscope equipped with an HBO 100-W mercury arc lamp [Leica Microsystems (Canada), Richmond Hill, ON] equipped with 525/50, 645/75 nm barriers and 470/40, 560/40 nm excitation filters.

3.2.6 Statistical Analysis. Analyses were conducted using SPSS version 16.0 (SPSS Inc., Chicago, Illinois, U.S.A). Multiple linear regression (MLR) was performed on un-transformed data to identify key influencing variables for trends in $[TE]_D$, bed sediment $[TE]^{Total}$, floc $[TE]^{Total}$, and individual sediment/floc reactive fractions. The relevant variable identified by the MLR to explain the most variance was subsequently used in linear regression analysis with the dependent variable of interest. T-tests were to test for significant differences of mean $[TE]^{Total}$ (floc vs. sediment) and constituent phase concentrations (floc vs sediment, within elements, sites). Unless otherwise indicated, for
all statistical analyses sample size was n = 6, and the significance level applied was $\alpha = 0.05$.

3.3 Results & Discussion

3.3.1 Floc versus Bed Sediment TE Sequestration. Floc was an important TE-sink, significantly concentrating TEs (Cu, Ni, As, Co, Ag) 1.5-55x above that of surficial bed sediments across five of the six aquatic environments (Figure 3.1, Table S3). Exceptions to this trend were observed in the mine tailings impoundment lake where floc total TE concentrations ($[TE]^{total}$: $\mu molg^{-1}$) were either not significantly different ($[Ag]^{Total}$, $[Cu]^{Total}$) or significantly lower ($[As]^{Total}$, $[Co]^{Total}$, $[Ni]^{Total}$) than surficial "'sediment" concentrations (n.b. "sediment" in the mine impoundment is predominantly waste rock and tailings slurry discharge rather than classical sediments observed in less anthropogenically altered systems) as well as in the CSO, a <1 m deep drainage ditch receiving combined sewer overflow, where no significant difference was observed between floc versus sediment $[Co]^{Total}$ and $[Ag]^{Total}$. At all sites, Cu and Ni exhibited the strongest affinity for floc and always occurred in the highest concentrations, respectively ($[Cu]^{Total}$: 69.0 $\mu molg^{-1}$-0.43 $\mu molg^{-1}$; $[Ni]^{Total}$: 15.8 $\mu molg^{-1}$-0.36 $\mu molg^{-1}$; Figure 3.1,Table S3).

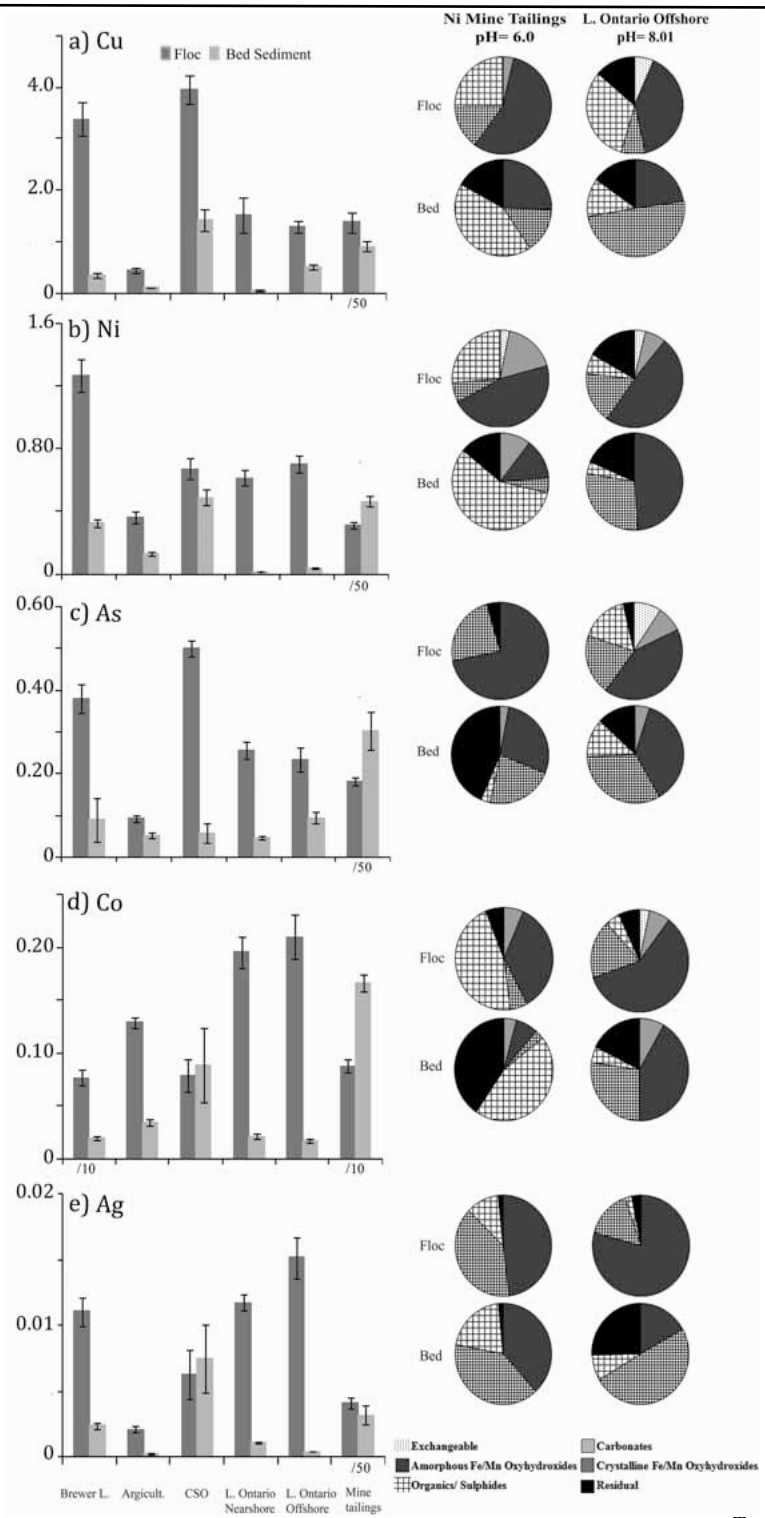

Figure 3.1. Floc and surficial (0-1 cm) bed sediment total TE concentrations ($[TE]^{Total}$: $\mu molg^{-1}$), as determined by the sum of sequential extraction steps across six aquatic ecosystems: a) copper, b) nickel, c) arsenic, d) cobalt, and e) silver. Mean (standard ± error values) are shown (n = 6). Sites marked with (/50, /10) had both floc and sediment concentrations divided by corresponding number before plotting for clarity. Representative relative percent partitioning (%) results from sequential extractions are shown in the right-hand-side of each panel for each corresponding element (a-e) for both the lowest pH site (mine tailings impoundment, pH = 6.0) and the highest pH environment (Lake Ontario, Offshore, pH = 8.01). For plotting clarity, only those fractions representing more than 3% of $[TE]^{Total}$ have been shown. For complete TE partitioning results see Table S3**.**

Floc $[TE]^{Total}$ was not predicted (MLR) by either aqueous TE concentrations ($[TE]_D$; <0.2 μm) or physico-chemistry (pH, °C, O_2, SPC) despite wide ranges in these parameters across sites (Tables S1, S5). This result suggests that floc-specific characteristics (i.e., structure, composition, and/or abundance of reactive sorbent phases), rather than system geochemical parameters known to be important to sorption processes[11] are more important controls on floc TE uptake. Consistent with this hypothesis, the enhanced TE reactivity of floc relative to the bed sediments (Figure 3.1, Table S3) was significantly explained by the concentration of floc organic matter (Figure 3.2, Table S5). However, secondary control of system pH on the relative floc-solution partitioning among specific TEs was observed and is discussed subsequently. Organic matter was a major constituent of floc, comprising 20-45% by mass, consistently significantly higher in floc compared to bed sediments across sites (6-17% by mass; Table S1). The single exception was within the mine tailings, which possessed not only substantially different "sedimentary" materials but also was natural organic matter (NOM)-poor (Table S1). Organic materials are commonly reported to be important for TE sequestration in aquatic systems.[11,24,26,28] The importance of floc-organic concentration as a control on floc TE reactivity is evident when comparing relative abundance ratios of floc:bed sediment TE concentrations ($TE^{Floc}/TE^{Sediment}$) to that of floc: bed sediment organic content ($C^{Floc}/C^{Sediment}$) (Figure 3.2). Highly significant positive correlations emerged indicating that the greater the accumulation of floc organic carbon relative to bed sediments ($C^{Floc}/C^{Sediment}$), the greater the relative difference in floc:bed TE concentration ($TE^{Floc}/TE^{Sediment}$) (Figure 3.2). Element-specific trends emerged within this result, with the greatest impact observed for Ni, where a 1 unit increase in $C^{Floc}/C^{Sediment}$ produced a 13.9 unit increase in $Ni^{Floc}/ Ni^{Sediment}$, decreasing in effect to that observed for As, of a 1.4 unit increase. Thus floc organic content is a key control underpinning enhanced floc TE reactivity relative to surficial bed sediments in close proximity (<0.5 m) irrespective of system physico-chemistry. Consistent with this organic matter control on floc TE sequestration, the NOM-poor mine tailings showed no enrichment for $C^{Floc}/C^{Sediment}$ and thus no significant enhancement of $TE^{Floc}/TE^{Sediment}$ was observed for all TEs investigated (Figure 3.2).

Floc-organics may be playing several roles facilitating enhanced TE reactivity, such as providing a large reactive surface area for TE sorption and/or for the collection/templating of solid sorbent phases (e.g., Fe oxyhydroxides, FeOOH [9,12,25]).

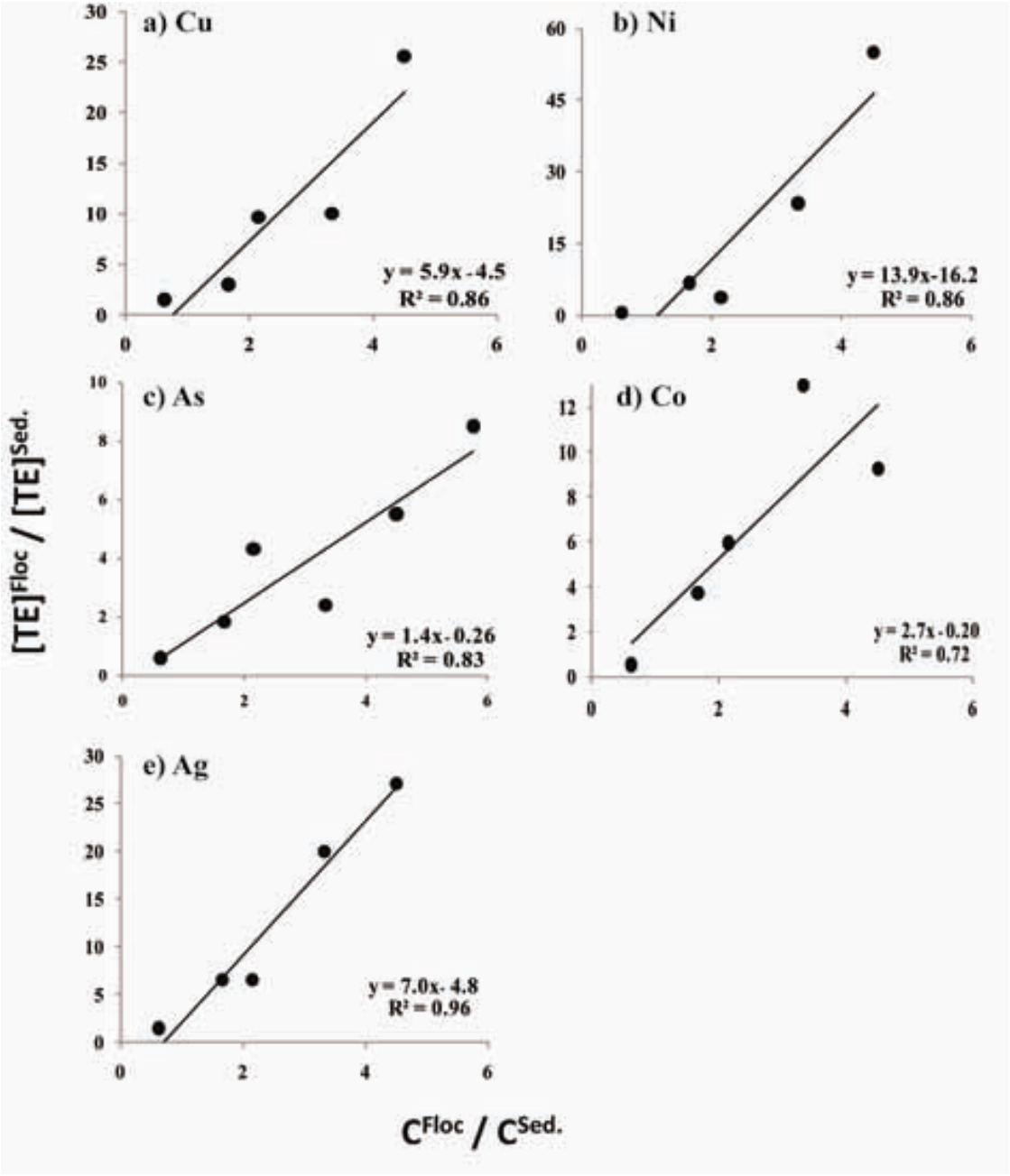

Figure 3.2 Relative abundance results comparing floc:sediment ratios of (1) total TE concentration ($[TE]^{Total}$: $\mu molg^{-1}$) to (2) organic content (g C/g dry weight) across sites. CSO flocs were excluded from the linear regression (LR) analysis, as there was little to no partitioning to this fraction despite high organic carbon concentrations (<3% for all TEs except As, which was included in LR). Ni is only significant at $p = 0.10$.

While increased floc TE reactivity was best predicted by floc organic concentrations, sequential extraction results indicated that TEs were not dominantly or consistently associated with this phase. Instead, the reducible amorphous Fe oxyhydroxide fraction, $[TE]^{A}$, was consistently the most important phase for floc TE retention across sites with [Ag, Ni, As, Co, Cu]^{A} constituting [43-79%, 30-53%, 30-70%, 38-68%, 32-70%] of $[TE]^{Total}$ concentrations respectively (Figure 3.1, Table S3). Floc $[TE]^{A}$ were also consistently significantly greater than bed $[TE]^{A}$ (up to an order of magnitude), except again, within the mine environment (Table S3). This result is similar to Stecko et al. (2000), who report a higher proportion of SPM Cu, Pb, and Zn within the easily reducible phase compared to bed sediments in an estuarine system.[14]

In contrast to suspended floc, TE partitioning within bed sediments was highly site and element-specific, with no single solid fraction accounting for the majority of TE retention across sites (Figure 3.1, Table S3). The organic/sulfide fraction was particularly important within the tailings sediments, consistent with the highly sulfidic nature of mine waste residues, while the Fe/Mn crystalline oxide minerals dominated both Lake Ontario bed sediment TE partitioning as well as specifically Ag partitioning across sites (Figure 3.1, Table S3). Thus, in contrast to a dominance of amorphous oxyhydroxides in floc TE sequestration across sites, bed sediment TE partitioning patterns were site specific and thus likely more reflective of both system geochemical parameters and element specific reactivity (Table S6).

3.3.2 Floc Organic-FeOOH Interactions. Floc from all sites had a significant proportion of organic matter (up to 45% by mass, Table S1). With the exception of the mine tailings, floc-organic concentrations (g C/g floc) were 2-16x greater than that of carbonate mineral, amorphous, and crystalline Fe/Mn oxyhydroxides concentrations and were always significantly greater than organic concentrations in surficial bed sediments (Table S1). Although enhanced TE reactivity of floc across sites was best predicted by floc organic content (Figure 3.2, Table S5), floc TE partitioning results indicate that TEs are not dominantly or consistently bound to this phase (Figure 3.1, Table S3). This suggests a possible alternate role for organics in floc TE sequestration. Floc organic content was a highly significant

($p<0.05$, $R^2=0.83$) positive control on the concentration of floc amorphous Fe oxyhydroxides (FeOOH), consistent with increased collection and/or templating of FeOOH associated with higher floc-organics (Figure 3.3). Floc-FeOOH concentrations were 2-to 26x greater than FeOOH within surficial sediments. Moreover, in contrast to floc-FeOOH, the majority of sediment associated Fe occurred as crystalline oxides, suggesting active processes of direct nucleation and precipitation, or collection of recently polymerized amorphous FeOOH, specifically by floc organic constituents. The correlation of floc-FeOOH concentrations to floc-organic concentrations rather than to water column pH or $[Fe]_D$ is also consistent with a bio-concentration of FeOOH linked to floc-organics at the microscale (Table S5). Strong organic-Fe associations are common in natural environments and are often indicative of microbial activity such as mineral coatings (e.g., FeOOH) on organic fibrils, metabolically mediated precipitation-dissolution reactions of FeOOH, and bacterial cells directly adsorbed onto oxyhydroxide surfaces.[9,12,25,35] While floc organic concentrations can include any floc associated detrital matter and refractory organics (e.g., humic and fulvic acids), here ESEM and epifluorescence microscopy with LIVE/DEAD fluorescent staining of floc samples revealed a high microbial cell density, a high degree of viability, and substantial organic-EPS fibril-mineral associations of floc (Figure 3.4). Iron mineral entrapment within microbial EPS was also consistently observed by TEM (Figure 3.4) and has been widely reported to be a consistent feature of floc organics.[1,3,6] These results are consistent with previous investigations reporting both higher viable bacterial counts in floc relative to surficial bed sediments[6,7,31] as well as the dominance of live microbial cells and EPS in overall floc structure.[3,6,31-34]

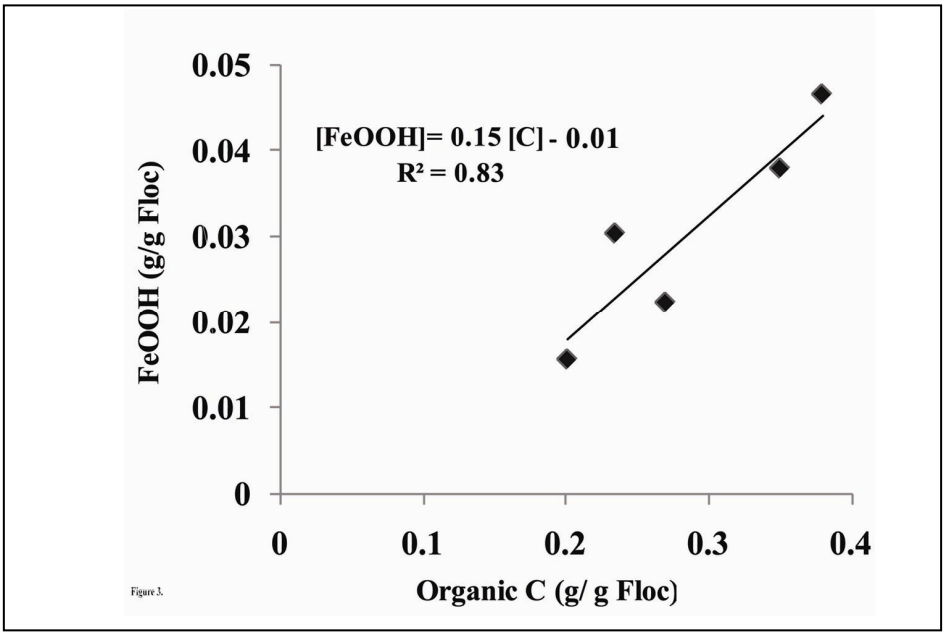

Figure 3.3 Floc organic carbon concentrations (g C/g floc) are positively correlated with floc amorphous Fe oxyhydroxide concentrations (estimated as ferrihydrite, g FeOOH/g floc). Floc in the mine tailing impoundment had higher floc-FeOOH concentrations than predicted by floc-organic carbon concentration alone and is not shown on the trend line.

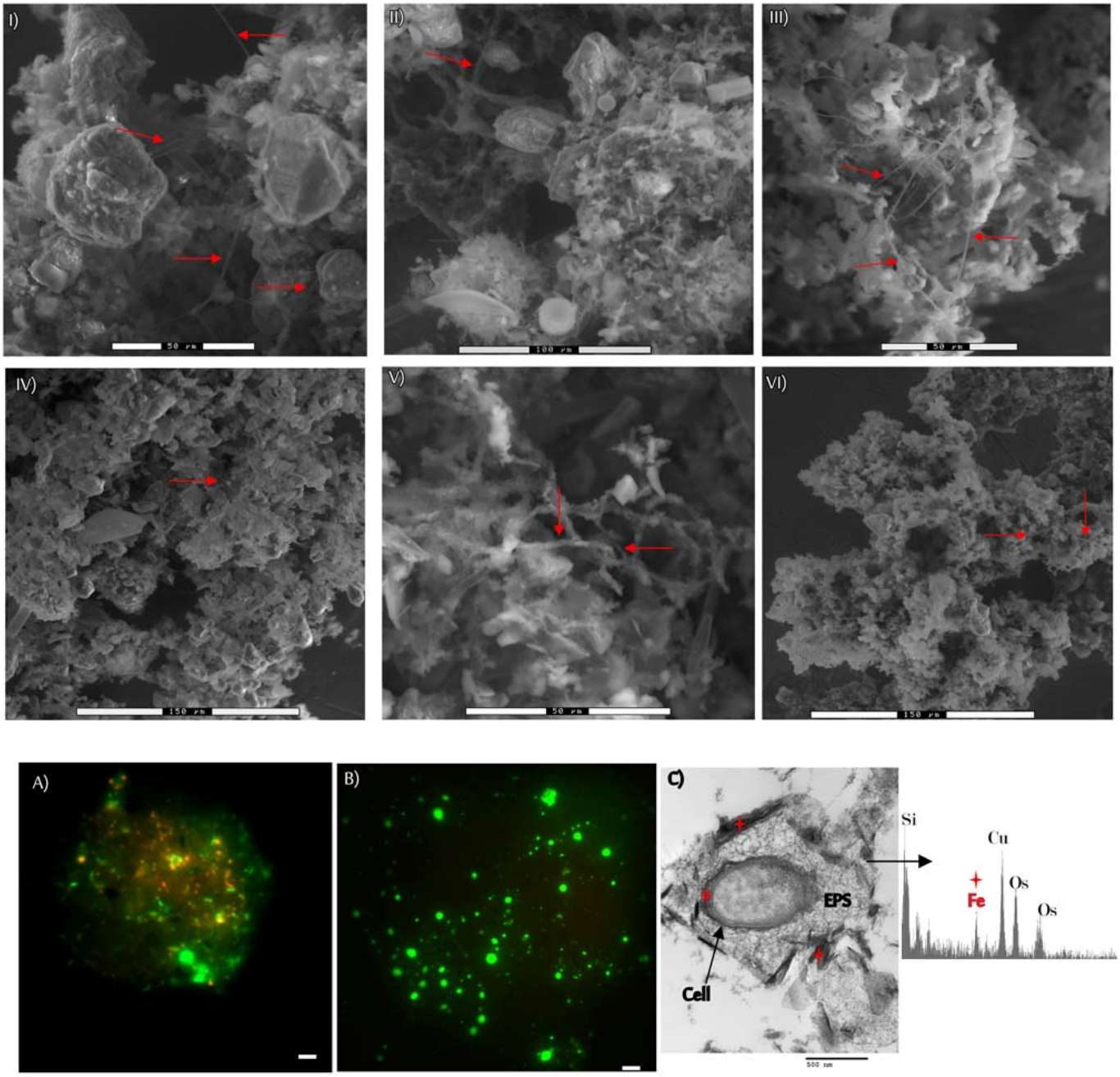

Figure 3.4. **I-VI)** Environmental Scanning Electron Micrographs (ESEM) of suspended floc samples across sites; from highest to lowest organic C content (g C/ g floc): (I) Combined Sewer Overflow (CSO); (II) Brewer Lake, Algonquin Park; (III) Nearshore L. ON; (IV) Offshore L. ON; (V) Agricultural Stream; and (VI) Ni mine tailings impoundment lake. Example exopolymeric (EPS) fibrils are indicated by red arrows. ESEMs included represent a range of differently scaled micrographs in order to visualize floc organic-EPS-mineral network as well as different textural elements at both the broader floc morphology and specific floc component scales. **A-B)** Live microbial community of floc for both A) the lowest organic content floc, Ni mine tailings; and B) the highest organic content floc, CSO. Epiflourescence images of flocs are stained for living bacteria (green) and dead (red). Scale bar represents 10µm. **C)** Representative transmission electron micrograph (TEM-EDS) of environmental floc sample exhibiting a bacterium (species unknown) with EPS and cell wall associated Fe (indicated by red stars). Peaks of Cu and Os are artifacts of sample preparation.

Further highlighting this floc organic-FeOOH relationship, comparative concentration factors (CF) relating the concentration of a TE within the amorphous oxyhydroxides fraction to the estimated abundance of amorphous oxyhydroxides in floc (CF^{TE} = $[TE]_A$ /[FeOOH]) indicate that TE reactivity of floc- FeOOH is far higher than that of surficial bed sediments. For example, a gram of floc-FeOOH retained up to 50x the amount of Cu compared to the observed Cu concentration associated with a gram of FeOOH within surficial bed sediments (Table S4). Thus, not only does increasing floc-organic accrual result in accumulation of floc-FeOOH, but also that these FeOOH are more efficient TE scavengers (Tables S1, S4). It has been previously demonstrated that bacterial-associated organic polymers preferentially induce the formation of less crystalline, and thus typically more reactive, Fe oxyhydroxides (e.g., ferrihydrite vs. goethite), and tend to slow re-crystallization to other forms.[27,28] This microbial-EPS-FeOOH interaction is thus likely important in flocs across sites, contributing both to the observed enhanced TE-reactivity of floc and specifically floc-FeOOH, as well as the dominance of FeOOH in floc-TE partitioning patterns. Interestingly, the results do not indicate an important role for amorphous Mn oxyhydroxides $[Mn]_A$ in floc. Although both FeOOH and $[Mn]_A$ have been observed to significantly impact TE behavior in aquatic systems[6,11,29,30] the mass of floc associated $[Mn]_A$ did not correlate to floc organic concentrations, nor did $[Mn]_A$ significantly correlate with floc $[TE]^{Total}$ (Table S5).

We hypothesize from these results that floc-organics are acting in a structural capacity, rather than as a direct sequestration role in floc TE uptake. That is, the large potential surface area and organic nature of floc provide a highly effective framework for the collection and/or templating of surface coatings of TE-reactive amorphous oxyhydroxide mineral phases (FeOOH). Oxyhydroxides are ubiquitous in aquatic systems and are known to tend to precipitate as surface coatings on other minerals and organic materials including bacterial/EPS surfaces.[9,13,25,26] This, in turn, would facilitate the sequestration of TEs associated with floc-FeOOH formation, imparting the FeOOH "signature" on floc-TE geochemistry across these widely differing sites. In contrast to the results observed for floc-FeOOH, CF for

floc-organics ($CF^{TE} = [TE]_C/[C]$) indicate that floc-organics were often less effective at concentrating TEs compared to bed sediment
associated organics (Table S4).

These novel results evidence that the organic rich nature of floc (EPS and living cells) exerts an important control over TE behavior, producing a floc-specific geochemistry that is both predictable and conserved across very different aquatic environments. Floc organics are likely providing the critical framework for the generation and concentration of FeOOH, the dominant floc TE scavenging phase, and also likely underpin enhanced TE reactivity of specifically floc-FeOOH.[9,21,22] The ability of floc-FeOOH to efficiently scavenge TEs despite constituting a low concentration is consistent with previous studies (e.g., ref 6); however, our results are the first to demonstrate linkages between floc organic biological materials, floc-FeOOH, and floc TE behavior, identifying a compartment dependent control on TE sequestration across highly variable aquatic systems.

3.3.3 System Effects on Floc TE Uptake. While floc-organic content principally controls TE reactivity through the development of amorphous FeOOH, secondary pH-dependent and element-specific trends emerged when assessing relative floc-solution partitioning for various elements across sites. Floc distribution coefficients (K_d^{TE} LKg^{-1}: $[TE]_{floc}/[TE]_D$ [36]) were calculated for Co, As, and Cu, which were consistently quantifiable in the aqueous phase ($[TE]_D$: <0.2 μm, Table S1). Floc K_d TE values ranged up to 3 orders of magnitude and were significantly correlated to system pH (Figure 3.5, Table S4). The importance of pH in dictating TE solid-aqueous partitioning has been widely reported (e.g., refs 11 and 36-38). Here, K_d^{Co} increased and K_d^{As} decreased with increasing system pH. Thus floc in the highest pH system (Lake Ontario, Toronto; pH = 8.01) had 1144x greater relative affinity for Co (divalent cation) uptake from the water-column and 30x lower affinity for As (oxyanion) than that of floc in the lowest pH system (Ni Mine Tailings; pH = 6.00). Further, FeOOH-specific concentration factors ($CF^{TE} = [TE]_A$ /[FeOOH]) exhibited the same pH-dependent relationships across sites: CF^{Co} increase while those for As decrease with system pH (Figure 3.5, Table S4). These linear relationships between

floc K_d^{TE} and specifically floc-FeOOH TE reactivity and pH across sites are consistent with floc-FeOOH surface reactively control on floc TE sorption (i.e., FeOOH typically exhibit pH_{zpc} values ranging between 6.5-8.0[36]). For example, floc-FeOOH scavenges 8x more Co in the highest pH system compared to the lowest pH system, resulting in a relatively higher floc K_d^{Co} value (Figure 3.5). In contrast, a relative decrease in floc uptake of As from the water-column at high pH is consistent with increasingly negative floc-FeOOH surfaces. Further, floc-FeOOH specific Kds for As and Co ($K_{dFeOOH}^{TE} = \log (CF^{TE}/[TE]_D)$) again exhibit anionic and cationic specific sorption behavior, consistent with the pH dependent acid-base reactivity of FeOOH surface sites (Table S4). These values are within the range of TE sorption studies using FeOOH in the literature.[12,36-38] Brewer Lake, Algonquin Park was an outlier the majority of observations (Figure 3.5, Table S4). Interestingly, K_d^{FeOOH} TE values are similar to TE sorption studies of bacteria- FeOOH composites (e.g., ref 12) suggesting possible synergistic effects between bacterial surfaces, EPS and FeOOH in floc. While cationic and anionic specific TE sorption behavior to FeOOH has been widely documented, this is the first field investigation to demonstrate consistent, predictable relationships between floc-FeOOH surface reactivity and element specific TE behavior across a range of aquatic systems.

Copper, the most abundant TE in floc from all sites, showed a distinct trend among the TEs examined. K_d^{Cu} did not significantly change with system pH, although floc CF^{FeOOH} values for Cu were significantly negatively correlated with system pH (i.e., inconsistent with classical cationic sorption to FeOOH; Table S4). However, K_d^{Cu} was positively correlated to mass of floc organic carbon (g C/g floc, $R^2 = 0.64$), indicating greater partitioning of Cu to floc from solution with increasing concentrations of floc organics, independent of system pH. Moreover, Cu had the highest affinity (i.e. CF) for both the FeOOH and organic fractions of all TEs (Table S4). Thus, although Cu affinity for FeOOH decreased with pH, in contrast to the other TEs, no measurable change in K_d^{Cu} was observed. This result suggests a possible redistribution of Cu to the floc organic fraction, associated with increased competitive sorption of other TEs to floc FeOOH as pH increases (Figure 3.1, Table S3).

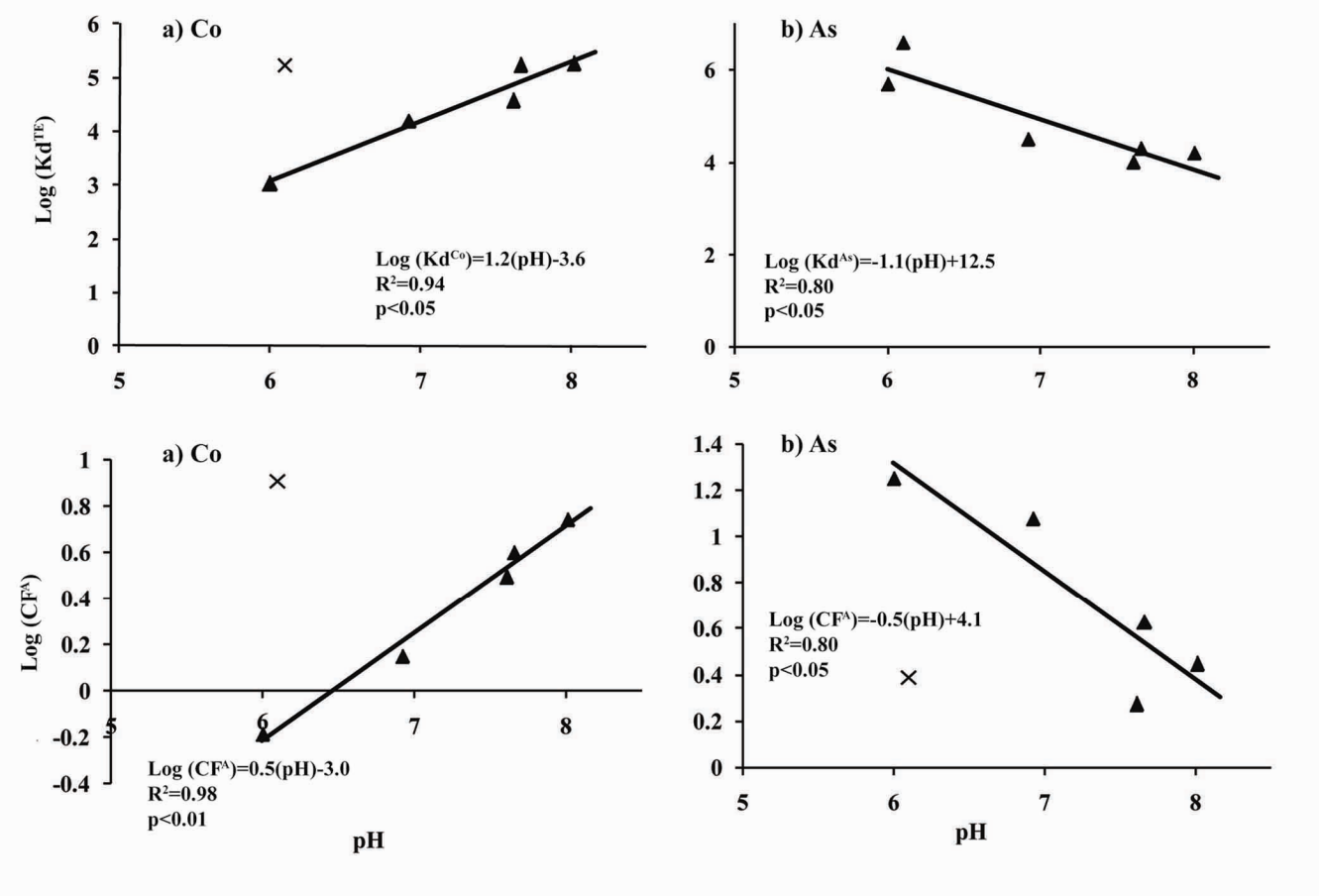

Figure 3.5 Distribution coefficients (K_d^{TE}, LKg^{-1}: $[TE]_{Floc}/[TE]_D$) and amorphous Fe oxyhydroxide (FeOOH) concentration factors (CFTE = [TE]A/[FeOOH]) versus system pH across sites for a) cobalt (Co) and b) arsenic (As). Brewer Lake, Algonquin Park (x) was an outlier for most observations, which may be due to competitive sorption processes between As and Co.[36]

Results of this field investigation show floc to be a geochemically distinct sedimentary compartment within aquatic systems with significant trace element scavenging capabilities, sequestering TEs in significantly greater concentrations than surficial bed sediments. Moreover, although suspended floc was collected in close proximity to bed sediments (<0.5 m), results indicate that sequestration and partitioning patterns of floc-associated TEs do not simply mirror TE patterns observed in proximate surficial bed sediments across a wide variety of systems. While previous studies have demonstrated the importance of oxyhydroxide minerals for TE retention in suspended particulates (e.g., refs 6 and 15), this is the first investigation demonstrating a consistent importance of amorphous Fe oxyhydroxides in floc TE geochemistry as well as the specific role of floc organic-FeOOH-TE interactions responsible for the increased floc TE reactivity.

Acknowledgment. The authors wish to thank Chris Jaskot, Brian Trapp, and Technical Operations of the National Water Research Institute for their assistance with the fieldwork. This work was funded by an NSERC Strategic Research Grant #350885; NSERC CGS scholarships were awarded to A.V.C. Elliott and J.M. Plach.

3.4 Supporting Information

TABLE S1: Physico-chemical conditions at sampling depth (<0.5m above the sediment-water interface) and mean trace element (TE) reactive sedimentary constituents of suspended flocs and surfical (0-1cm) bed sediments across the 6 aquatic systems investigated.

	System:	Brewer Lake	Agricultural	CSO	Mine Tailings	L. ON, offshore	L. ON, nearshore
Water Column	Depth of Sampling (m)	3.5	0.4	0.3	3	11.5	1.5
	Floc Concentration (mg/L)	1.4	3.1	3.2	1.2	1.5	1.4
	pH	6.01	7.61	6.92	5.95	8.01	7.66
	Temp. (°C)	15.7	14.9	18.7	14.97	7.1	8.5
	O_2 (mg/L)	8.5	8.5	5.9	5.32	12.4	12.2
	SPC µScm	101.2	75.4	1259	1870	345.2	350.8
	DIC (mg/L)	2.2 ± 0.06	65.3 ± 0.58	30.7 ± .0006	3.0 ±0	21.6 ± 0.59	23.5 ± 0.25
	DOC (mg/L)	5.4 ± 0.00	8.8 ± 0.14	4.07 ± 0.21	2.7 ± 0	2.4 ± 0.00	2.97 ± 0.38
	$[PO_4]$ mg/L	0.04 ± 0.01	0.25 ± 0.01	0.35 ± 0.03	0.09 ± 0.02	0.016 ± 0.02	0.015 ± 0.01
	$[SO_4]$ mg/L	5.47 ± 0.06	16.3 ±0.00	110.0 ± 4.04	967 ± 15.5	26.9 ± 0.12	28.3 ± 0.23
	$[NO_3]$ mg/L	0.5	1.3	1.9 ± 0.03	0.3 ± 0.03	0.14 ± 0.01	0.13 ± 0.01
	$[Fe]_D$ mg/L	0.05 ± 0.01	0.05 ± 0.01	0.13 ± 0.01	4.0 ± 1	0.02 ± 0.05	0.01 ± 0.00
	$[As]_D$ nmol/L	0.2	9.2	26	18.05	13.3	12.4
	$[Co]_D$ nmol/L	6.9	3.4	31.1	807	0.2	1.4
	$[Cu]_D$ nmol/L	8.1	17.1	47.7	520	19.7	25
	$[Ag]_D$ nmol/L	*	*	*	*	*	*
	$[Ni]_D$ nmol/L	*	*	6	60	*	17
Floc[a]	Carbonates (g/g)	0.08	0.07	0.04	0.5	0.14	0.14
	[FeOOH] (g/g)	0.047	0.016	0.038	0.36	0.03	0.022
	$[Mn]^A$ (µmol/g)	>6	>6	3.5	4.5	4.85	5.09
	$[Mn]^C$ (µmol/g)	3.6	4.2	0.005	1.2	0.61	0.36
	Organic C (g/g)	0.38	0.2	0.43	0.04	0.23	0.28
Bed[a]	Carbonates (g/g)	0.077	0.11	0.09	0.064	0.13	0.13
	[FeOOH] (g/g)	0.0025	0.012	0.01	0.27	0.005	0.006
	$[Mn]^A$ (µmol/g)	5.5	4.3	0.25	0.37	0.47	0.55
	$[Mn]^C$ (µmol/g)	1.6	2	0.11	0.11	0.14	0.18
	Organic C (g/g)	0.17	0.12	0.1	0.06	0.07	0.06

*indicates below procedural level of quantification (LOQ);((average of zeroes)+((standard deviation of zeroes)*3))*3 for all TEs LOQ=(0.05,0.2,8.0,0.2,5.0) nmol/L for Ag,As,Cu,Co and Ni, respectively.

[a] mean values (n=3). Standard devaition Organic C, Carbonates=10^{-1}, [FeOOH]=10^{-4}, $[Mn]^A$=$[Mn]^C$= 10^{-3}

**Mine site considered 'organic poor' due to significantly less organic carbon content of the floc compared to other sites and generally lower DOC and bed-sediment organic carbon content; 'organics' in the mine tailings constitute chemical additives during extraction/neutralization processes and thus are not representative of natural organic matter (NOM) formed within the water-column of less anthropogenically-altered systems (i.e NOM-poor)

TABLE S2: Bulk mineralogical composition of suspended aquatic floc and surficial (0-1cm) bed sediments across sites. Analysis identified the main cyrstalline components of floc and bed sediments to be similar within each site (Siemens d5005 x-ray diffractometer).

	Brewer Lake		Agricultural		CSO		Mine Tailings		L. ON, offshore		L. ON, Nearshore	
	Floc	Bed	Floc	Bed	Floc	Bed	Floc	Bed	Floc	Bed	Floc	Bed
Pyrite							26%	37%				
Mgnetite		3%				5%		3%	1%	2%	1%	1%
Quartz	25%	30%	32%	31%	8%	19%	14%	15%	17%	41%	14%	26%
Calcite			15%	13%	8%	15%			14%	12%	13%	12%
Anorthite/albite	22%	20%	20%	19%	5%	17%	18%	11%	19%	19%	19%	18%
Microcline	5%	7%	6%	6%	4%	5%	6%	6%	7%	6%	7%	7%
Mica		5%					5%	7%				
Dolomite/ankerite			6%	18%	4%	17%			7%	6%	8%	9%
Chlorite/Chloride		4%	3%	3%	2%	5%	8%	9%	11%	9%	11%	9%
Amphibole	2%	7%				2%	7%	6%	2%	3%	2%	2%
Smectite		4%										
Calcite												
Dolomite/ankerite	5%	4%										
Gypsum		2%										
Bassanite	1%											
Anhydrite	3%	2%										
Fibers	1%											
NaCl	2%											
Zeolite $2(KAlSiO_4)\cdot 3H_2O$	8%											
Illite			5%	3%	3%	2%			12%	2%	12%	10%
Organic	19%	14%	5%	2%			12%		2%		2%	
Amorphous, ect.	7%	6%	5%	4%	66%	5%	4%	4%	5%	4%	5%	5%

Table S3. Floc and surficial (0-1cm) bed sediment total trace element ($[TE]^{Total}$:µmol/g) and percent relative partitioning (%) to each of six, operationally defined reactive sedimentary fractions: 1=exchangeable; 2=carbonates/acid-soluble sulfides; 3=amorphous Fe/Mn oxyhydroxides; 4=crystalline Fe/Mn oxides; 5=oxidizable organics/sulfides; 6=residual. Complete sample digestion for the most contaminated (Ni mine tailings, Sudbury) and most remote (Brewer lake, Algonquin Park) sites did not exceed a 10% difference in comparison to totals obtained from the summation of the operationally defined fractions.

		Brewer Lake		Agricultural Stream		CSO		Nearshore, L. ON		Offshore, L. On		Mine Tailngs	
		Floc	Bed	Floc	Bed	Floc	Bed	Floc	Bed	Floc	Bed	Floc	Bed
	$[As]^{Total}$ µmol/g	**0.40**	**0.09**	**0.10**	**0.05**	**0.50**	**0.06**	**0.26**	**0.05**	**0.23**	**0.09**	**9.06**	**15.20**
	1	0.0	0.0	3.7	0.0	1.8	0.8	20.0	0.0	9.2	0.0	0.0	0.0
	2	8.5	8.5	6.5	4.8	20.0	6.0	0.2	5.1	8.9	4.7	0.3	3.0
	3	46.6	4.7	34.4	0.0	66.8	45.7	46.5	25.4	41.2	37.3	70.9	28.0
	4	0.0	74.7	34.4	82.8	7.8	12.6	18.2	59.1	20.6	32.5	23.8	22.0
	5	43.0	5.9	10.4	8.6	2.6	11.1	10.6	6.1	16.5	12.5	0.5	3.0
	6	2.2	6.2	10.5	3.7	0.6	23.8	4.8	4.3	3.6	13.0	4.4	43.0
	$[Co]^{Total}$ µmol/g	**1.2**	**0.19**	**0.13**	**0.03**	**0.08**	**0.09**	**0.2**	**0.02**	**0.21**	**0.02**	**0.86**	**1.64**
	1	1	2.3	0.6	0.7	7.6	0	3.2	0	3.3	0	0	1.3
	2	12.8	24	13.4	14.8	13.8	9.5	11.5	19.2	7	8	6.5	4.2
	3	51.3	33.2	44.6	0	68.8	18.4	50.3	37.1	60	43.9	35	7.1
	4	12.83	22.9	17.6	39.2	6.7	11	25.2	15.6	18.7	26.3	5.7	3
	5	8.34	10.8	6.3	19.1	2.2	18.3	4.8	7.2	4.9	4.5	46.7	44.6
	6	14.6	6.8	17.9	26.2	1.6	42.8	5	21.2	7	17.2	6	39.9
	$[Ag]^{Total}$ µmol/g	**0.012**	**0.0019**	**0.002151**	**0.0003**	**0.006**	**0.007**	**0.013**	**0.0005**	**0.01515**	**0.0007**	**0.21**	**0.16**
	1	1.3	0	0	0	0.72	0	0	0	0	0	0	0
	2	0.81	0	0	0	0.4	0	0	0	0	8	0	0
	3	40.7	51.3	43.7	0	63.5	14.1	60.5	16.9	79.2	16.9	47.1	38.3
	4	24.4	38.5	7.7	0	14.8	69.2	16.8	49.6	15.4	49.6	39.0	39.6
	5	16.6	5.13	0	0	0	3.8	7.56	8.3	2.2	5.3	10.7	20.5
	6	16.3	5.1	48.6	100	21.7	12.8	15.1	25.3	3.1	25.3	2.4	1.53
	$[Cu]^{Total}$ µmol/g	**3.40**	**0.35**	**0.43**	**0.11**	**3.94**	**1.42**	**1.52**	**0.06**	**1.29**	**0.12**	**70.00**	**45.30**
	1	0	1.5	0	0	0	0	6.1	18.6	6.4	0	0	0.5
	2	0	1	0	3.7	8.3	1	3.2	7.3	0	0	3.6	1.5
	3	18.3	16.7	17	0	73.8	9.7	33.3	24.5	39.9	22.7	56.3	25.4
	4	23	15.7	17	31.2	13.2	14	10.7	11.4	8	49.5	14.2	14.1
	5	40.4	50.5	30.8	32	4.7	59.1	30	20	32	12.8	24.8	42.5
	6	11.8	14.8	35.8	33	0	16.4	16.7	18.2	13.6	15	1.7	16.9
	$[Ni]^{Total}$ µmol/g	**1.27**	**0.33**	**0.36**	**0.13**	**0.67**	**0.49**	**0.61**	**0.01**	**0.71**	**0.03**	**15.80**	**23.30**
	1	1.8	0	1.7	0.6	7.1	0.24	3	0	3.8	0	3.1	0
	2	17.6	16.3	8.7	21.8	11.8	10.3	11.6	36.9	7	0	17.5	10.3
	3	35.7	27.7	34.7	25.5	56.8	26	41.2	30.1	48.8	48.9	46.5	13.3
	4	17.9	23.7	23.13	31.5	16.2	12.6	23.8	12.2	17.1	28.8	6.6	5
	5	8.9	19.5	5.8	7	2.5	18.6	5.1	5.6	6.7	4.01	26.3	57.6
	6	17.9	12.8	26	14.6	5.7	32.2	15.3	15.2	16.6	18.3	0	13.9
	$[Fe]^{Total}$ µmol/g	**785**	**439**	**301**	**130**	**566**	**408**	**274**	**75**	**277**	**92**	**5251**	**1770**
	1	0	0	1.14	6.15	3.53	1.23	0.23	0	0.36	0	0.95	3.39
	2	0	3.42	2.28	23.08	0.00	2.45	2.48	9.93	2.70	10.87	2.29	5.93
	3	74.52	48.75	43.96	13.85	82.83	51.47	67.02	26.49	67.39	23.91	62.73	17.26
	4	19.75	27.33	18.68	23.08	13.11	21.57	23.31	30.46	21.62	32.61	14.69	7.34
	5	2.55	6.83	1.82	24.62	0.53	23.28	0.95	6.62	1.80	5.43	2.29	12.43
	6	3.18	13.67	0.68	9.23	0.00	0.00	6.01	26.49	6.13	27.17	17.06	53.65
	$[As]^{Total}$ µmol/g	0.39	0.09									9.86	16.57
Total Digestion	**$[Co]^{Total}$ µmol/g**	1.29	0.21									0.83	1.52
	$[Ag]^{Total}$ µmol/g	0.01	0.002									0.20	0.18
	$[Cu]^{Total}$ µmol/g	3.48	0.35									73.65	49.09
	$[Ni]^{Total}$ µmol/g	1.17	0.35									16.57	21.52
	$[Fe]^{Total}$ µmol/g	766.2	423.7									5372.8	1846.6

Table S4. Mean aqueous trace element concentrations ($[TE]^D$,<0.2µm), associated distribution coefficents (Kd^{TE} L/Kg: $[TE]^{Floc}/[TE]^D$) and suspended floc and surficial (0-1cm) bed sediment concentration factors for both amorphous oxyhydroxides ($CF^A=[TE]^A/[FeOOH]$) and organic fractions ($CF^C= [TE]^C/[C]$) across sites.

	Brewer Lake	Agricultural	CSO	L. ON, Offshore	L. ON, Nearshore	Mine Tailings
$[As]_D$ nmol/L	0.2	9.2	26	13.3	12.4	18.05
$log(Kd^{As})$	6.3	4	4.4	4.2	4.3	5.7
$CF^{A\ Floc}$	2.44	1.88	8.78	2.81	4.3	18
$CF^{A\ Sed.}$	0.16	0	2.68	7.1	2.85	16.7
$CF^{C\ Floc}$	0.3	0.04	0.03	0.17	0.08	1.1
$CF^{C\ Sed.}$	0.03	0.11	0.03	0.17	0.04	7.6
$[Co]_D$ nmol/L	6.9	3.4	31.1	0.2	1.4	807
$log(Kd^{Co})$	5.3	4.6	4.4	6.1	5.2	3
$CF^{A\ Floc}$	8.1	3.1	1.41	5.5	4.1	0.65
$CF^{A\ Sed.}$	2.6	0	1.3	1.5	1.3	0.43
$CF^{C\ Floc}$	0.17	0.04	0.004	0.04	0.03	11.9
$CF^{C\ Sed.}$	0.12	0.2	0.77	0.01	0.03	12.3
$[Cu]_D$ nmol/L	8.1	17.1	47.7	19.7	25	520
$log(Kd^{Cu})$	5.8	4.4	4.9	4.8	5.2	5.1
$CF^{A\ Floc}$	13.3	4.3	72.9	17.2	23	101.8
$CF^{A\ Sed.}$	2.3	0	13.8	5.5	2.45	42.2
$CF^{C\ Floc}$	3.6	0.65	0.42	2	1.54	441
$CF^{C\ Sed.}$	1.1	0.86	40.1	24.1	0.2	312
$[Ni]_D$ nmol/L	*	*	6	*	17	60
$log(Kd^{Ni})$	*	*	5	*	4.5	5.4
$CF^{A\ Floc}$	9.6	7.8	10	11.5	11.4	20.4
$CF^{A\ Sed.}$	3.6	2.8	12.7	2.9	0.51	11.5
$CF^{C\ Floc}$	0.36	0.1	0.04	0.002	0.11	103.8
$CF^{C\ Sed.}$	0.38	0.23	4.34	0.02	0.09	223.7
$[Ag]_D$ nmol/L	*	*	*	*	*	*
$log(Kd^{Ag})$	*	*	*	*	*	*
$CF^{A\ Floc}$	0.1	0.06	0.1	0.4	0.38	0.27
$CF^{A\ Sed.}$	0.04	0	0.09	0.02	0.014	0.22
$CF^{C\ Floc}$	0.005	0.0009	0.002	0.001	0.004	0.56
$CF^{C\ Sed.}$	0.0006	0	0.23	0.0005	0.0007	0.55

Table S5. Correlation matrix values (Pearson) of suspended floc total trace element concentrations ($[TE]^{Total}$:µmol/g), mean aqueous trace element concentrations ($[TE]^{D}$,<0.2µm), physico-chemical conditions at sampling depth (<0.5m above the sediment-water interface) and concentration of TE-reactive sedimentary constituents of suspended flocs across the 6 aquatic systems investigated. Relative abundance results comparing floc:sediment ratios of (i) total TE concentrations $[TE]^{Floc}$/ $[TE]^{Sed.}$; (ii) mean organic content $[C]^{Floc}$/ $[C]^{Sed.}$; (iii) amorphous manganese phases $[Mn]^{A\ Floc}$/ $[Mn]^{A\ Sed.}$ and (iv) crystalline manganese phases $[Mn]^{C\ Floc}$/ $[Mn]^{C\ Sed.}$ evidence the accrual of floc-organics is a key factor contributing to enhanced TE sequestration.

Variables	pH	O_2 mg/L	°C	SPC (µScm)	$[Fe]_D$ mg/L	$[As]_D$ nmol/L	$[Co]_D$ nmol/L	$[Cu]_D$ nmol/L	$[Ag]_D$ nmol/L	$[Ni]_D$ nmol/L	Organic C (g/g)	$C^{Floc}/C^{Sed.}$	FeOOH (g/g)	$FeOOH^{Floc}/FeOOH^{Sed.}$	$[Mn]_A$ µmol/g	$[Mn]_{A\ floc}$ / $[Mn]_{A\ Sed.}$	$[Mn]_C$ µmol/g	$[Mn]_{C\ floc}$ / $[Mn]_{C\ Sed.}$
pH	1.00	0.63	-0.71	-0.04	-0.46	0.32	-0.43	0.11	-	0.21	0.13	0.42	-0.52	0.65	0.02	0.02	-0.25	-0.45
O_2 mg/L	0.63	1.00	-0.99***	-0.74	-0.92**	-0.30	-0.82*	-0.44	-	0.30	0.61*	0.98***	-0.12	0.28	0.31	0.96***	0.21	0.81**
°C	-0.71	-0.99***	1.00	0.65	0.87*	0.18	0.77	0.34	-	-0.28	0.65*	0.93***	0.21	0.20	-0.21	0.91***	0.38	0.83**
SPC (µScm)	-0.04	-0.74	0.65	1.00	0.89**	0.84*	0.88**	0.88**	-	0.04	-0.50	0.66*	0.01	0.00	-0.62	0.22	-0.	0.20
$[Fe]_D$ mg/L	-0.46	-0.92**	0.87*	0.89**	1.00	0.61	0.97***	0.71	-	-0.18	-0.77*	-0.60	0.41	-0.44	-0.30	0.40	-0.13	0.93***
$[As]_D$ nmol/L	0.32	-0.30	0.18	0.84*	0.61	1.00	0.70	0.97***	-	0.31	-0.04	0.50	-0.10	0.30	-0.94***	0.89**	-0.75*	0.90
$[Co]_D$ nmol/L	-0.43	-0.82*	0.77	0.88*	0.96***	0.70	1.00	0.82*	-	0.03	-0.77*	-0.60	0.44	-0.44	-0.30	0.40	-0.14	0.92***
$[Cu]_D$ nmol/L	0.11	-0.44	0.34	0.88**	0.71	0.96***	0.82*	1.00	-	0.39	-0.76*	-0.60	0.03	-0.42	-0.30	0.42	-0.17	0.92***
$[Ag]_D$ nmol/L	-	-	-	-	-	-	-	-	-	-	-	-	-	-	-	-	-	-
$[Ni]_D$ nmol/L	0.21	0.30	-0.28	0.04	-0.18	0.31	0.03	0.39	-	1.00	-0.78*	-0.50	-0.30	-0.40	-0.33	0.50	-0.30	0.86**
$[As]^{Floc}/[As]^{Sed.}$	0.08	-0.32	0.29	-0.15	-0.85	0.36	-0.53	-0.51	-	-0.41	0.94***	0.91***	0.31	0.65	0.33	0.30	-0.1	-0.78*
$[Co]^{Floc}/[Co]^{Sed.}$	0.67	0.89**	-0.9**	-0.78*	-0.52	-0.40	-0.52	-0.53	-	-0.46	0.61	0.9**	0.10	-0.69	-0.08	-0.13	-0.46	-0.20
$[Ag]^{Floc}/[Ag]^{Sed.}$	0.69	0.92***	-0.92	-0.65	-0.43	-0.24	-0.43	-0.42	-	-0.23	0.40	0.97***	-0.28	-0.73*	-0.2	0.00	-0.6	-0.20
$[Cu]^{Floc}/[Cu]^{Sed.}$	0.41	0.73**	-0.68	-0.62	-0.41	-0.30	-0.41	-0.10	-	-0.17	0.54	0.93**	-0.04	-0.54	-0.06	-0.043	-0.51	-0.30
$[Ni]^{Floc}/[Ni]^{Sed.}$	0.61	0.81**	-0.79*	-0.51	-0.35	-0.11	-0.35	-0.34	-	-0.11	0.30	0.92**	-0.36	-0.63	-0.2	0.10	-0.6	-0.20
$[Ag]^{Total}$ µmol/g	0.15	0.74	-0.74	-0.61	-0.57	-0.17	-0.40	0.52	-	0.25	0.14	0.20	0.30	0.70	-0.07	0.30	-0.50	0.60
$[As]^{Total}$ µmol/g	-0.38	0.50	-0.4	-0.87*	-0.59	-0.78	-0.54	0.72	-	0.00	0.45	0.20	0.40	-0.02	0.50	-0.42	0.21	0.47
$[Co]^{Total}$ µmol/g	-0.8*	-0.11	0.21	-0.55	-0.11	-0.76	-0.15	0.17	-	-0.33	0.75*	-0.35	0.7*	-0.40	0.50	0.60	0.50	0.12
$[Cu]^{Total}$ µmol/g	-0.79	-0.62	0.62	0.40	0.69	0.25	0.77	0.25	-	0.02	0.97***	0.52	0.88**	0.00	-0.5	0.31	-0.27	-0.59
$[Ni]^{Total}$ µmol/g	-0.8*	-0.12	0.20	-0.4	0.05	-0.47	0.08	0.48	-	-0.22	0.82**	-0.09	0.91**	-0.06	0.15	-0.22	0.13	0.05
Organic C (g/g)	0.13	0.61*	0.65*	-0.50	-0.77*	-0.04	-0.77*	-0.76*	-	-0.78*	1.00	0.71*	0.91**	0.40	-0.54	-0.09	-0.26	-0.84**
$C^{Floc}/C^{Sed.}$	0.42	0.98***	0.93***	0.66*	-0.60	0.50	-0.60	-0.60	-	-0.50	0.71	1.00	0.20	0.72	-0.56	0.45	-0.63	-0.72*
FeOOH (g/g)	-0.52	-0.12	0.21	0.01	0.41	-0.10	0.44	0.03	-	-0.30	0.91**	0.20	1.00	0.07	-0.30	0.37	-0.13	0.93***
$FeOOH^{Floc}/FeOOH^{Sed.}$	0.65	0.28	0.20	0.00	-0.44	0.30	-0.44	-0.42	-	-0.40	0.40	0.72	0.07	1.00	-0.41	0.77	-0.67	0.42
$[Mn]_A$ µmol/g	0.02	0.31	-0.21	-0.62	-0.30	-0.94***	-0.30	-0.30	-	-0.33	-0.55	-0.56	-0.30	-0.41	1.00	-0.95***	0.85**	-0.08
$[Mn]_{A\ floc}$ / $[Mn]_{A\ Sed.}$	0.02	0.96***	0.91***	0.22	0.40	0.89**	0.40	0.42	-	0.50	0.45	0.95**	0.37	0.77	-0.95***	1.00	-0.94***	0.30
$[Mn]_C$ µmol/g	-0.25	0.21	0.38	-0.	-0.13	-0.75*	-0.14	-0.17	-	-0.30	-0.63	-0.63	-0.13	-0.67	0.85**	-0.94***	1.00	-0.08
$[Mn]_{C\ floc}$ / $[Mn]_{C\ Sed.}$	-0.45	0.81**	0.83**	0.20	0.93***	0.90	0.92***	0.92***	-	0.86**	-0.72*	-0.72*	0.93**	0.42	-0.08	0.30	-0.08	1.00

*** signifance $\alpha \leq 0.01$
** signifance $\alpha \leq 0.05$
* signifance $\alpha \leq 0.1$

Table S6. Correlation matrix values (Pearson) of surficial (0-1cm) bed sediment total trace element concentrations ($[TE]^{Total}$:µmol/g), mean aqueous trace element concentrations ($[TE]^{D}$,<0.2µm), physico-chemical conditions at sampling depth (<0.5m above the sediment-water interface) and concentration of TE-reactive sedimentary constituents across the six aquatic systems investigated.

Variables	pH	O_2 mg/L	°C	SPC (µScm)	$[Fe]_D$ mg/L	$[As]_D$	$[Co]_D$	$[Cu]_D$	$[Ag]_D$	$[Ni]_D$	$[As]^{Total}$ µmol/g	$[Co]^{Total}$ µmol/g	$[Cu]^{Total}$ µmol/g	$[Ag]^{Total}$ µmol/g	$[Ni]^{Total}$ µmol/g	$[Fe]^{Total}$ g/g	FeOOH (g/g)	C (g/g)	$[Mn]_A$ µmol/g	$[Mn]_C$ µmol/g
pH	1.00	0.63	-0.71	-0.53	-0.63	0.32	-0.63	-0.61	-	-0.55	-0.62*	-0.98***	-0.63	-0.63	-0.76*	-0.92**	0.54	-0.87*	-0.58	-0.36
O_2 mg/L	0.63	1.00	-0.99***	-0.74	-0.92**	-0.30	-0.82*	-0.44	-	0.30	0.18	-0.53	-0.79	-0.77	-0.92**	-0.79	0.94**	-0.59	-0.29	-0.31
°C	-0.71	-0.99***	1.00	0.65	0.87*	0.18	0.77	0.34	-	-0.28	-0.17	0.61	0.73	0.71	0.91**	0.82*	-0.95**	0.68	0.39	0.39
SPC (µScm)	-0.53	-0.74	0.65	1.00	0.89**	0.84*	0.88**	0.88**	-	0.04	-0.46	-0.08	0.86*	0.83*	0.83*	0.84*	-0.65	-0.10	-0.38	-0.24
$[Fe]_D$ mg/L	-0.63	-0.92**	0.87*	0.89**	1.00	0.61	0.97***	0.71	-	-0.18	-0.15	0.37	0.95**	0.93**	0.92**	0.73	-0.78	0.31	-0.08	-0.06
$[As]_D$	0.32	-0.30	0.18	0.84*	0.61	1.00	0.70	0.97***	-	0.31	-0.39	-0.41	0.71	0.70	0.32	0.01	-0.15	-0.57	-0.83**	-0.69
$[Co]_D$	-0.63	-0.82*	0.77	0.88*	0.96***	0.70	1.00	0.82*	-	0.03	-0.17	0.33	0.99***	0.99***	0.89**	0.70	-0.64	0.16	-0.27	-0.28
$[Cu]_D$	-0.61	-0.44	0.34	0.88**	0.71	0.96***	0.82*	1.00	-	0.39	-0.43	-0.23	0.81*	0.81*	0.47	0.19	-0.28	-0.42	-0.73	-0.64
$[Ag]_D$	-	-	-	-	-	-	-	-	-	-	-	-	-	-	-	-	-	-	-	-
$[Ni]_D$	-0.55	0.30	-0.28	0.04	-0.18	0.31	0.03	0.39	-	1.00	-0.58	-0.34	0.00	0.03	-0.24	-0.29	0.28	-0.56	-0.54	-0.54
$[As]^{Total}$ µmol/g	-0.62*	0.18	-0.17	-0.46	-0.15	-0.39	-0.17	-0.43	-	-0.58	1.00	0.50	-0.09	-0.06	0.09	0.32	0.36	0.34	0.21	-0.02
$[Co]^{Total}$ µmol/g	-0.97***	-0.53	0.61	-0.08	0.37	-0.41	0.33	-0.23	-	-0.34	0.50	1.00	0.34	0.36	0.70	0.90**	-0.42	0.88**	0.61	0.37
$[Cu]^{Total}$ µmol/g	-0.63	-0.79	0.73	0.86*	0.95**	0.71	0.99***	0.82*	-	0.00	-0.09	0.34	1.00	0.99***	0.89**	0.71	-0.58	0.15	-0.30	-0.33
$[Ag]^{Total}$ µmol/g	-0.63	-0.77	0.71	0.83**	0.94**	0.70	0.99***	0.81*	-	0.03	-0.06	0.36	0.99***	1.00	0.88**	0.72	-0.54	0.14	-0.32	-0.37
$[Ni]^{Total}$ µmol/g	-0.76*	-0.91**	0.91**	0.82**	0.92**	0.32	0.89**	0.47	-	-0.24	0.09	0.70	0.89**	0.88**	1.00	0.94**	-0.75	0.58	0.16	0.07
$[Fe]^{Total}$ g/g	-0.92**	-0.79	0.81*	0.84**	0.73	0.01	0.70	0.19	-	-0.29	0.32	0.90**	0.71	0.72	0.94**	1.00	-0.62	0.75	0.35	0.17
FeOOH (g/g)	0.54	0.94**	-0.95**	-0.65	-0.78	-0.15	-0.64	-0.28	-	0.28	0.36	-0.42	-0.58	-0.54	-0.75	-0.62	1.00	-0.61	-0.40	-0.42
Organic C (g/g)	-0.86*	-0.59	0.68	-0.10	0.31	-0.57	0.16	-0.42	-	-0.56	0.34	0.88**	0.15	0.14	0.58	0.70	-0.61	1.00	0.88**	0.77*
$[Mn]_A$ µmol/g	-0.58	-0.29	0.39	-0.38	-0.08	-0.83**	-0.27	-0.73	-	-0.54	0.21	0.61	-0.30	-0.32	0.16	0.35	-0.45	0.87**	1.00	0.95**
$[Mn]_C$ µmol/g	-0.36	-0.31	0.39	-0.24	-0.06	-0.69	-0.28	-0.64	-	-0.54	-0.02	0.37	-0.33	-0.37	0.07	0.17	-0.53	0.75	0.94**	1.00

*** signifance $\alpha \leq 0.01$
** signifance $\alpha \leq 0.05$
* signifance $\alpha \leq 0.1$

3.5 References

(1) Droppo, I. G. Rethinking what constitutes suspended sediment. Hydrol. Processes 2001, 15 (9), 1551–1564.

(2) Milligan, T. G.; Hill, P. S. A laboratory assessment of the relative importance of turbulence, particle composition, and concentration in limiting maximal floc size and settling behaviour. J. Sea Res. 1998, 39, 227–241.

(3) Liss, S. N.; Droppo, I. G.; Flannigan, D. T.; Leppard, G. G. Floc architecture in waste-water and natural riverine systems. Environ. Sci. Technol. 1996, 30, 680–686.

(4) Costerton, J. W.; Cheng, K. L.; Geesey, G. G.; Ladd, T.; Nickel, J. C.; Dasgupta, M.; Marrie, T. J. Bacterial biofilms in nature and disease. Annu. Rev. Microbiol. 1987, 41, 35–464.

(5) Droppo, I. G.; Leppard, G. G.; Flannigan, D. T.; Liss, S. N. The freshwater floc: A functional relationship of water and organic and inorganic floc constituents affecting suspended sediment properties. Water, Air, Soil Pollut. 1997, 99 (1-4), 43–53.

(6) Plach, J. M.; Elliott, A. V. C.; Droppo, I. G.; Warren, L. A. Physical and ecological controls on freshwater floc trace metal dynamics. Environ. Sci. Technol. 2011, 45, 2157–2164.

(7) Droppo, I. G. Structural controls on floc strength and transport. Can. J. Civ. Eng. 2004, 31, 569–578.

(8) Leppard G. G. Evaluation of electron microscopic techniques for the description of aquatic colloids. In Environmental Particles; 1992; Vol. 1, pp 231_289.

(9) Chan, C. S.; Fakra, S. C.; Edwards, D. C.; Emerson, D.; Banfield, J. F. Iron oxyhydroxide mineralization on microbial extracellular polysaccharides. Geochim. Cosmochim. Acta 2009, 73, 3807–3818.

(10) Lovley, D. R.; Holmes, D. E.; Nevin, K. P. Dissimilatory Fe(III) and Mn(IV) reduction. In Advances in Microbial Physiology; 2004; Vol. 49, pp 219-286.

(11) Warren, L. A.; Haack, E. A. Biogeochemical controls on metal behaviour in freshwater environments. Earth Sci. Rev. 2001, 54, 261–320.

(12) Small, T. D.; Warren, L. A.; Roden, E. E.; Ferris, F. G. 1999. Sorption of strontium by bacteria, Fe(III) oxide and bacteria-Fe(III) oxide composites. Environ. Sci. Technol. 1999, 33, 4465–4470.

(13) Laurent, J.; Casellas, M.; Dagot, C. Heavy metals uptake by sonicated activated sludge: Relation with floc surface properties. J. Hazard. Mater. 2009, 162 (2_3), 652–660.

(14) Stecko, J. R. P.; Bendell-Young, L. I. Contrasting the geochemistry of suspended particulate matter and deposited sediments within an estuary. Appl. Geochem. 2000, 15, 753–775.

(15) Sondi, I.; Juracic, M.; Prohic, E.; Pravdic, V. Particulates and the environmental capacity for trace-metals- a small river as a model for a land-sea transfer system- the rasa river estuary. Sci. Total Environ. 1994, 155, 173–185.

(16) Santiago, S.; Thomas, R. L.; Larbaigt, G.; Corvi, C.; Rossel, D.; Tarradellas, J.; Gregor, D. J.; McCarthy, L.; Vernet, J. P. Nutrient, heavy-metal and organic pollutant composition of suspended and bed sediments in the Rhone river. Aquat. Sci. 1994, 56, 220–242.

(17) Cambell, P. F. C.; Lewis, A. G.; Chapman, P. M.; Crowder, A. A.; Fletcher, W. K.; Inber, B.; Luoma, S. N.; Stokes, P. M.; Winfrey, M. Panel on biologically available metals in sediments; PUB. No.BRCC27694. National Research Council of Canada: Ottawa, pp 3-27.

(18) Environment Canada. Analytical methods manual; Inland Waters Directorate, Water Quality Branch: Ottawa, 1979.

(19) Eaton, A. D.; Clesceri, L. S.; Rice, E. W.; Greenberg, A. E. Standard methods for the examination of water and wastewater; American Public Health Association, American Water Works Association, Water Environment Federation, Port City Press: Baltimore, MD, 2005.

(20) Haack, E. A.; Warren, L. A. Biofilm hydrous manganese oxyhydroxides and metal dynamics in acid rock drainage. Environ. Sci. Technol. 2003, 37, 4138–4147.

(21) Toner, B. M.; Santelli, C. M.; Marcus, M. A.; Wirth, R.; Chan, C. S.; McCollom, T.; Bach, W.; Edwards, K. Biogenic iron oxyhydroxide formation at mid-ocean ridge hydrothermal vents: Juan de Fuca Ridge. Geochim. Cosmochim. Acta 2009, 15, 388–403.

(22) Jackson, T. A.; West, M. M.; Leppard, G. G. Accumulation and partitioning of heavy metals by bacterial cells and associated colloidal minerals, with alteration, neoformation, and selective adsorption of minerals by bacteria, in metal-polluted lake sediment. Geomicrobiol. J. 2011, 28, 23–55.

(23) Cornell, R. M.; Schwertmann, U. The iron oxides: Structure, properties, reactions, occurrence and uses; VCH Verlagsgesellschaft mbH: Germany, 1996.

(24) Tessier, A.; Fortin, D.; Belzile, N.; DeVitre, R. R.; Leppard, G. G. Metal sorption to diagenetic iron and manganese oxyhydroxides and associated organic matter: narrowing the gap between field and laboratory measurements. Geochim. Cosmochim. Acta 1996, 60, 387–404.

(25) Chan, C. S.; De Stasio, G.; Welch, S. A.; Girasole, M.; Frazer, B. H.; Nesterova, M. V.; Fakra, S.; Banfield, J. F. Microbial polysaccharides template assembly of nanocrystal fibers. Science 2004, 303, 1656–1658.

(26) Dong, D. M.; Nelson, Y. M.; Lion, L. W.; Shuler, M. L.; Ghiorse, W. C. Adsorption of Pb and Cd onto metal oxides and organic material in natural surface coatings as determined by selective extractions: new evidence for the importance of Mn and Fe oxides. Water Res. 2000, 34 (2), 427–436.

(27) Kennedy, C. B.; Scott, S. D.; Ferris, F. G. Hydrothermal phase stabilization of 2-line ferrihydrite by bacteria. Chem. Geol. 2004, 212, 269–277.

(28) Schwertmann, U.; Wagner, F.; Knicher, H. Ferrihydrite-humic associations magnetic hyperfine interactions. Soil Sci. Soc. Am. J. 2005, 69, 1009–1015.

(29) Belzile, N.; Tessier, A. Interactions between arsenic and iron oxyhydroxides in lacustrine sediments. Geochim. Cosmochim. Acta 1990, 54, 103–109.

(30) Li., Y.; Wang, X. L.; Huang, G. H.; Zhang, B. Y.; Guo, S. H. Adsorption of Cu aand Zn onto Mn/Fe oxides and organic materials in the extractable fractions of river surficial sediments. Soil Sediment Contam. 2009, 18, 87–101.

(31) Droppo, I. G.; Liss, S. N.; Williams, D.; Nelson, T.; Jaskot, C.; Trapp, B. Dynamic existence of waterborne pathogens within river sediment compartments. Implications for water quality regulatory affairs. Environ. Sci. Technol. 2009, 43, 1737–1743.

(32) Guibaud G.; van Hullebusch, E.; Bordas, F.; s'Abzac, P.; Joussein, E. Sorption of Cd(II) and Pb(II) by exopolymeric substances (EPS) extracted from activated sludges and pure bacterial strains: Modeling of the metal metal/ligand ratio effect and role of the mineral fraction. Bioresour. Technol. 2009, 100 (12), 2959-2968.

(33) Dade, W. B.; Self, R. L.; Pellerin, N. B.; Moffet, A.; Jumars, P. A.; Norwell, A. R. M. The effects of bacteria on the flow behavior of clayseawater suspensions. J. Sediment. Res. 1996, 66, 39–42.

(34) Droppo, I. G.; Ongley, E. D. Flocculation of suspended sediment in rivers of southeastern Canada. Water Res. 1992, 28, 65–72.

(35) Mavrocordatos, D.; Fortin, D. Quantitative characterization of biotic iron oxides by analytical electron microscopy. Mineral. Soc. Am. 2002, 87, 940–946.

(36) Stumm, W.; Morgan, J. J. Aquatic Chemistry: Chemical Equilibria and Rates in Natural Waters, 3rd ed.; Wiley: New York, 1996.

(37) Munk, L; Faure, G. Effects of pH fluctuations on potentially toxic metals in the water and sediment of the Dillon Reservoir, Summit County, Colorado. Appl. Geochem. 2004, 19, 1065–1074.

(38) Grassi, M. T.; Shi, B.; Allen, H. E. Sorption of copper by suspended particulate matter. Colloids Surf, A 1997, 120 (1-3), 199–203.

CHAPTER 4: COLLABOARTIVE MICROBIAL FE REDOX CYCLING BY PELAGIC FLOC BATERIA ACROSS DIVERSE OXYGENATED AQUATIC SYSTEMS

Elliott, A.V.C., Plach, J.M., Droppo, I.G., and Warren, L.A
In review, Chemical Geology

ABSTRACT

$Fe^{(III)}$-reducing bacteria (IRB) and $Fe^{(II)}$-oxidizing bacteria (IOB) significantly impact the transformations and geochemical cycling of Fe. As these bacteria are thought to be differentially segregated to specific environments reflecting oxygen and pH restrictions on their respective metabolisms, their impacts on Fe biogeochemistry in pelagic environments has not been well investigated. Here we report the novel discovery of cooperative Fe-redox cycling bacterial consortia from diverse oxygenated ($O_2^{Sat.}$=1-103%), circumneutral freshwaters occurring within floc. Favourable microscale conditions are engineered through consortial aggregate formation, enabling both metabolisms within floc and thus the macroscale expansion of aero-intolerant IRB and IOB activity into presumed inhospitable oxic waters. Both environmental and experimentally enriched floc Fe metabolizing consortia included aero-intolerant IRB and microaerobic IOB together with oxygen-consuming organotrophic species. Genetically identified floc IOB and IRB differ from those associated with sediment/groundwater (IRB) and seep (IOB) habitats, indicating a likely greater environmental occurrence and diversity of Fe-bacteria than currently considered. These results identify a collaborative Fe-cycling strategy through aggregate formation and cooperation with aerobic species that substantively extends the potential environmental range of IRB-IOB impact on Fe geochemical cycling. Supporting this notion, experimental microcosm IRB-IOB-aerobe consortial aggregates generated unusual assemblages of co-occurring reduced and oxidized Fe minerals, not predicted by treatment oxygen levels, but also observed in environmental pelagic aggregate samples from similar system O_2 levels. These findings have large implications for the use of Fe minerals as geochemical proxies to constrain the chemistry and infer the history of atmospheric O_2 on early Earth and highlights that that the implementation of geochemical thermodynamic constraints alone as a guide to investigating and interpreting microbe-geosphere interactions may not accurately capture processes occurring *in situ*.

4.1 Introduction

Iron (Fe) is the fourth most abundant element on the Earth's surface, with $Fe^{(III)}/Fe^{(II)}$ redox transformations tied to the major biogeochemical cycles of other important elements including carbon, nitrogen and sulfur[1-4] and thus to planetary function. As redox transformations of Fe are often linked to physical transformations of associated minerals and Fe-bearing mineral phases, Fe-redox cycling also represents a major regulator of the bioavailability and ultimate fate of both inorganic contaminants (e.g. arsenic) and essential nutrients (e.g. PO_4^{2-}) within the biosphere [5-7]. The transformation of Fe in the major global pools is seen as the consequence of geologic processes over millions of years of Earth history, and microorganisms mediating $Fe^{(III)}/Fe^{(II)}$ redox cycling are deeply rooted in the universal phylogenetic tree, implicated in planetary biogeochemistry during the Archaean and early Proterozoic Eons e.g. [8, 9]. Thus microbes involved in Fe metabolism, having survived the shift from anoxic to widespread oxic conditions associated with planetary evolution, may have accordingly developed adaptive strategies enabling colonization and proliferation in the new oxygenated world.

However, in modern ecosystems, the prevailing paradigm is that $Fe^{(III/II)}$-redox cycling bacteria only occur in a select range of 'niche' environments due to perceived geochemical restrictions thought to differentially restrict where these organisms can sustain their metabolism. This has directed scientific investigation and accordingly our understanding of the biogeochemical Fe-redox cycle (Figure 4.1; i.e. discounting the oxygenated pelagic regions of aquatic systems). Specifically, dissimilatory $Fe^{(III)}$-reducing bacteria (IRB) activity is thought to be important only under bulk anoxic conditions (e.g. anoxic groundwater, non-sulfogenic hypolimnetic sedimentary zones) due to metabolic inhibition and toxicity by O_2 [10, 11]. Similarly, lithotrophic $Fe^{(II)}$-oxidizing bacteria (IOB) activity is considered exclusively restricted to pH <3.0 (e.g. acid mine drainage, [12] or to anoxic to low redox boundaries such groundwater seeps, the rhizosphere of wetland plants and biogenic iron oxyhydroxide (BIOS) mat communities [13-16] where IOB metabolism can compete with abiotic $Fe^{(II)}$oxidation [17-19]. Thus, the existence, ecology and potential geochemical roles for Fe-metabolizing bacteria, IRB and IOB,

in bulk oxygenated pelagic waters are unknown. Moreover, due to these differential restrictions on IRB (no O_2) and IOB (low O_2) metabolism, they are classically thought to occur in segregated environmental contexts, limiting the possibility of their co-occurrence and thus the potential for widespread, coupled microbial $Fe^{(III/II)}$-redox cycling. Such a strategy would have ecological benefits as well as biogeochemical ramifications.

An important emergent principle of geomicrobiology is that bacteria rarely interact with their environment in isolation; rather, they exist as multi-guild cooperatives within consortial aggregates[20-22] or biofilm communities[23-26]. In this manner, diverse lineages of environmental bacteria intimately co-exist and collectively influence biogeochemical cycling. Such cooperative adaptive strategies have been identified coupling anaerobic bacterial sulfur (S^0) reduction with autotrophic, oxygen-driven reduced sulfur oxidation in AMD consortial aggregates [27] as well as within marine methane and nitrogen metabolizing microbial consortia aggregates [20, 28]. Further, aggregate structures also allow for environmental microbial communities to cooperatively 'engineer' their immediate environment, providing hospitable microenvironments under bulk conditions thought to be toxic or inhibitory to sustainable substrate supplies[20, 21, 27, 29-31]. Thus environmental aggregates may well be important structures supporting Fe metabolism outside of classical geochemical niche environments. Indeed, emerging results from marine snow and "iron snow" aggregates in lakes of acid mine drainage systems indicate that Fe metabolizing bacteria can occur in pelagic systems, typically associated with diverse communities [32, 33].

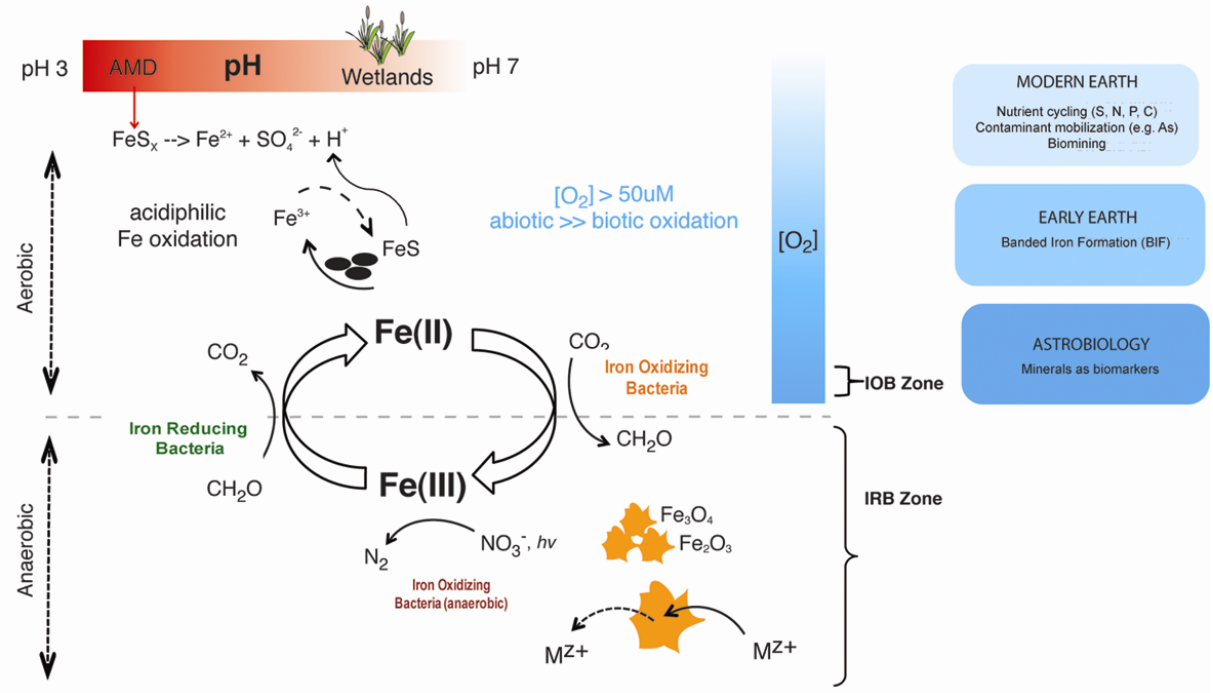

Figure 4.1. Geochemical niche of known $Fe^{(III/II)}$-redox cycling bacteria. The biogeochemical redox cycling of Fe has important implications for both ancient and modern planetary biogeochemistry as a control over Fe mobility, bioavailability and metal (M^{z+}) contaminant mobilization/sequestration reactions. However, $Fe^{(III/II)}$-redox cycling bacteria (IRB, IOB) are currently thought to be differentially segregated to a select range of geochemical 'niche' environments (i.e. O_2 ≤50µM or pH≤3.0). At pH>3.0, the rapid abiotic oxidation of $Fe^{(II)}$ by O_2 outcompetes microbial IOB catalysis of $Fe^{(II)}$ oxidation, limiting opportunity for survival. Similarly, IRB activity is restricted to anoxic conditions due to metabolism inhibition and toxicity of molecular oxygen. This has directed scientific investigation to date and accordingly our understanding of the biogeochemical Fe-redox cycle. However this view discounts the capacity of environmental bacterial communities to collectively engineer their immidate microenvironment through the creation of aggregates or biofilms; thus IRB and IOB may have a greater biogeography and importance to the global biogeochemical Fe-redox cycle than is currently appreciated.

The focus of this investigation was thus to evaluate whether iron-oxidizing bacteria (IOB) and iron-reducing bacteria (IRB) co-occur within in pelagic freshwater aggregates (here, 'flocs'). Flocs are complex aggregates of fine-grained inorganic particles (e.g. clays, silts, oxyhydroxides and carbonate minerals) within a network of active microbial communities and organics derived from microbial metabolism suspended within the water column [34, 35]. While floc structure, size and composition can vary considerably across aquatic systems and energy regimes[36-39] what is common among floc is the underlying microbial nature of their formation and stabilization, with bacterial-produced EPS acting as the dominant physical bridging mechanism between the floc components- microbial, mineral and organic [34, 35, 38]. Further, recent work has shown lacustrine floc aggregates to be extremely Fe rich with highly viable resident floc microbial communities driving the collection/nucleation of highly reactive amorphous $Fe^{(III)}$-oxyhydroxide minerals [39, 40]. This is similar to what has been observed within BIOS mat communities, a Fe-bacteria rich habitat[41, 42]. Thus flocs represent a highly attractive habitat for Fe metabolizing bacteria. Microbial $Fe^{(III/II)}$-redox cycling within oxygenated circumneutral freshwater pelagic flocs would require a syntrophic cooperative strategy to engineer favourable, intra-aggregate anoxic conditions required for IRB, and the maintenance of a stable IRB-produced $Fe^{(II)}$ source to sustain neutrophilic IOB metabolism. This would likely be facilitated by the extensive EPS network observed in freshwater flocs, limiting O_2 penetration in a manner similar to the identified role of EPS in preventing oxygenic-mediated inhibition of nitrogen fixation in *Cyanobateria*, and in marine snow aggregates[30, 43]. The generation of interior floc low-oxygen microenvironments would be further enhanced by O_2 consumption by floc-associated aerobic heterotrophic bacteria (e.g. [44, 45]). Decoupling the floc interior in this manner from bulk system oxygenated conditions would thus confer the functional capability of aero-intolerant floc IRB and $Fe^{(II)}$ requiring IOB bacteria to circumvent geochemical constraints that are predicted to preclude their survival under bulk oxic conditions. We hypothesized that this is indeed the case, and that freshwater pelagic floc would have co-occurring IRB and IOB across a wide range of O_2 concentrations from microoxic ($O_2^{Sat.}$= 1.0%) to

fully oxygenated ($O_2^{Sat.}$= 103%), enabled by the floc aggregate structure. We further hypothesized that Fe biominerals associated with floc would reflect these intra-floc micro-geochemical environments rather than bulk system oxygen levels. Thus the objectives of this field and experimental study were to: 1) determine if IRB and IOB co-occur in environmental pelagic floc collected from systems ranging from 1% O_2 saturation to 100% saturation and 2) experimentally demonstrate redox cycling of Fe under varying O_2 levels for environmental enrichments from pelagic floc.

4.2. Material and methods

4.2.1 Field investigation. Flocs were collected from diverse freshwater lakes located in the boreal forest and Great Lakes regions of Ontario, Canada (see Table S1 for detailed information on sites): i) pelagic region of Brewer L., a humic-stained, hard-water lake in Algonquin Park (45°35′15″N 78°18′07″W); ii) pelagic region of Coldspring L., a remote, groundwater fed lake, located in a restricted nature preserve area of Algonquin Park (45°85′28″N 78°82′17″W); and iii) the littoral zone of an urban public beach located on the north shore of L. Ontario (Sunnyside Beach, Toronto; 43°38′14″N 79°27′20″W). These sites were specifically chosen as they encompass an environmental gradient of pelagic oxygen conditions (1% to over 100% O_2 saturation), enabling our ability to test the hypothesis that bulk [O_2] will not inhibit floc enabled, coupled Fe redox cycling by co-occurring IRB and IOB directly *in situ*. Sampling campaigns at each site provided watercolumn survey information (Eh, pH, temperature, [O_2]: DataSonde-Surveyor 4A, Hydrolab Corporation, TX) and collected suspended floc samples over the summer of 2010 (14-June through 14-July). Flocs from all sites were collected using continuous flow centrifugation (CFC: Westfalia Model KA 2-06-075) whereby water (>2000L) was pumped (6Lmin^{-1}, 9470rpm) into CFC bowls [39, 40, 46]. Flocs were taken at calm and base flow conditions reflecting the majority of the year when flocs are in "equilibrium" with their flow conditions (i.e. carrying capacity of the flow will support a given floc size) and when settling and re-suspension would be minimal. Within Brewer and Coldspring lakes, flocs were collected simultaneously from two

discrete, non-mixing strata within the water column. Epilimnentic (above photic zone, 3.5m) and hypolimnetic (12.5m) flocs were collected from Brewer L.; metalimnetic (4.5m) and hypolimnetic (7.5m) flocs were collected and Coldspring L. (Table S1). Flocs at Sunnyside beach were collected at 0.5m (Table S1).

After collection, flocs for imaging analyses, culture isolations and laboratory microcosm enrichment experiments were stored at 4°C for a maximum of 12–16h prior to processing in the laboratory. Flocs for environmental community characterizations (16S, described below) and mineralogical analyses (XRD) were immediately frozen on dry ice and stored at -20ºC until processing. Bulk floc organic content was estimated by loss on ignition at 550ºC for 2h (g organic C/ g sediment). Further, transmission electron microscopy (TEM) was performed on environmental floc aggregates in order to visualize floc organic-EPS-bacterial associations and entrapped Fe-minerals within the *in situ* floc consortia network [39, 40]. Ultrastructure visualization of flocs followed a 4-fold multiprepatory technique as described previously [35], which allowed for detailed observations of floc associated cells and EPS. Briefly, ultrathin sections of floc were imaged using a JOEL 1200 Ex II TEMSCAN scanning transmission electron microscope (McMaster University, Canada) in transmission mode at an accelerated voltage of 80 kV. X-ray diffractometry (XRD; Siemens D5005 X-ray diffractometer, McMaster Analytic X-ray Diffraction Facimity, ON, CAN) was used to determine bulk mineralogical composition of flocs as described previously [47, 48].

4.2.2 Isolation and confirmation of targeted Fe-bacteria metabolism.

The objective of this field and laboratory investigation was to evaluate whether iron-oxidizing bacteria (IOB) and iron-reducing bacteria (IRB) co-occur within pelagic flocs across a range of oxygenated freshwater. As universal function genes that would genetically confirm the presence of either $Fe^{(III)}$ respiration or $Fe^{(II)}$ lithoautotrophic metabolic activity are currently lacking (as compared to, for example, dissimilatory sulphate reduction metabolism), the confirmation of these metabolisms required the use of geochemical, microbiological and molecular biological tools to demonstrate floc associated IRB and IOB occurrence and specifically metabolic activity (Figure 4.2). We took a functional biogeochemical

approach at addressing these questions by specifically culturing and characterizing bacterial consortial communities associated with $Fe^{(III)}$-reduction and $Fe^{(II)}$-oxidation activities. Here, the identification and characterization of Fe-bacteria involved (1) the isolation and confirmation of target Fe-metabolism (IRB, IOB) following widely applied targeted isolation approaches (*section 4.2.2.1*) as well as (2) laboratory microcosm co-enrichment experiments comparing $Fe^{(III)}$ and $Fe^{(II)}$ evolution as well as mineral formation associated with Fe-redox cycling consortia from environmental floc under increasing oxygen concentrations (*section 4.2.2.2*).

In the geomicrobiological literature, there is ambiguity surrounding the terms 'isolation' versus 'enrichment' cultures. Here, we use the term 'isolation' to specifically refer to our use of classical, well-accepted isolation protocols for Fe-bacterial metabolism: the opposing gradient tube method (IOB[14,49]) and heterotrophic ferric-iron reduction under strictly anoxic conditions (IRB[50]). Both these metabolic isolation procedures involved restricting available electron donors and acceptors over multiple generations (n>90, over 2 years) to sustain the metabolism of 'isolated' bacteria as well as testing ability to grow on other substrates (Figure 4.2). Positive results from targeted metabolic isolations relative to abiotic controls unequivocally demonstrate the presence of bacteria capable of completing that respective metabolism and these techniques has been used in a variety of recent and important studies on microbial Fe-metabolism (e.g.[51-54]). In contrast, we use the term 'enrichment' to refer to our microcosm experimentation on environmental floc samples (Figure 4.2). The goal of our microcosm enrichments was to test whether floc IRB and IOB could be simultaneously *co-enriched* from the same environmental floc samples under increasingly oxygenated concentrations and thus, in turn, provide insight into how aero-tolerant IOB and IRB operate under environmentally relevant (i.e. oxygenated) conditions. This is distinct from previous investigations in which separately isolated IOB and IRB from different environmental contexts are then experimentally added together to assess coupled microbial Fe redox (e.g. [13, 55]) and also from studies employing *in situ* observations and environmental sequencing of bulk communities to infer coupled IRB and IOB activity e.g. [32, 42].

4.2.2.1. Targeted Fe-bacteria isolation. Neutrophilic, microaerobic, $Fe^{(II)}$-oxidizing bacteria (IOB) were isolated using a modified gradient tube method [14, 49]. Opposing gradients of oxygen and $Fe^{(II)}$ (as $FeCl_2$) were created in screw-top glass vials (50mm x16 mm) and an aliquot of floc (~50 µL) was inoculated along a vertical axis, which allowed floc IOB to grow at the manufactured anoxic-oxic interface. Solid phase Fe-oxide bands were allowed to develop for ~4 weeks before approximately 10% of the band was extracted and similarly inoculated into a fresh gradient tube [54]. Negative controls were created both by i) inoculation with gamma-sterilized floc samples, and ii) empty (i.e. sample-free) tubes. Isolation of anaerobic, dissimilatory $Fe^{(III)}$-reducing bacteria (IRB) was accomplished using a modified *Shewanella putrefaciens* specific liquid media (pH=6.0, anoxic, 10mM $Fe^{(III)}$ (as Fe(III)-citrate), 10mM acetate) in the dark, as described previously[50]. Positive enrichments were scored on the evolution of $Fe^{(II)}$ (ferrozine assay[56, 57]) and colour change of the medium that accompanied microbial $Fe^{(III)}$-reduction[50,58]. All cultivated floc-IRB isolates (n>90 generations over two years) garnered in this investigation also metabolize synthetic solid-phase $Fe^{(III)}$ as ferrihydrite ($FeOOH^{Amorphous}$)[50]. Negative controls were created both by i) inoculation with gamma-sterilized floc samples, and ii) empty (i.e. sample-free) media.

Floc IOB and IRB isolated in this manner were identified by 16S rRNA sequencing and subsequent phylogenetic analysis. DNA from all cultured isolates from all sites were extracted in duplicate using the PowerSoil™ DNA Isolation Kit (Mo Bio Laboratories, Carlsbad, CA, USA) from excised Fe-oxide bands (IOB) or filtered solids (>0.22µm) (IRB) following the manufacturer-supplied protocols. Universal bacterial primers 27F and 1492R were used to amplify nearly the complete 16S rRNA gene and were subsequently purified with the QIA-quick PCR Purification kit (Qiagen) and ligated into the linear Plasmid Vector pCR4 supplied with the TOPO TA kit (Invitrogen). Cloning efficiency was improved by the addition of 3' A-overhangs post-amplification. Final products were transformed into One Shot Chemically Competent *Escherichia coli* (Invitrogen) by heat shock following the manufacturer's protocol. Sequencing was completed with ABI BigDye terminator chemistry, using a 3730 DNA analyzer (Applied Biosystems,

Foster City, CA and Institute for Molecular Biology and Biotechnology, McMaster University, ON, Canada). Phylogenetic analyses were conducted using MEGA version 5.0 software [59]. Multiple sequence alignments were accomplished using the MUSCLE algorithm, manually edited and regions of ambiguous alignment removed. Operational taxonomical units (OTUs) were binned at 97% similarity. Identified OTUS were subsequently analyzed against the NCBI (US) database using the mega-BLAST algorithm and also assigned to a taxonomical hierarchy proposed in Bergey's Manual of Systematic of Bacteriology, release 6.0., using the RDP classifier tool[60].The Maximum Likelihood tree-searching method was utilized for phylogenetic tree construction. Resulting phylogram topologies were bootstrapped 1,000 times to assess support for nodes.

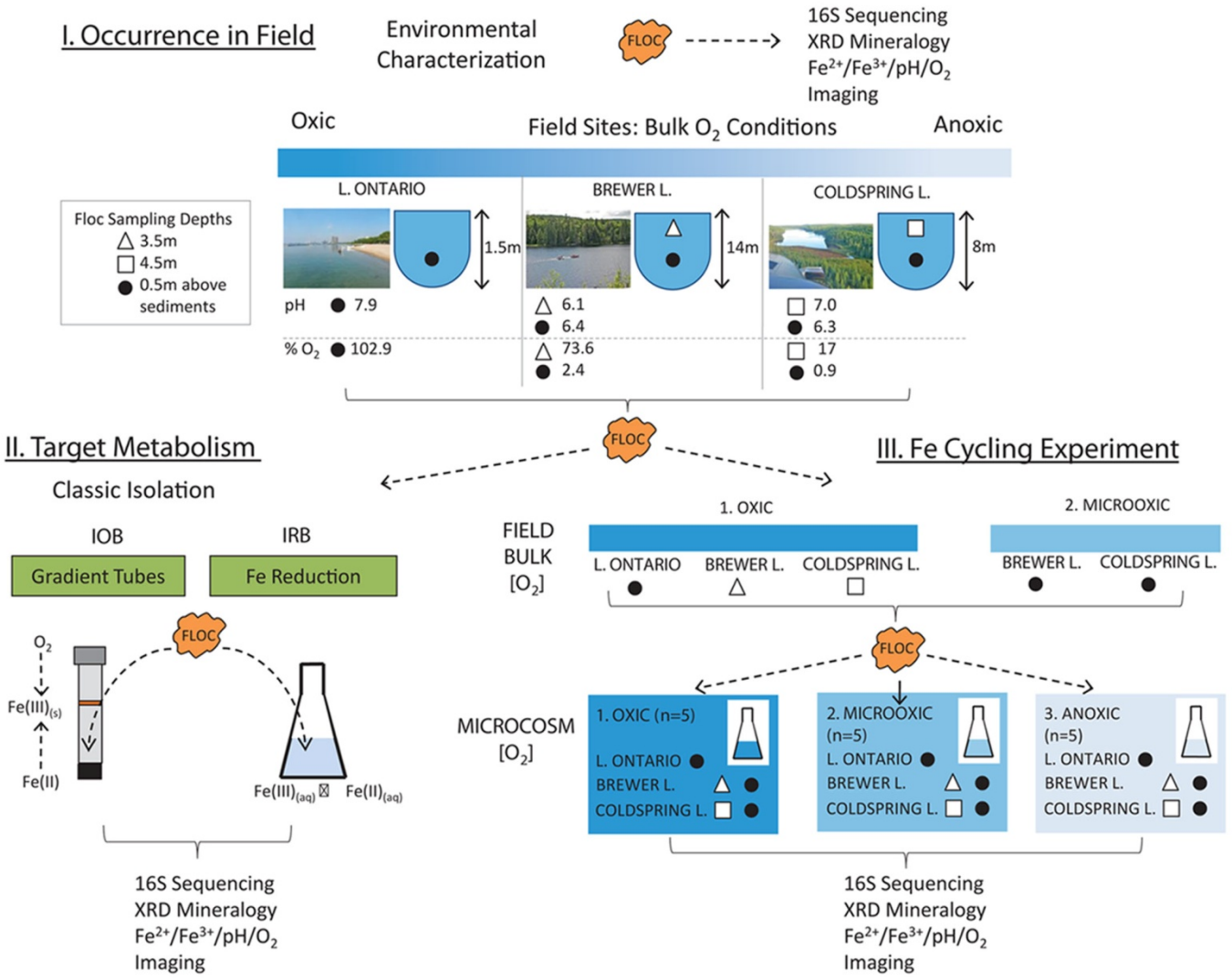

Figure 4.2. Investigation of a floc-hosted microbial Fe-redox wheel in oxygenated waters was completed using an integrated biogeochemical approach and assessed the potential for IRB and IOB activity: **i)** in the field, **ii)** using targeted isolation metabolic techniques, and **iii)** in laboratory microcosm co-enrichment experiments. Classical, isolation techniques were used to specifically cultivate and identify floc-associated IOB and IRB across all field sites and at all depths of sample collection. Laboratory microcosm enrichment experiments were additionally performed on parent floc samples from all sites (n=5, O_2 % Saturation: Brewer L. (epilimnion, 73.6%; hypolimnion, 2.4%;), Coldspring L. (metalimnion, 17%; hypolimnion, 0.9%;) and L. Ontario (littoral, 103%)) and were exposed to three oxygen levels: *anoxic*, $O_2^{Avg.}$= 0 mgL^{-1} ; *microoxic*, $O_2^{Avg.}$=0.19-0.22 mgL^{-1} and *oxic*, $O_2^{Avg.}$=6.0 mgL^{-}

4.2.2.2 Laboratory co-enrichment experiments.

Classic microbiology uses the term 'isolate' to describe a pure bacterial strain derived through axenic cultivation from a bulk community on selective media for a given metabolic pathway, i.e. to allow for the selective isolation of one organism over another. In contrast, 'enrichment' techniques describe the selection of multi-strain consortia or a mixed bacterial culture capable of performing a targeted metabolism (e.g. perchlorate reduction[61]); it is often the goal of classical microbiology, in turn, to physically reduce the diversity within mixed enrichment cultures so as to specifically assign a single organism to a specific metabolic process [62-64]. However, here, as the hypothesis is that syntrophic partnerships of IRB and IOB are required to enable Fe redox cycling in these floc, our goal is not to isolate/ reduce enrichments to pure strains but rather to enrich and sustain a mixed community capable of coupling these two aero-intolerant Fe metabolisms under pelagic (i.e. oxygenated) conditions. Indeed the overwhelming failure of traditional isolation culturing for retrieval of representative bacteria from most natural environmental communities[62, 65, 66] underscores the importance of ecological interactions and potential syntrophy in many relevant biogeochemical processes driven by microbial activity.

To assess microbial Fe-redox cycling by floc bacterial consortia under the range of oxygenated conditions occurring in our field sites, microcosm co-enrichment experiments were performed on environmental parent floc samples collected from all sites, from all depths of floc collection (Figure 4.2). A factorial experimental design was implemented to assess oxygen impact on floc Fe-bacteria under oxic ($O_2^{Average}$ = 6.0 mgL^{-}), microoxic ($O_2^{Average}$ = 0.19-0.22 mgL^{-1}) and anoxic (O_2 = 0 mgL^{-1}) conditions. By exposing each environmental floc sample from the three environmental systems that encompassed 1%-103% O_2 saturation levels to all three experimental O_2 treatment levels, we could then assess bulk oxygen impact on the ability of floc IRB-IOB to survive wide ranging oxygen conditions and whether there were any links between bulk oxygen concentration and floc associated biomineral formation. Experimental microcosms (5 environmental samples X 3 O_2 experimental treatment levels) tracked microbial community

dynamics (16S rRNA, described above), consortia morphology (imaging analyses) and Fe geochemistry ($Fe^{(II)}_{aq}$, $Fe^{(III)}_{aq}$, Fe biomineral formation (XRD)). We hypothesized that, as molecular oxygen is required for coupled IOB-IRB metabolism, floc Fe-bacteria isolates (*section 4.2.2.1*) would be co-enriched only within the oxygenated microcosms. Further, ferrous-Fe accumulation, indicative of IRB-activity, would accumulate in all three treatments. However, [$Fe^{(II)}$] across the experimental treatments would vary reflecting differential ongoing $Fe^{(II)}$-oxidation (both biotic and abiotic) under the three different oxygenated conditions. Thus, a negative-IOB control (i.e. IOB removed from enriched communities by incubation in anaerobic chamber, confirmed via 16S sequencing) comparatively assessed Fe-geochemical outcome (i.e. biominerals formed, $Fe^{(II)}$-accumulation) under oxygenated conditions. We hypothesized that varying experimental O_2 conditions, as well as IOB-removal in "IRB-only" controls, would influence Fe-biominerals formed by the enriched communities; reflecting the active Fe-bacterial metabolisms present as well as the generation of aggregate associated low oxygen/anoxic microenvironments, required to sustain active Fe-metabolism at these experimental oxygenated conditions.

All co-enrichment microcosms were set-up in minimal salts liquid media[50] spiked with acetate (electron donor, 10mM), ferric-$Fe^{(III)}$ (10mM as $Fe^{(III)}$-citrate; i.e. no $Fe^{(II)}$ source provided) and were maintained over multiple successive generations (N>50 over 2 years) in the dark. These $Fe^{(III)}$ and carbon concentrations were chosen i) to represent the relatively high overall total Fe content of *in situ* parent floc samples (up to 113 mg Fe/g floc, 0.6 mg organic C/ g floc; $Fe_{(aq)}$=0.02-9.72 mg/L. Table S1), and ii) to mimic electron donor and acceptor concentrations utilized in recent and important investigations of microbial Fe-redox transformations (e.g.[67-72]). Further, a soluble Fe source (<0.22μm) was used as to allow for the tracking of *in situ* bio-mineral formation within experimental microcosms (i.e. no exogenous Fe-mineral source introduced). Multiple investigations report that different species of IRBs are capable of reducing *both* solid phase and soluble $Fe^{(III)}$; (e.g.[67, 73, 74]) Similarly, all floc Fe-bacterial consortia enriched in laboratory microcosms here with soluble Fe also metabolize synthetic solid-phase $Fe^{(III)}$ as ferrihydrite

($FeOOH^{Amorphous}$). Furthermore, active reduction of soluble phase $Fe^{(III)}$ under oxygenated conditions results in the re-precipitation of ferric-Fe solids[19]. Thus, in addition to ferrous-Fe accumulation within oxygenated microcosms, the transition in speciation of Fe concentrations from soluble to solid phases can also be used as an indicator of Fe-bacterial activity under oxygenated conditions.

Microoxic treatment conditions ($O_2^{Average}$ = 0.19-0.22 mgL^{-1}) were achieved by setting flasks up at a liquid volume to flask volume ratio of 0.88, covered with a double-layer of aluminum foil to permit gas diffusion and left static, which produced similar microoxic conditions in previous studies[27, 50, 75]. Oxic treatment conditions were achieved by placing flasks at 175 r.p.m. on a Forma Orbital Shaker 420 (Controlled Environment Equipment, Marietta, OH, USA) which increase mixing and aeration of the solutions. Anoxic conditions were achieved by incubation in an anaerobic chamber. In the oxic treatments, oxygen concentrations started at 100% saturation and decreased over the first 12-24 hours before stabilizing at O_2^{Oxic} = 6.0 mgL^{-1}. Oxygenated microcosms do not accumulate $Fe^{(II)}$ the absence of acetate. Preservation of Fe-metabolic function (i.e. IOB and IRB activity) during and post the co-enrichment process was intermediately confirmed by re-growth trials in both i) opposing gradient tubes (IOB); and ii) *Shewanella putrefaciens* specific isolation media (IRB) as described above (*section 4.2.2).* Experimental control 'IRB-only systems' were created by eliminating oxygen-consuming members of the floc-consortia by incubation in an anaerobic chamber and was confirmed by 16S sequencing and visualization (fluorescent imaging, absence of IOB-sheathed morphotype).

Co-enrichment community identification (16S rRNA) on all experimental microcosms was completed as described above. In addition, identified sequences of the enrichment community were assigned to one of five putative function categories based on previous isolation results here (*section 4.2.2.1)* as well as documented metabolic capacity of comparison species (BLASTN, RDP): i. aerobe (oxygen reducing chemoorganotrophs and lithoautrophs, excluding IOB); ii. facultative anaerobe (aero-tolerant chemoorganotrophs documented to utilize multiple terminal electron acceptors including molecular oxygen and $Fe^{(III)}$); iii. obligate anaerobe

(aero-intolerant bacteria including fermentative bacteria, sulphate reducing and $Fe^{(III)}$-reducing bacteria); iv. $Fe^{(II)}$-oxidizing (IOB); and v. unclassifiable (Table S3)

4.2.2.3 Imaging analyses.

Environmental Scanning Electron Microscopy (ESEM) of experimental treatments provided visualization of enriched floc Fe-bacteria and the nature of physical consortia structure. Microbial consortia in batch experiments were sampled to preserve cell structural arrangements by gently filtering 1 mL of liquid sample onto sterile polystyrene vacuum column filters. Cells were always kept moist by continuously rising with sterile Mili-Q (200 mL) followed by gently agitating filter paper with Mili-Q (5 mL) to collect flocculated consortial aggregates that were then viewed immediately in an Phillips ElectroScan 2020 ESEM (McMaster University, Hamilton, Canada) operating at 20 kV. Epifluorescence microscopy was used to assess cell viability in microcosms across experimental oxygen regimes using the LIVE/DEAD BacLight Bacterial Viability (Molecular Probes). Samples (~50 µL) were incubated with 6µM SYTO 9 stain and 30 µM propidium iodide (final concentration) for 15min in the dark and spotted onto a gelatin-coated slide [0.25% gelatin and 0.01% KCr(SO4)2]. Slides were viewed using a Leica LEITZ DMRX epifluorescence microscope equipped with HBO 100-W mercury arc lamp [Leica Microsystems (Canada), Richmond Hill, ON] and 525/50, 645/75 nm barriers and 470/40, 560/ 40 nm excitation filters.

4.2.2.4 Geochemical analyses.

Quantification of $Fe^{(II)}$ evolution over the course of the experiment was accomplished by the ferrozine method, as described previously [56, 57]. Quantification of total aqueous Fe (`dissolved`, <0.22µm) and particulate Fe (>0.22µm) was accomplished by colorimetric analysis (Ultraspec 3000, UV/visible, spectrophotometer, Pharmacia Biotech, Cambridge, U.K) by the 1, 10 phenanthroline method (HACH, Co.). Experimental Fe-biomineral formation in microcosms was determined by powder X-ray diffraction (XRD) analysis (Siemens D5005 X-ray diffractometer) [47, 48]. Expected vs. unexpected biomineral assemblages were defined based on modeling on PHREEQC software.

4.3 Results/Discussion

4.3.1 Field observations and geochemistry.

All systems investigated were circumneutral (pH=6.1-7.9) but exhibited large differences in water column oxygen concentration, from microoxic (Coldspring L. hypolimnion= 0.10 mgL^{-1}) to super-saturated (littoral beach= 10.57 mgL^{-1}), as well as large differences in aqueous $Fe^{(II)}$ (0-5.6 mgL^{-1}) and $Fe^{(III)}$ (0.02-4.1 mgL^{-1}) concentrations (Table S1). Based on bulk system pH and O_2 values, only Coldspring L. hypolimnion meets the criteria of co-occurring low O_2 and $Fe^{(II)}$ presumed required to support neutrophilic IOB activity. None would be presumed favourable for active IRB metabolism.

Flocs (particle size, 200-350 µm) collected across sites were highly organic (14- 60% by mass) and Fe rich (13-113 mgg^{-}) (Table S1). Imaging analyses of floc aggregate further revealed consistent associations between resident floc microbial cells and nano-particulate Fe-minerals entrapped within a dense organic network of EPS (Figure 4.3). This apparent entrapment/collection of nano-particulate Fe-minerals by floc organics is consistent with the identified role of floc EPS in previous investigations[39, 40] and would provide both an accessible electron donor (Organic C) and acceptor (Fe) to potential floc IRB. Further, the observed extensive EPS network in these freshwater flocs would also likely limit O_2 penetration in a manner similar to the identified role of EPS in preventing oxygenic-mediated inhibition of nitrogen fixation in cyanobateria and in marine snow aggregates [30, 43]. The generation of interior low-oxygen microenvironments would be further enhanced by aerobic heterotrophic O_2 consumption within the floc aggregate by associated consortial members [76, 77]. This is again similar to the steep gradients in oxygen and pH reported within marine snow and cyanobacterial colonies (marcoscopic aggregates, >1mm), although these aggregates are seldom found to be anoxic unless they already occur in oxygen-minimum zones[30, 31, 33, 44, 78]. The prevention of O_2 penetration would allow for the proliferation of pelagic aero-intolerant Fe-metabolizing bacteria (i.e. IRB, IOB at the floc aggregate scale) under the wide range of bulk oxygen concentrations represented by our field sites.

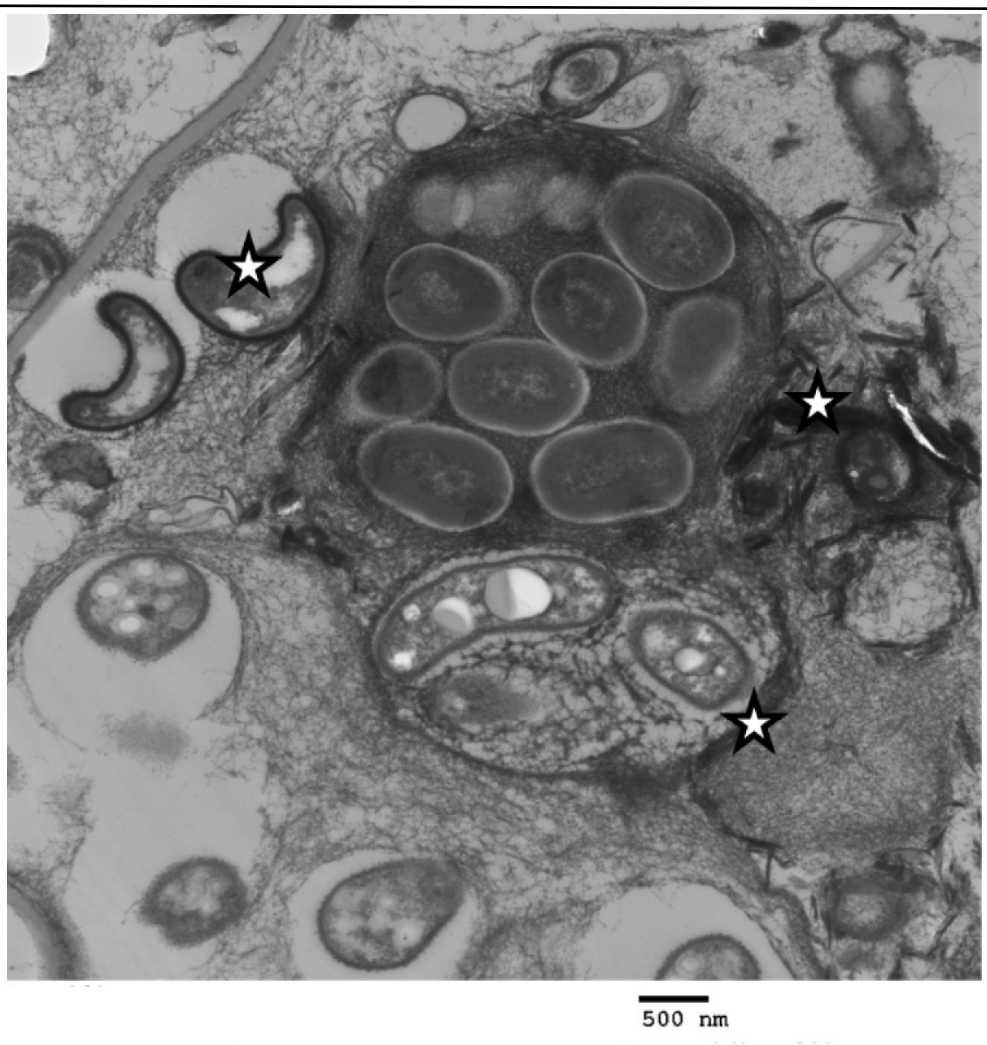

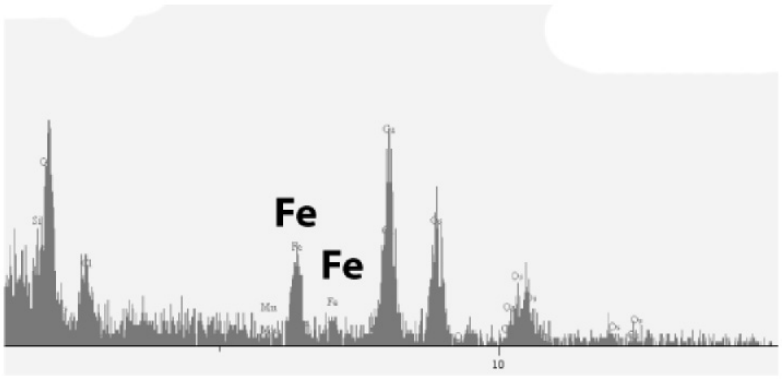

Figure 4.3 Suspended consortial aggregate formation by *in situ* floc bacteria. Aggregation and EPS production affords protection against bulk O_2 concentrations and thus provides a functional capability for the participating microorganisms to effectively circumvent geochemical constraints predicted to restrict their metabolisms at the bulk scale. White stars indicate particulate Fe (EDS).

4.3.2 Isolation of floc IOB and IRB.

Supporting the above hypothesis, classic targeted metabolic isolation techniques (Figure 4.2) reveal the universal presence of cultivable lithotrophic $Fe^{(II)}$-oxidizing (IOB) and heterotrophic $Fe^{(III)}$-reducing (IRB) bacteria in floc across the entire environmental range investigated. Isolated floc-IOB across all sites are restricted to the *Comamonadaceae* family of the *β-Proteobacteria* and closely grouped (Figure 4.4) with the well known filamentous $Fe^{(II)}$-oxidizing bacterium *Leptothrix spp.,* thought to be the most numerically dominant of any IOB in most freshwater environments [79]. In fact, the distinctive morphology and growth habit *in situ* of many neutrophilic IOB (i.e. filamentous sheaths) has often been used specifically for environmental identification of IOB as specific organisms (e.g.[80], [42, 55, 81]), and, further, to study their distribution ([80, 82]). A reason for the common reliance on morphology and growth habit *in situ* for IOB identification is that many species are enigmatic and have resisted laboratory cultivation efforts. Here, ESEM and fluorescent imaging of floc-IOB within isolation cultures similarly reveal a classic neutrophilic morphotype–i.e., sheathed cells, known from *Leptothrix spp.* (Figure 4.4, insert). However, phylogenetic analyses of floc IOB-isolates reveals that floc-IOB do not belong to the *Leptothrix* genus (NCBI, RDP, ML tree); the closest described species was identified as *Comamonas spp.* (>97% of clones). This genus has been previously isolated by gradient tube method from a circumneutral-pH groundwater seep[53] and found associated with BIOS Fe-redox communities[83]. However, this genus has not been previously documented to exhibit a sheathed morphotype. Furthermore, this is the first isolation of this class of IOB outside of geochemical niche environments perceived to be required for their occurrence and indicates a likely far greater environmental occurrence and diversity of sheathed IOB than currently considered.

In contrast to floc-IOB, which showed remarkable OTU consistency across sites, isolated floc-IRB from these field sites did not consist of a single genus (n>90 generations over 2 years) (Figure 4.5). Rather, isolation cultures exhibited consistently high diversity and multiple species composition associated with active Fe^{III} reduction under strictly anoxic conditions (Figure 4.5). Although *Geobacter*

spp. and *Shewenella spp.* have been identified as dominant IRB in anoxic environments (i.e. groundwater and bottom sediments, [84, 85] these genera were not identified in cultured isolates or bulk floc communities from any of the sites (Figure 4.5, Table S4). Here, the pelagically associated, aerobically occurring, floc IRB consisted of *Firmicutes, Bacteroidetes, Acidobacteria* and *α,β,γ,-Proteobacteria* groups.

The isolation and demonstration of both putative IOB and IRB activity from all environmental pelagic samples would not be predicted based on bulk oxygen values of these circumneutral systems ($O_2^{sat.}$=1.0-103%). Although some IRB are known to be aero-tolerant (e.*g. Shewenella spp.*) microbial $Fe^{(III)}$-reduction activity itself is thought to be exclusively restricted to anoxic environments due to metabolic inhibition and toxicity by O_2 [10, 11]. Similarly, the geochemical niche for neutrophilic IOB has a defined upper limit of 50µM dissolved oxygen concentration (i.e. $O_2^{sat.\ 15°C}$ =0.35%) which is based on the redox instability of $Fe^{(II)}$ at near neutral pH [17-19], i.e. rapid abiotic oxidation to $Fe^{(III)}$ eliminates the $Fe^{(II)}$ source required by IOB. Consequently, in order to sustain their respective Fe-metabolism within their parent oxygenated environments (Table S1), these isolated Fe-metabolizing floc bacteria must engage in a cooperative strategy to engineer favourable, intra-floc anoxic conditions required for IRB, and thus maintain a stable IRB-produced $Fe^{(II)}$ source for IOB. Consortial aggregate formation would enable both requirements and, indeed, this cooperative adaptive strategy has been identified coupling anaerobic bacterial sulfur (S^0) reduction with autotrophic, oxygen-driven reduced sulfur oxidation in AMD consortial aggregates [27].

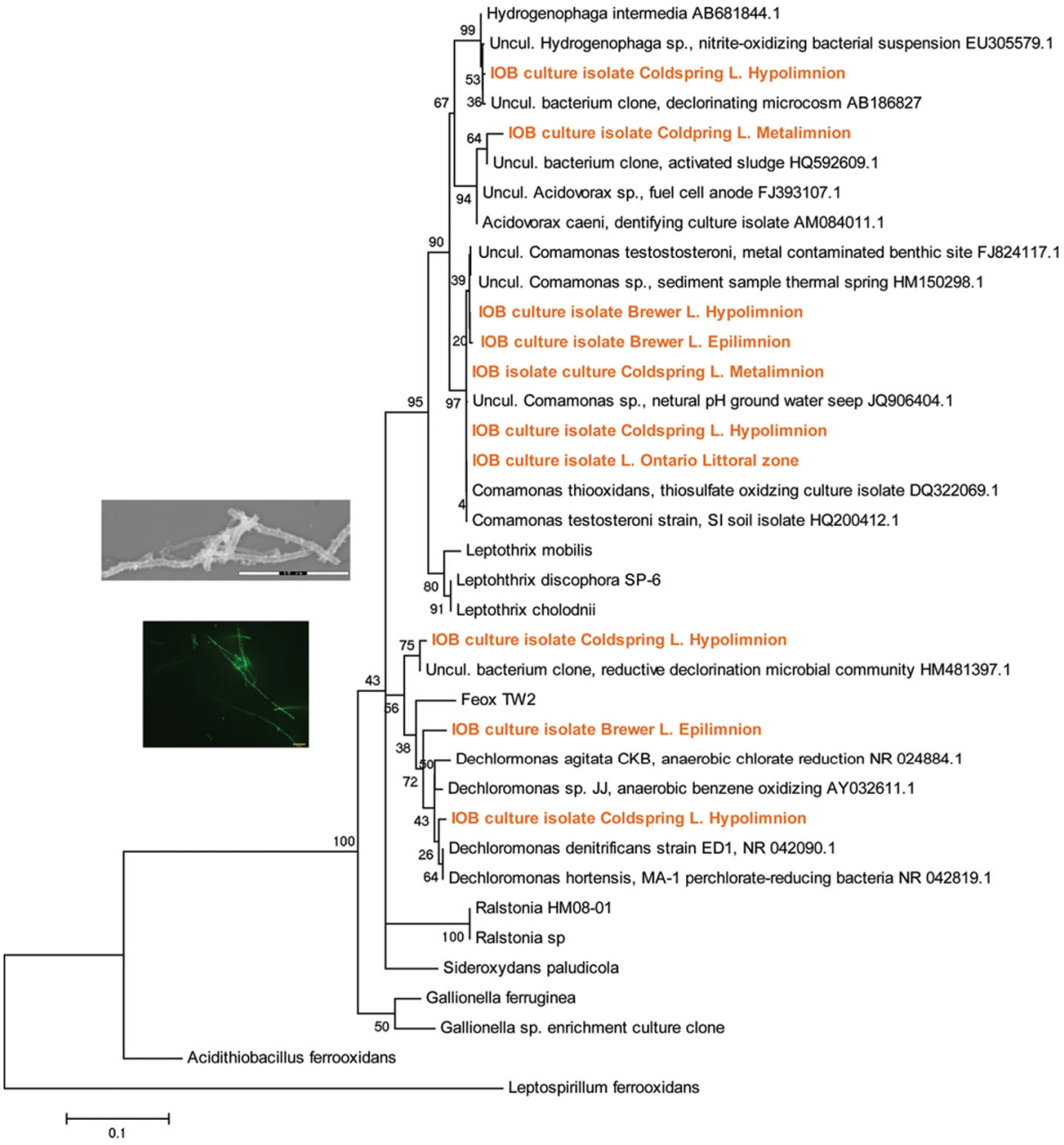

Figure 4.4 Phylogenetic tree (ML) of isolated floc-IOB (bolded orange) relative to classical neutrophilic IOB (black) known from bulk redox interfacial environments as well as acidophilic species. Note that all freshwater neutrophilic IOB isolated to date, including floc-IOB, belong to the β-proteobacteria group. Two species of bacteria known to complete anaerobic $Fe^{(II)}$ oxidation *Dechloromonas sp. and Acidovorax sp*. as well as hydrogen oxidization (*Hydrogenophaga sp*.) were also retrieved from gradient tubes (1-10% of clones)

.

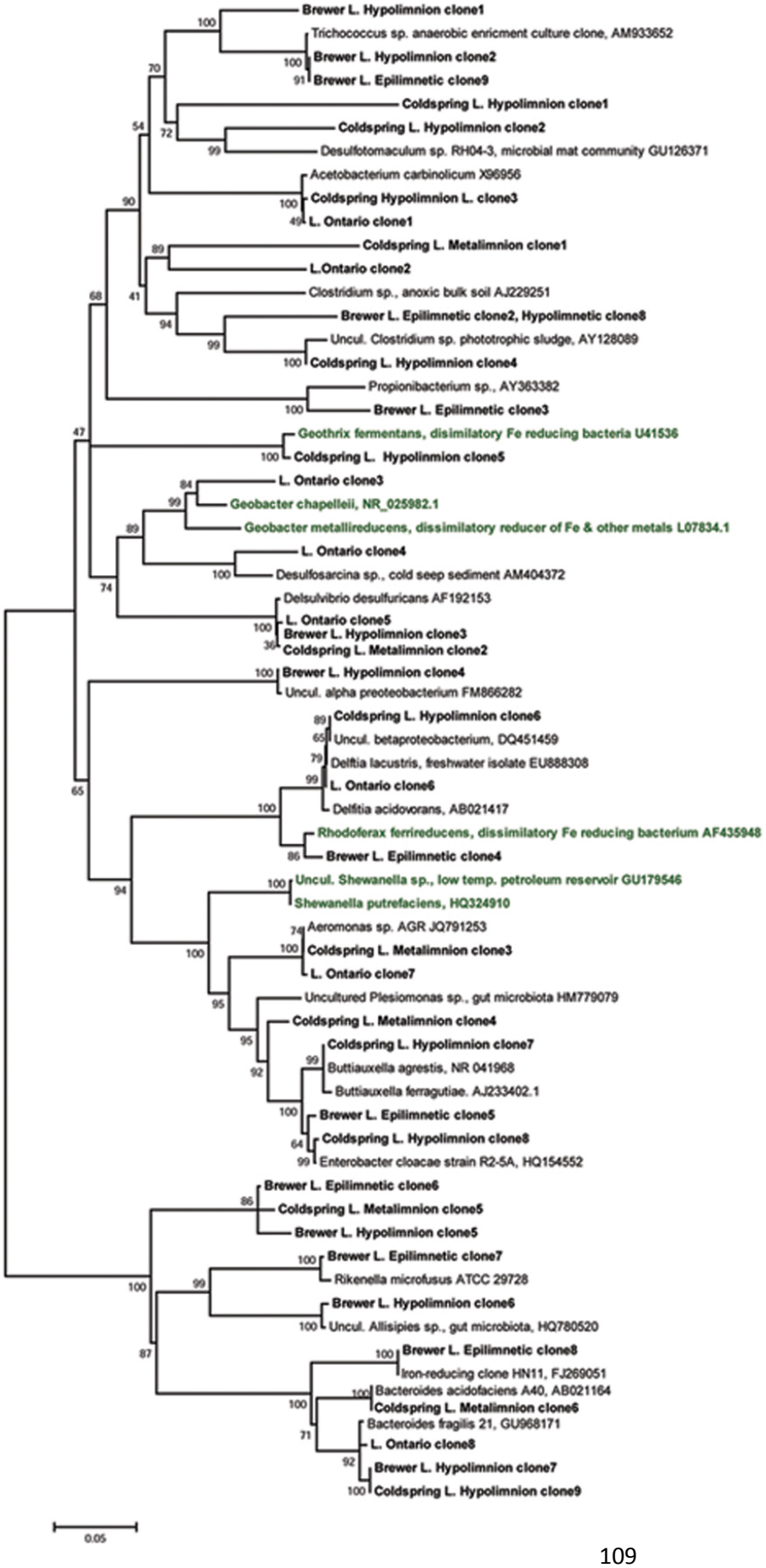

Figure 4.5

Phylogenetic tree (ML) of isolated floc-IRB (bolded black) relative to classical IRB known from bulk anoxic environments (green).

4.3.3 Microcosm co-enrichment experiments.

As the targeted isolation of floc IOB and IRB strains alone does not directly relate to metabolic activity *in situ*, experimental co-enrichment microcosms were utilized to assess the potential for active microbial Fe-redox cycling occurring under the range of oxygenated conditions represented in our field sites (Figure 4.2). Microcosm enrichments for all parent floc were each exposed to the three treatment O_2 levels and were maintained over multiple generations (N>60). As hypothesized, $Fe^{(II)}_{(aq)}$ accumulated in all microcosms and the greatest accumulation of $Fe^{(II)}$ occurred under strictly anoxic conditions (i.e. 100% $Fe^{(III)} \rightarrow Fe^{(II)}$) (Figures 4.5, S2). As also predicted, the microoxic and oxic conditions had varying [$Fe^{(II)}_{aq}$], reflecting co-occurring abiotic and biotic oxidation processes. However, all microcosms completely metabolized the provided soluble $Fe^{(III)}$ source (Figures 4.6, S2). In comparison, no $Fe^{(II)}$ accumulation was observed in any sterilized controls, or in the absence of acetate (i.e. abiotic and fermentative processes unimportant). Thus, the generation of $Fe^{(II)}$ can only be due to IRB-activity; i.e. microbial $Fe^{(III)}$-reduction occurred under anoxic, but also under microoxic and oxic conditions in all microcosms. Both IRB and IOB isolates were also successfully co-enriched and sustained over multiple generations in all microoxic and oxic microcosms for all sites (16S 98-100% identical to cultured isolates) (Figure 4.6, Table S3). Further, these IRB and IOB constituted 33 to 86% of the oxygenated microcosm communities at the time of sampling (% OTUs, Table S3). As no $Fe^{(II)}$ source was initially provided, floc-IOB isolates are thus being co-enriched and sustained (N- 60 generations) by biogenic $Fe^{(II)}$ within experimentally oxygenated conditions. As expected, oxygen-requiring floc-IOB were absent in anoxic microcosms (Figure 4.6, Table S3).

The accumulation of $Fe^{(II)}$ and the proliferation of IOB and IRB over successive generations within both oxygenated treatment conditions for all five environmental floc samples would only be possible if consortial aggregate formation occurred, enabling the development of interior anoxic microenvironments required to sustain anaerobic IRB-activity and a persistent $Fe^{(II)}$ source for microaerobic IOB (i.e. $O_2 \leq 50\mu M$[17]). Imaging analyses of oxygenated treatments confirmed the

presence consortial aggregates (Figures 4.6, S2). Experimental aggregates constituted 30-80µm macrostructures of cell dense and highly viable bacteria with clearly evident sheathed floc-IOB (Figures 4.6, S2). These structures were not observed in anoxic microcosms, indicating molecular oxygen may trigger consortial aggregate formation. Mineralogical analyses of biomineral assemblages associated with experimentally developed consortial aggregates are also consistent with the creation of differentiated microscale conditions and active Fe-redox cycling within oxygenated microcosms (Table 1). The formation and co-existence of both reduced $Fe^{(II)}$-mineral phases (siderite, $Fe^{(II)}$-carbonate; magnetite, mixed $Fe^{(III)}/Fe^{(II)}$ oxide) and oxidized $Fe^{(III)}$-mineral phases (hematite, goethite (microoxic only), $Fe^{(III)}$oxides) was observed. $Fe^{(II)}$-mineral formation is not predicted under these oxygenated conditions (PHREEQC), due to rapid abiotic oxidation and formation of $Fe^{(III)}$, but would be supported by an aggregate interior anoxic zone. Further, in comparison, 'IRB-only' control microcosms (i.e. IOB-members eliminated from floc consortia by incubation in anaerobic chamber, confirmed by 16S sequencing) grown under microoxic conditions resulted in the precipitation of vivianite ($Fe^{(II)}$-phosphate), pyrite ($Fe^{(II)}$-sulfide), a higher proportion of siderite (23% in IRB-only vs. 2% in microoxic microcosms with IRB-IOB), and decreased deposition of nano-particulate amorphous $Fe^{(III)}$ (Table 1). This suggests that floc-IOB may be depleting the aqueous $Fe^{(II)}$ pool within experimental microcosms and thus preventing formation of ferrous minerals and/or utilizing ferrous minerals directly as metabolic substrates.

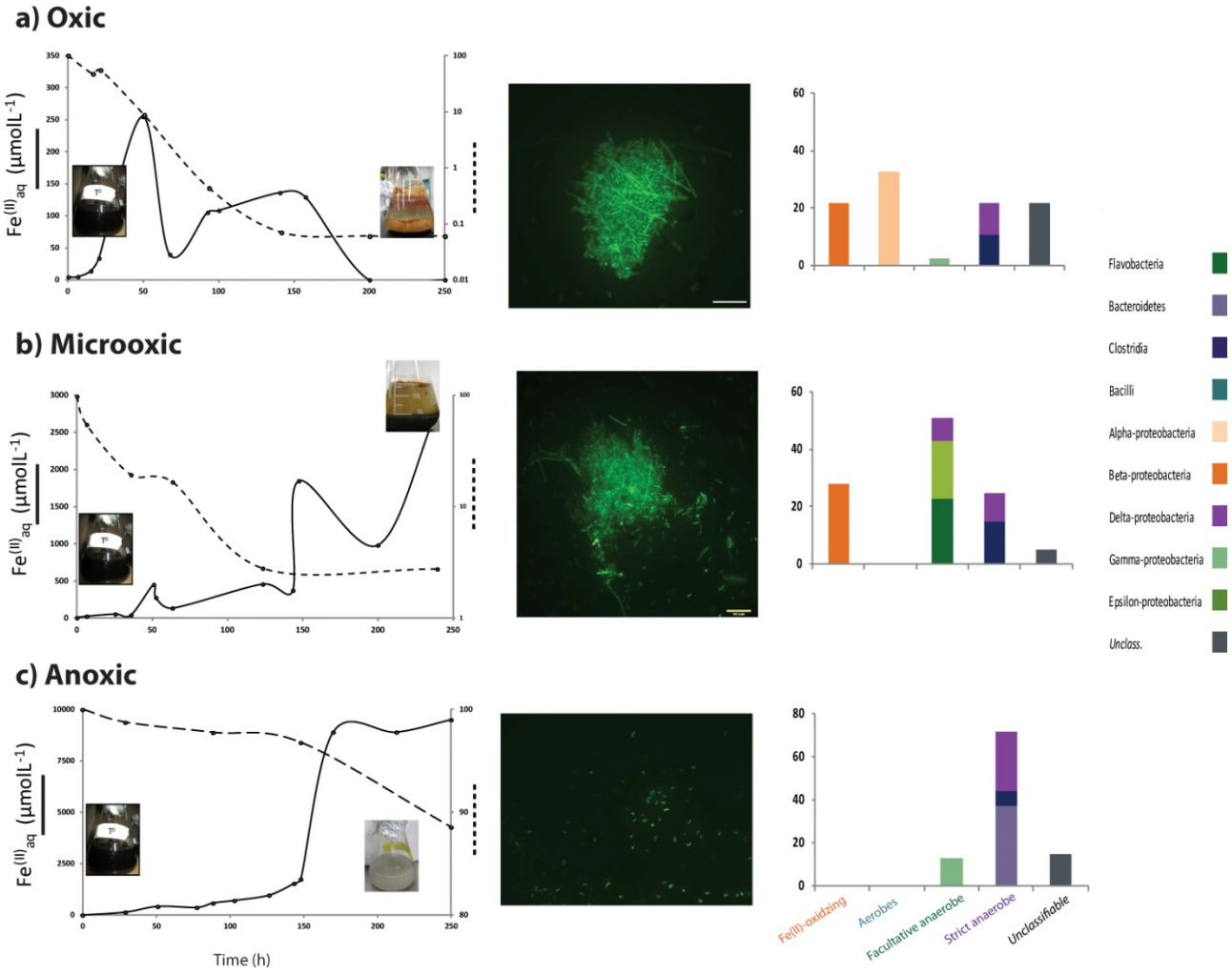

Figure 4.6 Subset of experimental co-enrichment microcosm results evaluating the influence of molecular oxygen concentrations on floc Fe-bacteria. A factorial experimental design was implemented and assessed the impact of **(a)** oxic, **(b)** microoxic, and **(c)** anoxic conditions on Fe-geochemistry (*first column*), consortia aggregate structure (*second column*) and community structure (16S, *third column*) of co-enriched Fe-redox cycling floc consortia. Evolution and accumulation of ferrous-Fe (µmolL- ; solid lines), changes in speciation of total Fe (as % change, dashed lines) from dissolved (<0.22µm) to solid phases (>0.22µm) as well as Fe-mineralogical analyses (XRD, Table 1) indicate co-occurring IRB and IOB activity within oxygenated microcosms (*see sections 2.2.2; 3.2*). Note differences in axis ranges between oxygen regimes. Epifluorescence imaging of enrichments revealed suspended bacterial consortia structures with dense EPS network and close aggregations of cells, including sheathed floc-IOB, in oxygenated treatments only. Genetic analyses indicate the presence of previously isolated IRB and IOB (*see section 2.2.1*) together with aerobic and facultatively aerobic (i.e. oxygen-consuming) species (% clones, third column). IOB and other oxygen consuming members of microcosm enrichment communities were absent after incubation under strictly anoxic conditions, as expected. Experiments were performed on nascent parent flocs from all sites of sample collection (n= 5 sites* 3 oxygen treatments); for results for all treatments for all floc samples collected see Figure S2, Tables 4.1, S3, S4.

Table 4.1 Mineralogical composition (XRD) of bio-minerals formed by floc Fe-metabolizing bacteria enriched in experimental microcosms (oxic, microoxic, anoxic). Results for all sites of floc sample collection are shown, (n= 5 sites * 3 oxygen treatments). Each column represents site of origin of parent floc sample. Control 'IRB-only' microcosms were generated by removing oxygen-comsuming members (including IOB) from enriched floc consortia by incubation in anaerobic chamber and confirmed by 16S sequencing. 'IRB-only' microcosms did not generate detectable levels of ferrous Fe in the oxic treatment, nor was there any detectable bio-mineral formation (N/A).

	Brewer L. Epilimnetic	**Brewer L. Hypolimnetic**	**Coldspring L. Metalimnetic**	**Coldspring L. Hypolimnetic**	**L. ON Littoral**	Control IRB only'
Oxic Microcosms						
Hematite	8%	8%	~8%	~8%	10%	N/A
Magnetite	~14%	~14%	9%	14%	14%	N/A
Siderite $FeCO_3$	-	-	1%	1%	-	N/A
Amorphous Fe Compounds	73%	73%	75%	70%	71%	N/A
Vivianite, $Fe_3(PO_4)2{\cdot}8H_2O$	-	-	-	-	-	N/A
$NaKSO_4$	-	-	-	-	-	N/A
Other materials	5%	5%	7%	7%	5%	N/A
Microoxic Microcosms						
Hematite	13%	9%	10%	8%	9%	8%
Magnetite	15%	10%	11%	10%	12%	10%
Goethite	2%	4%	4%	5%	3%	-
Siderite $FeCO_3$	2%	1%	-	5%	5%	22%
Amorphous Fe Compounds	66%	68%	75%	69%	68%	39%
Vivianite, $Fe_3(PO_4)2{\cdot}8H_2O$	1%	-	-	-	-	17%
$NaKSO_4$	-	2%	-	-	2%	-
Other materials	1%	6%	1%	4%	1%	5%
Anoxic Microcosms						
Pyrite	3%	6%	1%	5%	3%	
Siderite $FeCO_3$	10%	10%	10%	10%	10%	
Amorphous Fe Compounds	25%	25%	25%	25%	25%	
Vivianite, $Fe_3(PO_4)2{\cdot}8H_2O$	50%	50%	50%	50%	50%	
$NaKSO_4$	-	2%	-	-	2%	
Other materials	1%	1%	1%	1%	1%	

To date, previous investigations of coupled microbial $Fe^{(III/II)}$-redox cycling have used independently isolated IOB and IRB from different environmental contexts and subsequently experimentally assessed their artificially combined impact (e.g. [55]). This study represents the first investigation assessing microbial Fe-redox transformations by *simultaneously co-enriching* IOB and IRB from the same parent environmental sample. Moreover, 16S analysis of consortial aggregates in experimental microoxic and oxic microcosms indicate that observed consortia (Figures 4.6, S2) are not comprised of a simple co-association between the previously isolated IOB (autotroph) and IRBs (anaerobic heterotrophs). Rather, experimentally developed consortia aggregates within oxygenated conditions constitute highly functionally diverse bacterial communities representing a range of physiologies in terms of their response to oxygen, including aero-intolerant IRB and IOB (98-100% similarity to initial isolates) together with oxygen-consuming bacteria (aerobic heterotrophs, facultative anaerobic heterotrophs; Figure 4.6, Table S3). Importantly, 'IRB-only' control microcosms (i.e. prior elimination of oxygen-requiring members by incubation over multiple generations in anaerobic chamber, confirmed by 16S sequencing) within the oxic treatment did not produce the consortial aggregate structure, or accumulate $Fe^{(II)}$, as would be expected with metabolic activity, and showed overall low viability (Figure S3). These results are highly suggestive that specific collaborations between aero-intolerant Fe-bacteria and oxygen-consuming species are required to sustain microbial Fe-metabolism activity under oxygenated regimes.

The accumulation of $Fe^{(II)}_{(aq)}$ sufficient to produce ferrous mineral phases under experimental microoxic and oxic regimes underscores the role of the aggregate structure in generating differentiated geochemical microenvironments and provides for a persuasive argument for the widespread environmental occurrence of aggregate-associated microbial Fe-redox cycling at the microscale under oxygenated conditions. Supporting this notion, similar Fe-biomineral assemblages were also observed for environmental parent floc samples collected from microoxic/oxic field system conditions, including the presence of oxygen-sensitive ferrous Fe-minerals and $Fe^{(II)}_{(aq)}$ (Tables 1, S2). Further, the same IRB-IOB-aerobe consortial members

identified in Fe-cycling enrichment microcosms constitute 26 to 50% of environmental *in situ* floc bacterial communities inhabiting oxygenated systems (% OTU, Table S4). Phototrophic resident floc microbes (i.e. *Chloroflexi, Cyanobateria spp*.) constituted the major differences between enriched vs. *in situ* floc consortia (co-enriched consortia incubated in the dark). Interestingly, the same Fe-biomineral assemblage was formed within each experimental O_2 regime across the five original field floc samples, despite their original occurrence under widely differing original bulk O_2 conditions in the parent environments. Oxygen levels appear to exert a macroscale regulatory role on the microscale ***relative*** activities of aero-intolerant aggregate IRB and IOB and thus the Fe biominerals formed.

These findings have large implications for the use of Fe^{III}/Fe^{II} bearing minerals as geochemical proxies to constrain the chemistry and infer the history atmospheric O_2 on early Earth. The ability to decouple from increasing bulk O_2 via EPS production and aggregate formation would have been an highly adaptive strategy for anaerobic microorganisms enabling survival and colonization in an oxygenating world. In turn, this would have potentially profoundly influenced the Fe mineral record. For example, highly redox-reactive siderite ($Fe^{(II)}CO_3$) is considered a product only of anoxic reducing environments (Eh $\leq$ -0.2, [19]). Further, once produced, its inherent instability in the presence of molecular oxygen has been utilized to both delineate the pattern and timing of the oxygenation of Earth as well as to place upper bounds on Archean pO_2 (e.g. [86]). Similarly, mixed valence magnetite ($Fe^{(II)}Fe^{(III)}{}_2O_4$) is stable only under reducing conditions at relatively alkaline pH [19] and its accumulation in Precambrian banded iron formations (BIFs) has been used as evidence specifically of sedimentary-compartment IRB activity. However, here, floc microcosm enrichments actively produce siderite and magnetite associated with suspended aggregate structure formation under bulk oxygen conditions ranging from 0.19 to 6.0mgL^{-1}; the same mineral suite was also observed in floc from microoxic field environments. Further, Fe-mineral phases that are expected to form only under specific Eh/pH conditions (e.g. goethite vs. hematite vs. siderite) were co-produced within the same experimental floc system and again observed within environmental floc collected from oxic field sites. This similarly

indicates the formation of a variety of fine-grained minerals not predicted by bulk external solution oxygen conditions (Tables S1, S2).

4.3.4 The floc-hosted microbial Fe-redox wheel.

The production of pelagic aggregate structures by floc bacteria represents an ecological strategy enabling cooperating microbes to engineer their micro-geochemical environments and thus expand their environmental habitat range into conditions considered inhospitable at the macroscale (Figure 4.7). EPS production and aerobic organotrophic activity occurring within the aggregate exterior inhibit oxygen penetration, enabling the generation of interior anoxic microsites, facilitating anaerobic IRB-activity and the subsequent accumulation of their metabolic end-products (i.e. $Fe^{(II)}$) which would otherwise rapidly oxidize in the presence of O_2. Further, we suggest that observed floc-IOB filamentous morphotype serves a functional role in their metabolism (Figures 4.6, S2). Filamentous and sheathed IOB are enigmatic organisms and the role of their morphotype in their biology and $Fe^{(II)}$-oxidation metabolism has been considerably debated. Nevertheless, neutrophilic IOB are thought highly environmentally restricted as they require simultaneous access to both $Fe^{(II)}$ and molecular O_2 to sustain their metabolism, a relatively rare geochemical niche at the macroscale. Here, IOB filaments were observe to penetrate the floc aggregate consortial (Figures 4.6, S2); i.e., IOB may then occur within *both* interior and exterior regions, thus enabling simultaneously access to $Fe^{(II)}$ (inner anoxic core) and O_2 (outer oxygenated zone) (Figure 4.7). The filament morphotype may thus enable IOB to overcome the physical hurdle of their required substrates being separated by several 10's of microns. Indeed many sheathed-IOB have a reported much higher tolerance of environmental bulk O_2 concentrations then their stalked-IOB counterparts (*Gallionella spp.*)[87] and thus this collaboration of a sheathed IOB, the non-classical IRB isolated in the investigation, and oxygen-consuming organotrophic bacteria may then represent an evolutionary adaptation specific to the collaborative, aerobic microbial Fe-redox cycle.

Our results identify a new ecological strategy involving aggregate formation through the collaboration of diverse metabolic guilds of bacteria, which *collectively* influence the occurrence, products and effects of microbial Fe-redox transformations

in planetary zones not previously considered to be important sites for active Fe-metabolism. We show that the floc consortial aggregate structure enables anaerobes, requiring oxygen-sensitive substrates, to extend their habitat range into the vast pelagic oxygenated regions of lakes and oceans, indicating that diagenesis and metabolite transformation likely begins before pelagic flocs reach bed sediments. Here, field results reveal that both floc total organic content and amorphous $Fe^{(III)}$-mineral concentration decrease with increasing water column depth, while crystalline $Fe^{(III)}$-mineral content remains constant (Table S1). As it has been well established that heterotrophic IRB preferentially metabolize amorphous vs. crystalline Fe minerals, this observed shift in floc composition may be a result of *in situ* IRB-mediated diagenesis under oxygenated conditions during settling, accounting for the occurrence of redox-sensitive ferrous Fe minerals in bulk floc (vivianite, siderite, magnetite) and dissolved ferrous-$Fe^{(II)}$ detected in oxygenated water-columns across sites. This has large implications in models of ancient and modern Fe biogeochemistry. Here, the unexpected Fe-biomineral assemblages formed in Fe-redox cycling microcosms under varying O_2 regimes mirror those observed within *in situ* floc samples collected from systems at those specific O_2 concentrations, confirming the environmental activity of these cooperative Fe-metabolisms and the formation of a consistent suite of Fe biominerals associated with this activity. These results not only reveal ecological control of floc biogeochemistry across systems but also highlight bulk system [O_2] influences on the nature of Fe biominerals formed.

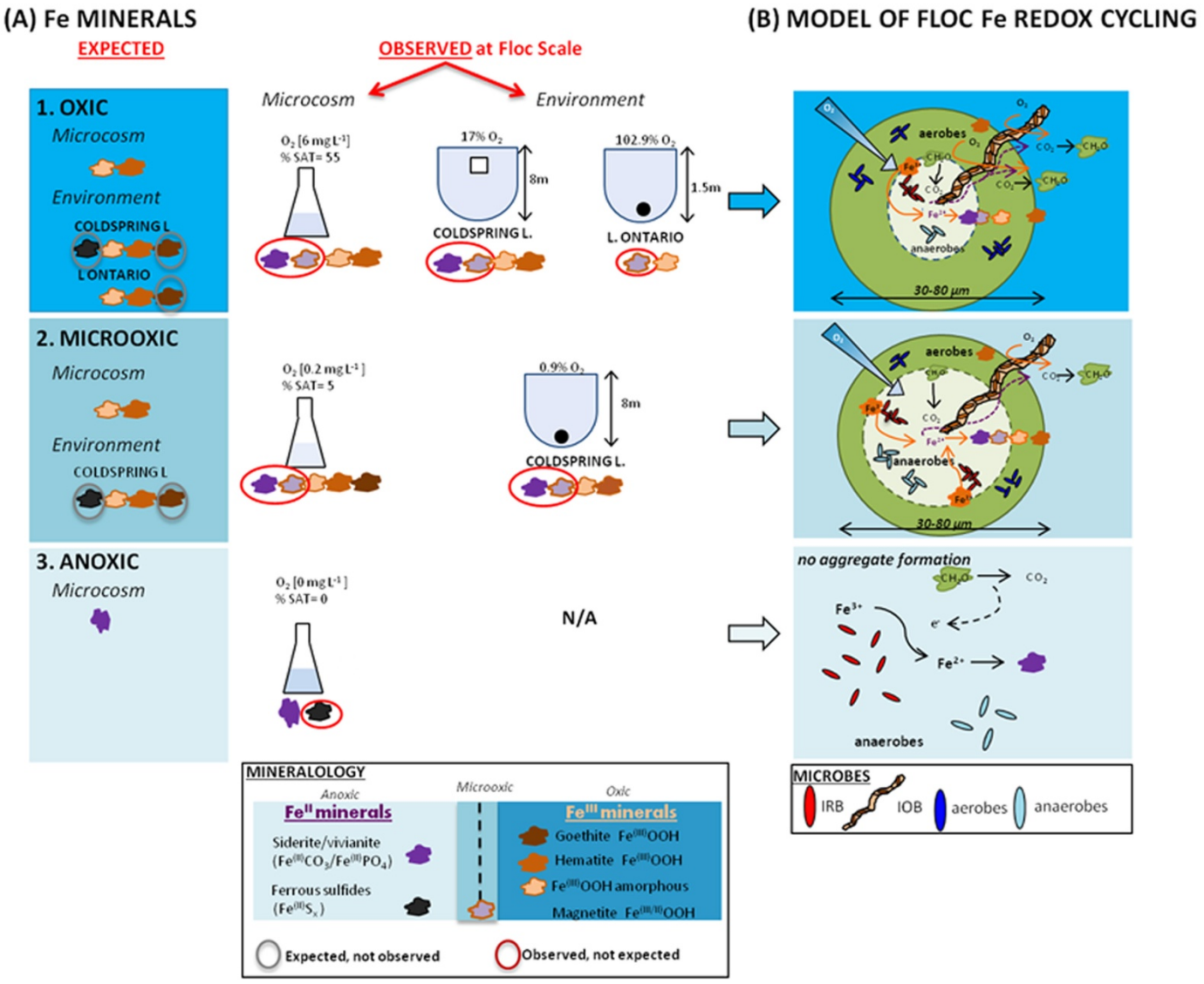

Figure 4.7 (A) Predicted and observed Fe minerals in microcosm and field sites and **(B)** proposed model of Fe redox cycling enabled by ecological collaborations between aero-intolerant IOB, IRB and oxygen-consuming aerobic bacteria species at the floc scale. In this model, aggregate formation by floc consortia, associated dense EPS-network, and aerobic heterotrophic activity contributes to decreased oxygen penetration into the floc aggregates. This results in the development of internal anoxic conditions, facilitating IRB and the subsequent accumulation of $Fe^{(II)}$, sustaining microaerobic, lithoautotrophic IOB floc species. As a result of this collaborative microbial Fe-redox cycling, redox-sensitive $Fe^{(II)}$-biominerals were produced in microcosm aggregates that were not predicted by experimental bulk O_2 values, but were consistent with those observed *in situ*.

4.4 Conclusions

Microbial Fe-redox bacteria (IRB, IOB) have been historically considered restricted to very specific and separate geochemical 'niche' environments and thus thought to possess a very restricted biogeography and low overall importance to the global biogeochemical Fe redox cycle. However, here we have identified collaborating floc $Fe^{(III)}$-reducing (IRB) and $Fe^{(II)}$-oxidizing (IOB) bacteria within consortial micro-aggregates (~30-80µm) across diverse oxygenated ($O_2^{Sat.}$=1-103%) aquatic systems not predicted to sustain microbial Fe metabolism. Not only does this discovery reframe the environmental range of microbial metabolism impact on Fe biogeochemical cycling, it also highlights an important emergent principle of microbial ecology, namely diverse, whole, environmental microbial communities are commonly associated with important processes occurring in the environment. Our results illustrate adoption of this notion of the microbial collective is critical to understanding macroscale system biogeochemistry. For example, many of the bacteria that are involved in $Fe^{(II)}$ metabolism and deposition of $Fe^{(III)}$ hydroxides are enigmatic, including sheathed IOB such as *Leptothrix spp.* This is the first study to identify the importance of cooperation in sustaining such microorganisms in the laboratory, i.e. aggregate IOB require an IRB, rather than a simple $Fe^{(II)}$ media salt, in order to provide an accessible $Fe^{(II)}$ source at environmentally relevant conditions. In turn, the resulting structural partnership, including collaboration with aerobic bacteria, generates necessary anoxic microenvironments enabling both Fe-metabolisms and results in unexpected Fe biomineral assemblages. Our results indicate that floc microbial Fe cycling, with attendant implications for nutrient and contaminant behaviour in oxygenated waters requires investigation, as do the potential implications of pelagic floc associated Fe-biominerals for geochemical interpretation. These results are exciting in identifying the widespread potential for the occurrence of a fully coupled microbial Fe redox wheel in oxygenated waters, as well as indicating that such cooperatives are likely operating in the other redox sensitive major biogeochemical cycles.

4.5 References

1. Boyd, P. W. & Ellwood, M. J. The biogeochemical cycle of iron in the ocean. *Nature Geosci* 3, 675-682 (2010).

2. Li, Y., Yu, S., Strong, J. & Wang, H. Are the biogeochemical cycles of carbon, nitrogen, sulfur, and phosphorus driven by the "FeIII–FeII redox wheel" in dynamic redox environments? *J Soils Sediments* 12, 683-693 (2012).

3. Senn, D. B. & Hemond, H. F. Nitrate Controls on Iron and Arsenic in an Urban Lake. *Science* 296, 2373-2376 (2002).

4. Shi, D., Xu, Y., Hopkinson, B. M. & Morel, F. M. M. Effect of Ocean Acidification on Iron Availability to Marine Phytoplankton. *Science* 327, 676-679 (2010).

5. Islam, F. S. *et al*. Role of metal-reducing bacteria in arsenic release from Bengal delta sediments. *Nature* 430, 68-71 (2004).

6. Warren, L. A. & Haack, E. A. Biogeochemical controls on metal behaviour in freshwater environments. *Earth-Science Reviews* 54, 261-320 (2001).

7. Stumm, W. & Sulzberger, B. The cycling of iron in natural environments: considerations based on laboratory studies of heterogeneous redox processes. *Geochimica et Cosmochimica Acta* 56, 3233-3257 (1992).

8. Konhauser, K. O. *et al*. Could bacteria have formed the Precambrian banded iron formations? *Geology* 30, 1079-1082 (2002).

9. Walker, J. C. G. Suboxic diagenesis in banded iron formations. *Nature* 309, 340-342 (1984).

10. Arnold, R. G., Hoffmann, M. R., DiChistinia, T. J. & Picardal, F. W. Regulation of Dissimilatory Fe(III) Reduction Activity in *Shewanella putrefaciens*. *Applied and Environmental Microbiology* 56, 2811-2817 (1990).

11. Lovely, D. R. in *Environmental Microbe-Metal Interactions* (ed Lovely, D. R.) 3-30 (ASM Press, Washington, DC, 2000).

12. Baker, B. J. & Banfield, J. F. Microbial communities in acid mine drainage. *FEMS Microbiol. Ecol.* 44, 139-152 (2003).

13. Bloethe, M. & Roden, E. E. Microbial Iron Redox Cycling in a Circumneutral-pH Groundwater Seep. *Appl. Environ. Microbiol.* 75, 468-473 (2009).

14. Emerson, D. & Floyd, M. M. Enrichment and isolation of iron-oxidizing bacteria at neutral pH. *Environ. Microbiol.* 397, 112-123 (2005).

15. Emerson, D. & Weiss, J. V. Bacterial iron oxidation in circumneutral freshwater habitats: Findings from the field and the laboratory. *Geomicrobiol. J.* 21, 405-414 (2004).

16. Weber, K. A., Achenbach, L. A. & Coates, J. D. Microorganisms pumping iron: anaerobic microbial iron oxidation and reduction. *Nature Reviews Microbiology* 4, 752-764 (2006).

17. Druschel, G. K., Emerson, D., Sutka, R., Suchecki, P. & Luther, G. W.,III. Low-oxygen and chemical kinetic constraints on the geochemical niche of neutrophilic iron(II) oxidizing microorganisms. *Geochim. Cosmochim. Acta* 72, 3358-3370 (2008).

18. Singer, P. C. & Stumm, W. Acidic mine drainage: the rate-determining step. *Science* 167, 1121-23 (1970).

19. Langmuir, D. in *Aqueous Environmental Geochemistry* (ed McConnin, R.) (Prentice Hall, Upper Saddle River, New Jersey, 1997).

20. Dekas, A. E., Poretsky, R. S. & Orphan, V. J. Deep-Sea Archaea Fix and Share Nitrogen in Methane-Consuming Microbial Consortia. *Science* 326, 422-426 (2009).

21. Kiorboe, T., Tang, K., Grossart, H. & Ploug, H. Dynamics of microbial communities on marine snow aggregates: colonization, growth, detachment, and grazing mortality of attached bacteria. *Appl. Environ. Microbiol.* 69, 3036-3047 (2003).

22. Simon, M., Grossart, H., Schweitzer, B. & Ploug, H. Microbial ecology of organic aggregates in aquatic ecosystems. *Aquat. Microb. Ecol.* 28, 175-211 (2002).

23. Konopka, A. Microbial ecology: searching for principles. *Microbe* 1, 175 (2006).

24. Costerton, J. W. *et al*. Bacterial biofilms in nature and disease. *Annual Reviews in Microbiology* 41, 435-464 (1987).

25. Hall-Stoodley, L., Costerton, J. W. & Stoodley, P. Bacterial biofilms: from the natural environment to infectious diseases. *Nature Reviews Microbiology* 2, 95-108 (2004).

26. Anderson, C. R., James, R. E., Fru, E. C., Kennedy, C. B. & Pedersen, K. In situ ecological development of a bacteriogenic iron oxide-producing microbial community from a subsurface granitic rock environment. *Geobiology* 4, 29-42 (2006).

27. Norlund, K. L. I. *et al*. Microbial Architecture of Environmental Sulfur Processes: A Novel Syntrophic Sulfur-Metabolizing Consortia. *Environ. Sci. Technol.* 43, 8781-8786 (2009).

28. Orphan, V. J., House, C. H., Hinrichs, K., McKeegan, K. D. & DeLong, E. F. Methane-Consuming Archaea Revealed by Directly Coupled Isotopic and Phylogenetic Analysis. *Science* 293, 484-487 (2001).

29. Warren, L. A. & Kauffman, M. E. Microbial Geoengineers. *Science* 299, 1027-1029 (2003).

30. Ploug, H., Kuhl, M., Bucholz-Cleven, B. & Jorgensen, B. B. Anoxic aggregtes- an ephemeral phenomenon in the pelagic environment? *Aquatic Microbial Ecology* 13, 285-294 (1997).

31. Ploug, H. *et al*. Carbon, nitrogen and O2 fluxes associated with the cyanobacterium Nodularia spumigena in the Baltic Sea. *The ISME journal* 5, 1549-1558 (2011).

32. Lu, S. *et al*. Insights into the structure and metabolic function of microbes that shape pelagic iron-rich aggregates (iron snow). *Appl. Environ. Microbiol.* (2013).

33. Balzano, S., Statham, P. J., Pancost, R. D. & Lloyd, J. R. Role of microbial populations in the release of reduced iron to the water column from marine aggregates. *Aquat. Microb. Ecol.* 54, 291 (2009).

34. Droppo, I. G. Rethinking what constitutes suspended sediment. *Hydrol. Process.* 15, 1551-1564 (2001).

35. Liss, S. N., Droppo, I. G., Flannigan, D. T. & Leppard, G. G. Floc architecture in wastewater and natural riverine systems. *Environmental science & technology* 30, 686 (1996).

36. Biggs, C. A. & Lant, P. A. Activated sludge flocculation: on-line determination of floc size and the effect of shear. *Water Res.* 34, 2542-2550 (2000).

37. Droppo, I. G. *et al*. Dynamic existence of waterborne pathogens within river sediment compartments. Implications for water quality regulatory affairs. *Environ. Sci. Technol.* 43, 1737-1743 (2009).

38. Droppo, I. G., Leppard, G. G., Flannigan, D. T. & Liss, S. N. The freshwater floc: a functional relationship of water and organic and inorganic floc constituents affecting suspended sediment properties. *Water Air Soil Pollut.* 99, 43-54 (1997).

39. Elliott, A. V. C., Plach, J. M., Droppo, I. G. & Warren, L. A. Comparative Floc-Bed Sediment Trace Element Partitioning Across Variably Contaminated Aquatic Ecosystems. *Environ. Sci. Technol.* 46, 209-216 (2012).

40. Plach, J. M., Elliott, A. V. C., Droppo, I. G. & Warren, L. A. Physical and Ecological Controls on Freshwater Floc Trace Metal Dynamics. *Environ. Sci. Technol.* 45, 2157-2164 (2011).

41. Fortin, D. & Langley, S. Formation and occurrence of biogenic iron-rich minerals. *Earth-Sci. Rev.* 72, 1-19 (2005).

42. Gault, A. G. *et al*. Microbial and geochemical features suggest iron redox cycling within bacteriogenic iron oxide-rich sediments. *Chem. Geol.* 281, 41-51 (2011).

43. Reddy, K. J., Soper, B. W., Tang, J. & Bradley, R. L. Phenotypic variation in exopolysaccharide production in the marine, aerobic nitrogen-fixing unicellular cyanobacterium Cyanothece sp. *World Journal of Microbiology and Biotechnology* 12, 311-318 (1996).

44. Alldredge, A. L. & Cohen, Y. Can microscale chemical patches persist in the sea? Microelectrode study of marine snow, fecal pellets. *Science* 235, 689-691 (1987).

45. Ploug, H., Iversen, M., Koski, M. & Buitenhuis, E. T. Production, oxygen respiration rates, and sinking velocity of copepod fecal pellets: Direct measurements of ballasting by opal and calcite. *Limnol. Oceanogr. 53 (2)*, 469-476 (2008).

46. Rees, T. F., Leenheer, J. A. & Ranville, J. F. Use of a single-bowl continuous-flow centrifuge for dewatering suspended sediments: Effect on sediment physical and chemical characteristics. *Hydrol. Process.* 5, 201-214 (1991).

47. Kulczycki, E., Fowle, D. A., Fortin, D. & Ferris, F. G. Sorption of cadmium and lead by bacteria-ferrihydrite composites. *Geomicrobiology Journal* 22, 299-310 (2005).

48. Fortin, D., Leppard, G. G. & Tessier, A. Characteristics of lacustrine diagenetic iron oxyhydroxides. *Geochimica et Cosmochimica Acta* 57, 4391-4404 (1993).

49. Emerson, D. & Moyer, C. Isolation and characterization of novel iron-oxidizing bacteria that grow at circumneutral pH. *Appl. Environ. Microbiol.* 63, 4784-4792 (1997).

50. Kostka, J. E. & Nealson, K. H. in *Techniques in Microbial Ecolgy* (eds Burlage, R. S., Atlas, R., Stahl, D., Geesey, G. & Sayler, G.) (Oxford University Press, Inc., New York, New York, 1998).

51. Francis, C. A., Obraztsova, A. Y. & Tebo, B. M. Dissimilatory metal reduction by the facultative anaerobe Pantoea agglomerans SP1. *Appl. Environ. Microbiol.* 66, 543-548 (2000).

52. Lentini, C. J., Wankel, S. D. & Hansel, C. M. Enriched iron(III)-reducing bacterial communities are shaped by carbon substrate and iron oxide mineralogy. *Frontiers in Microbiology* 3 (2012).

53. Roden, E. E. *et al*. Extracellular electron transfer through microbial reduction of solid-phase humic substances. *Nature Geosci* 3, 417-421 (2010).

54. Swanner, E. D., Nell, R. M. & Templeton, A. S. Ralstonia species mediate Fe-oxidation in circumneutral, metal-rich subsurface fluids of Henderson mine, CO. *Chem. Geol.* 284, 339-350 (2011).

55. Roden, E. E., Sobolev, D., Glazer, B. & Luther, G. W. Potential for microscale bacterial Fe redox cycling at the aerobic-anaerobic interface. *Geomicrobiol. J.* 21, 379-391 (2004).

56. Stookey, L. L. Ferrozine---a new spectrophotometric reagent for iron. *Anal. Chem.* 42, 779-781 (1970).

57. Viollier, E., Inglett, P. W., Hunter, K., Roychoudhury, A. N. & Van Cappellen, P. The ferrozine method revisited: Fe(II)/Fe(III) determination in natural waters. *Appl. Geochem.* 15, 785-790 (2000).

58. Lin, B. *et al*. Phylogenetic and physiological diversity of dissimilatory ferric iron reducers in sediments of the polluted Scheldt estuary, Northwest Europe. *Environ. Microbiol.* 9, 1956-1968 (2007).

59. Tamura, K. *et al*. MEGA5: Molecular Evolutionary Genetics Analysis Using Maximum Likelihood, Evolutionary Distance, and Maximum Parsimony Methods. *Molecular Biology and Evolution* 28, 2731-2739 (2011).

60. Wang, Q., Garrity, G. M., Teiedje, J. M. & Cole, J. R. Naive Bayesian classifier for rapid assignmnet of rRNA aequences into the new bacterial taxonomy. *Appl. Environ. Microbiol.* 73, 5261 (2007).

61. Attaway, H. & Smith, M. Reduction of perchlorate by an anaerobic enrichment culture. *J. Ind. Microbiol.* 12, 408-412 (1993).

62. Vartoukian, S. R., Palmer, R. M. & Wade, W. G. Strategies for culture of 'unculturable' bacteria. *FEMS Microbiol. Lett.* 309, 1-7 (2010).

63. Gerhardt, P., Murray, R., Wood, W. A. & Krieg, N. R. in *Methods for general and molecular bacteriology* (American Society for Microbiology Washington, DC, 1994).

64. Jokinen, C. C. *et al*. An enhanced technique combining pre-enrichment and passive filtration increases the isolation efficiency of Campylobacter jejuni and Campylobacter coli from water and animal fecal samples. *J. Microbiol. Methods* (2012).

65. Eilers, H., Pernthaler, J., GlÃ¶ckner, F. O. & Amann, R. Culturability and In Situ Abundance of Pelagic Bacteria from the North Sea. *Appl. Environ. Microbiol.* 66, 3044-3051 (2000).

66. Jeanthon, C. *et al*. Diversity of cultivated and metabolically active aerobic anoxygenic phototrophic bacteria along an oligotrophic gradient in the Mediterranean Sea. *Biogeosciences Discussions* 8, 4421 (2011).

67. Shelobolina Evgenya, S. *et al*. Isolation of phyllosilicate-iron redox cycling microorganisms from an illite-smectite rich hydromorphic soil. *Frontiers in Microbiology* 3 (2012).

68. Coby, A. J., Picardal, F., Shelobolina, E., Xu, H. & Roden, E. E. Repeated Anaerobic Microbial Redox Cycling of Iron. *Appl. Environ. Microbiol.* 77, 6036-6042 (2011).

69. Fritzsche, A. *et al*. Fast microbial reduction of ferrihydrite colloids from a soil effluent. *Geochim. Cosmochim. Acta* 77, 444-456 (2012).

70. Miot, J. *et al*. Iron biomineralization by anaerobic neutrophilic iron-oxidizing bacteria. *Geochim. Cosmochim. Acta* 73, 696-711 (2009).

71. Kappler, A., Johnson, C. M., Crosby, H. A., Beard, B. L. & Newman, D. K. Evidence for equilibrium iron isotope fractionation by nitrate-reducing iron(II)-oxidizing bacteria. *Geochim. Cosmochim. Acta* 74, 2826-2842 (2010).

72. Lovely, D. R., Stolz, J. F., Nord, G. L. & Phillips, E. J. P. Anaerobic production of magnetite by a dissimilatory iron reducing microogranism. *Nature* 330, 252 (1987).

73. Reguera, G. *et al*. Extracellular electron transfer via microbial nanowires. *Nature* 435, 1098-1101 (2005).

74. Roden, E. E. Geochemical and microbiological controls on dissimilatory iron reduction. *Comptes Rendus Geoscience* 338, 456-467 (2006).

75. Warren, L. A., Norlund, K. L. I. & Bernier, L. Microbial thiosulphate reaction arrays: the interactive roles of Fe(III), O2 and microbial strain on disproportionation and oxidation pathways. *Geobiology* 6, 461-470 (2008).

76. Han, Y., Liu, J., Guo, X. & Li, L. Micro-environment characteristics and microbial communities in activated sludge flocs of different particle size. *Bioresource technology* 124, 252-258 (2002).

77. Li, B. & Bishop, P. L. Micro-profiles of activated sludge floc determined using microelectrodes. *Water research*, 1248-1258 (2004).

78. Ploug, H. & Grossart, H. Bacterial production and respiration in aggregates-a matter of the incubation method. *Aquat. Microb. Ecol.* 20, 21-29 (1999).

79. Emerson, D., Fleming, E. J. & McBeth, J. M. Iron-Oxidizing Bacteria: An Environmental and Genomic Perspective. *Annual Review of Microbiology, Vol 64, 2010* 64, 561-583 (2010).

80. Ferris, F. G., Hallberg, R. O., Lyven, B. & Pedersen, K. Retention of strontium, cesium, lead and uranium by bacterial iron oxides from a subterranean environment. *Appl. Geochem.* 15, 1035-1042 (2000).

81. Emerson, D. & Moyer, C. L. Neutrophilic Fe-oxidizing bacteria are abundant at the Loihi Seamount hydrothermal vents and play a major role in Fe oxide deposition. *Appl. Environ. Microbiol.* 68, 3085-3093 (2002).

82. Fleming, E. J. *et al*. Hidden in plain sight: discovery of sheath-□forming, iron □oxidizing Zetaproteobacteria at Loihi Seamount, Hawaii, USA. *FEMS Microbiol. Ecol.* (2013).

83. Fru, E. C., Piccinelli, P. & Fortin, D. Insights into the Global Microbial Community Structure Associated with Iron Oxyhydroxide Minerals Deposited in the Aerobic Biogeosphere. *Geomicrobiol. J.* 29, 587-610 (2012).

84. Thamdrup, B. in *Advances in Microbial Ecology* (ed Schink, B.) (Kluwer Academic/Plenum Publishers, New York, 2000).

85. Lovley, D. R., Holmes, D. E. & Nevin, K. P. in *Advances in Microbial Physiology* (ed Pool, R. K.) (Academic Press, 2004).

86. Rasmussen, B. & Buick, R. Redox state of the Archean atmosphere: Evidence from detrital heavy minerals in ca. 3250â€“2750 Ma sandstones from the Pilbara Craton, Australia. *Geology* 27, 115-118 (1999).

87. Emerson, D. & Revsbech, N. P. Investigation of an Iron-Oxidizing Microbial Mat Community Located near Aarhus, Denmark: Field Studies. *Applied and Environmental Microbiology* 60, 4022-4031 (1994).

4.6 Supporting Information

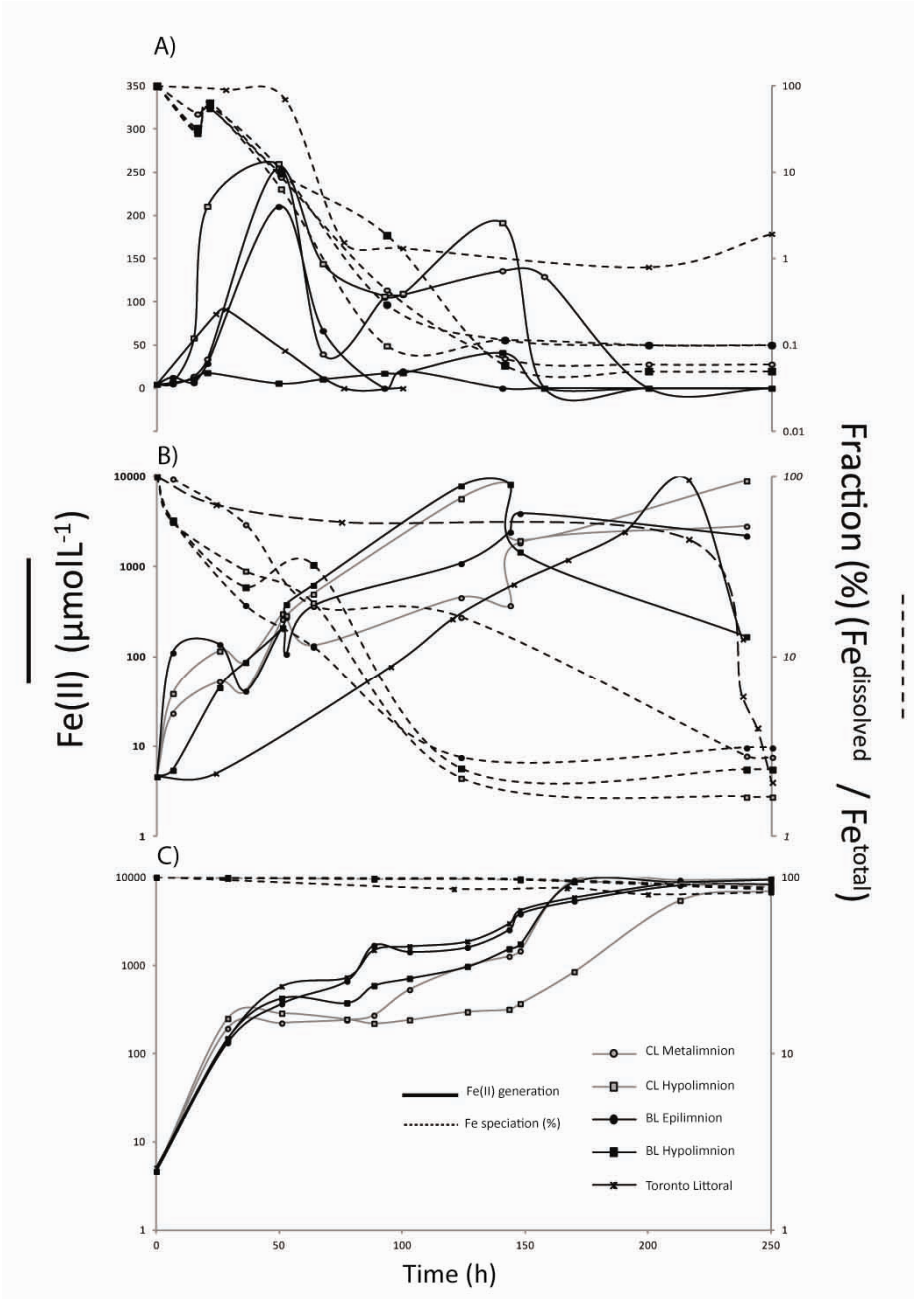

Figure 4.S1. Ferrous-Fe accumulation (µmol/L, solid lines) and changes in speciation of total Fe (as % changes, dashed lines) from dissolved (<0.22µm) to solid phases (>0.22µm). Results for all experimental treatments ((a) oxic, (b) microoxic, and (c) anoxic) for all sites of floc collection are shown (n= 5 sites* 3 oxygen treatments). Data shown here present Fe-geochemical outcome of a single generation (N=60th) of co-enrichment experiments over 250h. Data points represent mean ± SEM (n=3). Ferrous-Fe accumulated under all experimentally oxygenated conditions and all microcosm co-enrichments completely metabolized the provided soluble ferric-Fe source (*see sections 4.2.2.2; 4.3.2*) Note differences in scales.

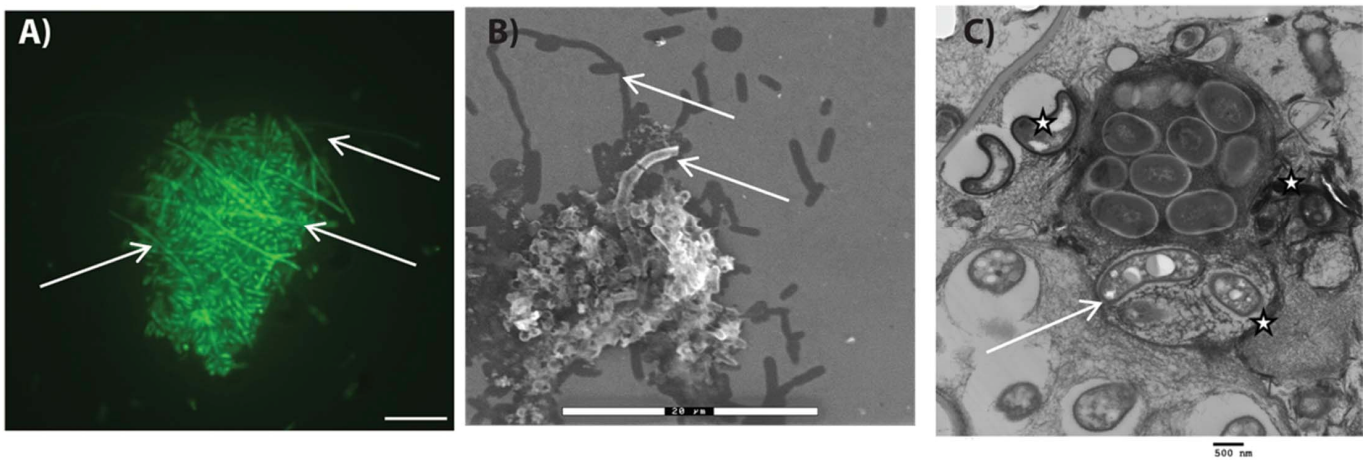

Figure 4.S2. Suspended consortial aggregate formation by co-enriched floc Fe-bacteria **(A,B)** and **(C)** *in situ* floc bacteria. Aggregation and EPS production affords protection against bulk oxygen concentrations and thus provides a functional capability for the participating microorganisms to effectively circumvent geochemical constraints predicted to restrict their metabolism at the bulk scale. These consortial structures were only observed in bulk oxygenated conditions, and only in collaboration with aerobic bacteria. White arrows highlight sheathed floc IOB associating with enriched consortial aggregates; white starts inidcate particulate Fe (EDS).

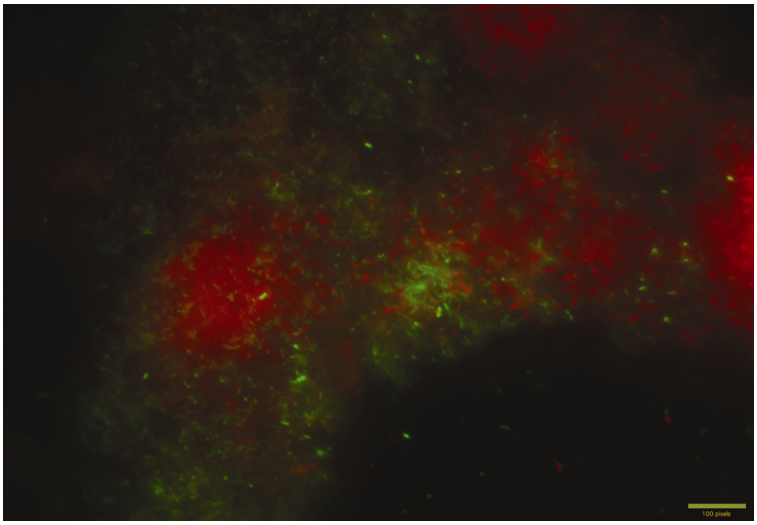

Figure 4.S3 Fluorescent LIVE (green) and DEAD (red) image of control 'IRB-only' microcosms grown in oxic treatment. 'IRB-only' microcosms were generated by first removing oxygen-consuming members from enriched floc consortia by incubation for multiple generations under anoxic conditions; confirmed by 16S sequencing. These microcosms i) did not accumulate Fe(II) over the course of the experiment, ii) generate discrete aggregate consortial structures, and iii) showed much lower overall viability (red). 100 pixels = 20μm

TABLE S1: Physico-chemical conditions at sampling depth of floc collection. DIC= dissolved inorganic carbon; DOC= dissolved organic carbon. Aqueous nutrient concentrations were quantified onsite by HACH spectrophotometer (sulphate, phosphate, nitrate, Fe total)

Site:	Coldspring L. Hypolimnetic	Brewer L. Hypolimnetic	Coldspring L. Metalimnetic	Brewer L. Epilimnetic	L. ON, Littoral
Water Column physico-chemistry					
[Oxygen] (% sat.)	0.9	2.4	17.1	73.6	102.9
pH	6.3	6.4	6.6	6.1	7.9
Depth of Sampling (m)	7.5	12.5	4.5	3.5	1.0
Temp. (°C)	11.6	5.305	19.28	21.4	14.0
[Fe(II)] mg/L	5.6 ± 0.2	3.6 ± 0.2	0.05 ± 0.00	0.09 ± 0.00	-
[Fe(III)] mg/L	4.12 ± 0.02	2.14 ± 0.02	1.79 ± 0.00	0.08 ± 0.00	0.02 ± 0.00
DIC mg/L	6.7 ± 0.17	2.0 ± 0.14	1.6 ± 0.00	2.2 ± 0.78	21.2 ± 0.10
DOC mg/L	8.1 ± 0.06	7.9 ± 0.14	6.2 ± 0.10	9.4 ± 0.80	2.33 ± 0.06
[Sulphate] mg/L	1.2 ± 0.06	4.6 ± 0.1	4.39 ± 0.01	4.63 ± 0.39	26.4 ± 0.21
[Phosphate] mg/L	0.06 ± 0.01	0.06 ± 0.01	0.02 ± 0.01	0.05 ± 0.01	0.015 ± 0.01
[Nitrate] mg/L	14.2 ± 0.00	0.53 ± 0.06	0.18 ± 0.00	0.43 ± 0.05	0.13 ± 0.01
Suspended flocs					
Floc Concentration (mgL)	6.09 ± 0.54	4.2 ± 0.54	3.1 ± 0.03	1.0 ± 0.01	1.4 ± 0.1
Mean floc particle size (d50)	200.0	300	245	250	350
[Organic C] (g/g)	0.5	0.17	0.6	0.4	0.14
[Amorphous Fe] mg/g	37.5	12.0	67.7	22.2	7.1
[Crystalline Fe] mg/g	47.5	15.2	45.5	11.5	5.8

TABLE S2: Mineralogical composition (XRD) of environmental suspended floc aggregates.

	Coldspring L. Hypolimnetic	Coldspring L. Metalimnetic	L. ON Littoral
Quartz	4%	3%	23%
Plagioclase	16%	~10%	-
Ankerite	4%	3%	1%
Kaolinite	10%	5%	-
Hematite	4%	8%	-
Magnetite	6%	8%	2%
Siderite $FeCO_3$	4%	4%	-
Amorphous Fe Compounds	37%	47%	5%
Organic	10%	5%	16%
Other materials	5%	7%	2%
Calcite	-	-	19%
Anorthite/albite	1%	1%	9%
Microcline	-	-	4%
Mica/Illite	-	-	5%
Chlorite	-	-	4%
Amphibole	1%	1%	1%
Smectite	1%	1%	6%
Dolomite	-	-	5%

TABLE S3: Sequencing (16S rRNA, ~1500bp) results of Fe-metabolizing consortial co-enriched in experimental microcosms (***oxic, microoxic, anoxic***). Results for all s ites of floc sample collection are shown (n= 5 sites * 3 oxygen treatments). Identified sequnces (OTU= 97% sequence similarity) were assigned to one of five putative function categories based on isolation results here and also documented metabolic capacity of comparison species (BLASTN, RDP):
i. aerobe (**Aer.**: oxygen reducing chemoorgantrophs and lithoautrophs, excluding IOB); **ii.** facultative anaerobe (**Fac.**: aero-tolerant chemoorganothrophs able to utilize multiple terminal electron acceptors (TEAs) including molecular oxygen); **iii.** obligate anaerobe (**Ana.**: aero-intolerant bacteria including fermentative bacteria, sulphate reducing and Fe(III)-reducing bacteria); **iv.** microaerobic Fe(II)-oxidizing (**IOB**); and **v.** unclassifiable (UN.). For clarity, only OTUs representing >1% of sequences are shown.28

L. Ontario, Littoral

No. Clones	Taxonomial Assigment	Sequence Identification	Similarity (%)	Function Assignment	Ref.
10	Actinobacteria	Arthrobacter sp.	98%	Aer.	7,8,9
2	Actinobacteria	Micromonsopora sp.	98%	Aer.	60
4	Beta-proteobacteria	Comamonas sp.	98%	IOB	61
3	Beta-proteobacteria	Delfita sp.	97%	Fac.	19,,21
10	Firmicutes	Bacillus silvestris	97-98%	Fac.	10,11
6	Firmicutes	Paenibacillus sp.	98%	Fac.	35,36
10	Firmicutes	Sporosarcina sp.	96-97%	Fac.	50,51
8	Gamma-proteobacteria	Xanthomonas sp.	99%	Aer.	62
2	Gamma-proteobacteria	Pseudomonas sp.	97-98%	Fac.	42,59
55					
6	Bacteroidetes	unclass. Chitinophagaceae	100%	UN	
1	Bacteroidetes	Bacteroidetes	100%	UN	
8	Beta-proteobacteria	Comamonas sp.	98%	IOB	61
3	Beta-proteobacteria	Simplicispira sp.	98%	Fac.	47
3	Beta-proteobacteria	Delfita sp.	98%	Fac.	19,21
6	Beta-proteobacteria	Alicycliphilus sp.	97%	Ana.	5
3	Delta-proteobacteria	Desulfovibrio desulfuricans	99%	Ana.	26,27
3	Delta-proteobacteria	Desulfobacteraceae	100%	UN	
3	Firmicutes	Bacillus silvestris	98%	Fac.	10,11
10	Gamma-proteobacteria	Xanthomonas sp.	97-98%	Aer.	62
46					
6	Bacteroidetes	Bacteroidetes	100%	UN	
8	Beta-proteobacteria	Delfita sp.	94-96%	Fac.	19,21
6	Delta-proteobacteria	Desulfosarcina sp.	96-97%	Ana.	23
4	Delta-proteobacteria	Desulfobacteraceae	100%	UN	
2	Delta-proteobacteria	Desulvibrio desulfuricans	99%	Ana.	26,27
6	Firmicutes	Acetobacterium sp.	94-96%	Ana.	1,2
13	Firmicutes	Clostridium XI	99%	Ana.	64,67
8	Gamma-proteobacteria	Aeromonas sp.	97-98%	Fac.	3,4,68
53					

Brewer L. Hypolimnetic

No. Clones	Taxonomial Assigment	Sequence Identification	Similarity (%)	Function Assignment	Ref.
3	Alpha-proteobacteria	unclass. Rhodocyclaceae	98%	Fac.	46
11	Bacteriodetes	unclass. Porphyromonadaceae	100%	UN	
3	Beta-proteobacteria	Comamonas sp.	97-98%	IOB	61
4	Firmicutes	Acetobacterium sp.	97%	Ana.	1,2
10	Firmicutes	unclass. Clostridiales	99%	Ana.	64,, 1,2, 15
11	Firmicutes	Clostridium sp.	96-97%	Ana.	64,,67
3	Gamma-proteobacteria	Pseudomonas sp.	96-98%	Fac.	42,59
3	Gamma-proteobacteria	unclass. Enterobacteriaceae	92-97%	Ana.	30,69
Sum **48**					
7	Bacteriodetes	unclass. Porphyromonadaceae	100%	UN	
10	Bacteroidetes	Bacteroides	98-99%	Ana.	12,13
10	Beta-proteobacteria	Comamonas sp.	96-98%	IOB	61
4	Beta-proteobacteria	Propionivibrio sp.	98%	Ana.	39,41
7	Firmicutes	unclass. Clostridiales	100%	Ana.	64,67
5	Firmicutes	Lysinibacillus	98%	Fac.	33,34
6	Gamma-proteobacteria	unclass. Enterobacteriales	98%	Ana.	30,69, 15
Sum **49**					
4	Alpha-proteobacteria	Sinorhizobium sp.	94%	Ana.	48
12	Firmicutes	Trichococcus sp.	98-99%	Fac.	55,56
4	Firmicutes	Lysinibacillus	96-98%	Fac.	33,34
2	Bacteroidetes	unclass. Porphyromonadaceae	100%	UN	
2	Bacteroidetes	Alistipes sp.	98%	Ana.	6
6	Bacteroidetes	Bacteroides	98%	Ana.	12,13
2	Clostridia	unclass. Clostridiales	100%	Ana.	64,68
6	Delta-proteobacteria	Desulfovibrio sp.	96-99%	Ana.	26,27
Sum **38**					

Brewer L. Epilimnetic

No. Clones	Taxonomial Assigment	Sequence Identification	Similarity (%)	Function Assignment	Ref.
6	Beta-proteobacteria	Comamonas sp.	97-98%	IOB	61
8	Beta-proteobacteria	Dechloromonas sp.	97%	Ana.	65
4	Firmicutes	Acetobacterium sp.	97%	Ana.	1,2
12	Bacteroidetes	Cloacibacterium sp.	95-98%	Fac.	16
6	Bacteroidetes	unclass. Flavobacteriaceae	100%	UN	
7	Gamma-proteobacteria	Pseudomonas sp.	95-98%	Fac.	42,59
36					
2	Actinobacteria	Propionibacterium sp.	98%	Ana.	41
4	Bacteroidetes	Bacteroides sp.	97-99%	Ana.	12,13
8	Beta-proteobacteria	Comamonas sp.	97-98%	IOB	61
15	Beta-proteobacteria	Delftia lacustris	99%	Aer.	18
6	Beta-proteobacteria	Rhodoferax sp.	98%	Fac.	46
4	Beta-proteobacteria	Curvibacter sp.	99%	Fac.	17
4	Delta-proteobacteria	Desulfovibrio desulfuricans	97-98%	Ana.	26,27
5	Bacteroidetes	unclass. Flavobacteriaceae	100%	UN	
4	Gamma-proteobacteria	Enterobacter sp.	94-97%	Fac.	30
52					
2	Actinobacteria	Propionibacterium sp.	98%	Ana.	41
10	Bacteroidetes	Bacteroides sp.	98-99%	Ana.	12,13
6	Bacteroidetes	Rikenella sp.	97-99%	Ana.	43
8	Bacteroidetes	unclass. Bacteroidales	100%	UN	
2	Bacteroidetes	unclass. Flavobacteriaceae	100%	UN	
4	Beta-proteobacteria	Rhodoferax sp.	98%	Fac.	46
4	Firmicutes	unclass. Clostridiales	99%	Ana.	64,67
10	Firmicutes	Trichococcus sp.	97-99%	Fac.	55,56
6	Gamma-proteobacteria	Enterobacter sp.	94-97%	Fac.	30,69
52					

Coldspring L. Hypolimnetic

No. Clones	Taxonomial Assigment	Sequence Idenfitifcation	Simillarity (%)	Function Assignment	Ref.
8	Bacteroidetes	Flavobacterium sp.	98%	Fac.	31,32
2	Beta-proteobacteria	Comamonas sp.	95%	IOB	61
3	Beta-proteobacteria	Delftia acidovorans	99%	Fac.	20,21
10	Beta-proteobacteria	unclass. Rhodocyclaceae	94%	UN	
7	Epsilon-proteobacteria	Sulfuricurvum sp.	96-98%	Fac	52
3	Delta-proteobacteria	Desulfovibrio spp.	99%	Ana.	26,27
9	Firmicutes	unclass. Veillonellaceae	94%	UN	
Sum **42**					
4	Acidobacteria	Geothrix sp.	95%	Ana.	70
12	Beta-proteobacteria	Comamonas sp.	95%	IOB	61
11	Beta-proteobacteria	Delftia acidovorans	99%	Fac.	20,21
3	Delta-proteobacteria	Desulfovibrio sp.	97-98%	Ana.	26,27
11	Epsilon-proteobacteria	Sulfuricurvum sp.	98-99%	Fac.	51,52
6	Delta-proteobacteria	unclass. Geobacteraceae	95-97%		
4	Gamma-proteobacteria	Enterobacter cloacae	98%	Fac.	30
3	Gamma-proteobacteria	Pantoea sp.	94%	Fac.	37,38
3	Gamma-proteobacteria	Pseudomonas sp.	96%	Fac.	42,59
Sum **57**					
4	Acidobacteria	Geothrix sp.	95%	Ana.	70
8	Bacteroides	Bacteroides sp.	97-99%	Ana.	12,13
2	Firmicutes	unclass. Veillonellaceae	100%	UN	
3	Beta-proteobacteria	Delftia acidovorans	97-99%	Fac.	20,21
2	Firmicutes	Acetobacterium sp.	97%	Ana.	1,2
2	Firmicutes	Desulfotomaculum sp.	98%	Ana.	22
3	Firmicutes	Clostridium sp.	96%	Ana.	64
4	Gamma-proteobacteria	Buttiauxella agrestis	99%	Ana.	14,15
4	Gamma-proteobacteria	Enterobacter cloacae	98-99%	Fac.	30
Sum **32**					

Coldspring L. Metalimnetic

No. Clones	Taxonomial Assigment	Sequence Identification	Similarity (%)	Function Assignment	Ref.
15	Alpha-proteobacteria	Ahrensia sp.	97-98%	Aer.	66
10	Beta-proteobacteria	Comamonas sp.	95%	IOB	61
10	Beta-proteobacteria	unclass. Rhodocyclaceae	100%	UN	
5	Delta-proteobacteria	Desulfovibrio sp.	97-99%	Ana.	26,27
5	Firmicutes	Acetobacterium sp.	96-97%	Ana.	1,2
	Gamma-proteobacteria	Pseudomonas sp.	96%	Fac.	42,59
45					
12	Bacteroidetes	Flavobacterium sp.	94-98%	Fac.	31,32
2	Bacteroidetes	Cloacibacterium sp.	98%	Fac.	16
17	Beta-proteobacteria	Comamonas sp.	95%	IOB	61
9	Firmicutes	Tissierella creatinini	97-98%	Ana.	53,54
1	Delta-proteobacteria	Desulfuromonas sp.	97%	Ana.	28,29
3	Delta-proteobacteria	unclass. Bdellovibrionaceae	100%	UN	
5	Delta-proteobacteria	unclass. Desulfuromondales	95%	UN	
12	Gamma-proteobacteria	Aeromonas sp.	95-97%	Fac.	10,11
61					
6	Bacteroidetes	unclass. Bacteroidales	96-98%	UN	
18	Bacteroidetes	Bacteroides sp.	99%	Ana.	12,13
11	Delta-proteobacteria	Desulfovibrio sp.	95-98%	Ana.	26,27
4	Firmicute	Robinsoniella sp.	98%	Ana.	44,45
6	Gamma-proteobacteria	Aeromonas sp.	98%	Fac.	10,11
5	Gamma-proteobacteria	Plesiomonas sp.	97%	Fac.	40,71
50					

TABLE S4: Enviromental sequencing (16S rRNA) results of parent suspended floc samples for all sites (n= 5). OTUs were binned at 97% and analyzed against the NCBI (US) database using MEGA BLAST analysis and also assigned to a taxonomical hierarchy proposed in Bergey's Manual of Systematic of Bacteriology, release 6.0., using the RDP classifier tool.

Results indicate that floc Fe-redox cycling consortia enriched in experimental microcosms constitute 26 to 50% of the in situ floc bacterial community (% OTU, bold font).

Phototrophic bacterial lineages in the parent floc samples account for the majority of bacteria taxons not enriched in experimental microcosms (expected). Also identified in parent flocs were a wide range of aerointolerant bacteria and bacteria of known strict anaerobic metabolism including anoxygenic phototrophs, sulphur oxidizing and sulfur reducing bacteria. For clarity, only OTUs representig at least 1% of sequences are shown.

Toronto Beach, Littoral floc

Phylum	OTU	Taxonomial Assigment (RDP)	NCBI Identification (MEGA BLAST)	Similarity (%)
Actinobacteria	1	**Arthrobacter sp.**	**Arthrobacter albus**	97
	2	Propionibacterium	Uncultured hydrocarbon seep bacterium	99
Bacteroidetes	3	**unclass. Chitinophagaceae**	**bacterium clone ORSPEP_c06**	98
	4	unclass. Flavobacteriaceae	Uncultured bacterium clone	97
Chloroflexi	5	unclass. Chloroflexi	Uncultured Ktedobacteria	98
Firmicutes	6	Carnobacterium sp.	Carnobacterium sp. enrichment	98
	7	**Acetobacterium sp.**	**Acetobacterium sp. R6T**	98
	8	**Lactobacillus sp.**	**Lactobacillus ruminis**	95
	9	**Clostridium XI**	**Uncultured bacterium clone**	98-99
	10	Clostridium XI	uncultured Peptostreptococcaceae	95
	11	Pasteuria sp.	planctomycete str. 535	98
Planctomycetes	12	unclass. Planctomycetaceae	Uncultured bacterium clone	95
	13	Planctomyces sp.	Uncultured bacterium clone	97
Proteobacteria				
Alpha class	14	Pedomicrobium sp.	Uncultured bacterium clone	92
	15	Rhodobacter sp.	uncultured bacterium clone	95-97
	16	Rhodobacter sp.	Uncultured bacterium clone	99
	17	Sphingomonas sp	Uncultured bacterium clone	98
	18	unclass. Alphaproteobacteria	Uncultured bacterium clone	95
	19	unclass. Rhizobiales	uncultured bacterium clone	96-97
	20	unclass. Rhizobiales	uncultured bacterium clone	96
	21	unclass. Rhizobiales	uncultured alpha proteobcaterim	97
	22	unclass. Rhizobiales	Uncultured proteobacterium clone	98
	23	unclass. Rhizobiales	Uncultured Rhizobiaceae	96
	24	unclass. Rhodobacteraceae	Uncultured bacterium clone	93
Beta class	25	**Delfitia sp.**	**Delfitia sp.**	97-99
	26	**Comamonas sp.**	**Comamonas sp.**	99
Delta class	27	**Desulfovibrio sp.**	**Desulfovibrio desulfuricans**	98
Gamma class	28	**Xanthomonas sp.**	**Xanthomonas sp.**	98-99
	29	Steroidobacter sp.	Uncultured bacterium clone	99
Planctomycetes	30	unclass. Planctomycetaceae	Uncultured bacterium clone	95
	31	Planctomyces sp.	Uncultured bacterium clone	97
Verrucomicrobia	32	Spartobacteria (genera incertae	Uncultured Verrucomicrobia bacterium	96
	33	Luteolibacter sp.	Uncultured Verrucomicrobiales bacterium	97-99
	34	unclass. Verrucomicrobiaceae	Uncultured bacterium clone	96

Brewer L., Epilimnetic floc

Phylum	OTU	Taxonomial Assigment (RDP)	NCBI Identification (MEGA BLAST)	Similarity (%)
Actinobacteria	1	Nocardioides sp.	uncultured bacterium	96
	2	**Propionibacterium sp.**	uncultured bacterium	99
Bacteroidetes	3	**unclass.Flavobacteraceae**	**uncultured Cloacibacterium sp.**	95
	4	Flavobacterium sp.	uncultured bacterium	98
	5	Fluviicola sp.	uncultured bacterium	94
	6	**unclass. Bateroidales**	uncultured Bacteroidetes bacterium	98
Chloroflexi	7	Dehalogenimonas sp.	Uncultured bacterium clone	96-99
	8	unclass. Anaerolineaceae	uncultured Chloroflexi bacterium	94-96
Firmicutes	9	**Trichococcus sp.**	Trichococcus palustris strain	99
	10	**Acetobacterium sp.**	uncultured bacterim	97
Proteobacteria				
Beta class	11	Albidiferax sp.	uncultured bacterium	99
	12	**Comamonas sp.**	**Uncultured Commamonas sp.**	98
	13	**Curvibacter sp.**	**uncultured bacterium**	97
	14	**Dechloromonas sp.**	**Decholormonas sp. JJ**	97
	15	Dechloromonas sp.	uncultured bacterium	98
	16	**Rhodoferax sp.**	**uncultured bacterium**	98
Epsilon class	17	unclass. Alcaligenaceae	Uncultured bacterium	97
Gamma class	18	Sulfurimonas sp.	Uncultured bacterium	97
	19	Pseudomonas sp.	Uncultured gamma proteobacterium	97
	20	**Pseudomonas sp.**	**Uncultured Pseudomonas sp.**	99
	21	Methylobacter sp.	Uncultured Methylobacter	98
Candidate Division Tm7	22	TM7_genera_incertae_sedis	Uncultured bacterium	97

Brewer L., Hypolimnetic floc

Phylum	OTU	Taxonomial Assigment (RDP)	NCBI Identification (MEGA BLAST)	Similarity (%)
Actinobacteria	1	Illumatobacter sp.	Uncultured bacterium	97
	2	unclass. Micrococcineae	Uncultured bacterium	99
Bacteroidetes	3	Ferruginibacter sp.	Ferruginibacter alkalilentus	98
	4	**unclass. Porphyromonadaceae**	**Uncultured bacterium**	95
Chloroflexi	5	Bellilinea sp.	Uncultured bacterium clone	97
	6	Dehalogenimonas sp.	Uncultured bacterium clone	96-99
Chlorobi	7	Ignavibacterium sp.	Uncultured Chlorobiales bacterium	98
Firmicutes	8	**Trichococcus sp.**	uncultured bacterium clone	97
	9	**unclass. Costridiales**	uncultured bacterium clone	98'
	10	**unclass. Bacillales**	uncultured bacterium clone	96
Planctomycetes	11	Gemmata sp.	Uncultured bacterium clone	98
Proteobacteria				
Alpha class	12	unclass. Alphaproteobacteria	Uncultured bacterium	92
Beta class	13	**Comamonas sp.**	**Comamonas sp.**	99
	14	**Propionivibrio sp.**	**Uncultured bacterium**	98
	15	unclass. Betaproteobacteria	Candidatus Nitrotoga arctica	99
	16	unclass. Neisseriaceae	Uncultured bacterium	94
Delta class	17	unclassified deltaproteobacteria	cultured bacterium iron snow	98
	18	**Desulvibrio sp.**	**uncultured bacterium clone**	99
Gamma class	19	Methylobacter sp.	Uncultured Methylobacter sp. Clone	99
	20	unclass. Gammaproteobacteria	uncultured bacterium clone	96
Verrucomicrobia	21	Spartobacteria (genera_incertae_sedis)	Uncultured Verrucomicrobia bacterium	94
Candidate Division Tm7	22	TM7_genera_incertae_sedis	uncultured bacterium clone	97

Coldspring L., Hypolimnetic floc

Phylum	OTU	Taxonomial Assigment (RDP)	NCBI Identification (MEGA BLAST)	Similarity (%)
Acidobacteria	1	unclass. Acidimicrobiaceae	Uncultured bacterium	97
	2	**Geothrix sp.**	**uncultured Geothrix sp.**	96
Actinobacteria	3	unclass. Actinomycetales	Uncultured Sporichthyaceae	97
	4	unclass. Actinomycetales	uncultured actinobacterium	98
	5	unclass. Micrococcineae	uncultured bacterium	98
Chloroflexi	6	unclass. Anaerolineaceae	uncultured bacterium	98
	7	unclass. Chloroflexi	uncultured Chloroflexi	91
Cyanobacteria	8	Family I	Uncultured cyanobacterium	98
	9	Family II	uncultured Synechococcus sp.	99
	10	Family II	Synechococcus sp. Itu14s11	99
	11	Family II	Cyanobium sp. JJNV	99
	12	Family II	Uncultured cyanobacterium	98-99
	13	Family XIII	Cyanobacterium enrichment culture clone	96
Firmicute	14	**Bacillus sp.**	**uncultured Bacillus sp.**	98
Planctomycetes	15	Zavarzinella sp.	Uncultured bacterium	99
Proteobacteria				
Beta class	16	Albidiferax sp.	Albidiferax sp.	98
	17	**Comamonas sp.**	**uncultured bacterium**	98
	18	Dechloromonas	uncututred bacteriuam	97
	19	Sulfuritalea sp.	Fe-reducing enrichment culture clone	98
	20	unclass. Betaproteobacteria	Uncultured bacterium clone DR368	94
	21	unclass. Betaproteobacteria	Uncultured beta proteobacterium	93
	22	unclass. Betaproteobacteria	Uncultured beta proteobacterium	93
	23	unclass. Rhodocyclaceae	Uncultured Azospira sp.	99
	24	**unclass. Rhodocyclaceae**	**Uncultured bacterium**	97
Delta class	25	**unclass. Geobacteraceae**	**Uncultured Geobacter sp**	97
	26	unclass. Deltaproteobacteria	uncultured soil bacterium	92
	27	**unclass. Desulfobacterales**	**Uncultured Desulfobacteraceae bacterium**	95
Gamma class	28	Coxiella sp.	Uncultured gamma proteobacterium	95
	29	Methylobacter sp.	Methylobacter tundripaludum	95
	30	**Pseudomonas sp.**	**Uncultured Pseudomonas sp. Clone**	99
	31	unclass. Methylococcaceae	Uncultured bacterium	96
Verrucomicrobia	32	Spartobacteria (genera incertae sedis)	Uncultured Verrucomicrobia bacterium	97-99
Candidate Division Tm7	33	TM7 (genera incertae sedis)	Uncultured bacterium	96-99

Coldspring L., Metalimnetic floc

Phylum	OTU	Taxonomial Assigment (RDP)	NCBI Identification (MEGA BLAST)	Similarity (%)
Actinobacteria	1	Illumatobacter sp.	Uncultured bacterium	99
	2	unclass. Micrococcineae	Uncultured bacterium	98
	3	unclass. Actinomycetales	Uncultured Sporichthyaceae bacterium	98
	4	unclass. Actinobacteria	Uncultured bacterium	96
Bacteroidetes	5	**Cloacibacterium sp.**	Uncultured bacterium	
	6	Sediminibacterium sp.	Uncultured Bacteroidetes bacterium	97
	7	**Bacteroides sp.**	**Uncultured bacterium**	99
	8	unclass. Sphingobacterides	Uncultured bacterium clone	95
	9	**unclass. Flavobacteriales**	**Uncultured Flavobacterium sp.**	93
Chloroflexi	10	Bellilinea sp.	Uncultured bacterium clone	97
	11	Heliothrix sp.	Chloroflexaceae bacterium enrichment culture	95
	12	unclass. Anaerolineaceae	denitrifying bacterium enrichment culture	95
	13	Unclass. Chloroflexi	Uncultured bacterium	96
Chlorobi	14	unclass. Chlorobia	uncultured Chlorobia bacterium	97
Cyanobacteria	15	Cryptomonadaceae sp.	Uncultured bacterium clone	97-98
	16	Family II	Uncultured bacterium clone	99
	17	Family XIII	Planktothrix sp.	96-97
Firmicute	18	**Bacillus sp.**	**uncultured Bacillus sp.**	98
	19	unclass. Clostridiales	Uncultured bacterium	
Fusobacter	20	unclass. Fusobacteriaceae	Uncultured Fusobacteria	98
Planctomycetes	21	Zavarzinella sp.	Uncultured bacterium	99
Proteobacteria				
Alpha class	22	unclass. Alphaproteobacteria	Uncultured bacterium	92
Beta class	23	Acidovorax sp.	Uncultured bacterium	98
	24	**Comamonas sp.**	Uncultured bacterium	99
	25	Dechloromonas sp.	Uncultured bacterium	97
	26	**unclass. Rhodocyclaceae**	Uncultured bacterium	98
Delta class	27	**unclass. Desulfuromonadales**	**Uncultured bacterium clone**	95
Gamma class	28	Methylobacter sp	Uncultured Methylobacter	99
	29	**Pseudomonas sp.**	**Pseudomonas veroni**	96
	30	unclass. Methylococcaceae	Uncultured bacterium	96
Verrucomicrobia	31	Spartobacteria (genera incertae sedis)	Uncultured Verrucomicrobia bacterium	97-99
Candidate Division Tm7	32	TM7 (genera incertae sedis)	Uncultured bacterium	96-99

1. W.E. Balch, S. Schoberth, R. S. Tanner, R.S. Wolfe, "Acetobacterium, a new genus of hydrogen-oxidizing, carbon dioxide-reducing, anaerobic bacteria," *Int J Syst Bacteriol.* **27**, 355 (1997).

2. H. Kobayashi, K. Endo, S. Sakata, D. Mayumi, H. Kawaguchi, M. Ikarashi, Y. Miyagawa, H. Maeda, K. Sato, "Phylogenetic diversity of microbial communities associated with the crude-oil, large- insoluble-particle and formation-water components of the reservoir fluid from a non-flooded high-temperature petroleum reservoir," *J Biosci Bioeng.* **113**, 204 (2012).

3. M. L. Edwards, A. K. Lilley, T. H. Timms-Wilson, I. P. Thompson, I. Cooper, "Characterisation of the culturable heterotrophic bacterial community in a small eutrophic lake (Priest Pot)," *FEMS Microbiol Ecol.* **35**, 295 (2006).

4. E. S. McLeod, Z. Dawood, R. MacDonald, M. C. Oosthuizen, J. Graf, P. L. Steyn, V. S. Brözel, "Isolation and Identification of Sulphite- and Iron Reducing, Hydrogenase Positive Facultative Anaerobes from Cooling Water Systems," *Syst Appl Microbiol.* **21**, 297 (1998).

5. T. Mechichi, E. Stackebrandt, G. Fuchs, "Alicycliphilus denitrificans gen. nov., sp. nov., a cyclohexanol-degrading, nitrate-reducing beta-proteobacterium," *Int J Syst Evol Microbiol*. **53**, 147 (2003).

6. M. Rautio, E. Eerola, M. L. Väisänen-Tunkelrott, D. Molitoris, P. Lawson, M. D. Collins, H. Jousimies-Somer, "Reclassification of Bacteroides putredinis (Weinberg et al., 1937) in a new genus Alistipes gen. nov., as Alistipes putredinis comb. nov., and description of Alistipes finegoldii sp. nov., from human sources," *Syst Appl Microbiol*. 26, 182 (2003).
7. K. Gorlach, R. Shingaki, H. Morisaki, T. Hattori, "Construction of Eco-collection of Paddy Field Soil Bacteria for Population Analysis," *J Gen Appl Microbiol.* 40, 509 (1994).

8 W. L. van Veen, "Biological oxidation of manganese in soils," *Antonie Van Leeuwenhoek* **1**, 657 (1973).

9 M. L. Edwards, A. K. Lilley, T. H. Timms-Wilson, I. P. Thompson, I. Cooper, "Characterisation of the cultivable heterotrophic bacterial community in a small eutrophic lake (Priest Pot)," *FEMS Microbiol Ecol.* **35**, 295 (2006).

10 H. Rheims, A. Frühling, P. Schumann, M. Rohde, E. Stackebrandt, "Bacillus silvestris sp. Nov., a new member of the genus Bacillus that contains lysine in its cell wall," *Int J Syst Bacteriol.* **49**, 795 (1999).

11 D. R. Boone, Y. Liu, Z. J. Zhao, D. L. Balkwill, G. R. Drake, T. O. Stevens, H. C. Aldrich, "Bacillus infernus sp. nov., an Fe(III)- and Mn(IV)-reducing anaerobe from the deep terrestrial subsurface," *Int J Syst Evol Microbiol.* **45**, 441 (1995).

12 H. Wexler, "Bacteroides: the Good, the Bad, and the Nitty-Gritty," *Clin Microbiol Rev.* **20**, 593 (2007).

13 . S. T. Tay, V. Ivanov, W. Q. Zhuang, J. H. Tay, "Presence of Anaerobic Bacteroides in Aerobically Grown Microbial Granules," *Microb Ecol.* **44**, 278 (2002).

14 H. E. Müller, D. J. Brenner, G. R. Fanning, P. A. Grimont, P. Kämpfer, "Emended description of Buttiauxella agrestis with recognition of six new species of Buttiauxella and two new species of Kluyvera: Buttiauxella ferragutiae sp. nov., Buttiauxella gaviniae sp. nov., Buttiauxella brennerae sp. nov., Buttiauxella izardii sp. nov., Buttiauxella noackiae sp. nov., Buttiauxella warmboldiae sp. nov., Kluyvera cochleae sp. nov., and Kluyvera georgiana sp. nov." *Int J Syst Bacteriol* 46, 50 (1996).
15 P. K. Wüst, M. A. Horn, H. L. Drake, "Clostridiaceae and Enterobacteriaceae as active fermenters in earthworm gut content," *ISME Journal* 5, 92 (2011).

16. T. D. Allen, P. A. Lawson, M. D. Collins, E. Falsen, R. S. Tanner, "Cloacibacterium normanense gen. nov., sp. nov., a novel bacterium in the family Flavobacteriaceae isolated from municipal wastewater," *Int J Syst Evol Microbiol.* **56**, 1311 (2006).

17. L. Ding, A. Yokota, "Curvibacter fontana sp. nov., a microaerobic bacteria isolated from well water," *J Gen Appl Microbiol.* **56**, 267 (2010).

18 N. O. G. Jørgensen, K. K. Brandt, O. Nybroe, M. Hansen, "*Delftia lacustris* sp. nov., a peptidoglycan-degrading bacterium from fresh water, and emended description of *Delftia tsuruhatensis* as a peptidoglycan-degrading bacterium," *Int J Syst Evol Microbiol.* 59, 2159 (2009).
19 A. Wen, M. Fegan, C. Hayward, S. Chakraborty, L. I. Sly, "Phylogenetic relationships among members of the *Comamonadaceae,* and description of *Delftia acidovorans* (den Dooren de Jong 1926 and Tarnaoka *etal.* 1987) gen. nov., comb. now." *Int J Syst Bacteriol* 49, 567 (1999)

20 M. L. Edwards, A. K. Lilley, T. H. Timms-Wilson, I. P. Thompson, I. Cooper, "Characterisation of the culturable heterotrophic bacterial community in a small eutrophic lake (Priest Pot)," *FEMS Microbiol Ecol.* **35**, 295 (2006).

21. S. S. Adav, D. J. Lee, J. Y. Lai, "Microbial community of acetate utilizing denitrifiers in aerobic granules," *App Microbiol Biotechnol.* **85**, 753 (2010).

22. V. Vandieken, C. Knoblauch, B. B. Jørgensen, "Desulfotomaculum arcticum sp. nov., a novel spore-forming, moderately thermophilic, sulfate-reducing bacterium isolated from a permanently cold fjord sediment of Svalbard," *Int J Syst Evol Microbiol.* **56**, 687 (2006).

23. H. Rütters, H. Sass, H. Cypionka, J. Rulkötter, "Monoalkylether phospholipids in the sulfate-reducing bacteria Desulfosarcina variabilis and Desulforhabdus amnigenus," *Arch Microbiol.* **176**, 435 (2001).

24. I. Neria-González, E. T. Wang, F. Ramírez, J. M. Romero, C. Hernández-Rodríguez, "Characterization of bacterial community associated to biofilms of corroded oil pipelines from the southeast of Mexico," *Anaerobe* **12**, 122 (2006).

26 . D. R. Lovley, E. J. Phillips, "Reduction of uranium by Desulfovibrio desulfuricans," *Appl Environ Microbiol.***58**, 850 (1992).

27. M. P. Bryant, L. L. Campbell, C. A. Reddy, M. R. Crabill, "Growth of Desulfovibrio in Lactate or Ethanol Media Low in Sulfate in Association with H2-Utilizing Methanogenic Bacteria," *Appl Environ Microbiol.***3**, 1162 (1997).

28. E. E. Roden, D. R. Lovley, "Dissimilatory Fe(III) Reduction by the Marine Microorganism *Desulfuromonas acetoxidans,*" *Appl Environ Microbiol*. **3**, 743 (1993).

29. K. Finster, J. D. Coates, W. Liesack, N. Pfennig, "Desulfuromonas thiophila sp. nov., a New Obligatory Sulfur-Reducing Bacterium from Anoxic Freshwater Sediment," *Int J Syst Bacteriol.* **47**, 754 (1997).

30. D. Moreels, G. Crosson, C. Garafola, D. Monteleone, S. Taghavi, J. P. Fitts, D. van der Lelie. "Microbial community dynamics in uranium contaminated subsurface sediments under bio-stimulated conditions with high nitrate and nickel pressure," *Environ Sci Pollut Res Int.* **15**, 481, (2008).

31. B. J. Paster, W. Ludwig, W. G. Weisburg, E. Stackebrandt, R. B. Hespell, C. M. Hahn, H. Reichenbach, K. O. Stetter, C. R. Woese, "A Phylogenetic Grouping of the Bacteroides, Cytophagas, and Certain Flavobacteria," *Syst Appl Microbiol.* **6**, 34 (1985).

32. Z. W. Wang, Y. H. Liu, X. Dai, B. J. Wang, C. Y. Jiang, S. J. Liu, "Flavobacterium saliperosum sp. nov., isolated from freshwater lake sediment," *Int J Syst Evol Microbiol.* **56**, 439 (2006).

33. C. S. Lee, Y. T. Jung, S. Park, T. K. Oh, J. H. Yoon, "Lysinibacillus xylanilyticus sp. nov., a xylan-degrading bacterium isolated from forest humus," *Int J Syst Evol Microbiol.* **60**, 281 (2010).

34 J. M. Cerrato, J. O. Falkinham, A. M. Dietrich, W. R. Knocke, C. W. McKinney, A. Pruden, "Manganese-oxidizing and -reducing microorganisms isolated from biofilms in chlorinated drinking water systems," *Water Research* **44**, 3935 (2010).

35. X .Li, L. R. Krumholz, "Influence of nitrate on microbial reduction of pertechnetate," *Environ Sci Technol.* **42**, 1910 (2008).

36. B. Pettersson, K. E. Rippere, A. A. Yousten, F. G. Priest, "Transfer of *Bacillus lentimorbus* and *Bacillus popilliae* to the genus *Paenibacillus* with emended descriptions of *Paenibacillus lentimorbus* comb. nov. and Paenibacillus popilliae comb. nov." *Int J Syst Bacteriol* **49**, 531 (1999).

37. C. A. Francis, A. Y. Obraztsova, B. M. Tebo, "Dissimilatory Metal Reduction by the Facultative Anaerobe *Pantoea agglomerans* SP1," *Appl Environ Microbiol.* **66**, 543 (2000).

38. F. Gavini, J. Mergaert, A. Beji, C. Mielcarek, D. Izard, K. Kersters, J. De Ley, "Transfer of *Enterobacter agglomerans* (Beijerinck 1888) Ewing and Fife 1972 to *Pantoea* gen. nov. as *Pantoea agglomerans* comb. nov. and Description of *Pantoea dispersa* sp. nov." *Int J Syst Bacteriol.* **39**, 337 (1989).

39 A. Grabowski, B. J. Tindall, V. Bardin, D. Blanchet, C. Jeanthon, "Petrimonas sulfuriphila gen. nov., sp. nov., mesophilic fermentative bacterium isolated from a biodegraded oil reservoir," *Int J Syst Evol Microbiol.* **55**, 1113 (2005).

40. H. S. Pilar, R. R. De Garcia, "Prevalence of Plesiomonas shigelloides in aquatic environments," *Int J Environ Health Res.* **7**, 115 (1997).

41. B. Schink, "Mechanisms and Kinetics of Succinate and Propionate Degradation in Anoxic Freshwater Sediments and Sewage Sludge," *Microbiology* **131**, 643 (1984).

42. R. G. Arnold, T. J. DiChristina, M. R. Hoffmann, "Inhibitor studies of dissimilative Fe(III) reduction by Pseudomonas sp. strain 200 ("Pseudomonas ferrireductans")," *Appl Environ Microbiol.* **52**, 281 (1986).

43. B. J. Paster, F. E. Dewhirst, I. Olsen, G. J. Fraser, "Phylogeny of Bacteroides, Prevotella, and Porphyromonas spp. and related bacteria," *J Bacteriol.* **176**, 725 (1994).

44. M. A. Cotta, T. R. Whitehead, E. Falsen, E. Moore, P. A. Lawson, "Robinsoniella peoriensis gen. nov., sp. nov., isolated from a swine-manure storage pit and a human clinical source," *Int J System Evol Microbiol.* **59**, 150 (2009).

45. U. S. Justesen, M. N. Skov, E. Knudsen, H. M. Holt, P. Søgaard, T. Justesen, "16S rRNA Gene Sequencing in Routine Identification of Anaerobic Bacteria Isolated from Blood Cultures," *J Clin Microbiol.* **48**, 946 (2010).

46. K. T. Finneran, C. V. Johnsen, D. R. Lovley, "Rhodoferax ferrireducens sp. nov., a psychrotolerant, facultatively anaerobic bacterium that oxidizes acetate with the reduction of Fe(III)," *Int J Syst Evol Microbiol.* **53**, 669 (2003).

47. R. Schulze, S. Spring, R. Amann, I. Huber, W. Ludwig, K. H. Schleifer, P. Kämpfer, "Genotypic diversity of Acidovorax strains isolated from activated sludge and description of Acidovorax defluvii sp. nov." *Syst Appl Microbiol*. **22**, 205 (1999).

48. G. Nick, P. de Lajudie, B. D. Eardly, S. Suomalainen, L. Paulin, X. Zhang, M. Gillis, K. Lindström, "*Sinorhizobium arboris* sp. nov. and *Sinorhizobium kostiense* sp. nov., isolated from leguminous trees in Sudan and Kenya," *Int J Syst Bacteriol*. **49**, 1359 (1999).

49. C. S. Zou, M. H. Mo, Y. Q. Gu, J. P. Zhou, K. Q. Zhang, "Possible contributions of volatile-producing bacteria to soil fungistasis," *Soil Biol Biochem.* **39**, 2371 (2007).

50. S. Y. An, T. Haga, H. Kasai, K. Goto, A. Yokota, "Sporosarcina saromensis sp. nov., an aerobic endospore-forming bacterium," *Int J Sys Evol Microbiol.* **57**, 1868 (2007).

51. K. Watanabe, K. Watanabe, Y. Kodama, K. Syutsubo, S. Harayama, "Molecular characterization of bacterial populations in petroleum-contaminated groundwater discharged from underground crude oil storage cavities," *Appl Environ Microbiol*. **66**, 4803 (2000).

52. Y. Kodama, K. Watanabe, "Sulfuricurvum kujiense gen. nov., sp. nov., a facultatively anaerobic, chemolithoautotrophic, sulfur-oxidizing bacterium isolated from an underground crude-oil storage cavity*," Int J Syst Evol Microbiol*. **54**, 2297 (2004).

53. C. Harms, A. Schleicher, M. D. Collins, J. R. Andreesen, "Tissierella creatinophila sp. nov., a Gram-positive, anaerobic, non-spore-forming, creatinine-fermenting organism," *Int J Syst Bacteriol.* **48**, 983 (1998).

54. J.W. Bae, J. R. Park, Y. H. Chang, S. K. Rhee, B. C. Kim, Y. H. Park, "Clostridium hastiforme is a later synonym of Tissierella praeacuta," *Int J Syst Evol Microbiol*. **54**, 957 (2004).

55. M. Bunge, A. Wagner, M. Fischer, J. R. Andreesen, U. Lechner, "Enrichment of a dioxin-dehalogenating Dehalococcoides species in two-liquid phase cultures," *Environ Microbiol*. **10**, 2670 (2008).

56J. R. Liu, R. S. Tanner, P. Schumann, N. Weiss, C. A. McKenzie, P. H. Janssen, E. M. Seviour, P. A. Lawson, T. D. Allen, R. J. Seviour, "Emended description of the genus Trichococcus, description of Trichococcus collinsii sp. nov., and reclassification of Lactosphaera pasteurii as Trichococcus pasteurii comb. nov. and of Ruminococcus palustris as Trichococcus palustris comb. nov. in the low-G+C Gram-positive bacteria," *Int J Syst Evol Microbiol*. **52**, 1113 (2002).

57 B. Austin, S. Garges, B. Conrad, E. E. Harding, R. R. Colwell, U. Simidu, N. Taga, "Comparative study of the aerobic, heterotrophic bacterial flora of Chesapeake Bay and Tokyo Bay," *Appl Environ Microbiol.* **37**, 704 (1979).
58. M. J. Wolin, E. A. Wolin, N. J. Jacobs, "Cytochrome-producing anaerobic Vibrio, Vibrio succinogenes, sp. nov." *J Bacteriol*. **81**, 911 (1961).

59 . P. D. Nguyen, C. G. Van Ginkel, C. M. Plugge, "Anaerobic degradation of long-chain alkylamines by a denitrifying Pseudomonas stutzeri," *FEMS Microbiol. Ecol.* **66**, 136 (2008).

60 R. M. Kroppenstedt *et al.*, "Eight new species of the genus Micromonospora, Micromonospora citrea sp. nov., Micromonospora echinaurantiaca sp. nov., Micromonospora echinofusca sp. nov. Micromonospora fulviviridis sp. nov., Micromonospora inyonensis sp. nov., Micromonospora peucetia sp. nov., Micromonospora sagamiensis sp. nov., and Micromonospora viridifaciens sp. nov." *Syst. Appl. Microbiol.* **28**, 328 (2005).

61. M. Bloethe, E. E. Roden, "Microbial Iron Redox Cycling in a Circumneutral-pH Groundwater Seep," *Appl. Environ. Microbiol.* **75**, 468 (2009).

62. J. Wiegel, "Xanthobacter *Wiegel, Wilke, Baumgarten, Opitz and Schlegel 1978, 573* ," , 555 (2005). Bergey's Manual of Systematic of Bacteriology

63. A. Teske, D. Nelson, "The Genera *Beggiatoa* and *Thioploca*," 784 (2006). In: The Prokartoyes, 3rd Ed.

64. X. Wang, J. Yang, X. Chen, G. Sun, Y. Zhu, "Phylogenetic diversity of dissimilatory ferric iron reducers in paddy soil of Hunan, South China," *Journal of Soils and Sediments* **9**, 568 (2009).

65 J. G. Lack, S. K. Chaudhuri, R. Chakraborty, L. A. Achenbach, J. D. Coates, "Anaerobic biooxidation of Fe(II) by Dechloromonas sp.m," *Microb. Ecol.* **43**, 424 (2002).

66. N. Krieg, "Ahrensia *Uchino, Hirata, Yokota and Sugiyama 1999, 1* VP *(Effective publication: Uchino, Hirata, Yokota and Sugiyama 1998, 208*," , 167 (2005).

67 Dobbin, Paul S., et al. "Dissimilatory Fe (III) reduction by Clostridium beijerinckii isolated from freshwater sediment using Fe (III) maltol enrichment."*FEMS microbiology letters* 176.1 (1999): 131-138.

68 Knight, Victoria, and Richard Blakemore. "Reduction of diverse electron acceptors by Aeromonas hydrophila." *Archives of microbiology* 169.3 (1998): 239-248.

69 Wang, Pi-Chao, et al. "Isolation and characterization of an Enterobacter cloacae strain that reduces hexavalent chromium under anaerobic conditions."*Applied and Environmental Microbiology* 55.7 (1989): 1665-1669.

70 Coates, John D., et al. "Geothrix fermentans gen. nov., sp. nov., a novel Fe (III)-reducing bacterium from a hydrocarbon-contaminated aquifer." *International journal of systematic and evolutionary microbiology* 49.4 (1999): 1615-1622.

71 McLeod, Elise S., et al. "Isolation and identification of sulphite-and iron reducing, hydrogenase positive facultative anaerobes from cooling water systems." *Systematic and applied microbiology* 21.2 (1998): 297-305.

CHAPTER 5: SEASONAL CHANGES IN MICROBIAL COMMUNITY STRUCTURE, $FE^{(III/II)}$ REDOX CYCLING, AND TRACE ELEMENT GEOCHEMISTRY OF PELAGIC FLOCS IN A CIRCUMNEUTRAL, REMOTE LAKE

Elliott, A.V.C., and Warren, L.A
Submission to Environmental Science & Technology, July 2013

ABSTRACT

Evaluation of lacustrine floc Fe, Pb, and Cd biogeochemistry over seasonal (summer-winter) and water column depth (4.5, 7.5m) scales reveals depth-independent seasonally significant differences in floc Fe biominerals and trace element (TE: Pb, Cd) sequestration, driven by floc microbial community shifts. No depth dependent floc [Fe] or [TE] differences were evident between the 4.5m ('metalimnetic') and 7.5m ('hypolimnetic') depths for either season. However, winter floc total [TE] were significantly lower than summer total [TE], due to the declining abundance and reactivity of floc-FeOOH phases under ice ($[FeOOH]^{Summer}$= 37-77mgg^{-1} vs. $[FeOOH]^{Winter}$= 0.3-7mgg^{-1}). Further, while high summer floc [$Fe^{(III)}OOH$] was observed at both depths, winter floc [Fe] was dominated by $Fe^{(II)}$ phases. This observed seasonal change in both the nature and concentrations of floc Fe-phases was independent of water column [Fe], O_2, and pH, but was significantly correlated to floc bacterial community membership. Bioinformatic modelling (Unifract, PCA analyses) of *in situ* and experimental Fe-bacteria enrichment microcosm results identified temperature-driven seasonal shifts in floc microbial communities occurred; specifically the dominance of Fe metabolisms within summer floc to ancillary Fe reducing and S metabolizing bacteria within winter flocs. The temperature driven seasonal floc community functional shifts, most importantly the wintertime loss of floc associated microbial $Fe^{(II)}$-oxidizing capability and concomitant increases of S-metabolizing bacteria, alters dominant floc Fe minerals from $Fe^{(III)}$ to $Fe^{(II)}$ phases. This resulted in observed decreased floc TE sequestration during winter stratification, not predicted by water column geochemistry.

5.1 Introduction

The biogeochemistry of suspended sedimentary materials/suspended particulate matter (SPM) has received a great deal of attention in the last several decades. This is due to the: i) ability of SPM to sequester large quantities of trace elements (TE) relative to bottom sediments, ii) important role of SPM as a vector for TE transport, iii) link SPM plays between the highly bioavailable aqueous phase and bed sediment (classical TE-sink) aquatic system compartments and iv) biologically flocculated nature of suspended particulates (i.e. 'flocs'), such that flocs are regarded as mobile biofilms (1-8). Flocs may be derived from overland wash-off of soil aggregates, re-suspended bottom sedimentary materials and/or formed directly in suspension via a complex flocculation process (6). Regardless of their origin, the development and stabilization of suspended flocs are highly influenced by the activity of floc-colonizing bacteria and associated extracellular polymeric substances (EPS) (e.g. 6, 9-11). While floc structure, size and composition can vary considerably across aquatic systems and energy regimes (5, 12-14) what is common among floc is this underlying microbial nature of its formation and stabilization, with bacterial-produced EPS acting as the dominant physical bridging mechanism between the floc components- microbial, mineral and organic (6, 10, 12). This substantive biological nature of floc, as well as microbial influences on floc architecture and development, suggests that the resident floc microbial community will influence floc geochemistry in ways not currently captured by geochemical models, i.e., linkages amongst microbial metabolism and geochemical microenvironment development.

Recent work has shown lacustrine floc aggregates possess a distinct and conserved geochemistry, microbiology and composition from bed sedimentary materials in close proximity across varying aquatic systems and energy regimes (4, 5, 14, 15). Importantly, resident floc microbial communities were found to facilitate the concentration of TEs specifically though the collection/nucleation of highly reactive amorphous $Fe^{(III)}$-oxyhydroxide minerals (FeOOH), identifying a water column solid phase with differing controls over TE behavior than bed sedimentary materials (4, 5). More recently, Elliott et al. 2013 (*unpublished data)* demonstrated

that collaborating putative $Fe^{(III)}$-reducing (IRB) and $Fe^{(II)}$-oxidizing (IOB) floc bacteria within consortial micro-aggregates (80µm) couple $Fe^{(III)}$-reduction with $Fe^{(II)}$-oxidation across diverse oxygenated ($O_2^{Sat.}$=1-103%) aquatic systems, not expected to sustain microbial Fe-metabolism. Steep microscale gradients in oxygen and pH under bulk oxic conditions have been similarly reported within marine snow and cyanobacterial colonies (macroscopic aggregates, >1mm) (16-20). Elliott et al. 2013 also demonstrated the co-formation and occurrence of reduced and oxidized Fe biominerals in floc; not expected under the bulk system oxic concentrations but reflective of interior aggregate low oxygen/ anoxic conditions. This discovery suggests highly dynamic floc Fe-biogeochemistry, and therefore TE sequestration/mobilization, driven by microbial Fe-metabolism within the floc microhabitat.

Pelagic flocs will be exposed to highly differing physicochemical conditions as a function of water column depth as well as season. However, no studies to date of the microbial community structure and geochemistry of lacustrine suspended flocs (and of other pelagic aggregates, including marine snow) have assessed either seasonal or depth dependent changes in floc Fe/TE biogeochemistry or potential linkages to underlying floc microbial community functioning. Thus the objectives of this investigation were to characterize floc: i) bacterial community structure, ii) Fe-geochemistry, iii) Pb and Cd partitioning over depth and seasonal scales in a temperate, remote lake, and iv) experimentally assess floc microbial $Fe^{III/II}$-redox transformations under identified factors influencing floc biogeochemistry *in situ*. This was accomplished with an integrated biogeochemical approach, combining 454 16S amplicon sequencing, bioinformatics and hierarchal clustering of whole bacterial communities, with Fe-bacterial enrichment methodologies as well as solid phase TE and mineralogical analyses of floc aggregates to reveal biogeochemical linkages.

5.2. Material and methods

5.2.1 Field investigation. Summer (2010-August) and winter (2011-March) sampling campaigns were conducted at Coldspring Lake, a remote, groundwater fed lake only accessible by float plane within the nature preserve area of Algonquin Park, ON, Canada (45°85′28″N 78°82′17″W) (Figure 5.1). This system was selected due to steep water column gradients in important variables known to regulate Fe-geochemistry during both summer and winter stratification periods ($[O_2]$, $[Fe^{(II)}]$, $[Fe^{(Total)}]$, $[S^{2-}]$, $[NO_3^{2-}]$) (Figure 5.1, Table S1). Further, very high hypolimnetic $Fe_{aq}^{(II)}$ and metalimnetic $Fe_{aq}^{(III)}$ ('dissolved', <0.22μm) concentrations (>>1mg/L) occur, indicating differential supersaturation of ferrous, ferric and iron bearing mineral phases with water column depth (i.e. 'floc building' reactions). These Fe concentrations are significantly greater than average Fe concentrations known from hardrock and/or boreal lacustrine waters for both pristine and impacted systems (1.3-533μgL^{-1}) (21)

Sampling campaigns during each season provided i) *in situ* water column physicochemical data (redox potential (Eh), pH, temperature, dissolved oxygen $[O_2]$, conductivity (SPC): DataSonde-Surveyor 4A, Hydrolab Corporation, TX); ii) quantification of major inorganic species (nitrate, phosphate, sulphate, sulphide: DR/2010 HACH spectrophotometer), iii) quantification of $Fe^{(II)}_{aq}$, $Fe^{(III)}_{aq}$ (22, 23), TE_{aq} ('dissolved', <0.22μm) and iv) suspended floc samples. Flocs from each seasonal campaign were simultaneously collected from 4.5m (summer metalimnion) and 7.5m (hypolimnion) water column depths using continuous flow centrifugation (CFC: Westfalia Model KA 2-06-075) whereby water (>2000L) was pumped (6$Lmin^{-1}$) into CFC bowls with a rotational speed of 9470rpm (4, 5, 24). Floc samples were collected for mineralogical analysis (XRD), imaging analyses (TEM), trace element analyses (TEs: Pb, Cd; sequential extractions), 16S sequencing and targeted isolations/enrichments of Fe-bacteria. After collection, flocs for sequential extractions (25, 26) and 16S community analyses were immediately frozen on dry ice and stored in the dark at -20°C prior to processing in the laboratory. Flocs for Fe-bacteria (IRB, IOB) enrichments were stored in the dark at 4°C for a maximum of 8–16h.

5.2.2 Floc Fe and TE characterization. Floc associated Fe and TE concentrations were quantified in triplicate using a sequential extraction technique (25, 26), partitioning floc Fe-phases and associated TEs into six operationally defined solid phases: i. exchangeable (loosely bound), ii. acid-soluble (i.e. associated with carbonates); iii. easily reducible amorphous Fe/Mn oxyhydroxides (i.e. FeOOH); iv. reducible crystalline Fe/Mn oxides (i.e. hematite, goethite); v. oxidizable phases (i.e. associated with organics/sulfide phases) and vi) residual (i.e. bound within mineral lattices). Sequential extractions selectively dissolved each floc solid fraction, concomitantly releasing any Fe and TEs associated with that solid phase into the supernatant. TE concentrations were subsequently quantified in triplicate by inductively coupled plasma mass spectrometry (ICP-MS: Perkin Elmer SCIEX ELAN 6100, Woodbridge, ON, Canada). Floc associated Fe was quantified using the Ferrozine assay, as described previously (23, 27). Total floc Fe ($[Fe]^{Total}$; mgg^{-1}) and $[TE]^{Total}$ ($\mu molg^{-1}$) were determined by summing the individual concentrations in each of the defined fractions, providing a means to quantify whole-floc Fe and TE concentrations as well as their partitioning among the differentially reactive solid-phase floc constituents. Bulk floc organic content was estimated by loss on ignition at 550ºC for 2h (g organic C/ g sediment).

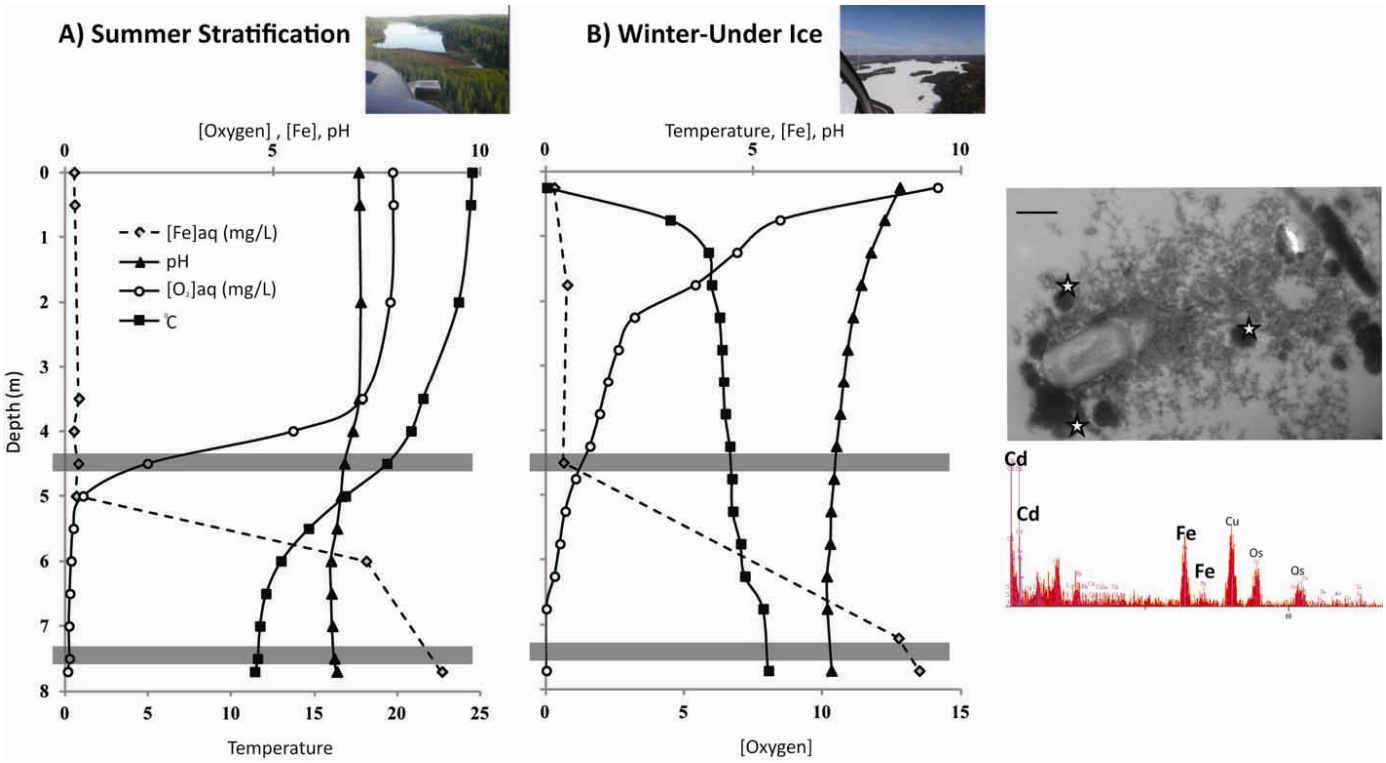

Figure 5.1 Seasonal geochemistry of A) summer stratification and B) winter stratification of Coldspring Lake, Algonquin Park, ON. Grey bars correspond to depth of suspended floc collection for each sampling campaign: 4.5m (summer metalimnion) and 7.5m (hypolimnion). Note differences in x-axes. TEM and EDS analyses revealed consistent association of floc microbial cells, and Fe-Cd precipitates entrapped within organic EPS matrix (insert).

5.2.3 Summer vs. winter Fe-bacterial communities. Floc associated Fe-bacterial consortia were characterized using targeted metabolic isolation techniques for IRB and IOB (28, 29), as well as laboratory microcosm co-enrichment experimentation on whole-floc communities, as described previously (30) and modified by (Elliott et al. 2013, *unpublished data*) for summer floc communities. Briefly, targeted metabolic cultivation techniques were used for isolation and demonstration of Fe-redox (i.e., IOB, IRB) activity within flocs. Isolations for neutrophilic, microaerobic, $Fe^{(II)}$-oxidizing bacteria (IOB) via a modified gradient tube method (28, 29) were incubated at 22°C (i.e. summer) and at 4°C (i.e. winter) in the dark. Demonstration of anaerobic, dissimilatory IRB activity was accomplished using a modified *Shewanella putrefaciens* specific liquid media under strictly anoxic conditions (pH=6.0, 10mM $Fe^{(III)}$ (as $Fe^{(III)}$-citrate), 5mM acetate) in the dark (30). Negative controls were created by i) inoculation with γ-sterilized floc samples, and ii) empty (i.e. sample-free) media. Laboratory co-enrichment experiments assessed the potential for coupled Fe-metabolism in winter and summer environmental floc samples from both sampling depths. Co-enrichment microcosms tracked microbial community dynamics (16S rRNA, Sanger sequencing), aggregate formation (imaging analyses) and Fe geochemistry ($Fe^{(III)}/Fe^{(II)}_{aq}$, Ferrozine assay, (23, 27)), Fe-biomineral formation (XRD, (31, 32)) under conditions mimicking either winter (~4°C) or summer (~22°C) temperatures. All microcosms were conducted under microoxic conditions, confirmed by monitoring ($\mathbf{O_2}^{\textbf{Avg. Summer Microcosms}}$= 0.29-0.39 mgL^{-1}; $\mathbf{O_2}^{\textbf{Avg Winter Microcosms}}$= 0.32-0.40 mgL^{-1}). To achieve these microoxic conditions, flasks were set up at a liquid to flask volume ratio of 0.88, covered with a double-layer of aluminum foil permitting gas diffusion and left static (33, 34). Enrichment microcosms constituted liquid mineral salts media (30) (pH=6.0), spiked with acetate (electron donor, 10mM), ferric-$Fe^{(III)}$ (10mM as $Fe^{(III)}$-citrate; i.e. no $Fe^{(II)}$ source provided) and maintained over multiple generations (n=~60 generations, over ~1.5 years) in the dark. A soluble-phase Fe source was used to assess *in situ* bio-mineral formation within experimental microcosms (i.e. no exogenous Fe-mineral source introduced). These experimental $Fe^{(III)}$ and carbon concentrations reflect the relatively high overall total Fe content of *in situ* parent

floc samples (up to ~135.5 mg Fe/g floc, 0.6 mg organic C/ g floc; $Fe_{(aq)}$=0.43-9.9 mg/L Table S1), and mimic electron donor and acceptor concentrations from recent investigations of microbial Fe-redox transformations e.g. (35-39). Negative controls consisted of i) inoculation with γ-sterilized floc samples, and ii) empty (i.e. sample-free) co-enrichment media. Preservation of Fe-metabolic function post microcosm experiment was confirmed by re-growth trials in isolation media as described above i.e. IOB, opposing gradient tubes (28, 29) and IRB, *Shewanella putrefaciens* isolation media (30).

5.2.4 Whole floc and Fe-bacteria community identification. Total community DNA was extracted in duplicate from parent floc samples (whole floc community) and laboratory co-enrichments (Fe-bacteria community) using the PowerSoil DNA Isolation Kit (MO Bio Laboratories, Carlsbad, CA) according to the manufacturer's instructions. Pyrosequencing was carried out by Mr. DNA Next Generation Sequencing and Bioinformatics Services (Shallowater, TX, U.S.A), using a Roche 454 FLX genome sequencer system and FLX Titanium reagents (Roche Applied Sciences, IN, U.S.A (40, 41). The universal Eubacterial primers 27F (5'-AGRGTTTGATCMTGGCTCAG) and 530R (5'-CCGCNGCNGCTGGCAC) were used to amplify approximately 500bp of the variable regions V1 to V3, generating ~5000-6000 sequences per sample (post editing). In addition, Sanger sequencing (16S rDNA) of microcosm co-enrichments targeted a greater length of the 16S and thus improved specific identification of Fe-metabolizing bacteria enriched within the experimental microcosms and *in situ* communities. Universal bacterial primers 27F and 1492R (~1500 bp) were used to amplify almost the complete 16S rRNA gene and were subsequently purified with the QIA-quick PCR Purification kit (Qiagen) and ligated into the linear Plasmid Vector pCR4 supplied with the TOPO TA kit (Invitrogen). Cloning efficiency was improved by the addition of 3' A-overhangs post-amplification. Final products were transformed into One Shot Chemically Competent *Escherichia coli* (Invitrogen) by heat shock following the manufacturer's protocol. Sequencing was completed with ABI BigDye terminator chemistry, using

a 3730 DNA analyzer (Applied Biosystems, Foster City, CA and Institute for Molecular Biology and Biotechnology, McMaster University, ON, Canada).

The Ribosomal Database Project (RDP) Pyrosequencing pipeline was used to process and analyze sequences derived from 454 sequencing (Michigan State University; http://pyro.cme.msu.edu/index.jsp (42)) including: alignment, clustering, and dereplication. All sequences (both 454 and Sanger 16S) were analyzed against the NCBI (US) database using the mega-BLAST algorithm and also assigned to a taxonomical hierarchy using the RDP classifier tool. Representative sequence identification and classification from all OTUs (binned at 97% similarity) was performed using the Basic Local Alignment Search Tool (BLAST) and RDP classification tool (43). Further phylogenetic analyses were conducted using MEGA version 5.0 software (44). Multiple sequence alignments were accomplished using the MUSCLE algorithm, manually edited and regions of ambiguous alignment removed. The Maximum Likelihood (ML) tree-searching method was used for phylogenetic tree construction for both 454 and Sanger 16S sequences. Phylogram topologies were bootstrapped 1,000 times to assess support for nodes and subsequently used as input files for UniFrac analyses.

5.2.5 Community clustering and PCA analyses. Unifrac (http://bmf.colorado.edu/unifrac (45, 46)) is a phylogenetic distance metric and clustering algorithm applied in a wide variety of medical microbiological and human 'microbiome' (e.g. (47-49)) as well as environmental studies (e.g. (50-52), which enables comparisons of entire *in situ* communities across environments or sampling points. Here, Unifrac was used to evaluate changes in i) whole *in situ* floc and ii) floc Fe-bacteria consortial communities (enrichments) across seasons (summer-winter) and with water column depth (4.5m vs. 7.5m). Unifrac is distinct from other widely used metrics in that it accounts for the different degrees of similarity between 16S rRNA gene sequences and thus garners more information than comparable taxon-based metrics that bin 16S rRNA genes based on 97-99% similarity; reducing the impact of utilization of arbitrary OTU thresholds prior to statistical analyses (46). Further, both the delineation of the relative importance of changes in

community membership (here defined as the presence/absence of specific bacterial lineages, $UniFrac^{Unweighted}$) versus changes in bacterial lineage abundance (i.e. overall community structure, $UniFract^{Weighted}$) in contributing to variations and clustering patterns observed between floc communities were assessed (46, 53). The Unifract Significance test (46) was used to assess pair-wise differences between each floc community using both weighted ($P^{Weighted}$) and unweighted ($P^{Unweighted}$) Unifrac metrics. Multivariate statistic measures, hierarchal clustering (UPGMA) and Principle Coordinates Analyses (PCA), were used to compare floc communities simultaneously (45). The first three principle components of PCA were subsequently regressed with site physicochemical and floc composition data to identify which variables have the largest impact on floc community membership ($UniFrac^{Unweighted}$) and overall floc community structure ($UniFract^{Weighted}$) (53).

5.3 Results & Discussion

5.3.1 Field observations and seasonal geochemistry. Both depths of floc collection (4.5m, 7.5m) were of circumneutral pH (6.54-6.88) across summer and winter sampling campaigns (Figure 5.1, Table S1). During the summer sampling campaign, these depths corresponded to metalimnetic and hypolimnetic regions, between which dissolved oxygen concentrations decreased from oxygenated to microoxic conditions (Summer-$O_2^{Sat.}$: 21.3% to 0.5). Concomitantly, both $Fe_{(aq)}^{(Total)}$ and $Fe_{(aq)}^{(II)}$ significantly ($p<0.01$) increased with water column depth (~8x, 300x respectively) as did sulphide (4x) and nitrate (80x) concentrations (Figure 1, Table S1). Further, during the summer sampling campaign, both depths of floc collection were within the photic zone (1% light level=7.3m).

The water column during winter stratification showed very similar depth dependent trends. Water column [O_2] exhibited a similar decrease from oxygenated to microoxic conditions over these two depths, however was relatively less saturated compared to the summer %O_2 values (Winter-O_2^{Sat}: 10.4% to 0.21%) (Figure 1, Table S1). Both winter $[Fe_{(aq)}]^{Total}$ and $[Fe^{(II)}]_{(aq)}$ again significantly ($p<0.01$) increased with water column depth (~6x, 300x respectively) as did

sulphide (~3.6x) and nitrate (122x) concentrations (Figure 1, Table S1). Notably, $[Fe^{(II)}]_{(aq)}$ decreased under ice relative to summer concentrations (~2-14x) despite lower *in situ* oxygen levels. Water column temperature, $[O_2]$, and $[Fe^{(II)}]_{(aq)}$ were the only variables identified to exhibit significant seasonal variations (i.e. $Summer^{4.5m.}$ vs. $Winter^{4.5m.}$; $Summer^{7.5m}$ vs. $Winter^{7.5m}$). Water column temperature exhibited the greatest seasonal variation and was 6-15°C cooler during winter months, consistent with the temperate locality of Coldspring Lake (45°85′28″N 78°82′17″W).

PHREEQC modelling was used to identify expected dominant Fe-phases with depth. Water column $[Fe_{(aq)}]^{Total}$ ranged from 1.3-9.9mgL^{-1} in summer months and 0.43-8.5mgL^{-1} in winter months. Modelling results identified supersaturation of amorphous Fe-phases ($Fe^{(III)}OOH^{Amorphous}$) and hematite ($Fe_2O_3$) at both depths for both summer and winter stratification periods; consistent with the demonstrated occurrence of these phases through XRD analyses of environmental floc samples (Tables S1, S2). However, modeling did not predict the observed summer associated co-existence of reduced $Fe^{(II)}$-mineral phases (siderite, $Fe^{(II)}$-carbonate; magnetite, mixed $Fe^{(III)}/Fe^{(II)}$ oxide) and oxidized $Fe^{(III)}$-mineral phases (hematite, $Fe^{(III)}OOH^{Amorphous}$) in floc (Figure 5.2, Tables S1, S2) for both sampling depths (only magnetite observed for winter floc samples). Goethite was also predicted to occur but was not detected in either seasonal set of depth dependent floc samples. Rather, contrasting observed *in situ* floc Fe-mineral results, modelling predicted the largest observable differences in Fe-phases would occur with water column depth, not between seasons. However, observed floc Fe-mineralogy significantly varied only with season, showing no difference between depths for each season (Figure 2, Table S1). Significantly higher concentrations of floc $[Fe]^{Total}$ were observed in summer flocs compared to winter flocs ($[Fe]^{Total\ Sumner}$= 89-140 mg/g; $[Fe]^{Total\ Winter}$= 64-68 mg/g; Figure 2). Further, a large seasonal shift in the nature of the Fe-phases associated with flocs was observed, despite no evident significant variation between *in situ* summer vs. winter water column $[Fe_{(aq)}]^{Total}$, $[Fe^{(II)}]_{aq}$, $[O_2]^{Sat}$, or Eh (Figure 1, Table S1) at depth. Sequential extraction and XRD results indicate that the majority of summer floc-associated Fe was amorphous iron oxyhydroxides ($Fe^{(III)}OOH$), with crystalline-$Fe^{(III)}$ phases becoming relatively more important with depth (Figure 2,

Table S1). This result is consistent with previous studies on summer floc within epilimnentic and littoral zones whereby the majority of floc Fe was associated with reducible FeOOH phases (4, 5, 15). In contrast, here, winter floc samples contained very low concentrations of FeOOH ($[FeOOH]^{Winter}$=0.3-7mgg^{-1} vs. $[FeOOH]^{Summer}$=37-77 mgg^{-1}) with the majority of Fe associated with organics and/or sulphides (i.e. oxidizable phases) consistent with $Fe^{(II)}$ rather than $Fe^{(III)}$. Further, winter floc crystalline ferric iron concentrations were ~0.5 that of summer flocs but constituted 45-55% of total floc-associated Fe ($[Fe_{(C)}]^{Winter}$= 23-25mgg^{-1}). Thus both a decrease in the total abundance of floc [Fe], as well as a shift from dominantly $Fe^{(III)}$ to $Fe^{(II)}$ phases occurred in winter floc compared to summer floc despite minimal summer-winter physicochemical water column variation (Figure 5.1, Table S1). In contrast, while substantive differences in water column physicochemistry were evident between the two sampling depths for both seasons, little observable difference between 4.5m ('metalimnetic') and 7.5m (hypolimnetic) floc Fe-geochemistry for either season emerged.

The seasonal shift in floc Fe phases from summer amorphous FeOOH to winter crystalline $Fe^{(III)}$ and $Fe^{(II)}$ phases was associated with a significant decrease ($p<0.01$) in winter floc TE sequestration (Figure 5.2b,c). Winter floc $[Pb]^{Total}$ and $[Cd]^{Total}$ were 6-12x to 4-16x lower relative to summer values, respectively. Floc $[TE]^{Totals}$ were not significantly predicted (MLR) by either $[TE]_{aq}$ or water column physicochemistry (Table S1), highlighting that floc-specific characteristics (i.e. abundance and nature of reactive sorbent phases), are likely more important controls on floc TE uptake. Consistent with this notion, lower winter floc $[TE]^{Totals}$ were significantly correlated to the declining abundance of floc-FeOOH phases under ice (R^2= 0.85-0.99, $p< 0.01$) (Figure S2). Declining winter floc $[TE]^{Totals}$ were not significantly correlated to abundance of other floc solid phases ([Organic C], $[Fe^{(C)}]$, $[Fe^{(Oxidizable)}]$, $[Mn^{(Amorph)}]$, $[Mn^{(C)}]$; consistent with the previously observed dominating TE sequestration control of floc FeOOH (4, 5). Element specific trends emerged: a 1 unit decrease in floc-FeOOH produced a 5.9 unit decrease in floc $[Pb]^{Total}$ but only a 0.12x unit decrease in floc $[Cd]^{Total}$, indicating a higher seasonal impact on Pb-uptake associated with changing floc Fe phases (Figure S2). Further,

comparative concentration factors (CF= $[TE]^{FeOOH}$/[FeOOH]) identify a decrease the reactivity of FeOOH phases in winter flocs (Table S4). Correspondingly, floc TE partitioning to amorphous FeOOH phases substantially decreased under ice, accounting for only 0-12% of winter total floc TE concentrations compared to 35-60% of total summer floc TE concentrations (Figure 2b,c). Winter floc-TE partitioning was instead dominated by oxidizable phases (Figure 5.2).

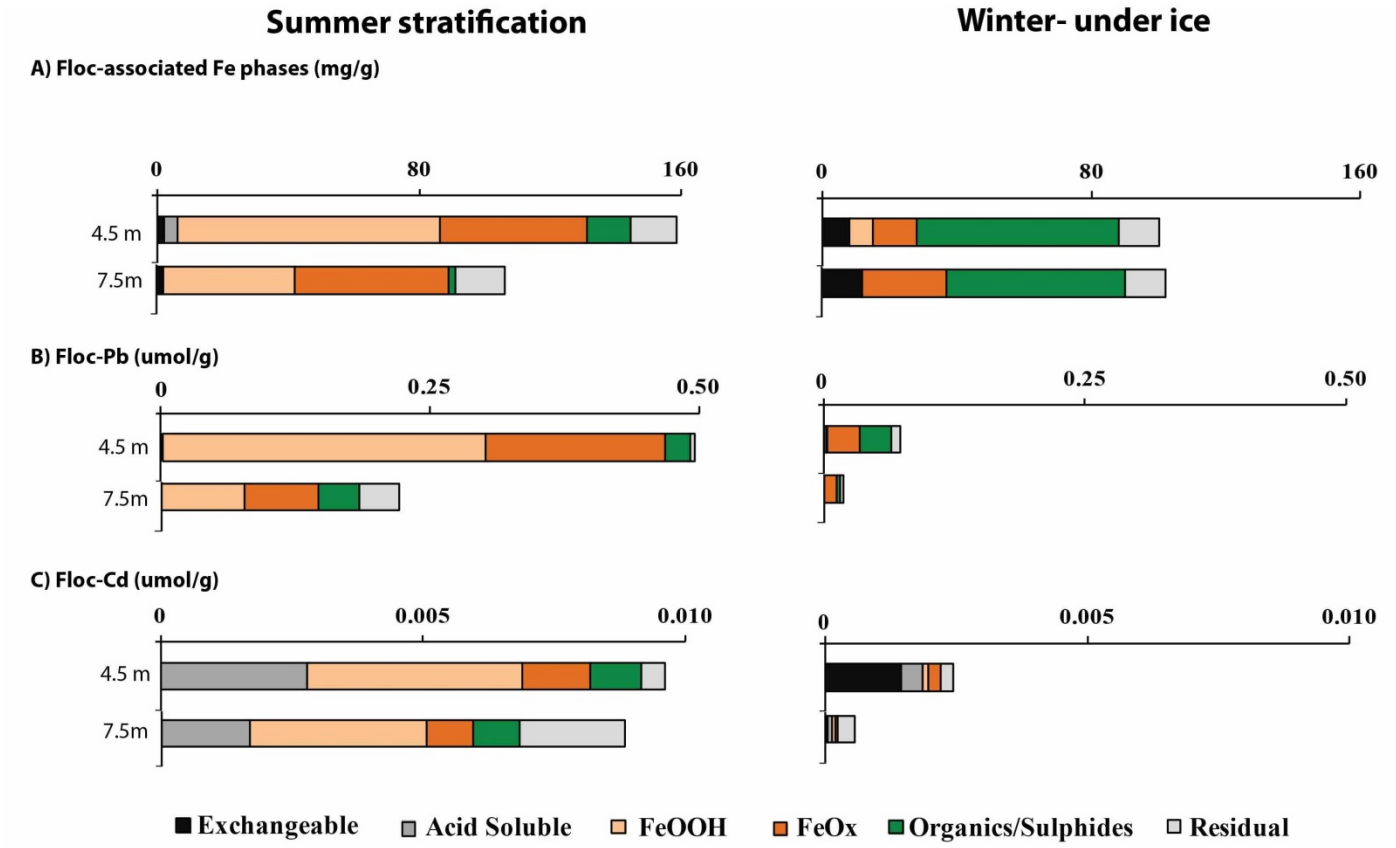

Figure 5.2 Seasonal comparison of the concentration and nature of Fe-phases within *in situ* flocs and subsequent impacts on TE behaviour. Results shown are A) floc-associated Fe (mg/g) and B,C) TE partitioning (Pb, Cd; μmol/g) as determined sequential extraction and operational partitioning into six, operationally, defined sedimentary fractions (see methods). Results indicate a significant decline in $[Fe]^{Total}$ associated within winter flocs, as well as specifically FeOOH phases, corresponding to a large increase in Fe associated with the oxidizable phases in winter. Observed seasonal shifts in Fe phases is mirrored in TE partitioning and, further, resulted in a decrease in floc TE -uptake in winter (B,C, Table 1).

5.3.2 Seasonal turnover of in situ floc bacterial communities. Mirroring above results for floc Fe and TE patterns, evaluation of floc bacterial community dynamics indicates significant seasonal changes in floc bacterial community membership and overall structure, but not between depths for each season (Figures 5.3, 5.4a). Floc bacterial community membership ($Unifrac^{Unweighted}$) and overall structure ($Unifrac^{Weighted}$) were statistically highly conserved with water column depth for summer and winter (summer: $P^{Weighted}$=0.52, $P^{Unweigted}$=0.41; winter: $P^{Weighted}$=0.32, $P^{Unweigted}$=0.21; Figures 3, S2). This result is distinct from other investigations on lacustrine bacterial community dynamics, even for relatively shallow systems comparable to Coldspring L. e.g.(54) and is suggestive of a high degree of conservation in pelagic floc community functioning and metabolic potential across metalimnetic and hypolimnetic zones in this system. Indeed, summer flocs at both depths consist of similarly abundant and co-existing lineages (% OTUs, 97-100% 16S similarity) of known C-cycling and Fe-cycling bacteria (Figure 4a). Specifically, summer floc phylotypes from both depths consist of known CH_4 oxidising (*Verrumicrobia, Methylomonas*), fermentative (*Bacteriodetetes, Flavobacterium*), anoxygenic phototrophic (*Cholorfelxi, Chlorobium*) and oxygenic phototrophic (*Cyanobacteria*) capabilities together with previously identified (Elliott et al. 2013, *unpublished data)* putative floc IOB (*Comamonas spp*.) and IRB (OTUs from *Acidobacteria, Bacteriodetes, Veillonellaceae, Aeromonas, Plesiomonas, Clostridium*) were identified (corresponding Fe-metabolic ability confirmed for both depths, discussed below, *section 5.3.3*). Known oxygenic and anoxygenic photosynthetic bacteria (*Chloroflexi, Chlorobi, Cyanobacteria*) were the most abundant of any metabolic guild in both summer floc communities (Figure 5.4a) reflecting the lighted nature of nearly the entire water column during the summer (1% light level = 7.3m).

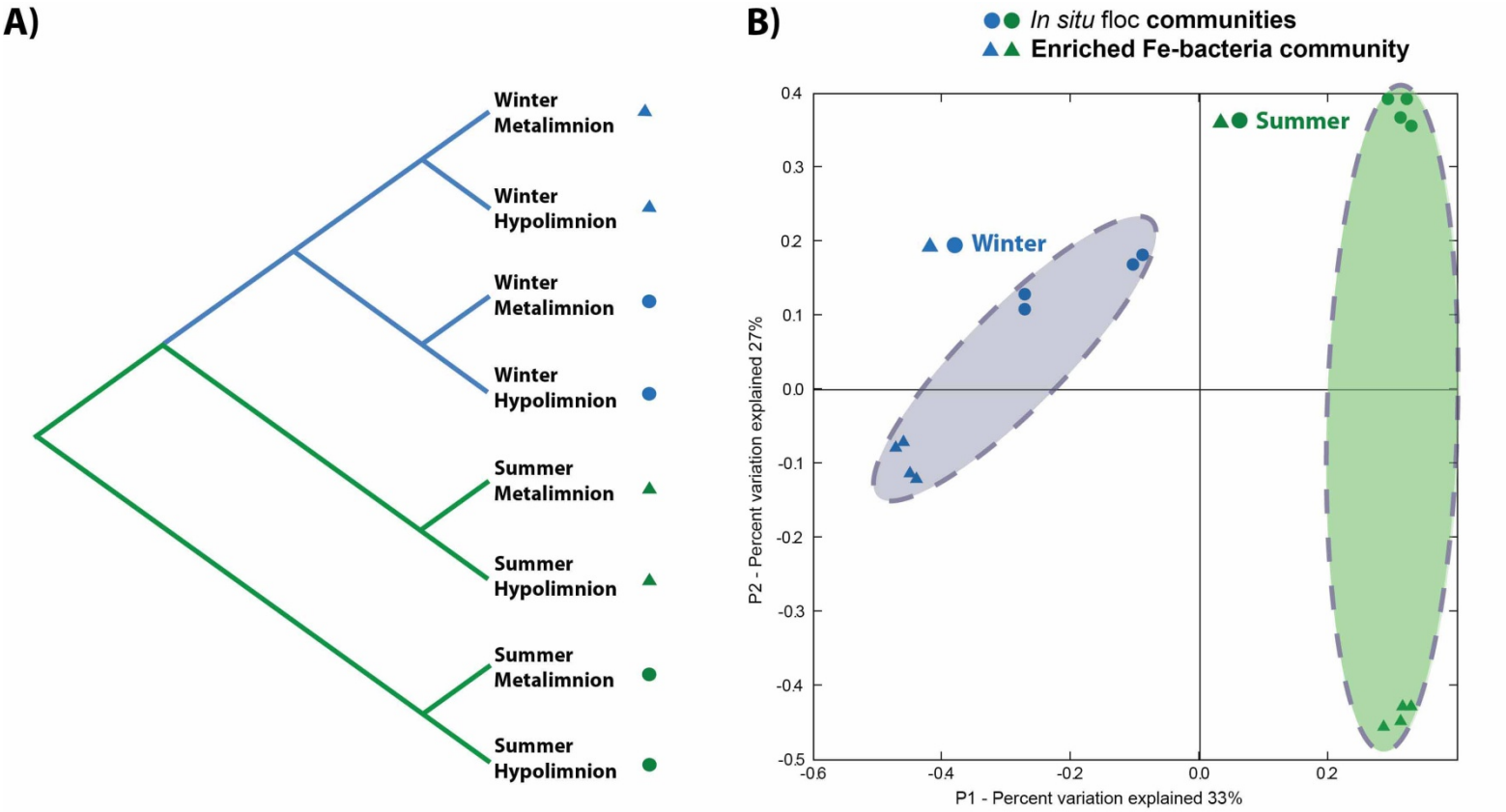

Figure 5.3. Analysis of *in situ* floc and enriched floc Fe-bacterial communities with weighted Unifrac—$_{\text{Weighted}}$ metrics. Results indicate that both overall community structure (Unifrac$^{\text{Weighted}}$) as well as community membership (Unifrac$^{\text{Unweighted}}$, see Figure S1) only significantly varies with season. *In situ* summer vs. winter time communities only largely diverge along the PC1 axis, which was significantly correlated to water column temperature (R^2=0.81, $p<0.05$), and clearly separates all winter samples from summer samples. This large seasonal divergence between *in situ* communities was magnified during co-enrichments for floc Fe-bacteria, highlighted by black double arrow. UPGMA clustering (tree) indicates samples from Fe bacteria enrichments resemble each other more than their parent flocs, highlighting the conserved nature within season of the Fe-bacterial community with depth down the water column.

Winter floc bacterial communities were highly significantly different from their summer counterparts ($P^{Unweigted}$=<0.01-0.05; $P^{Weighted}$=0.03-0.06; Figures 5.3, S1) and exhibit both a reduced genetic diversity (*γ-Protobacteria* lineages constituted 32-40% of OTUs) as well as reduced range of co-existing metabolic guilds of bacteria (Figure 5.4a). Heavy ice and snow cover (Figure 5.1), eliminating light input into the water column, resulted in the complete removal of identified putative summer photosynthetic organisms from the winter floc community (Figure 5.4a). Furthermore, entire 'summer' bacterial lineages disappeared from the winter floc community, including all summer OTUs of the *Acidobacteria, Actinobacteria* and *β-Proteobacteria* lineages (all but a single *Delfitia* OTU, constituting ~2% of the winter community at 4.5m); i.e. not simply phototrophic organisms disappeared under ice. In addition, putative summer floc IOB and IRB taxa, previously linked to Fe-redox cycling within summer flocs, were not detected. Instead, winter floc bacterial communities largely shifted to known anaerobic guilds (*Clostridiales, Dehalococcoidetes* groups) and S-metabolizers (*Sulfuricurvum spp, Sulfurimonas spp., Desulfovibrio* sp.) together with aerobic CH_4 oxidising bacteria (*Methylobacter spp., Methylosoma spp.*), despite the oxic water column. Furthermore, winter floc communities also showed a higher degree of variation with depth compared to their summer counterparts and uncluster during PCA analyses (Figures 5.3, S2). Comparison of weighted vs. unweighted Unifract results indicates this variance can be mostly attributed to differences in the relative abundance of bacterial lineages, rather than the presence/absence of specific lineages with depth. Specifically, known anaerobic S-oxidizing (*Sulfuricurvum spp, Sulfurimonas spp.*), S-reducing (*Desulfovibrio* sp.) and methanotrophic (*Methylobacter spp., Methylosoma spp.*) phylotypes were dominant within the winter 4.5m floc community (Figure 5.4a). In contrast, the winter hypolimnetic floc community was significantly less diverse, with members of *Dehalococcoidetes* (metal respiring phylotypes of *Chloroflexi* lineage*)* and *Pseudomonas* group*s* constituting ~80% of the total OTUs.

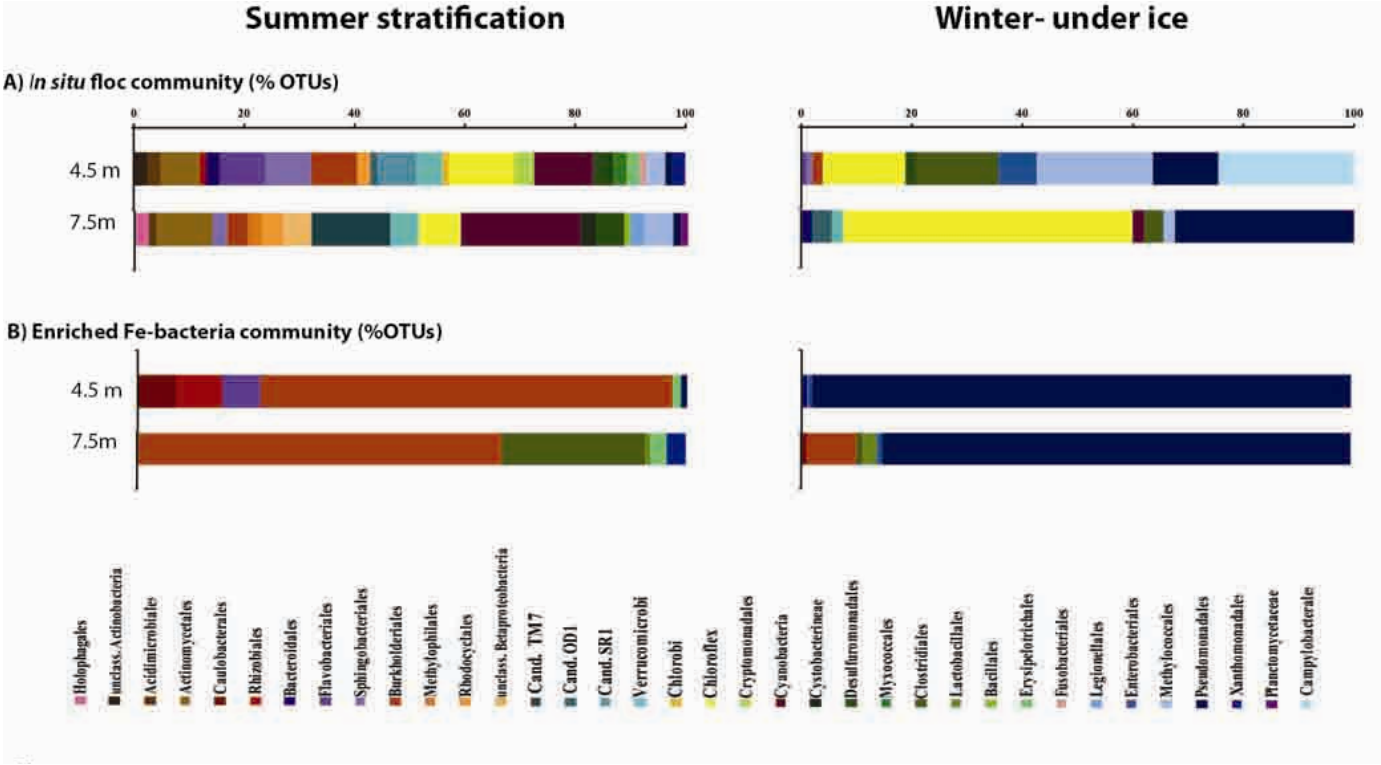

Figure 5.4 Classification of OTUs for whole *in situ* floc and enriched floc Fe-bacterial communities. Results are shown for A) *in situ* floc community and B) experimentally enriched Fe-bacterial floc community for both summer (left column) and winter (right column) sampling periods (% OTUS, Order classification). For clarity, only sequences representing more than 1% of the total community are shown.

5.3.3 Identified environmental drivers of in situ floc bacterial community shifts. Principal coordinate analyses (PCA) coupled with regressions of identified principle components (PCs) with system physicochemical and floc composition variables provide insight into which environmental factors have the largest impact on seasonal floc community dynamics (53). If many independent environmental factors drive the observable variation between seasons (i.e., Figures 5.3, S1), the first two to four PCs will explain a minimal fraction of the variation in the data (e.g. ΣPC1-PC4=~41% (46)). Here, the first three PCs describe ~75% of the seasonal variation observed with UniFrac^{Weighted} metrics (i.e. community structure) (Figure 5.3) suggesting few independent factors contribute to seasonal floc bacterial community turnover. In contrast, with UniFrac^{UnWeighted} (i.e. community membership), the first three PCs only describe ~55% of the variation among samples; identifying a greater number of independent factors contributed to the presence/absence of specific bacterial lineages within flocs (*section 5.3.4*). This is also likely reflective of the complete removal of identified putative summer photosynthetic community members from the winter floc community, driven by the elimination of light input into the water column; a key difference in seasonal *in situ* floc bacterial community membership (presence/absence data not compatible with regressions with Unifrac metrics). Further, although cessation of light input into the water column eliminated phototrophs from the floc communities, other phylotypes and corresponding metabolic guilds of bacteria exhibited dramatic seasonal changes in relative abundance and appearance/disappearances from the *in situ* communities, suggesting that additional factors contribute to observed whole-community turnover. However, when comparing winter vs. summer flocs, UniFrac^{Unweighted} performed similarly to UniFrac^{Weighted} analyses (Figures 5.3, S1), identifying seasonal patterns in community membership and overall community structure are highly correlated in Coldspring Lake.

In addition to light inputs, water column temperature, [O_2], and [$Fe^{(II)}$] exhibited large seasonal variations (i.e. Summer$^{4.5m}$ vs. Winter$^{4.5m.}$; Summer$^{7.5m}$ vs. Winter$^{7.5m}$) (Table S1) suggesting one or some combination of these variables is linked to the observed turnover in floc microbial communities and corresponding

shift of dominant bacterial metabolisms from summer Fe and C-cycling guilds to winter S and C-cycling guilds (Figure 5.4a). Both the decrease of $[O_2]$ under ice as well the increased relative abundance of S-redox cycling and other aero-intolerant phylotypes in winter communities highlight that declining redox conditions may be an important predictor of the observed seasonal differences in floc bacterial community structure. However, here, $[O_2]$ (mgL^{-1}, $\%^{Sat.}$) did not significantly correlate with any of the first three principle components in $UniFrac^{Weighted}$ ($R^2<0.20$, $p>>0.1$) analyses. Rather, water column temperature was identified as the most important parameter explaining observed seasonal differences in floc bacterial community structure. Under $UniFrac^{Weighted}$ (community structure) analyses, PC1 correlated significantly with temperature ($R^2=0.81$, $p<0.05$) and clearly separates all winter samples from summer samples (Figure 3). Winter communities from the two sampling depths also diverge only along this PC1 axis. Other potentially important water column parameters (i.e. O_2 mgL^{-1}, $O_2^{\%\ Sat.}$, pH, $Fe^{(Total)}$, $Fe^{(II)}$, $Fe^{(III)}$, nitrate, sulphate, sulifide, phosphate, SPC, Eh) did not significantly correlate with any of the first three PCs using $UniFrac^{Weighted,Unweighted}$ metrics for analyses,.

The identification of water column temperature as the best predictor of observed seasonal changes in floc community composition and diversity may reflect ecological (i.e. direct microorganism response to decreasing temperature) and/or geochemical (i.e. temperature may function as an integrating variable that provides a combined index of water column conditions) mechanisms. There are a number of physicochemical and ecological characteristics that are known to co-vary and/or are directly or indirectly impacted by seasonal temperature changes (e.g., $[O_2]$, organic C concentration and structure, nutrient availability, energy regime) and these factors together may have contributed to the observed changes in floc community composition. However no statistically significant ($R^2<0.28$, $p>>0.1$) relationships were found between temperature and water column variables (Table S1), suggesting direct ecological responses to cold conditions are likely more important. Temperature is a known important physiological constraint on bacteria; altering competitive outcomes or reducing the net growth of individual taxa that are less able to survive under cold winter conditions. In this manner, cold-adapted guilds of floc

bacteria may have out-competed summer communities during the onset of winter stratification, contributing to the statistically significant turnover (i.e. Figures 3, S1) in the overall community. Consistent with the latter ecological role of temperature affecting seasonal floc communities, NCBI MEGABLAST analyses revealed that the closest related sequences of the 'booming' winter γ-*Proteobacteria* groups are in fact OTUs specifically from (permanently) cold environments. These include, for example, *Methylobacter spp*. from Fe-rich snow, Arctic wetland soils, high altitude lakes and hypoxic bottom water from permafrost thaw ponds. Similarly, ~30% of winter *Clostridiales* members were *Acetobacterium spp*. OTUs most closely related to bacteria from Canadian low-temperature bio-degraded oil reservoirs, anoxic bottom sediments, subsurface aquifer sediment and Fe-reducing enrichment cultures. Psychrophilic and cold-tolerant microorganisms such as these adapt by producing cold-acclimation enzymes, allowing for associated metabolisms to be sustained at rates comparable to mesophiles at warmer temperatures (e.g. 33).

3.4 Seasonal changes in identity and activity of enriched floc Fe-bacteria.

The absence of summer Fe-redox cycling bacteria (i.e. previously identified floc putative IRB and IOB) from *in situ* winter floc communities based on genetic analyses (16S) suggests that either different bacterial species are mediating floc $Fe^{(III)}$-reduction and $Fe^{(II)}$-oxidizing activities under ice or these Fe-metabolic guilds are no longer present. The lack of universal functional genes precludes genetic markers of either $Fe^{(III)}$ respiration or $Fe^{(II)}$ lithoautotrophic activity. Thus, here, targeted metabolic isolation techniques for IRB and IOB (28, 29), as well as attempted co-enrichment (IRB+IOB) experimentation on whole-floc summer and winter communities experimentally exposed to summer (22°C) and winter (4°C) temperatures, were used to (i) confirm $Fe^{(III)}$-reduction and $Fe^{(II)}$-oxidation activity within flocs, (ii) identify putative guilds mediating these reactions, and iii) identify Fe biominerals formed under these differing microbial community and temperature regimes.

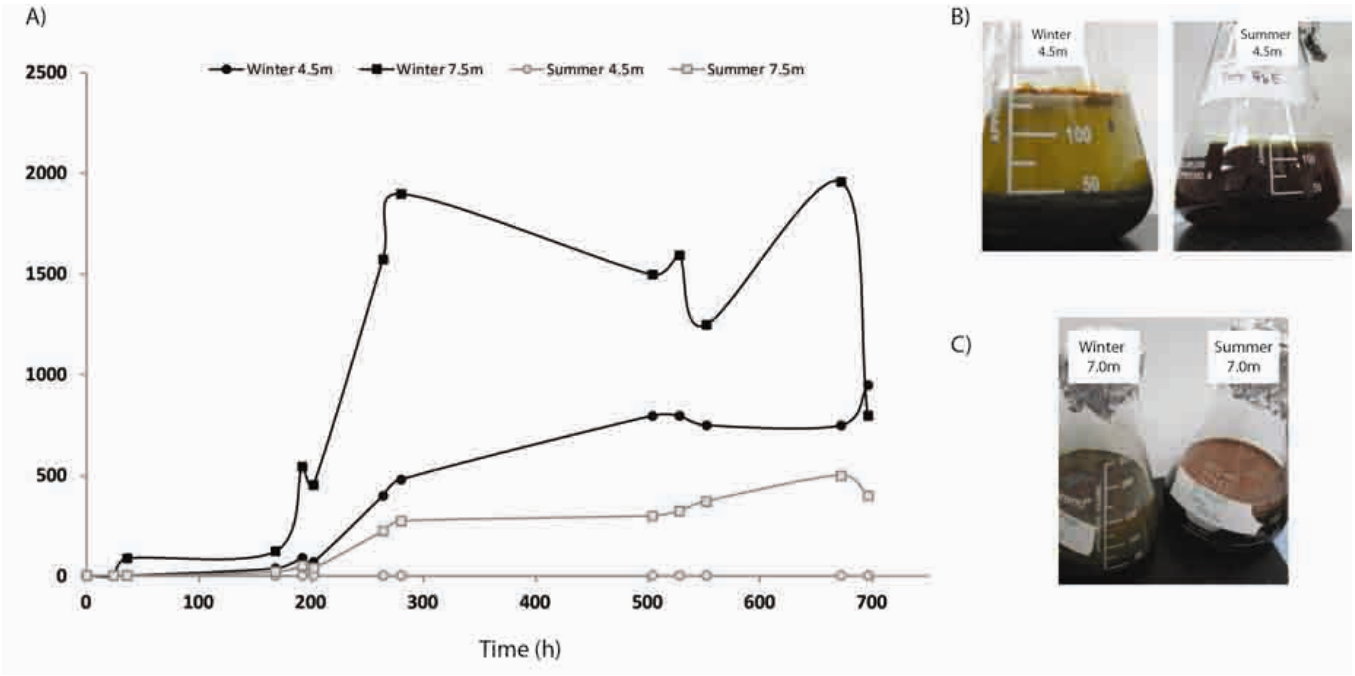

Figure 5.5 . $Fe^{(II)}$ accumulation (µmol/L) in cold microoxic enrichment microcosms. Data shown here present Fe-geochemical outcome of a single generation (N=40th) of enrichment experiments over 700h. Data points represent mean ± SEM (n=3). Summer floc Fe-bacteria communities showed none (4.5m) to diminished (7.5m) capacity to reduce ferric iron in microcosms incubated at 4°C, as evidenced by decreased ferrous Fe accumulation **(A)** and inability to clear media **(B, C)** over the course of 700h.

Attempted isolations of winter microaerophilic IOB in opposing-gradient tubes (4°C and 22°C) as well as attempted co-enrichments (i.e. winter IRB and $Fe^{(III)}$ source provided to stimulate IOB-metabolism of biogenic $Fe^{(II)}$ instead of a $Fe^{(II)}$ media salt; 4°C and 22°C) were unsuccessful; confirming the absence of this metabolic guild within winter floc consortia communities. This contrasts results from summer floc communities which revealed the universal presence of cultivable lithotrophic $Fe^{(II)}$-oxidizing (IOB) using both opposing-gradient tubes as well as within co-enrichments at 22°C (Elliott et al. 2013, *unpublished data*). Declining water column temperature under ice was specifically identified (Unifrac, PCA) as a driver of observed seasonal turnover of whole floc community composition, and also likely specifically contributed to IOB guild removal. That is, for a bacterium to grow on $Fe^{(II)}$ as a sole energy source is a physiological challenge. Of all the potential lithotrophic energy sources, the oxidation of $Fe^{(II)}$ yields the lowest Gibbs free energy (G°) for cellular metabolism with energetic yield estimates as low as 29 kJ mol^{-1}. Further, neutrophilic IOB must also outcompete the rapid abiotic oxidation kinetics of $Fe^{(II)}$ at pH>3, to gain access to their energy source. Thus, the added physiological stress due to the onset of seasonally cold conditions, and consequent decrease in metabolic rates, may have rendered floc-IOB unable to sustain their specialized metabolism resulting in their loss from winter floc communities at both depths. This hypothesis is supported by a recent study (54), which demonstrated decreased ability of IOB isolates to compete with abiotic oxidation kinetics with decreasing temperature. Temperature is also a known important physiological control on the rate of $Fe^{(II)}$-oxidation by phototrophic IOB (55). Here, not only were isolation attempts for putative IOB from winter flocs unsuccessful, the previously established summer IOB also did not show positive growth in opposing gradient tubes incubated in cold conditions (~4°C). This result is also consistent with high optimal growth temperatures (25-37°C) reported for a number of other neutrophilic $Fe^{(II)}$-oxidizers, and that of closely related lithoautotrophic *Leptothrix discophora,* which also shows none to limited oxidizing ability (using Mn^{II}) below 8°C (56). The winter absence and summer presence of resident floc-IOB guilds (i.e. $Fe^{(II)}$ oxidizing) would explain the observed winter

accumulation of floc $Fe^{(II)}$, reduction in amorphous FeOOH solid phases and reduced floc [TE], and higher summer observed floc [FeOOH] and floc [TE] under similar water column *in situ* physicochemical conditions for both seasons (Figure 2a, Table S1).

In contrast to seasonally dependent occurrence of floc $Fe^{(II)}$-oxidizing (IOB) ability, culture isolation results indicated $Fe^{(III)}$-reducing (IRB) activity was conserved in floc across seasons under strictly anoxic conditions (Figure S3). Further, enrichment experiments assessed *in situ* operation of the winter IRB community under cold microoxic conditions. Previously established summer Fe-redox cycling consortia (Figure 5.4b) were also exposed to these same experimental cold conditions for comparison**.** $Fe^{(II)}_{(aq)}$ accumulated in all winter floc microcosms under cold, oxygenated conditions (Figure 5.5). However, previously established enrichments (22°C) of summer floc Fe-bacteria showed none ($Summer^{4.5m.}$) to diminished ($Summer^{7.5m}$) capacity to reduce $Fe^{(III)}$ in microcosms incubated at 4°C, as evidenced by decreased $Fe^{(II)}$ accumulation and inability to clear media (30) (Figure 5). This result suggests a distinct, cold adapted, winter floc IRB community that differs from those IRB associated with IOB under warm 'summer' conditions. Genetic and bioinformatic analyses confirm that winter IRB communities were statistically significantly different from their summer counterparts (Figures 3, S1) and, further, constituted bacteria of known 'accessory' IRB metabolism (i.e. phylotypes of known fermentative (*Pelobacter, Clostridales*) and sulfur-reducing physiology (SRB; D*esulvibrio spp*.) (Figure 4b). In microbial fermentative metabolism, there is no electron transport chain as in respiration; rather electrons from NADH generated during glycolysis are transferred to the carbon source itself (55). It is thought that $Fe^{(III)}$ serves as a supplementary electron acceptor during this process, disposing excess reducing power (55). Similarly, SRB such as *Desulvibrio spp*. are known to use a variety of electron acceptors in addition to $Fe^{(III)}$, including sulphate and nitrate, which were present in trace amounts within enrichment media (30). Further, *Pseudomonas* OTUs, which exhibit extreme metabolic flexibility with documented metabolisms including fermentation, $Mn^{(II)}$ oxidation as well as dissimilatory reduction of NO_3^{2-}, $Fe^{(III)}$, and Mn (57), constituted ~70-80% of both

Winter$^{4.5m}$ and Winter$^{7.5m}$ enrichment communities. Thus, in addition to the temperature driven removal of observed putative floc IOB taxa from winter floc communities (i.e. elimination of Fe oxidation capability from floc), experimental results also indicate the replacement of summer floc IRB with cold-adapted accessory Fe reducing, S-reducing and fermentative phylotypes.

The observed significant seasonal shift in identity and ecology of dominant floc Fe-bacterial consortial community members within enrichments (summer: IOB-IRB-aerobes; winter: fermenters-SRB-*Pseudomonas*) significantly impacted observable geochemical outcomes of floc Fe-bacterial activity. Results indicate the successful co-enrichment (22°C) of putative summer floc IOB and IRB within aggregated consortial structures (30-80 µm) (Figure 5.6a), enabling active microbial $Fe^{(III)}$-reducing and $Fe^{(II)}$-oxidizing activities at the aggregate scale, decoupled from experimentally oxygenated conditions (Elliott et al., 2013, *unpublished data*). Further, summer consortial aggregate IOB-IRB-aerobe activity resulted in the formation and co-existence of both reduced $Fe^{(II)}$-mineral phases (siderite, $Fe^{(II)}$-carbonate; magnetite, mixed $Fe^{(III)}/Fe^{(II)}$ oxide) and oxidized $Fe^{(III)}$-mineral phases (hematite, goethite (microoxic only), $Fe^{(III)}$oxides) (Table S3) that are not predicted (PHREEQC) based on experimental oxygenated conditions. In contrast, enriched (4°C) winter consortial community (fermenters-SRB-*Pseudomonas*) showed decreased $Fe^{(II)}$ accumulation in cold microcosms, consortial aggregates showed lower overall viability (Figure 6b), had no visibly apparent sheathed floc-IOB (again consistent with their absence from this community) (Figure 6a,b), and did not form mixed valence $Fe^{(III/II)}$ bio-mineral assemblages ($FeOOH^{Amorphous}$ and hematite only, Table S3). Further, also in contrast to their summer counterparts at warmer temperatures, winter consortial aggregates became completely entombed in ferric Fe solids over the course of the enrichment experiment (i.e. showed an inability to localize $Fe^{(III)}$ precipitation) (Figure 5.6d,e). This is an extremely maladaptive outcome of winter floc ferric-iron reduction activity and suggests that summer IOB activity likely aided to localize Fe-mineralization in summer consortia. That is, IOB are thought to form Fe oxide-encrusted sheaths/stalks morphologies in order to locate the electron transfer process close to the cell, as well as provide a means for

the cell to escape encrustation by $Fe^{(III)}$(hydr)oxides (FeOOH); thus, with IOB absence, this localization ability is lost from the winter enriched Fe-bacterial community (28,30). Furthermore, the changing ecology of winter floc ferric iron reducing community, and corresponding slower overall rate of $Fe^{(II)}$ accumulation in cold conditions, is likely another contributing factor to the apparent inhibition of floc IOB to sustain their metabolism *in situ* during winter months (as the energetic yield of $Fe^{(II)}$ oxidation is very low, large amounts of $Fe^{(II)}$ are required in order to provide enough energy for growth). Importantly, these results show that the turnover in Fe-bacterial community membership (Figure 5.3, S1) can be specifically linked to changed geochemical outcome of Fe-bacterial activity under the same initial experimental physicochemical and Fe-geochemical regime (Figures 5.5, 5.6, Table S3), providing a persuasive argument that the observed similar *in situ* Fe-bacterial community changes over seasonal scales underpin significant shifts in floc $Fe^{(III)/(II)}$-phases despite similar seasonal system physicochemical regimes. Indeed, the Fe-biomineral assemblages formed in Fe-bacterial enrichment microcosms by respective summer and winter enriched communities mirror those observed within seasonal *in situ* parent floc samples, identifying the formation of a consistent suite of Fe biominerals associated with these summer and winter floc Fe-metabolisms (Table S1, S3).

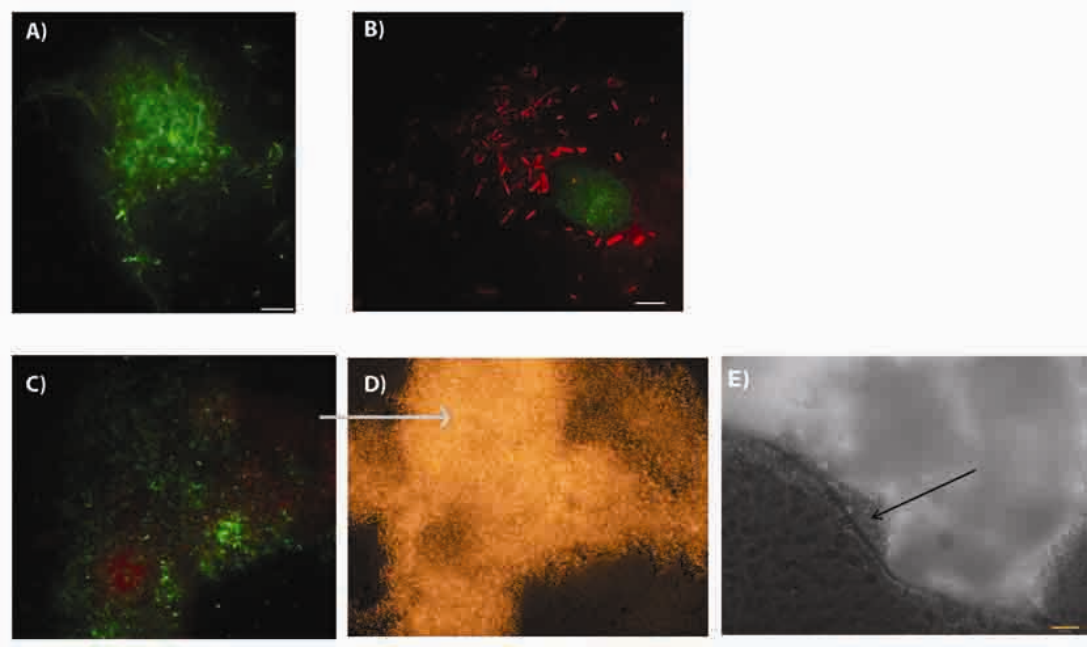

Figure 5.6. Fluorescent LIVE/DEAD (A,B,C) and light microscopy (D, E) of consortial aggregates of enriched floc Fe-bacteria. In contrast to summer Fe-bacteria consortia enriched under warm, microoxic conditions **(A),** winter floc Fe-bacteria consortial aggregates **(B)** showed lower overall viability and had no visibly apparent sheathed floc-IOB. Also in contrast to their summer counterparts, winter consortial aggregates became completely entombed in ferric Fe solids over the course of the enrichment experiment (i.e. inability to localize $Fe^{(III)}$ precipitation) **(C, D, E).** D) light microscope image showing orange Fe-precipitates**.** E) greyscale light microscope image showing entombed winter Fe-bacterial cells (still visible along the edges of $Fe^{(III)}_{(s)}$, indicated by black arrow). A,B,C) 100 pixels=10µm; C,D,E) 100pixels=20µm.

3.4 *In situ* seasonal shifts in floc community membership and floc Fe geochemistry. As discussed, the greatest observable seasonal difference in floc Fe-geochemistry *in situ* was the shift in the nature and concentrations of floc-associated Fe phases, despite similar seasonal water column trends in [$Fe^{(II)/(III)}$], [O_2], pH (Figures 5.1, 5.2; Table S1). Contrasting summer floc-Fe, floc amorphous $Fe^{(III)}$-minerals (FeOOH) decreased in winter flocs (10-100x), $Fe^{(II)}$ phases increased (4-27x), and crystalline $Fe^{(III)}$ minerals comprised 45-55% of total floc-$Fe^{(III)}_{(s)}$. This changing nature and concentration of floc solid phase Fe constituents resulted in significant decreased floc TE sequestration during winter stratification, not predicted by water column geochemistry. However, changing floc-[Fe] were significantly correlated to the observed turnover of floc community membership (Figure S1). That is, under $UniFrac^{Unweighted}$, winter and summer samples do not show a large divergence on PC1 (Figure S1), which also significantly correlates with water column temperature (R^2=0.83, p=0.01). Instead, PC2 clearly separates all winter samples from summer samples (Figure S1). PC2 was significantly correlated with both the concentration of floc associated Fe-crystalline phases ([Fe_C], $p<0.05$, R^2=0.85), as well as the increases in organic and/or sulphide associated Fe (i.e. concentration of oxidizable $Fe^{(II)}$ phases) within winter flocs ([Fe_{OS}], $p<0.05$, R^2=0.93). Water column physicochemical parameters ([O_2], pH, $Fe_{aq}^{(Total)}$, $Fe_{aq}^{(II)}$, [nitrate], [sulphate], [phosphate], SPC) did not correlate with PC2.

The identified significant relationship of floc bacterial community membership ($UniFrac^{Unweighted}$) and floc associated Fe-phases could be reflective, singly or in combination, of i) the activities of *in situ* floc communities acting on floc Fe-phases or, in contrast, ii) that changing floc Fe-phases drives a turnover of floc community membership. For example, the winter absence of resident floc-IOB guilds (i.e. ferrous-Fe utilizing) is consistent with the accumulation of floc ferrous-iron solid phases in winter flocs, contributing to the overall shift to $Fe^{(II)}$ dominated floc Fe under ice rather than $Fe^{(III)}$ as observed in summer samples (Figure 5.2, Table S1). Further, the observed emergence of SRB in winter flocs (Figure 5.4) would have contributed to the accumulation of ferrous-Fe phases, and decrease of [FeOOH], through the abiotic reduction of floc ferric-Fe phases by biogenic

sulphides. This is consistent with the observable increase in aqueous sulphide concentrations under ice as well as with the majority of winter floc-Fe being associated with organics and/or sulphides (i.e. oxidizable phase, Table S1, Figure 5.2). In contrast, the large seasonal decrease in available $Fe^{(III)}_{(s),}$ more specifically FeOOH, would have negatively impacted resident pelagic floc putative IRB community membership. That is, amorphous FeOOH (e.g. ferrihydrite) are considered the most bioavailable $Fe^{(III)}_{(s)}$ occurring in soils and sediments as they are the least crystalline and most soluble phase of the common oxy(hydr-)oxides at pH> 4 (as compared to goethite (α-FeOOH) or hematite (α-Fe_2O_3)(56)). Accordingly, amorphous FeOOH are known to support the greatest extent and highest rates of Fe-reduction in laboratory incubations with model putative IRB (57, 58). In contrast, crystalline $Fe^{(III)}_{(s)}$ are considered significantly less bioavailable for Fe-metabolism, supported by increasing evidence of the limited ability of model IRB to reduce crystalline $Fe^{(III)}_{(s)}$ (39). Furthermore, it has recently been experimentally demonstrated that changing from amorphous FeOOH to crystalline $Fe^{(III)}_{(s)}$ substrates specifically shifts cultivable IRB communities from dominantly $Fe^{(III)}$-respiring (i.e. *Geobacter spp.*) to fermenting and sulfate-reducing organisms which, in turn, were better capable of reducing more recalcitrant Fe phases (39). Here, very similar shifts from putative summer floc IRB to winter floc associated accessory IRB fermenting and sulfate-reducing phylotypes within both the *in situ* whole floc and targeted enriched IRB communities were observed (Figure 5.4). Thus, changes in FeOOH abundance and availability of $Fe^{(III)}$ associated with the loss of IOB from winter floc may play a role in the observed shift in putative IRB community membership to dominantly fermenting and/or sulfate reducing organisms, which are capable of directly or indirectly reducing more recalcitrant Fe phases.

Results of this field investigation provide insight into linkages among the geochemical properties of suspended flocs in a pristine, remote site as well as the interplay between floc-associated bacteria, floc-reactive solid phases and TE sequestration. Results indicate that observed temperature-driven seasonal changes in floc bacterial community structure likely specifically contributed to the removal

of floc IOB metabolic guilds from the winter flocs, thus extinguishing the potential for coupled microbial Fe-redox transformations under ice, contrasting results described previously for summer flocs (Elliott et al. 2013, *unpublished data*). Moreover, significant seasonal changes in floc microbial ecology corresponded to large seasonal differences in observable floc Fe and TE biogeochemistry. Regressions with PCAs derived from $Unifrac^{Unweighted}$ metrics (Figure S1) identify this observed turnover of floc community membership significantly correlated specifically to the changing nature and concentration of floc solid phase Fe constituents, while overall floc community structure ($Unifrac^{Weighted}$) significantly correlated with water column temperature. These results reveal that ecological drivers of floc-specific characteristics are an important control of floc Fe and TE geochemistry. Furthermore, these results expand our understanding of the geomicrobiological controls and interactions of environmental bacterial communities in Fe-biogeochemical cycling as well as bacterial processes with the potential to affect TE sequestration in pelagic environments.

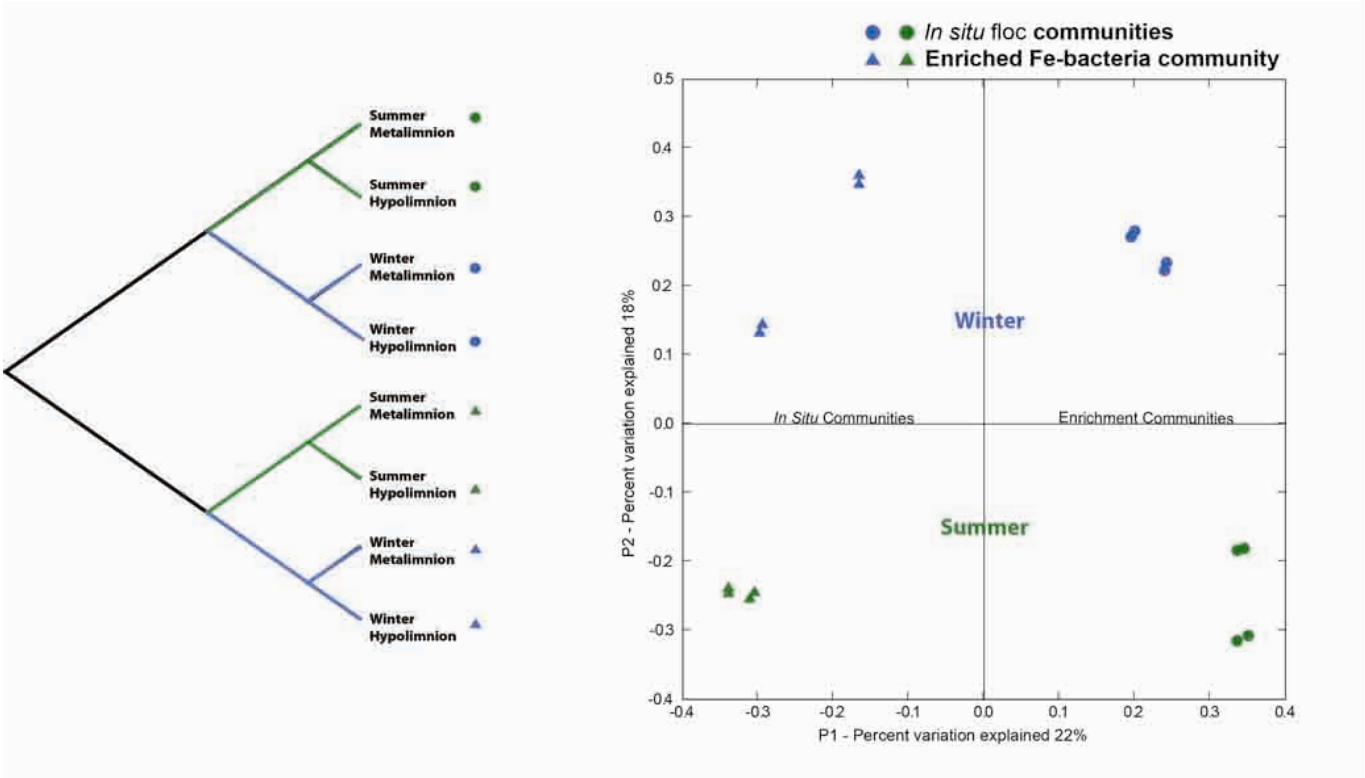

Figure S1. Analysis of in situ and enriched floc Fe-bacterial communities with unweighted Unifrac metrics. Results indicate that floc community membership significantly varies with season, but not with water column depth. Here, PC2 clearly separates *in situ* floc summer vs. winter communities, and significantly correlated to seasonal changes in the concentrations and nature of floc associated Fe-phases (*see main text*).

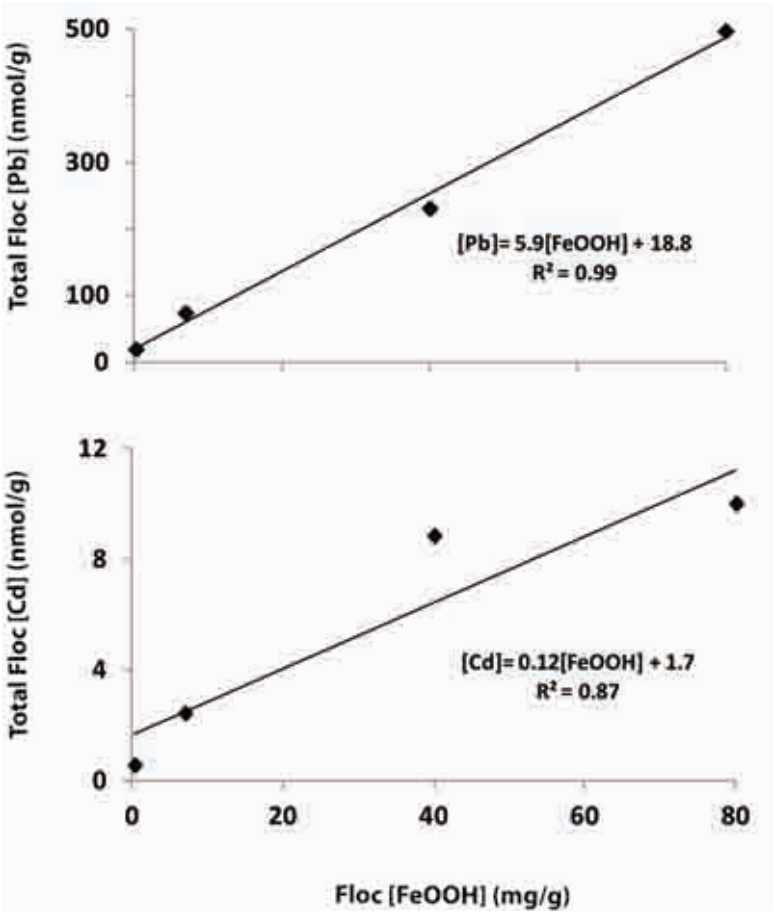

Figure S2. Total floc trace element concentrations (TEs: Pb, Cd) are positively correlated with the concentration of floc-associated amorphous Fe (oxy) hydroxides ([FeOOH]).

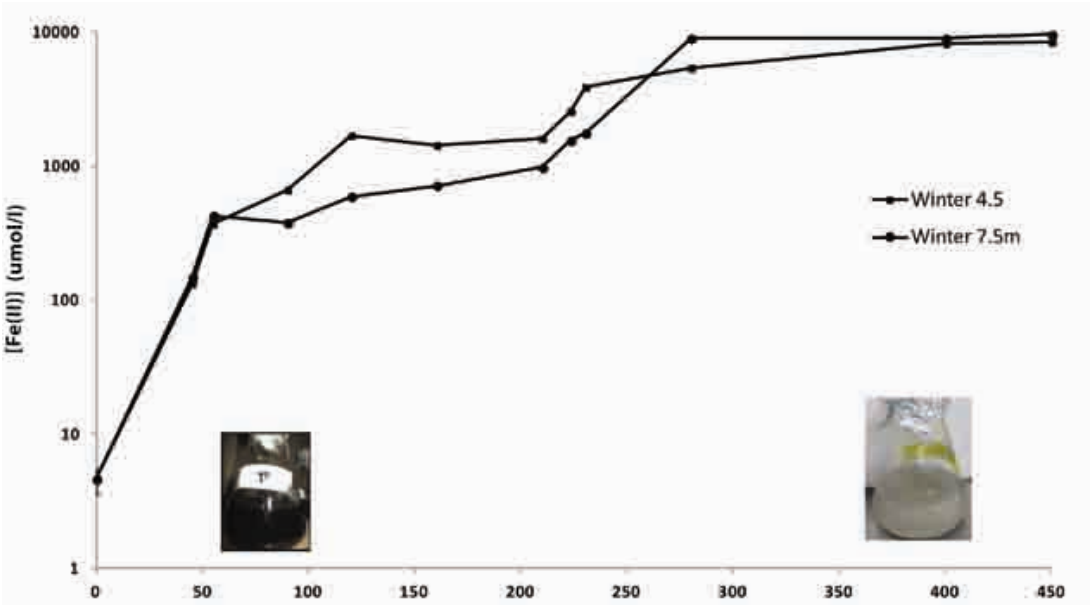

Figure S3. Ferrous iron accumulation (umol/L) by enriched winter floc Fe-bacterial communities (4.5m, 7.5m) under strictly anoxic conditions. Data shown here represent Fe-geochemical outcome of a single generation (N=40th) of enrichment experiments over 450h.

Table 51. Field observations and seasonal geochemistry during summer and winter stratification periods of Coldspring Lake, Algonquin Park, ON, CAN (45°85'28"N 78°82'17"W).

		Summer		Winter	
	Site:	4.5m	7.5m	4.5m	7.5m
Water column	[Oxygen] (mg/L)	1.98	0.06	1.08	0.026
	[Oxygen] (sat %)	21.3	0.5	10.4	0.21
	Temperature (C)	19.36	11.4	4.5	5.4
	SPC (us/cm)	31	90	39	63
	pH	6.72	6.54	6.94	6.88
	[Fe]total (mg/L)	1.3 ± 0.1	9.9 ± 0.1	0.43 ± 0.1	8.5 ± 0.1
	[Fe(II)] (mg/L)	0.02 ± 0.0	5.9 ± 0.0	0.07 ± 0.0	0.42 ± 0.0
	[Nitrate] (mg/L)	0.18 ± 0.00	14.2 ± 0.00	0.1 ± 0.00	12.2 ± 0.00
	[Sulphate] (mg/L)	4.39 ± 0.01	1.2 ± 0.06	3.2 ± 0.01	1.6 ± 0.06
	[Pb] (nmol/L)	1.0	2.4	0.7	2.6
	logKd	5.7	5.0	5.0	3.8
	[Cd] (nmol/L)	0.27	0.34	0.9	3.6
	logKd	4.6	4.4	3.3	2.1
[b]***Suspended flocs***	[Organic C] (g/g)	0.6	0.5	0.4	0.4
	[Acid-soluble Phase-Fe] mg/g	4.2	0.2	0.01	-
	[Amorphous FeOOH] mg/g	77	38	7	0.3
	[Crystalline Fe(OH)] mg/g	45	47	13	25
	[Oxidizable Phase-Fe] mg/g	13.5	2.1	60.7	53
Fe-minerals (XRD)	Hematite	8%	4%	7%	4%
	Magnetite	8%	6%	6%	~9%
	Amorphous Fe Compounds	47%	~37%	~82%	81%
	Siderite $FeCO_3$	4%	4%	-	-

a Values are means (n=3), standard deviation: [Pb], [Cd]= 10^{-2}
b Values are means (n=3), standard deviation = 10^{-1}

Table S2. Abiotic modelling (PHREEQC) was used to identify expected dominant Fe-phases with depth during both summer and winter stratification periods. Physicochemical and geochemical paramters (Table S1) were used to formulate input files; redox S(-2)/S(6) couple was used for modeling for all depths of sample collection.

				logK			logK			logK			logK
Phase	**Formula**	**SI**	**log IAP**	**(292k, 1atm)**	**SI**	**log IAP**	**(292k, 1atm)**	**SI**	**log IAP**	**(292k, 1atm)**	**SI**	**log IAP**	**(292k, 1atm)**
Anglesite	PbSO4	-10.1	-17.9	-7.8	-9.9	-17.8	-7.9	-10.0	-17.9	-7.9	-11.3	-19.2	-7.9
Cd(OH)2	Cd(OH)2	-15.1	-1.4	13.7	-15.6	-1.9	13.7	-14.3	-0.6	13.7	-15.2	-1.5	13.7
CdSO4	CdSO4	-19.9	-19.8	0.1	-21.3	-20.9	0.4	-19.8	-19.1	0.7	-21.0	-20.4	0.7
Fe(OH)3(a)	Fe(OH)3	**3.1**	8.0	4.9	**4.0**	8.9	4.9	**3.3**	8.2	4.9	**4.6**	9.5	4.9
FeS(ppt)	FeS	-0.9	-4.8	-3.9	**1.8**	-2.1	-3.9	-0.5	-4.4	-3.9	**0.9**	-3.0	-3.9
Goethite	FeOOH	**8.8**	8.0	-0.8	**9.4**	8.9	-0.5	**8.4**	8.2	-0.2	**9.8**	9.5	-0.3
Hausmannite	Mn3O4	-31.2	31.2	62.4	-31.8	32.7	64.6	-33.8	32.7	66.5	-33.3	33.0	66.2
Hematite	Fe2O3	**19.5**	15.9	-3.6	**20.7**	17.8	-2.9	**18.8**	16.5	-2.3	**21.5**	19.1	-2.4
Mackinawite	FeS	-0.2	-4.8	-4.7	**2.6**	-2.1	-4.7	**0.2**	-4.4	-4.7	**1.6**	-3.0	-4.7
Manganite	MnOOH	-13.7	11.6	25.3	-13.2	12.1	25.3	-13.2	12.2	25.3	-13.1	12.2	25.3
Melanterite	FeSO4:7H2O	-8.6	-10.8	-2.3	-6.6	-9.0	-2.4	-7.9	-10.4	-2.5	-7.7	-10.1	-2.5
Pb(OH)2	Pb(OH)2	-7.9	0.5	8.4	-7.5	1.2	8.6	-8.3	0.6	8.9	-9.3	-0.4	8.9
Pyrite	FeS2	**8.6**	-10.1	-18.6	**12.0**	-6.9	-18.9	**9.9**	-9.2	-19.1	**11.7**	-7.4	-19.1
Pyrochroite	Mn(OH)2	-7.2	8.0	15.2	-6.7	8.5	15.2	-6.9	8.3	15.2	-6.7	8.5	15.2
Pyrolusite	MnO2:H2O	-27.1	15.2	42.3	-27.9	15.7	43.7	-28.9	16.1	44.9	-28.8	15.9	44.7
Sulfur	S	-3.2	1.8	5.0	-2.9	2.3	5.2	-2.9	2.5	5.4	-2.4	2.9	5.4
Vivianite	Fe3(PO4)2:8H2O	-2.5	-43.5	-36.0	**0.4**	-35.6	-36.0	-4.9	-40.9	-36.0	-0.5	-36.5	-36.0

Table S3. Minerological composition (XRD) of 'biominerals' formed by enriched floc Fe-bacterial community under microoxic condtions. Each column represents site of origin of parent floc sample

	Summer Stratification		Winter Stratification	
	4.5m	7.5m	4.5m	7.5m
Hematite	10%	8%	22%	25%
Magnetite	11%	10%		
Geothite	4%	5%	3%	4%
Siderite $FeCO_3$	-	5%	-	-
Amorphous Fe Compounds	75%	69%	75%	70%
$NaKSO_4$	-	-	2%	-
Other materials	1%	4%	1%	1%

5.1 References

1. Sondi, I.; JuraÄ, M.; Prohi, E.; Pravdi, V. Particulates and the environmental capacity for trace metals: A small river as a model for a land-sea transfer system: the Rasa River estuary. *Sci. Total Environ.* 1994, *155,* 173-185.

2. Santiago, S.; Thomas, R.L.; Larbaigt, G.; Corvi, C.; Rossel, D.; Tarradellas, J.; Gregor, D.J.; McCarthy, L.; Vernet, J.P. Nutrient, heavy metal and organic pollutant composition of suspended and bed sediments in the Rhone River. *Aquat. Sci.* 1994, *56,* 220-242.

3. Stecko, J.R. and Bendell-Young, L. Contrasting the geochemistry of suspended particulate matter and deposited sediments within an estuary. *Appl. Geochem.* 2000, *15,* 753-775.

4. Plach, J.M.; Elliott, A.V.C.; Droppo, I.G.; Warren, L.A. Physical and Ecological Controls on Freshwater Floc Trace Metal Dynamics. *Environ. Sci. Technol.* 2011, *45,* 2157-2164.

5. Elliott, A.V.C.; Plach, J.M.; Droppo, I.G.; Warren, L.A. Comparative Floc-Bed Sediment Trace Element Partitioning Across Variably Contaminated Aquatic Ecosystems. *Environ. Sci. Technol.* 2012, *46,* 209-216.

6. Droppo, I.G. Rethinking what constitutes suspended sediment. *Hydrol. Process.* 2001, *15,* 1551-1564.

7. Bockelmann, U.; Manz, W.; Neu, T.R.; Szewzyk, U. Characterization of the microbial community of lotic organic aggregates in the Elbe River of Germany by cultivation and molecular methods. *FEMS Microbiol. Ecol.* 2000, *33,* 157-170.

8. Bockelmann, U.; Manz, W.; Neu, T.R.; Szewzyk, U. Investigation of lotic microbial aggregates by a combined technique of fluorescent in situ hybridization and lectin-binding-analysis. *J. Microbiol. Methods* 2002, *49,* 75-87.

9. Droppo, I.G. Structural controls on floc strength and transport. *Canadian Journal of Civil Engineering* 2004, *31,* 569-578.

10. Liss, S.N.; Droppo, I.G.; Flannigan, D.T.; Leppard, G.G. Floc architecture in wastewater and natural riverine systems. *Environmental science & technology* 1996, *30,* 686.

11. Hall-Stoodley, L.; Costerton, J.W.; Stoodley, P. Bacterial biofilms: from the natural environment to infectious diseases. *Nature Reviews Microbiology* 2004, *2,* 95-108.

12. Droppo, I.G.; Leppard, G.G.; Flannigan, D.T.; Liss, S.N. The freshwater floc: a functional relationship of water and organic and inorganic floc constituents affecting suspended sediment properties. *Water Air Soil Pollut.* 1997, *99,* 43-54.

13. Biggs, C.A. and Lant, P.A. Activated sludge flocculation: on-line determination of floc size and the effect of shear. *Water Res.* 2000, *34,* 2542-2550.

14. Droppo, I.G.; Liss, S.N.; Williams, D.; Nelson, T.; Jaskot, C.; Trapp, B. Dynamic existence of waterborne pathogens within river sediment compartments. Implications for water quality regulatory affairs. *Environ. Sci. Technol.* 2009, *43,* 1737-1743.

15. Plach, J.M. and Warren, L.A. Differentiating natural organic matter roles in freshwater floc and bed sediment lead dynamics. *Chem. Geol.* 2012, *305,* 97-105.

16. Alldredge, A.L. and Cohen, Y. Can microscale chemical patches persist in the sea? Microelectrode study of marine snow, fecal pellets. *Science* 1987, *235,* 689-691.

17. Ploug, H.; Kuhl, M.; Bucholz-Cleven, B.; Jorgensen, B.B. Anoxic aggregtes- an ephemeral phenomenon in the pelagic environment? *Aquatic Microbial Ecology* 1997, *13,* 285-294.

18. Ploug, H.; Adam, B.; Musat, N.; Kalvelage, T.; Lavik, G.; Wolf-Gladrow, D.; Kuypers, M.M.M. Carbon, nitrogen and O2 fluxes associated with the cyanobacterium Nodularia spumigena in the Baltic Sea. *The ISME journal* 2011, *5,* 1549-1558.

19. Ploug, H. and Grossart, H. Bacterial production and respiration in aggregates-a matter of the incubation method. *Aquat. Microb. Ecol.* 1999, *20,* 21-29.

20. Balzano, S.; Statham, P.J.; Pancost, R.D.; Lloyd, J.R. Role of microbial populations in the release of reduced iron to the water column from marine aggregates. *Aquat. Microb. Ecol.* 2009, *54,* 291.

21. Wetzel, R.G. *Limnology: lake and river ecosystems.* Access Online via Elsevier: 2001;

22. Viollier, E.; Inglett, P.W.; Hunter, K.; Roychoudhury, A.N.; Van Cappellen, P. The ferrozine method revisited: Fe(II)/Fe(III) determination in natural waters. *Appl. Geochem.* 2000, *15,* 785-790.

23. Stookey, L.L. Ferrozine---a new spectrophotometric reagent for iron. *Anal. Chem.* 1970, *42,* 779-781.

24. Rees, T.F.; Leenheer, J.A.; Ranville, J.F. Use of a single-bowl continuous-flow centrifuge for dewatering suspended sediments: Effect on sediment physical and chemical characteristics. *Hydrol. Process.* 1991, *5,* 201-214.

25. Haack, E.A. and Warren, L.A. Biofilm Hydrous Manganese Oxyhydroxides and Metal Dynamics in Acid Rock Drainage. *Environ. Sci. Technol.* 2003, *37,* 4138-4147.

26. Tessier, A.; Campbell, P.G.C.; Bisson, M. Sequential extraction procedure for the speciation of particulate trace metals. *Anal. Chem.* 1979, *51,* 844-851.

27. Viollier, E.; Inglett, P.W.; Hunter, K.; Roychoudhury, A.N.; Van Cappellen, P. The ferrozine method revisited: Fe(II)/Fe(III) determination in natural waters. *Appl. Geochem.* 2000, *15,* 785-790.

28. Emerson, D. and Moyer, C. Isolation and characterization of novel iron-oxidizing bacteria that grow at circumneutral pH. *Appl. Environ. Microbiol.* 1997, *63,* 4784-4792.

29. Emerson, D. and Floyd, M.M. Enrichment and isolation of iron-oxidizing bacteria at neutral pH. *Environ. Microbiol.* 2005, *397,* 112-123.

30. Kostka, J.E. and Nealson, K.H. Isolation, cultivation and characterization of iron- and manganese- reducin bacteria, In *Techniques in Microbial Ecolgy,* Burlage, R.S., Atlas, R., Stahl, D., Geesey, G. and Sayler, G., Eds.; Oxford University Press, Inc.: New York, New York, 1998;

31. Kulczycki, E.; Fowle, D.A.; Fortin, D.; Ferris, F.G. Sorption of cadmium and lead by bacteria-ferrihydrite composites. *Geomicrobiology Journal* 2005, *22,* 299-310.

32. Fortin, D.; Leppard, G.G.; Tessier, A. Characteristics of lacustrine diagenetic iron oxyhydroxides. *Geochimica et Cosmochimica Acta* 1993, *57,* 4391-4404.

33. Norlund, K.L.I.; Southam, G.; Tyliszczak, T.; Hu, Y.; Karunakaran, C.; Obst, M.; Hitchcock, A.P.; Warren, L.A. Microbial Architecture of Environmental Sulfur Processes: A Novel Syntrophic Sulfur-Metabolizing Consortia. *Environ. Sci. Technol.* 2009, *43,* 8781-8786.

34. Warren, L.A.; Norlund, K.L.I.; Bernier, L. Microbial thiosulphate reaction arrays: the interactive roles of Fe(III), O2 and microbial strain on disproportionation and oxidation pathways. *Geobiology* 2008, *6,* 461-470.

35. Shelobolina Evgenya, S.; Hiromi, K.; Huifang, X.; Jason, B.; Xiong, M.Y.; Tao, W.; Bl?the Marco; Eric, R. Isolation of phyllosilicate-iron redox cycling microorganisms from an illite-smectite rich hydromorphic soil. *Frontiers in Microbiology* 2012, *3,*

36. Coby, A.J.; Picardal, F.; Shelobolina, E.; Xu, H.; Roden, E.E. Repeated Anaerobic Microbial Redox Cycling of Iron. *Appl. Environ. Microbiol.* 2011, *77,* 6036-6042.

37. Miot, J.; Benzerara, K.; Morin, G.; Kappler, A.; Bernard, S.; Obst, M.; FÃ©rard, C.; Skouri-Panet, F.; Guigner, J.; Posth, N.; Galvez, M.; Brown Jr., G.E.; Guyot, F. Iron biomineralization by anaerobic neutrophilic iron-oxidizing bacteria. *Geochim. Cosmochim. Acta* 2009, *73,* 696-711.

38. Hegler, F.; Schmidt, C.; Schwarz, H.; Kappler, A. Does a low-pH microenvironment around phototrophic FeII-oxidizing bacteria prevent cell encrustation by FeIII minerals? *FEMS Microbiol. Ecol.* 2010, *74,* 592-600.

39. Lentini, C.J.; Wankel, S.D.; Hansel, C.M. Enriched iron(III)-reducing bacterial communities are shaped by carbon substrate and iron oxide mineralogy. *Frontiers in Microbiology* 2012, *3,*

40. Dowd, S.E.; Callaway, T.R.; Wolcott, R.D.; Sun, Y.; McKeehan, T.; Hagevoort, R.G.; Edrington, T.S. Evaluation of the bacterial diversity in the feces of cattle using 16S rDNA bacterial tag-encoded FLX amplicon pyrosequencing (bTEFAP). *BMC Microbiology* 2008, *8,* 125.

41. Wolcott, R.D.; Gontcharova, V.; Sun, Y.; Dowd, S.E. Evaluation of the bacterial diversity among and within individual venous leg ulcers using bacterial tag-encoded FLX and titanium amplicon pyrosequencing and metagenomic approaches. *BMC Microbiology* 2009, *9,* 226-237.

42. Cole, J.R.; Wang, Q.; Cardenas, E.; Fish, J.; Chai, B.; Farris, R.J.; Kulam-Syed-Mohideen, A.S.; McGarrell, D.M.; Marsh, T.; Garrity, G.M.; and Tiedje, J.M. The Ribosomal Database Project: improved alignments and new tools for rRNA analysis. *Nucleic Acids Research* 2009, *37,* D145.

43. Wang, Q.; Garrity, G.M.; Teiedje, J.M.; Cole, J.R. Naive Bayesian classifier for rapid assignmnet of rRNA aequences into the new bacterial taxonomy. *Appl. Environ. Microbiol.* 2007, *73,* 5261.

44. Tamura, K.; Peterson, D.; Peterson, N.; Stecher, G.; Nei, M.; Kumar, S. MEGA5: Molecular Evolutionary Genetics Analysis Using Maximum Likelihood, Evolutionary Distance, and Maximum Parsimony Methods. *Molecular Biology and Evolution* 2011, *28,* 2731-2739.

45. Lozupone, C.A.; Hamady, M.; Knight, R. UniFrac – An online tool for comparing microbial community diversity in a phylogenetic context. *BMC Bioinformatics* 2006, *7,* 371.

46. Lozupone, C. and Knight, R. UniFrac: a New Phylogenetic Method for Comparing Microbial Communities. *Appl. Environ. Microbiol.* 2005, *71,* 8228-8235.

47. Turnbaugh, P.J.; Hamady, M.; Yatsunenko, T.; Cantarel, B.L.; Duncan, A.; Ley, R.E.; Sogin, M.L.; Jones, W.J.; Roe, B.A.; Affourtit, J.P. A core gut microbiome in obese and lean twins. *Nature* 2008, *457,* 480-484.

48. Cui, Z.; Zhou, Y.; Li, H.; Zhang, Y.; Zhang, S.; Tang, S.; Guo, X. Complex sputum microbial composition in patients with pulmonary tuberculosis. *BMC microbiology* 2012, *12,* 276.

49. Koenig, J.E.; Spor, A.; Scalfone, N.; Fricker, A.D.; Stombaugh, J.; Knight, R.; Angenent, L.T.; Ley, R.E. Succession of microbial consortia in the developing infant gut microbiome. *Proceedings of the National Academy of Sciences* 2011, *108,* 4578-4585.

50. Werner, J.J.; Knights, D.; Garcia, M.L.; Scalfone, N.B.; Smith, S.; Yarasheski, K.; Cummings, T.A.; Beers, A.R.; Knight, R.; Angenent, L.T. Bacterial community structures are unique and resilient in full-scale bioenergy systems. *Proceedings of the National Academy of Sciences* 2011, *108,* 4158-4163.

51. Evans, S.E. and Wallenstein, M.D. Soil microbial community response to drying and rewetting stress: does historical precipitation regime matter? *Biogeochemistry* 2012, *109,* 101-116.

52. Yavitt, J.B.; Yashiro, E.; Cadillo-Quiroz, H.; Zinder, S.H. Methanogen diversity and community composition in peatlands of the central to northern Appalachian Mountain region, North America. *Biogeochemistry* 2012, *109,* 117-131.

53. Lozupone, C.A.; Hamady, M.; Kelley, S.T.; Knight, R. Quantitative and Qualitative Î² Diversity Measures Lead to Different Insights into Factors That Structure Microbial Communities. *Appl. Environ. Microbiol.* 2007, *73,* 1576-1585.

54. Shade, A.; Jones, S.E.; McMahon, K.D. The influence of habitat heterogeneity on freshwater bacterial community composition and dynamics. *Environ. Microbiol.* 2008, *10,* 1057-1067.

55. Ehrlich, H.L. and Newman, D.K. Geomicrobiology. 2009,

56. Langmuir, D. *Aqueous Environmental Geochemistry.* Prentice Hall: Upper Saddle River, New Jersey, 1997;

57. Langley, S.; Gault, A.; Ibrahim, A.; Renaud, R.; Fortin, D.; Clark, I.D.; Ferris, F.G. A Comparison of the Rates of Fe(III) Reduction in Synthetic and Bacteriogenic Iron Oxides by Shewanella putrefaciens CN32. *Geomicrobiol. J.* 2009, *26,* 57-70.

58. Mark Jensen, M.; Thamdrup, B.; Rysgaard, S.; Holmer, M.; Fossing, H. Rates and regulation of microbial iron reduction in sediments of the Baltic-North Sea transition. *Biogeochemistry* 2003, *65,* 295-317.

CHAPTER 6: CONCLUDING STATEMENTS

The combined results of this dissertation provide new knowledge and insight into linkages among the geochemical properties of suspended flocs in aquatic environments and, in turn, the interplay between floc-associated bacteria, floc-reactive solid phases and trace element uptake. This work adds to the field of geomicrobiology by identifying important roles for pelagic floc bacterial communities as 'geochemical agents'[1]. Resident floc bacteria and associated EPS were found to influence floc trace element and Fe geochemistry by: i) facilitating the scavenging of TEs specifically through the collection/nucleation of highly reactive amorphous Fe^{III}-oxyhydroxide minerals ($Fe^{(III)}OOH_{(s)}$) (*Chapter 3*); ii) the potential for active participation in floc-associated $Fe^{(III/II)}$-redox and thus Fe-mineral formation and dissolution reactions (*Chapters 4, 5*) ; and, iii) through their ability to collaboratively modify the geochemical conditions of their immediate microenvironment as a result of natural metabolic processes and activities (*Chapters 4, 5*).

The results of the field investigation of floc-bed sediment trace element behavior (*Chapter 3*) demonstrate that the organic rich nature of floc exerts an important control over trace element (TEs: Ag, As, Cu, Ni and Co) geochemistry in aquatic environments. To date a number of studies have demonstrated floc to be a significant TE sorbant (e.g., ref 13). However, very few investigations have specifically assessed suspended floc TE partitioning patterns or constituent phases responsible for TE uptake[6,14-16] and none to date have compared floc TE concentrations and partitioning patterns across a suite of variably impacted natural aquatic systems. The goal of Chapter 3 was to address these gaps in understanding through specific inclusion of floc in assessment of freshwater TE behavior. Floc organics were found to provide the critical framework for the generation and concentration of amorphous Fe oxyhydroxides (FeOOH), the dominant floc TE scavenging phase. Highlighting this floc organic-FeOOH relationship, comparative concentration factors indicated not only the enrichment of the FeOOH-phase in floc relative to surficial bed sediments, but also that TE reactivity of floc-FeOOH is far

higher than that of surficial bed sediments. Thus both the greater abundance and higher reactivity of floc-FeOOH contribute to the observed enhanced TE uptake by flocs relative to bed sediments across widely varying and differentially contaminated aquatic systems.

This work has also made important discoveries that expand our understanding of microbial metabolic impacts on key biogeochemical cycles, evidencing the previously unknown expansion of aero-intolerant ferric-iron reducing (IRB) and ferrous-iron oxidizing (IOB) environmental bacterial communities into the oxygenated pelagic regions of aquatic environments (*Chapters 4, 5*). These findings have large implications in current models of modern and ancient Fe biogeochemistry and highlight that the implementation of geochemical thermodynamic constraints alone as a guide to investigating and interpreting microbe-geosphere interactions may not accurately capture processes occurring *in situ.* Furthermore, IRB and IOB microbial metabolisms are hypothesized to be ancient and microbial-mediated $Fe^{(II)}/Fe^{(III)}$ redox transformations have been implicated in planetary biogeochemistry as early as the Archaean and early Proterozoic Eons[2, 3]. Thus the finding of a modern co-occurrence and close association of IRB-IOB-aerobe bacterial consortia within pelagic floc aggregates, although highly speculative, could then represent the result of an evolutionary adaption of these ancient aero-intolerant Fe-metabolisms to increasing oxygen conditions of early Earth. That is, the advent of oxygenation would affect the water column biosphere not only though the diversification of chemolithoautotrophs (i.e. advent of IOB), but also result in the suppression of obligatory anaerobic metabolism to anoxic bottom sediments. However, a significant ecological advantage would be available to those anaerobic microorganisms able to both decouple from increasing bulk O_2 via EPS production and aggregate formation, but also form new associations, syntrophic or collaborative, with the newly evolving mega-metabolic guild of microorganisms, the aerobes. This strategy would have allowed ancient anaerobic metabolism to colonize and proliferate in the new oxygenated world. Further, in modern systems, this could translate to a widespread adaptive strategy of aero-intolerant microorganisms, such as Fe-metabolizers, that

serves to extend these otherwise highly restricted aero-intolerant species into a far broader range of environments. The identification of IRB-IOB-aerobe consortia in pelagic environmental bacterial communities, where O_2 concentrations are saturated, and successful co-enrichments under increasing oxygen regimes, supports this hypothesis.

Results detailed in Chapters 4 and 5 also highlight important principles of geomicrobiology. For example, findings from this doctoral research support the principle that bacteria rarely interact with their environment in isolation; rather, they exist as multi-guild cooperatives often associated with macrostructures such as consortial aggregates (e.g.[4, 5]) or sessile biofilm communities[6-8]. In this manner, diverse lineages of environmental bacteria intimately co-exist and *collectively* influence biogeochemical cycling. Furthermore, that this microbial-scale cooperation may not be captured by bulk scale physico-chemical characterizations. Such collective impacts on biogeochemical cycling, while appreciated, are still not well understood. Here, experimental microcosm IRB-IOB-aerobe consortial aggregates generated unusual assemblages of co-occurring reduced and oxidized Fe minerals, not predicted by treatment oxygen levels, but also observed in environmental pelagic aggregate samples from similar system O_2 levels. The accumulation of $Fe^{(II)}_{(aq)}$ sufficient to produce ferrous mineral phases under experimental microoxic and oxic regimes underscores the role of the aggregate structure in generating differentiated geochemical microenvironments and provides a persuasive argument for the widespread environmental occurrence of aggregate-associated microbial Fe-redox cycling at the microscale under oxygenated conditions.

The results of this dissertation highlight that adopting notions of microbial-scale cooperation, as well as an appreciation of the capacity of microorganisms to ecologically orchestrate their immediate microenvironment, more widely into biogeochemical investigations will enable us to better capture processes occurring *in situ* and advance our biogeochemical understanding of both modern and ancient planetary function. For example, many of the bacteria that are involved in $Fe^{(II)}$ metabolism and deposition of $Fe^{(III)}$ hydroxides have not been obtained in pure

culture, including many sheathed IOB such as *Leptothrix spp.* Chapter 4 details the first study, to our knowledge, to identify the importance of syntrophy in sustaining such microorganisms in the laboratory. That is, resident floc IOB require an IRB, rather than a simple $Fe^{(II)}$ media salt, in order to provide an accessible $Fe^{(II)}$ source under environmentally relevant (i.e. oxygenated) conditions. In turn, the resulting structural partnership, including collaboration with oxygen-consuming aerobic bacteria, provides the necessary geochemical microenvironment that enables both Fe metabolisms. Furthermore, this doctoral work also highlights hat although advances in molecular biology continue to generate powerful tools that can improve our ability to identify environmental bacteria as well as our understanding of microbial community functioning, an overemphasis on genetics can largely ignore the microbial ecology of bacterial communities and that findings from genomics without ecological and biogeochemical characterization can be difficult to link to processes occurring within natural systems. Here, experimentation on co-enrichment cultures and isolation of targeted microbial metabolism are techniques allowed for the identification of particular physiological types within environmental floc bacterial communities, and as well as the identification and characterization of microbial interactions in the context of targeted biogeochemical cycles.

These combined results of this dissertation indicate that floc microbial Fe cycling, with attendant implications for nutrient and contaminant behaviour in oxygenated waters requires further investigation, as do the potential implications of floc associated Fe-biominerals for geochemical interpretation. Further, these results are impelling in identifying the widespread potential for the occurrence of a fully coupled microbial Fe redox wheel in oxygenated waters as well as indicating that such microbial cooperatives are likely operating in the other redox sensitive major biogeochemical cycles.

6.1 References

References

1. Ehrlich, H. L. & Newman, D. K. Geomicrobiology. (2009).

2. Konhauser, K. O. *et al*. Could bacteria have formed the Precambrian banded iron formations? *Geology* **30**, 1079-1082 (2002).

3. Walker, J. C. G. Suboxic diagenesis in banded iron formations. *Nature* **309**, 340-342 (1984).

4. Norlund, K. L. I. *et al*. Microbial Architecture of Environmental Sulfur Processes: A Novel Syntrophic Sulfur-Metabolizing Consortia. *Environ. Sci. Technol.* **43**, 8781-8786 (2009).

5. Dekas, A. E., Poretsky, R. S. & Orphan, V. J. Deep-Sea Archaea Fix and Share Nitrogen in Methane-Consuming Microbial Consortia. *Science* **326**, 422-426 (2009).

6. Warren, L. A. & Kauffman, M. E. Microbial Geoengineers. *Science* **299**, 1027-1029 (2003).

7. Konopka, A. Microbial ecology: searching for principles. *Microbe* **1**, 175 (2006).

8. Gault, A. G. *et al*. Seasonal Changes In Mineralogy, Geochemistry and Microbial Community of Bacteriogenic Iron Oxides (BIOS) Deposited in a Circumneutral Wetland. *Geomicrobiol. J.* **29**, 161-172 (2012).